1061

Intrinsic Decomposition of Sodium Nitrate and Potassium Nitrate

Dissertation by
Carolyn Margaret Kramer
December 1980

Z. A. Munir
Dissertation Committee Chair
Material Science Division
Department of Mechanical Engineering
University of California, Davis

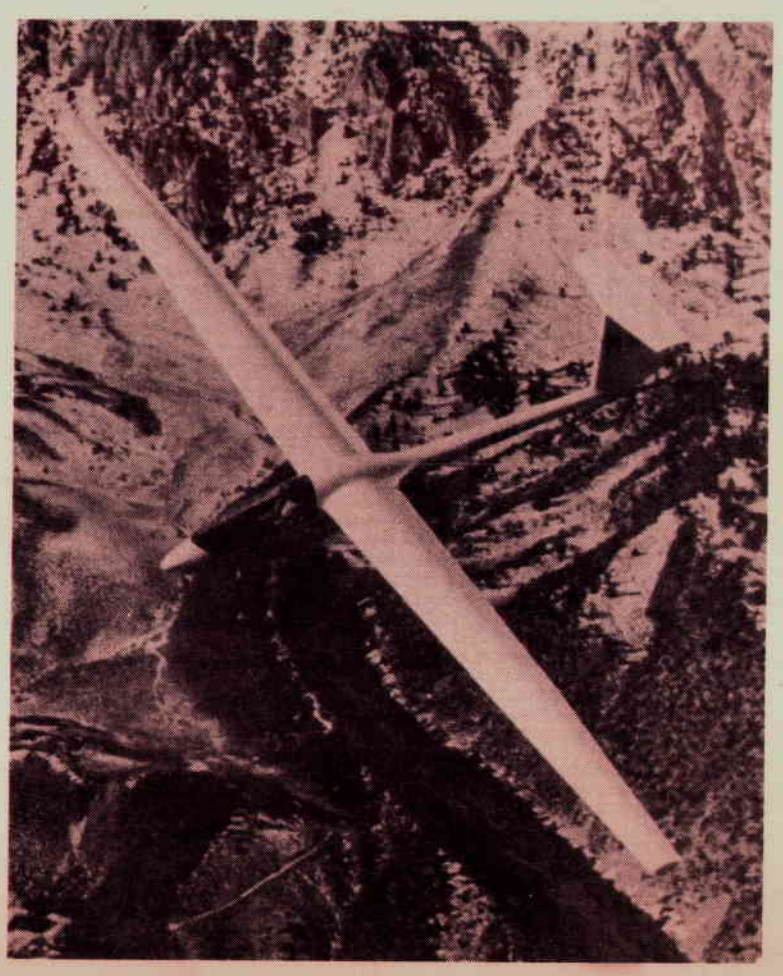

"Solar Powered"
Photo courtesy of George Uveges

INTRINSIC DECOMPOSITION OF SODIUM NITRATE AND POTASSIUM NITRATE

Dissertation by

Carolyn Margaret Kramer
Division of Materials Science and Engineering
Department of Mechanical Engineering
University of California, Davis

Z. A. Munir
Dissertation Committee Chair

Carolyn Margaret Kramer
December 1980
Materials Science

INTRINSIC DECOMPOSITION OF SODIUM NITRATE AND POTASSIUM NITRATE

Abstract

The decomposition of $NaNO_3$ and KNO_3 has been studied in air, argon, and vacuum with these experimental techniques: differential scanning calorimetry (DSC), chemical analysis, thermogravimetry (TG) and mass spectrometry (MS). Above 840 ($\pm$ 10) and 820 ($\pm$ 20) K, for $NaNO_3$ and KNO_3 respectively, endothermic decomposition reactions were evident in DSC experiments. These decomposition reactions caused the alkalinity to increase and the amount of nitrite to increase in the nitrates. A statistical screening technique, in conjunction with chemical analysis, determined that of ten selected variables that cause decomposition, temperature was the most important variable. The presence of carbon dioxide or water vapor, high gas flow rates, and low purity of the salts also enhanced decomposition. Salt samples were decomposed in argon where it was observed that the nitrates decomposed almost entirely to nitrite as low as 624 K, a process which was enhanced by corrosion of the stainless steel containers that were used.

Vaporization and decomposition of the nitrates occurred concurrently at 630 K in addition to vaporization of the decomposition products, superoxide and peroxide. The intrinsic (noncondensible) decomposition products of $NaNO_3$ and KNO_3 are N_2, NO and O_2. Nitrogen and nitric oxide are the initial decomposition products and oxygen is a product that appears in

increasing proportions as decomposition proceeds and at higher temperatures. The rates of weight loss in TG experiments were proportional to the surface area of the salt. In vacuum, the rates of weight loss were 0.12 and 0.17 $mg\text{-}cm^{-2}\text{-}min^{-1}$ for $NaNO_3$ and KNO_3, respectively, at 740 K. The activation enthalpies for $NaNO_3$ and KNO_3 are, respectively, 36.6 and 34.9 $kcal\text{-}mole^{-1}$ ($\pm$ 4.9 $kcal\text{-}mole^{-1}$ for a 90% confidence limit) from 630 K to 750 K in vacuum. The rates of weight loss in static air were approximately 1% of the rates of weight loss of the nitrates in vacuum.

CONTENTS

TABLES

ILLUSTRATIONS

I. INTRODUCTION

In the late 1800's sodium and potassium nitrate were shipped by "solar-powered" vessels. The largest and swiftest of these sailing ships was the Preussen[1], which is shown in Figure 1. Now molten sodium and potassium nitrate have become candidates for heat transfer and energy storage fluids in solar thermal electric power plants.[2] Thus these salts have shifted from being transported by solar energy to transporting and transforming solar energy.

Solar electric power plants use thermal energy from the sun to generate steam for turbines that generate electrical power. In one type of power plant, shown in Figure 2, the sun's rays are focused by a field of heliostats (sun-tracking mirrors) onto an elevated tower, through which a heat transfer fluid is pumped to absorb the focused energy. The heat transfer fluid can be contained in pipes that are heated by the sun or can directly absorb the focused energy.[3,4] The heated fluid is conveyed to heat exchangers that generate steam.

Effective use of solar insolation for electrical power generation necessitates energy storage so that continuous power can be supplied from a diurnal energy source.[5] Ideally, the heat transfer fluid that generates steam would also be the sensible-heat thermal storage medium.

Several studies[2,6] have suggested criteria for the heat transfer and thermal energy storage fluids: melting point less than 523 K, thermal stability to 850 K, high heat capacity per gram, low vapor pressure, compatibility with structural metals, and low cost. Satisfying these criteria are certain molten salts and molten metals,[6-10] outstanding among which are the nitrate mixtures of sodium and potassium.[11-13]

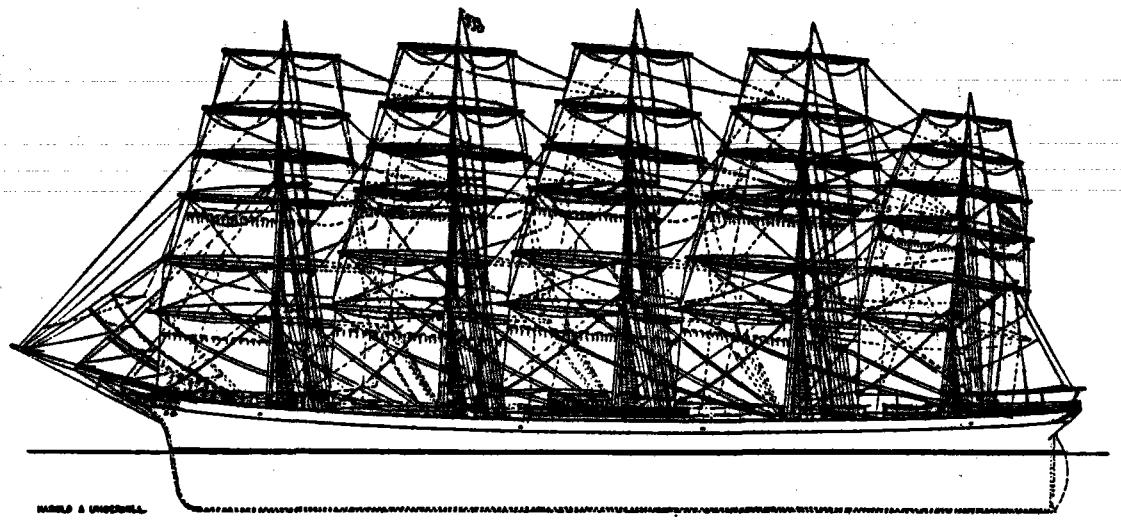

Figure 1. The Preussen

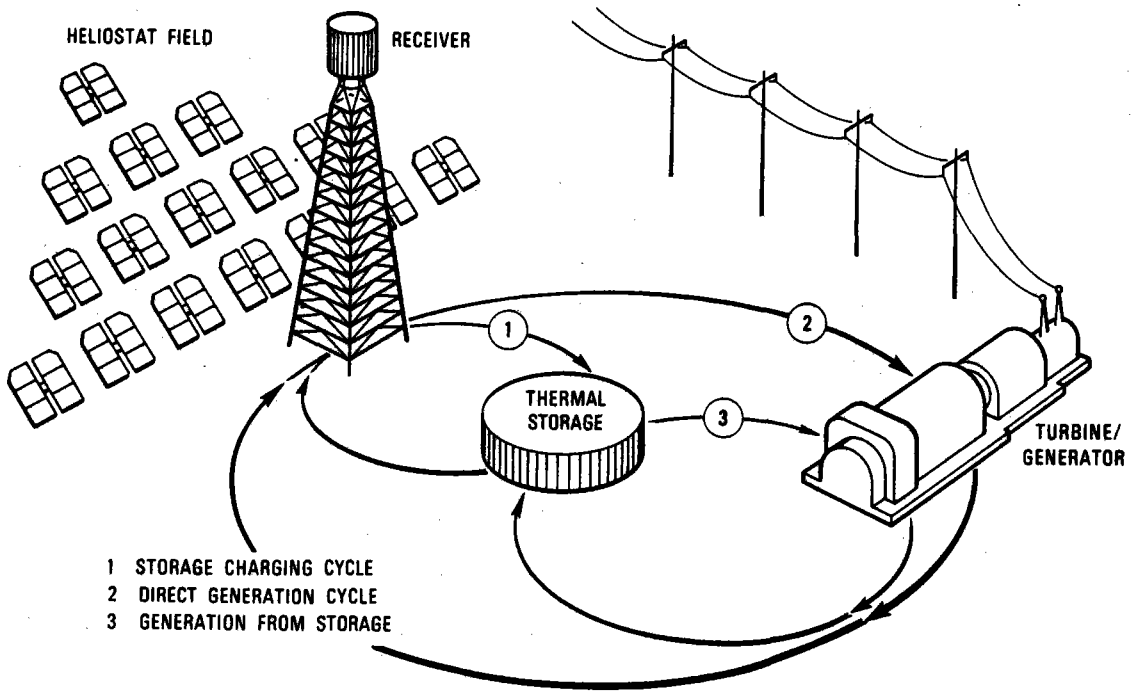

Figure 2. A Schematic of a Solar Central Receiver

These nitrates are among the lowest-melting-point anhydrous salts known.[14] These salts are also very inexpensive and relatively noncorrosive,[8] particularly when compared with other molten salts,[6] such as $LiNO_3$, or liquid metals, such as sodium. Another important characteristic of sodium and potassium nitrate is their relative chemical stability in air,[15] which can greatly simplify the design and reduce the cost of the solar power plant.[9,16]

Of course the nitrates of sodium and potassium have many other applications. Among these are: fertilizer,[1] electrochemical solvents,[17] electrolytes for thermal batteries,[18] ion exchange media for strengthening glass,[19,20] and oxidants in pyrotechnics.[21] The desirable heat transfer characteristics of the nitrates have been utilized in salt baths for heat treatment of aluminum[22,23] and steel[14] alloys and for controlling the temperature of chemical production processes.[7,8] These salts have also been considered for nuclear reactor coolants.[24,25]

Several commercial mixtures of $NaNO_3$ and KNO_3 have been marketed: Houdry salt (45 w/o $NaNO_2$ - 55 w/o KNO_3),[15,7] draw salt (46 w/o $NaNO_3$ - 54 w/o KNO_3),[26] and HTS* (40 w/o $NaNO_2$ - 7 w/o $NaNO_3$ - 53 w/o KNO_3).[11,12,17-29] The latter has become the most popular mixture because of its low melting point, 415 K. The lowest melting point of any $NaNO_3$ - KNO_3 mixture is 498 K. The melting point of Houdry salt is as low as that of HTS; however, the greater percentage of nitrite makes it more expensive than HTS. For solar thermal electric applications, draw salt has been the prime candidate because it is less expensive than HTS or Houdry salt and has an acceptable melting point.[2]

In these various applications the molten nitrate salts have been heated to as high as 870 K, the exact temperature depending on the

*HTS = heat transfer salt.

duration of use and economic factors.[7,15] At these elevated temperatures a number of deleterious phenomena have been observed: increasing viscosity, increasing melting point or density, and formation of insoluble or corrosive products. The causes can be traced to decomposition or some other chemical reaction of the salts.

The most common of the reactions may be classified as follows: nitrite formation, decomposition to oxide, reaction with CO_2 or H_2O, or vaporization. The chemical reactions that describe these phenomena for $NaNO_3$ (or KNO_3) are

$$NaNO_3 \rightarrow NaNO_2 + \frac{1}{2} O_2 \text{ (nitrite formation)} \quad (1)$$

$$2NaNO_3 \rightarrow Na_2O + \frac{5}{2} O_2 + N_2 \text{ (decomposition to oxide)} \quad (2)$$

$$2NaNO_3 + CO_2 \rightarrow Na_2CO_3 + N_2 + \frac{5}{2} O_2 \text{ (carbonate formation)} \quad (3)$$

$$2NaNO_3 + H_2O \rightarrow 2NaOH + N_2 + \frac{5}{2} O_2 \text{ (hydrolysis)} \quad (4)$$

$$NaNO_{3(\ell)} \rightarrow NaNO_{3(g)} \text{ (vaporization)} \quad (5)$$

However, even if degradation does occur by Reactions (1)-(4), the salt quality can be ameliorated by a number of processes[15,24,30] which regenerate the nitrate or nitrite salts.

The chemical behavior of $NaNO_3$ and KNO_3 is complex because of the multiple conjugate, consecutive, and reversible reactions that occur.[31] In particular, Reaction (2) is an overall reaction that may proceed by various steps involving N_xO_y gas species. Also, the nitrite ($NaNO_2$) produced in Reaction (1) may also undergo decomposition reactions that obscure the behavior of nitrate salts alone.

The objective of this study was to remove the ambiguity from the reaction mechanisms and rates of decomposition of molten sodium and

potassium nitrate. To this end, I studied the decomposition of sodium and potassium nitrate in air, vacuum, and argon. The types of experiments and the parameters of interest depended on the details of chemical reactions (1) - (5), a discussion of which we turn to next. This is followed by a description of the experimental techniques and the experimental results.

II. SALT CHEMISTRY

When one contemplates practical uses of nitrates, it is important to know the maximum temperature at which the salts may be used without decomposition due to reactions such as (1) through (4). Several investigators have assigned decomposition temperatures to the nitrates and nitrites as described in Table 1. These temperatures vary over several hundred kelvins because of the variety of experimental techniques used and their sensitivity. Furthermore, the decomposition reactions that were observed in these experiments were not the same. For instance, some authors observed nitrate to be decomposing when nitrite started to form while others observed decomposition when oxide started to form. All agree, however, that nitrates and nitrites of Na and K may be used as heat-transfer fluids at least to temperatures 50-100 K greater than their melting points without noticeable decomposition.

Unfortunately, for solar power plants, the heat-transfer fluids must be relatively stable, for some time, at temperatures above 800 K, over 250 K above the melting points of these salts. For this application it is necessary to have more information on the onset and rate of each decomposition reaction that sodium and potassium nitrate can undergo. In the remainder of this chapter I describe what is known in, and what can be derived from, the existing literature.

II A. Gaseous Equilibria

A description of the many possible reactions in which $NaNO_3$ and KNO_3 may participate is complicated by the gaseous equilibria of nitrogen, oxygen, and their compounds.[31] Stern[31] concluded that N_2 and

Table 1

Nitrate and Nitrite Salt Decomposition Temperatures

Salt	Decomposition Temperature (K)	Experimental Technique	Decomposition Observations	Reference
$NaNO_3$	1073	Observation of Gas Evolution	Rapid Decomposition to Oxide	27
$NaNO_3$	802	Measure P_{O_2}	P_{O_2} = 1 atm	33
$NaNO_3$	570	Knudsen Cell Effusion	NO(g) observed	21
$NaNO_3$	873	Thermogravimetry	Onset of Weight Loss	34
$NaNO_3$	861	Thermogravimetry	Onset of weight loss	35
$NaNO_3$	653	None	c	6
$NaNO_3$	1006[a]	Differential Thermal Analysis	Large Endotherm Occurred	36
$NaNO_3$	1029[b]	Differential Thermal Analysis	Large Endotherm Occurred	36
$NaNO_3$	783	Chemical Analyses	0.05% Nitrate Formed in 10 Minutes	37
KNO_3	1273	Observation of Gas Evolution	Rapid Decomposition to Oxide	27
KNO_3	806	Measure P_{O_2}	P_{O_2} = 1 atm	33
KNO_3	673	Literature Survey		6
KNO_3	958[a]	Differential Thermal Analysis	Large Endotherm Occurred	36
KNO_3	1027[b]	Differential Thermal Analysis	Large Endotherm Occurred	36
KNO_3	803	Chemical Analysis	0.05% Nitrite Formed in 10 Minutes	37
$NaNO_2$	593	None	c	6

Table 1 (continued)

Salt	Decomposition Temperature (K)	Experimental Technique	Decomposition Observations	Reference
$NaNO_2$	610	Chemical Analyses	Oxide Formed	38
$NaNO_2$	893	Thermogravimetry	Onset of Weight Gain	34
$NaNO_2$	1013	Thermogravimetry	Onset of Weight Loss	3
KNO_2	763	Chemical Analyses	Oxide Formed	38

[a]Salt mixed with Al_2O_3 powder
[b]Salt mixed with MgO powder
[c]Based on reviewers analysis of literature

O_2 are thermodynamically the most stable components compared with any of the N_xO_y species but pointed out that N_xO_y species are frequently products of nitrate and nitrite decomposition. In this section I discuss the thermodynamic stability and the kinetics of the interactions of the N_xO_y species in the temperature range 300-1000 K.

To demonstrate the thermodynamic stability of N_2 and O_2 I compared the free energies[32] of the gases NO, NO_2, N_2O, N_2O_3, N_2O_4, and N_2O_5 with the free energies of equivalent amounts of N_2 and O_2. The chemical equilibria I used to make the comparisons are given below; the comparisons are shown in Figures 3-8.

$$\frac{1}{2} N_2 + \frac{1}{2} O_2 \rightarrow NO \qquad (7)$$

$$\frac{1}{2} N_2 + O_2 \rightarrow NO_2 \qquad (8)$$

$$N_2 + \frac{1}{2} O_2 \rightarrow N_2O \qquad (9)$$

$$N_2 + 2O_2 \rightarrow N_2O_4 \qquad (10)$$

$$N_2 + \frac{3}{2} O_2 \rightarrow N_2O_3 \qquad (11)$$

$$N_2 + \frac{5}{2} O_2 \rightarrow N_2O_5 \qquad (12)$$

In most cases the free energies of formation of the N_xO_y species are negative (relative to N and O atoms); however, in agreement with Stern regarding the stability of N_2 and O_2, these energies are always greater than those for equivalent amounts of N_2 and O_2. The gas N_2O was not discussed by Stern, perhaps because it is the least stable species with respect to dissociation.

Based on thermodynamic considerations, all N_xO_y species will decompose to N_2 and O_2 above 300 K. Although the N_xO_y species are unstable

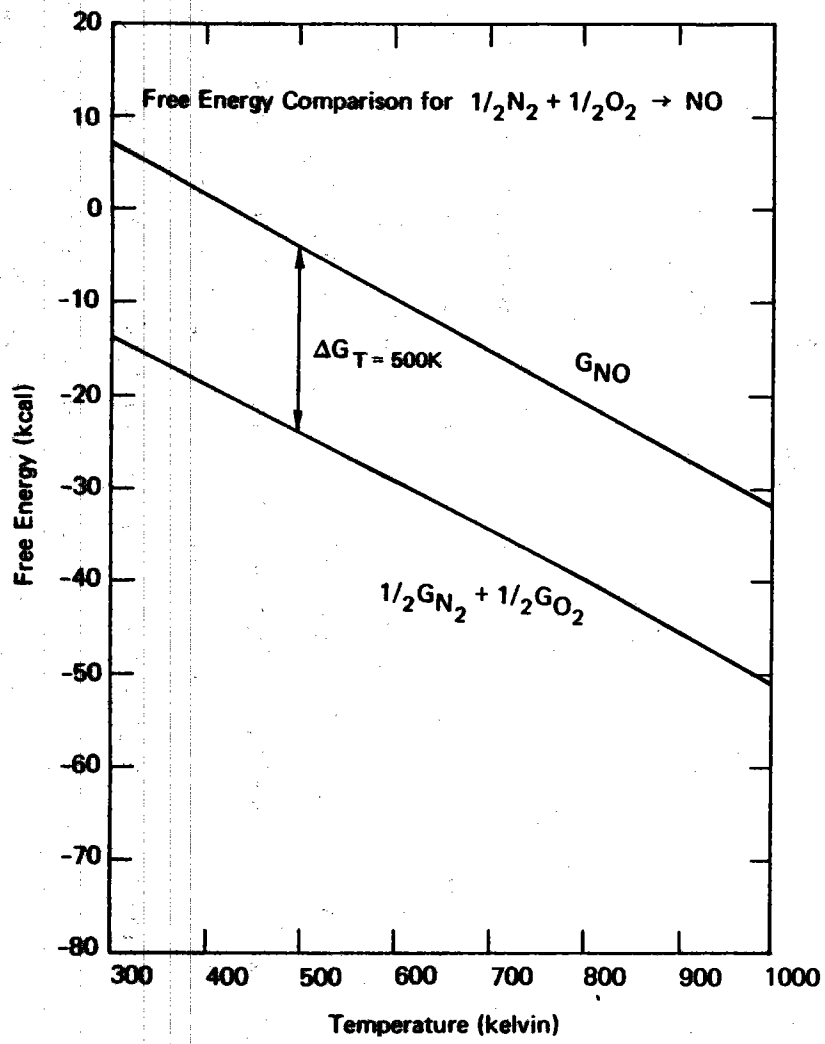

Figure 3. Comparison of the Free Energies of $\frac{1}{2}$ N_2, $\frac{1}{2}$ O_2 and NO

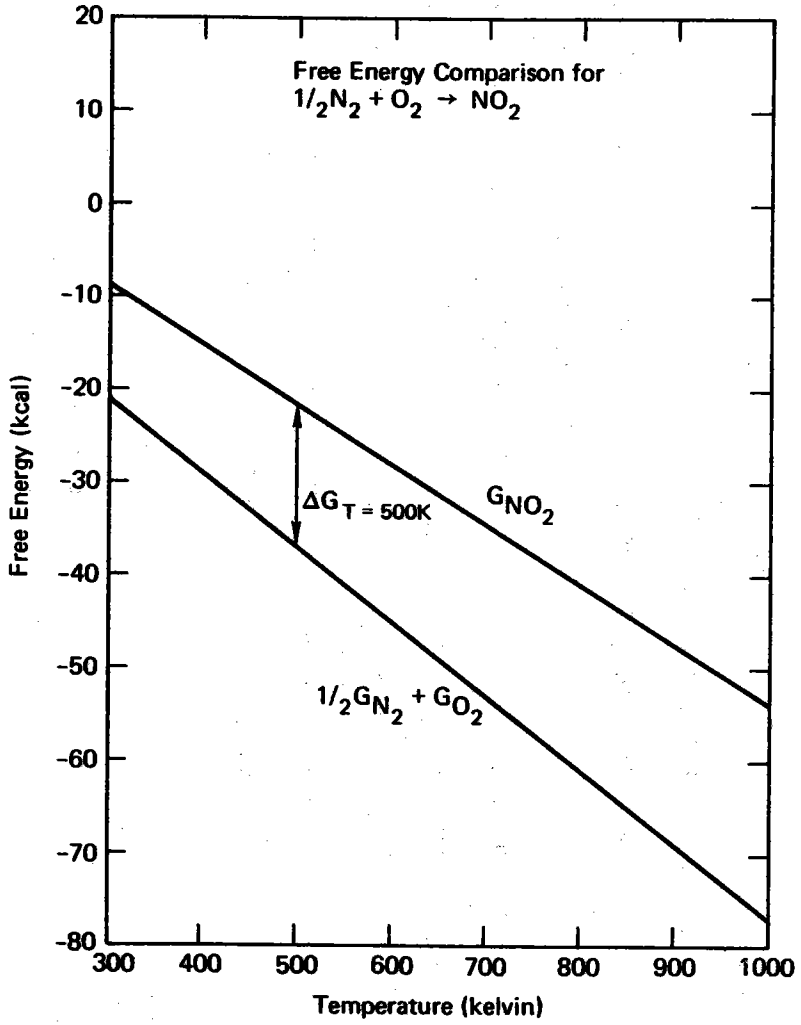

Figure 4. Comparison of the Free Energies of $\frac{1}{2}$ N_2, O_2 and NO_2

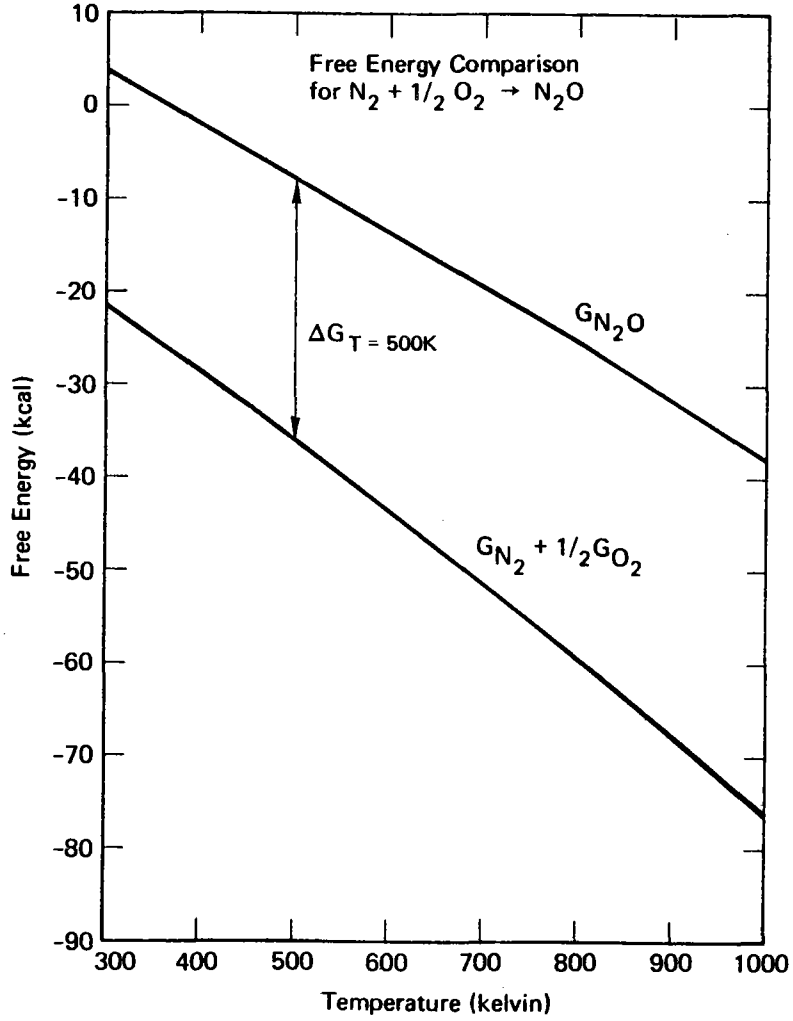

Figure 5. Comparison of the Free Energies of N_2, $\frac{1}{2}\ O_2$ and N_2O

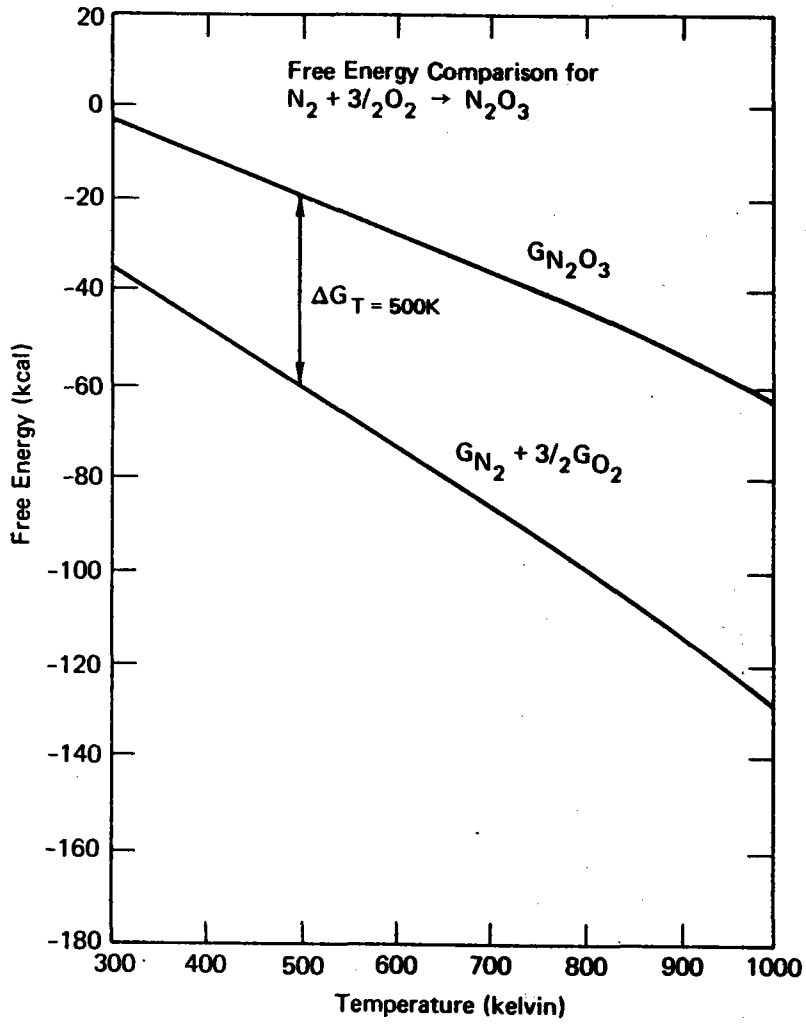

Figure 6. Comparison of the Free Energies of N_2, $\frac{3}{2}\ O_2$ and N_2O_3

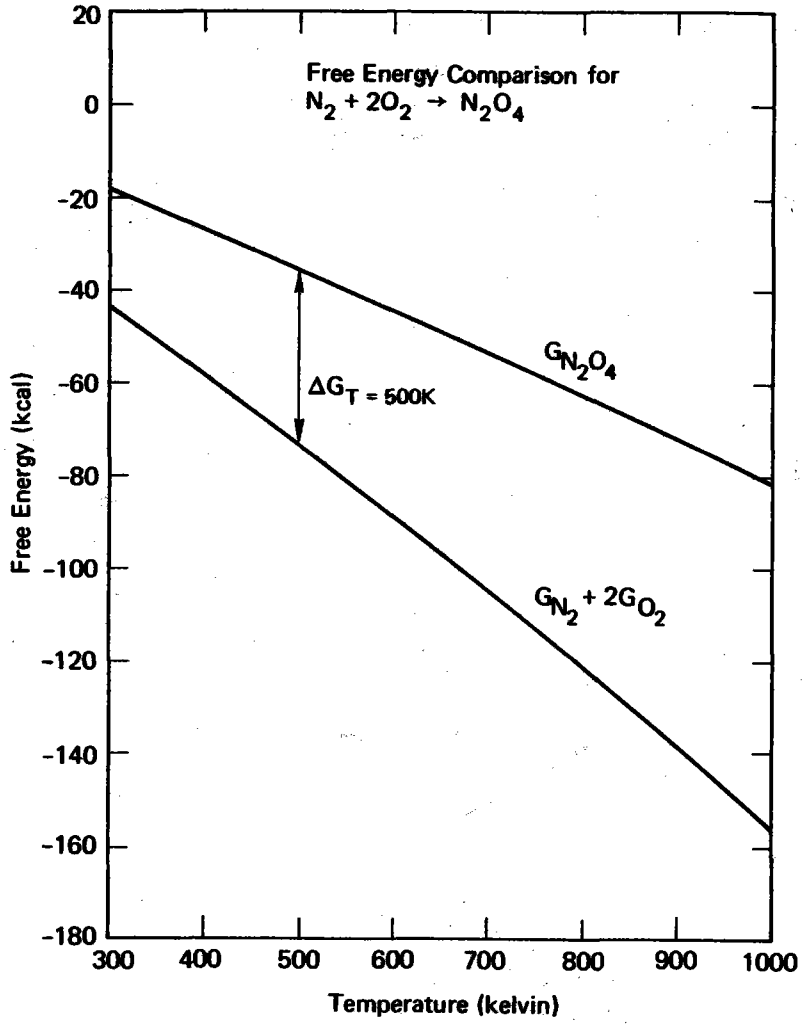

Figure 7. Comparison of the Free Energies of N_2, $2O_2$ and N_2O_4

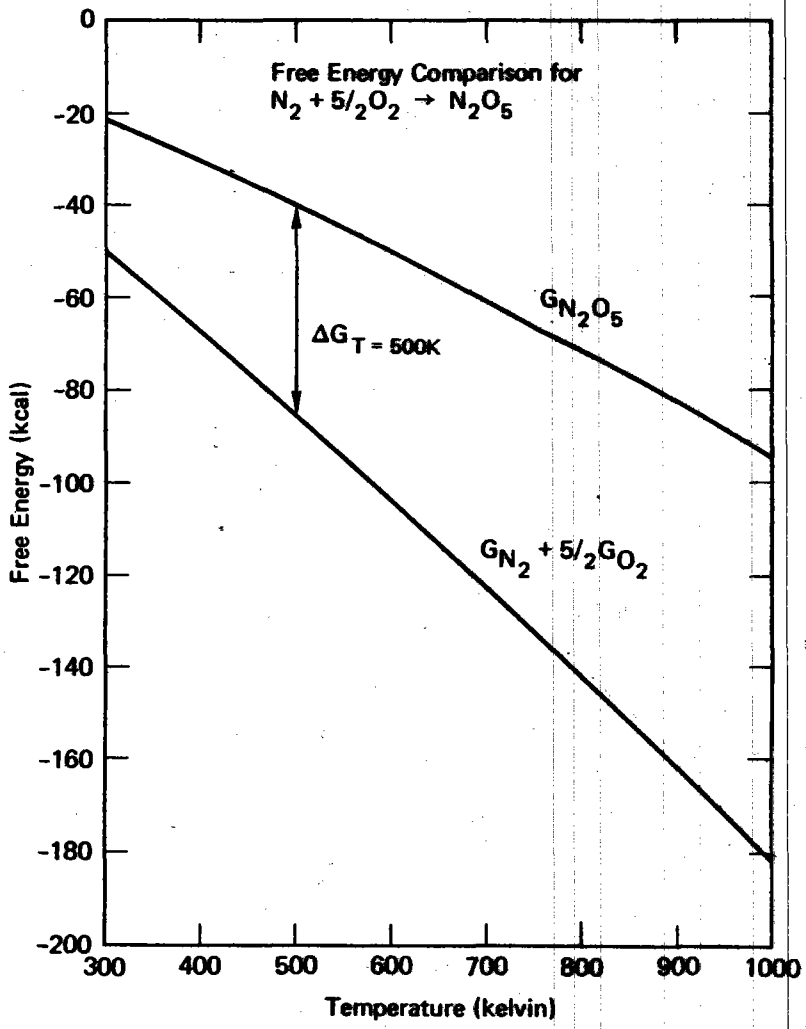

Figure 8. Comparison of the Free Energies of N_2, $\frac{5}{2}\ O_2$ and N_2O_5

with respect to dissociation to N_2 and O_2, the kinetics below 1000 K are in some instances prohibitively slow to establish equilibrium.[31] Therefore, if N_xO_y species are formed from a reaction such as nitrate decomposition, the N_xO_y species may be observed before they decompose to N_2 and O_2. One must consider these gaseous kinetics of N_xO_y species to correctly identify what species are nitrate decomposition products.

The gases N_2O_3, N_2O_4, and N_2O_5 decompose rapidly to NO and NO_2 in the temperature range 300 - 1000 K and therefore may be neglected.[31] Nitric oxide and nitrogen dioxide are the most likely N_xO_y species to to be observed. I performed a calculation of the degree of decomposition of NO at 1000 K using a gaseous chemical kinetics computer model[39,40] and found that in 3 hours at 1000 K, 3% of the NO had decomposed. However, reaction of NO, O_2, NO_2 is rapid enough below 1000 K that one must consider the reaction

$$NO + 1/2\ O_2 \rightarrow NO_2 \qquad (13)$$

The rate at which NO, O_2, and NO_2 approach equilibrium and the proportions of each at equilibrium are very temperature dependent. The free energy for Reaction (13) is shown in Figure 9. Note that from 300 to 1000 K the free energy changes from -9 to +5 kcals. Therefore significant amounts of reactants and products will be present at equilibrium over much of this temperature range. Reaction (13), the only interaction of the N_xO_y species that Stern considered significant, adds to the confusion regarding the identities and amounts of the gaseous nitrate decomposition products, particularly in air or oxygen.

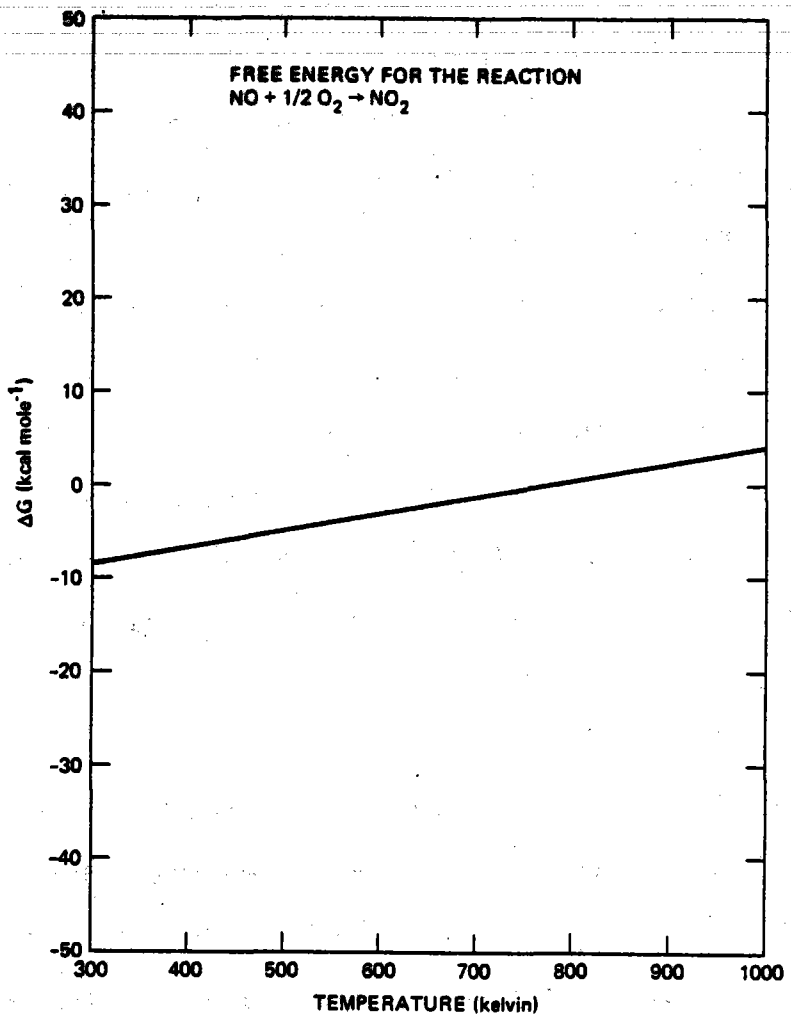

Figure 9. Free Energy of Reaction of NO, O_2 and NO_2

II B1. Nitrate and Nitrite Equilibria

Reaction (1) expresses the equilibrium of nitrite, nitrate, and oxygen. The equilibrium constant for this reaction, K_{eq} is related to the activities a_i of the reaction species as

$$K_{eq} = a_{MNO_2} a_{O_2}^{1/2} / a_{MNO_3} \quad , \tag{14}$$

where the activity of oxygen is assumed to be equal to the partial pressure (P_{O_2}) and M is either metal (Na or K). The complexity of this reaction can be grasped by comparing it to a similar oxyanionic decomposition such as

$$CaCO_3 \rightarrow CaO + CO_2 \quad , \tag{15}$$

where the equilibrium constant is

$$K_{eq} = \frac{a_{CaO} P_{CO_2}}{a_{CaCO_3}} = P_{CO_2} \quad . \tag{16}$$

The activities of CaO and $CaCO_3$ are assumed to be equal to unity because they are pure solid phases. Therefore, at a given temperature, the equilibrium pressure of carbon dioxide is fixed.

This situation contrasts to the oxygen, nitrate, and nitrite equilibrium where the nitrate and nitrite are totally miscible liquids. However, because they are believed to behave ideally,[41,42] one can substitute mole fractions X_i for the a_i in Eq. (14). Still, the equilibrium partial pressure of oxygen is not fixed solely by choosing a temperature, as is the equilibrium pressure of CO_2 for the carbonates; rather, it is determined by temperature, the free energy of Reaction (14) (which determines K_{eq}), and the ratio of the mole fractions of the nitrate and nitrite. The situation considerably simplifies if one chooses a temperature and a partial pressure of oxygen such that the equilibrium ratio of nitrate and nitrite in a molten salt mixture is

invariant. Table 2 summarizes several values of equilibrium constants determined in this way.

Table 2 also lists values for the enthalpies and entropies of reaction, ΔH° and ΔS°, respectively. These are related to the equilibrium constant via

$$-RT \ln(K_{eq}) = \Delta G = \Delta H - T\Delta S \quad (17)$$

and

$$\ln(K_{eq}) = \frac{-\Delta H}{RT} + \frac{\Delta S}{R} \quad (18)$$

In these equations ΔG is the free energy of the reaction, T is the absolute temperature, and R is the universal gas constant. The values of ΔH° and ΔS° that I calculated came from a least-squares fit of $\ln(K_{eq})$ versus 1/T with experimental values for K_{eq} and temperatures from the literature. The temperature dependencies of ΔH° and ΔS° were neglected. The average values of ΔH° and ΔS° are given for the temperature range. In Figures 10, 11, and 12 I have plotted the K_{eq} values given in the literature for sodium, potassium, and 50/50 sodium/potassium nitrate/ nitrite mixtures. Superimposed on the data are the least squares fits of $\ln(K_{eq})$ versus 1/T.

The slopes of the $\ln(K_{eq})$ versus 1/T in Figures 10-12 are very similar, approximately 25 kcal/mole, independent of the cation. The only exception to this was the data from Reference 44 which I believe to be anomalous (as did Paniccia and Zambonin[45]) because it is so much lower than the other values. The value of ΔS is somewhat higher for $NaNO_3/NO_2$ mixtures than for KNO_3/NO_2 mixtures, indicating that more sodium nitrite is present in $NaNO_3$ compared with potassium nitrite in KNO_3 at a given temperature.

Table 2

Determination of Equilibrium of Nitrate and Nitrite

Salt	Temperature Range (kelvin)	ΔH (kcal mole^{-1})	$\Delta H(\frac{kJ}{mole})^d$	ΔS (cal mole^{-1} K^{-1})	ΔS(J mole^{-1} K^{-1})^d	P_{O_2}	Experimental Technique	Reference
KNO_3/NO_2	823-1073	29.1±1.7 (28.4[a]) 26.4±1.1 (27.1[a]) 27.6±1.2 (30.0[a])	118. 113. 125.	24.4±1.2 (25.1[a]) (23.7[a]) (27.1[a])	105. 99.2 113.	1. atm	Gas Volume Changes NO_2^- Titration Combination of Above Techniques	41
KNO_3/NO_2	973-1073	31.3 (33.6[a])	140.	31.1[b] (33.6[a])	140.	1. atm	Gas Volume Changes	42
KNO_3/NO_2	873-973	26.0 (28.7[a])		22.9[b] (25.7[a])	108.	0.2 atm	NO_2^- Titration	43
$NaNO_3/NO_2$	873-973	24.5 (25.6[a])	107.	(25.6[a])	107.	1. atm	Gas Volume Changes	34
$NaNO_3/NO_2$	823-973	27.0 (28.4[a])	119.	(26.8[a])	112.			43
$(Na/K)NO_3/NO_2$	568-613	(2.2)[a]	9.2	13.3[a]	55.6	0.85 atm	NO_2^- Titration	44
$(Na/K)NO_3/NO_2$	500-700	27.2 (25.6[a])	107.	14.8 (23.8[a])	61.9	na[c]	Equilibrate to Constant Pressure; O_2, P,V Measured; NO_2^- Titration	45

[a]Calculated by the author using a least squares analysis method with the data given in the cited reference. Values of ΔH and ΔS without a superscript are those given in the cited reference.
[b]Reported in Reference 28.
[c]Not applicable to technique.
[d]Only values calculated by author are given in SI units.

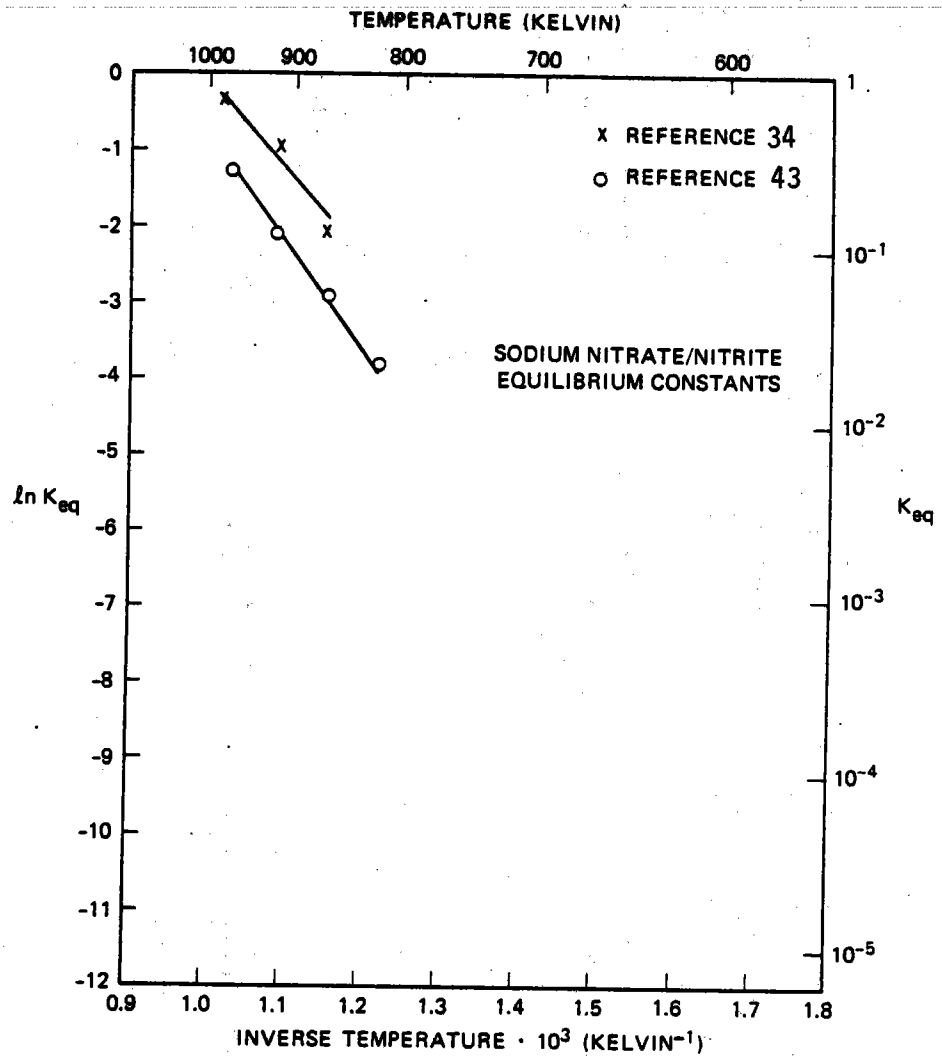

Figure 10. The Equilibrium Constants for $NaNO_3/NO_2$

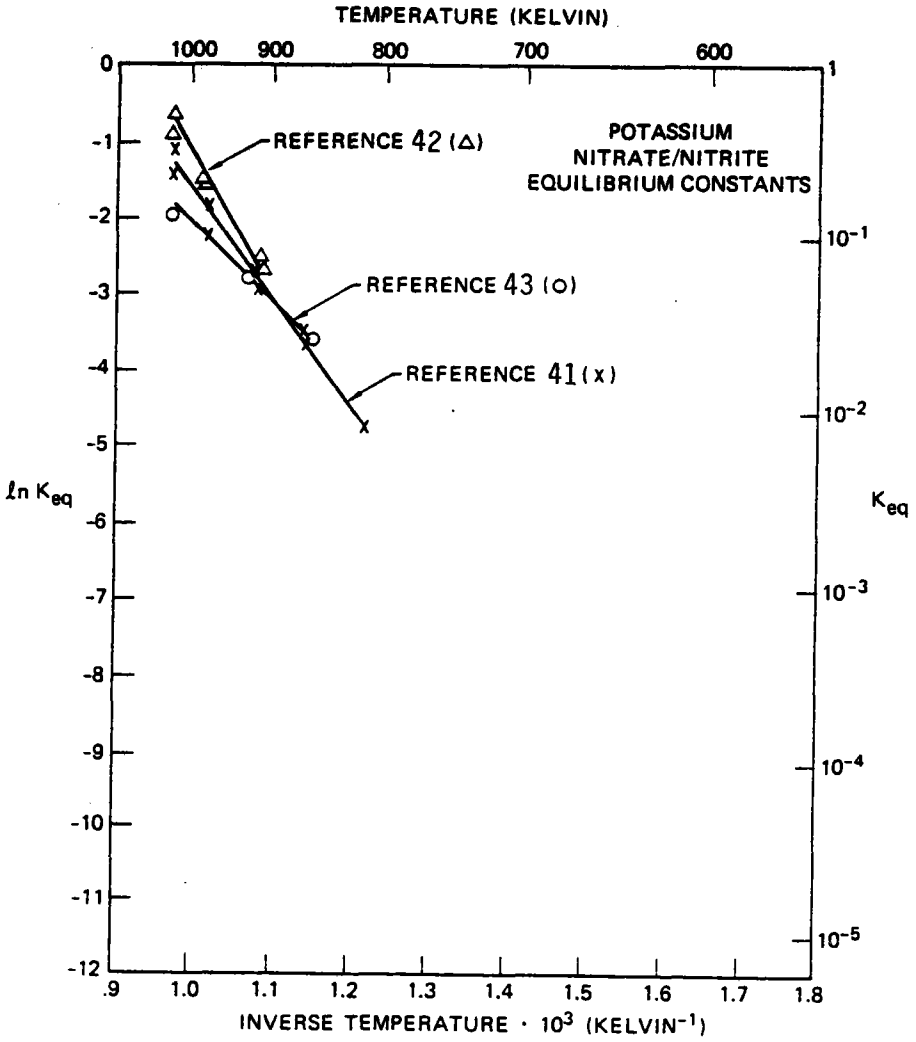

Figure 11. The Equilibrium Constants for KNO_3/NO_2

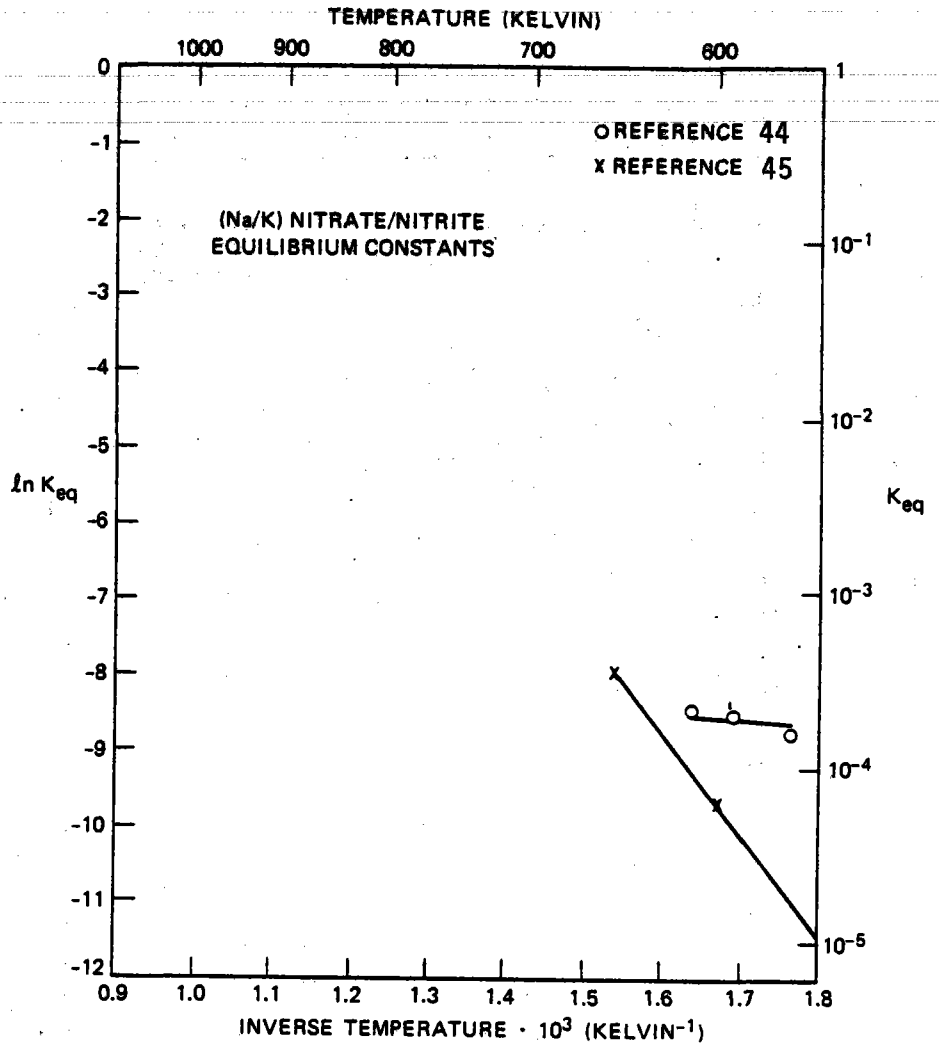

Figure 12. The Equilibrium Constants for (Na,K)NO_3/NO_2

To understand the significance of Reaction (1) in the temperatures of interest, 620-870 K, I calculated the amount of nitrite that would be present at equilibrium as follows. I chose values of K_{eq} from the nitrate chemistry review, Reference 31, to evaluate the extent of Reaction (1) as a function of temperature and P_{O_2}. For KNO_3/NO_2, the equilibrium constant I used was

$$\ln(K_{eq}) = (-27.5/RT)\ (\text{kcal mole}^{-1}) + 24.4/R\ (\text{cal mole}^{-1}\text{K}^{-1}). \qquad (19)$$

For $NaNO_3/NO_2$, Stern[31] gives several values for K_{eq} in the range 800-1000 K, which I fitted for convenience with the polynomial expression

$$\ln(K_{eq}) = -32.3 + .0493T - 1.80(10^{-5})T^2 \ . \qquad (20)$$

The activities of a_i of the salts are related to the O_2 partial pressure and equilibrium constant K_{eq} by Eq. (14). I separately investigated three partial pressures of oxygen: namely, 1. atm, 0.2 atm (as in air), and 0.0001 atm (similar to vacuum conditions). For each oxygen pressure I calculated the ratio X_{MNO_2}/X_{MNO_3} as a function of temperature from 500-1000 K. The results are illustrated in Figures 13 and 14 and tabulated in Appendix A. As the temperature is increased, the amount of nitrite rises. It is easily seen that at any temperature, increasing the partial pressure of oxygen suppresses nitrite formation in the melt, in accordance with the principle of le Chatlier. These figures also show that sodium salts have more NO_2^- when compared to potassium salts at a given temperature and pressure; however, the ratio of nitrite to nitrate in sodium differs from that calculated for potassium nitrate/nitrite mixtures by less than a factor of 2. One should also note that in air the molar ratio of nitrite to nitrate is less than 5% at 823 K

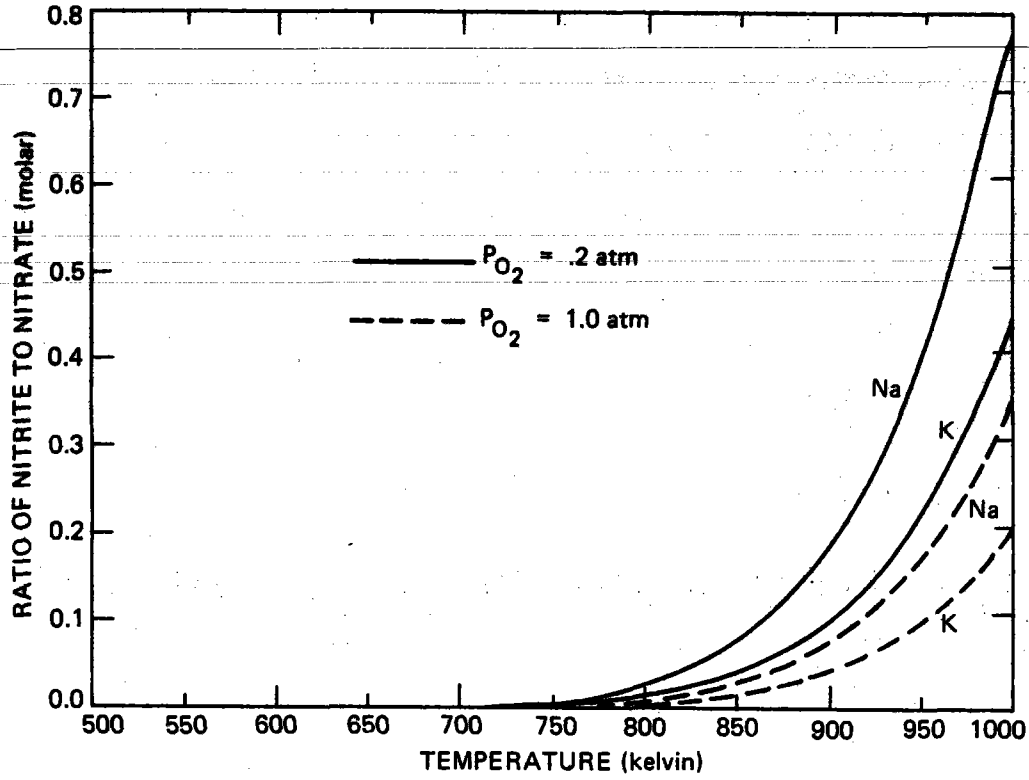

Figure 13. Equilibrium of Nitrates and Nitrites; P_{O_2} = 0.2, 1.0 atm

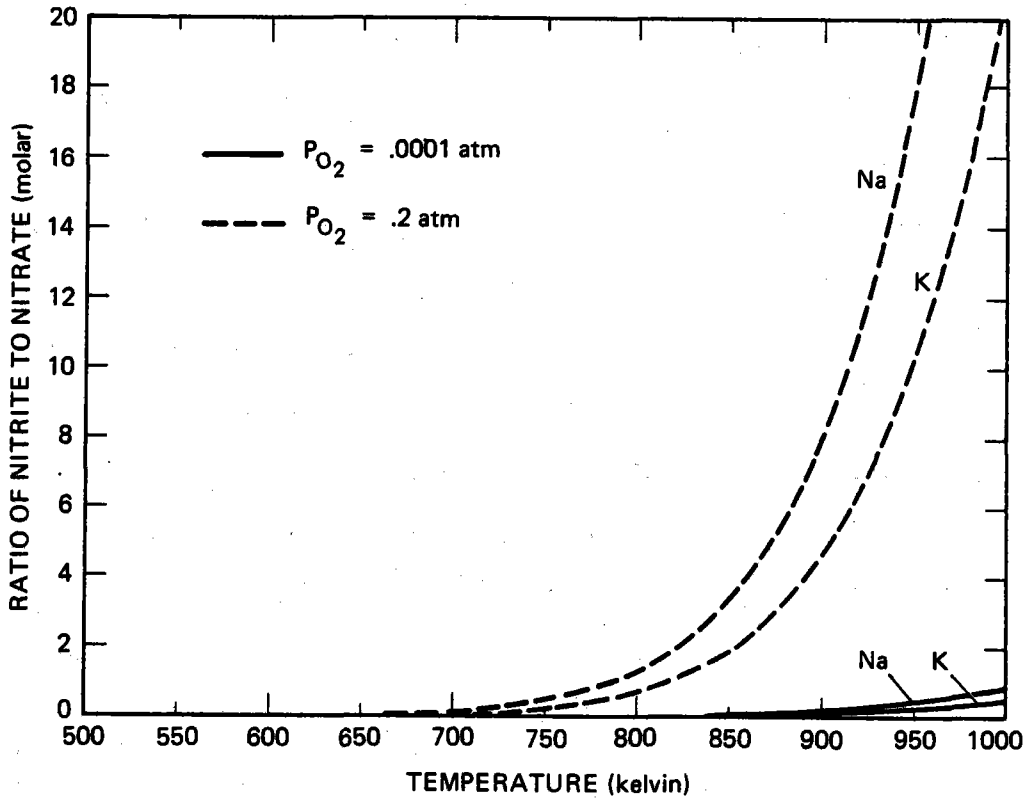

Figure 14. Equilibrium of Nitrates and Nitrites; P_{O_2} = 0.2, 0.0001 atm

for either Na or K, the upper temperature limit for solar power plants. However, at 0.0001 atm oxygen pressure, the ratio is 1-1.5, meaning that the amount of nitrite equals or exceeds the amount of nitrate. Because oxygen prevents nitrite formation, inert-gas blanketing to exclude oxygen is impractical although it has been suggested for commercial uses.[15]

Since very little thermodynamic information is available regarding the nitrates and the nitrites,[31] I used the equilibrium constant data (equations 19 and 20) to calculate the free energy of formation of the nitrite salts. In particular I used

$$\Delta G_{rxn} = G_{MNO_2} + \frac{1}{2} G_{O_2} - G_{MNO_3} \quad , \tag{21}$$

where I could insert known values of ΔG_{rxn} (calculated from the K_{eq} values and equation 17), G_{O_2} (from Reference 32), and extrapolated values of G_{MNO_3} (extrapolated from values given in Reference 32). The ΔG_{rxn} for $NaNO_3$ and KNO_3 is plotted in Figure 15. The equations I used for the free energies of formation of the nitrates, G_{MNO_3}, from 600-1000 K are

$$G_{NaNO_3} = -97.39 - (.0568)T \ \frac{kcal}{mole} \tag{22}$$

$$G_{KNO_3} = -104.6 - (.0596)T \ \frac{kcal}{mole} \tag{23}$$

From this information I calculated G_{MNO_2} for both $NaNO_2$ and KNO_2 from 600-1000 K. The values for G_{MNO_3} and G_{MNO_2} in 100 K intervals are listed in Table 3. These values of the free energy of formation of the nitrites and nitrates are used in the ensuing discussions of the decomposition reactions and reactions with water and carbon dioxide.

The temperature above which the products are favored in Reaction (1) or rather, where ΔG of Reaction (1) is equal to or less than zero,

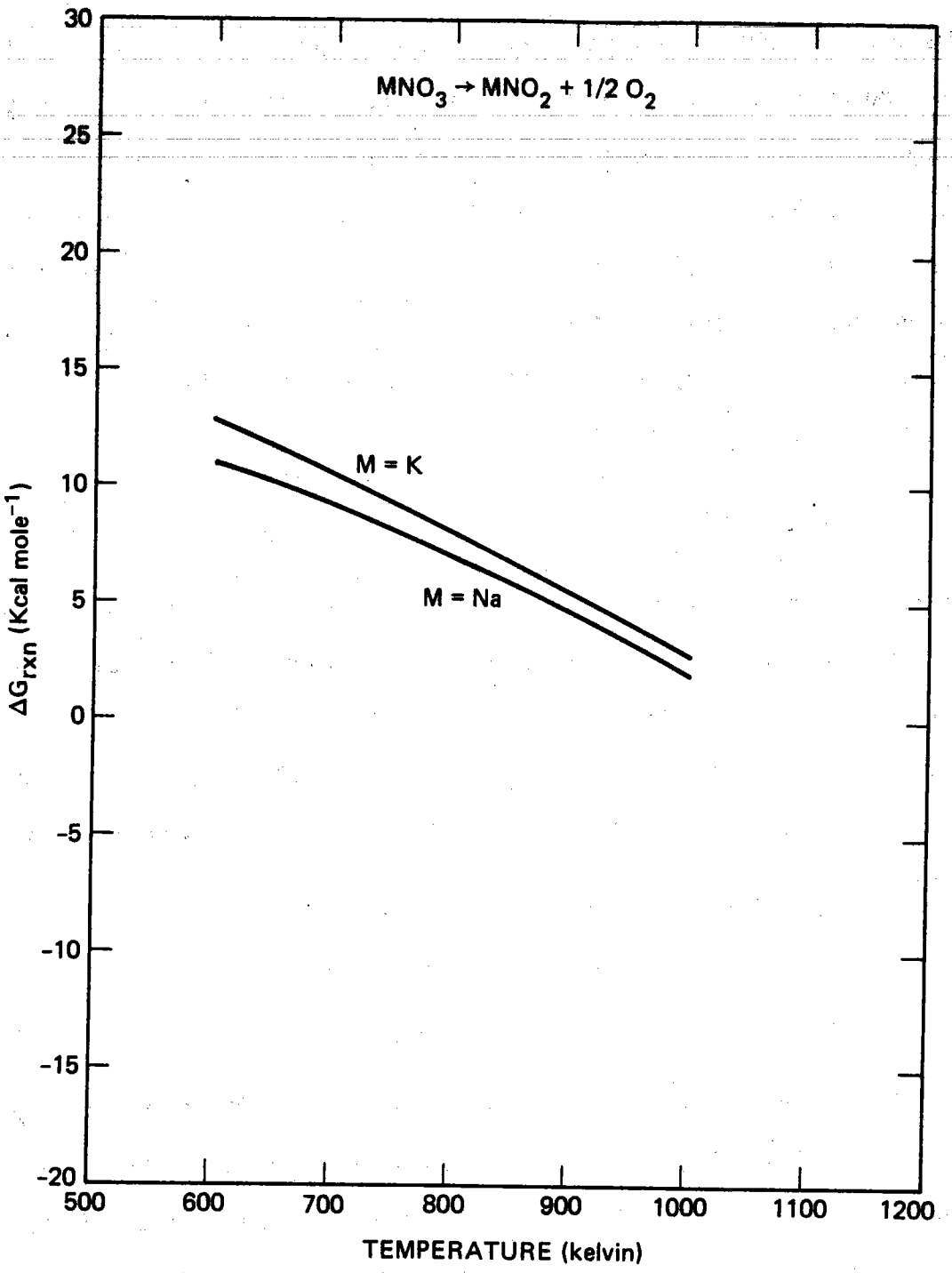

Figure 15. Free Energy for Nitrate/Nitrite Equilibria

TABLE 3

CALCULATED FREE ENERGIES OF FORMATION OF THE NITRATES AND NITRITES

Temperature (kelvin)	ΔG_{NaNO_3}		ΔG_{NaNO_2}		ΔG_{KNO_3}		ΔG_{KNO_2}	
	kcal/mole	kJ/mole	kcal/mole	kJ/mole	kcal/mole	kJ/mole	kcal/mole	kJ/mole
600	-131.49	-550.15	-104.47	-437.10	-140.42	-587.52	-112.21	-469.49
700	-137.22	-574.13	-109.97	-460.11	-146.36	-612.37	-117.83	-493.00
800	-142.83	-597.60	-115.31	-482.46	-152.28	-637.14	-123.38	-516.22
900	-148.51	-621.36	-120.18	-502.50	-158.24	-662.08	-128.92	-539.40
1000	-154.19	-645.13	-125.96	-527.02	-164.20	-687.01	-134.40	-562.33

can be calculated for Na and K nitrate/nitrite mixtures from (19) and (20) by setting $\ln(K_{eq})$ equal to 0. This temperature is 1086 K for sodium mixtures and 1127 K for potassium.

II B2. Nitrate and Nitrite Kinetics

The rate of formation of nitrite is important for characterizing the rate of decomposition of nitrates because the rate of formation may determine the rate at which other subsequent reactions occur. The kinetics of Reaction (1) for both sodium and potassium have been investigated by Freeman,[34,42] who determined forward and reverse reaction rates as well as activation energies. His experiments were performed under isothermal conditions in a constant pressure apparatus. Freeman assumed that first order kinetics were applicable to the reduction of nitrate. In other words, he assumed that the velocity

$$V_1 = k_1 X_{MNO_3} \tag{24}$$

was proportional to the amount of nitrate present in the sample. For the oxidation of nitrite he used the following expression for the velocity:

$$V_{-1} = k_{-1} P_{O_2}^{1/2} X_{MNO_2} \tag{25}$$

The terms k_1 and k_{-1} are called the rate constants for the reduction and oxidation reactions, respectively. Freeman[34] found that k_{-1} was proportional to the surface area of the salt exposed to the gas but that k_1 was not.

It is of greater practical interest to know the time needed for the nitrate and nitrite melts to equilibrate rather than the rate constants which are specific to the kinetic expression used. Molten

KNO_3 reached equilibrium with KNO_2 at 873 K in 300 minutes.[42] However, the reaction of KNO_2 with O_2 did not equilibrate in 300 minutes.[42] Freeman[34] observed that $NaNO_3$ reached equilibrium with $NaNO_2$ after 40 minutes at 973 K. At lower temperatures, the time required to reach equilibrium was much longer. Kust and Burke[44] kept their $(Na,K)NO_3$ samples at 568 K for 9-27 days to achieve equilibrium, although they stated that these durations were longer than necessary.

In summary, the equilibrium of nitrate and nitrite is a function both of the temperature and the oxygen pressure (fixed by the experimental configuration). The extent of formation of nitrite can be quite significant at high temperatures and low partial pressures of oxygen.

The next section discusses Reaction (2) and an analogous expression for decomposition of nitrite salts.

II C. Decomposition to Oxide

Sodium nitrate and potassium nitrate may decompose via several paths. As the temperature is elevated the nitrates of sodium and potassium may decompose to their corresponding nitrites.[31,34,42] The nitrites may decompose to oxide[46] according to

$$2MNO_2 \rightarrow M_2O + NO_2 + NO \qquad (26)$$

or

$$2MNO_2 \rightarrow M_2O + N_2 + 3/2\ O_2 \qquad (27)$$

Reaction (26) occurs above 603 K for $NaNO_2$ and above 683 K for KNO_2.[31] The NO_2 and NO produced in Reaction (26) can react with MNO_2 so that nitrate is formed as in the reactions[47,48]

$$2MNO_2 + 2NO \rightarrow 2MNO_3 + N_2 \qquad (28)$$

$$MNO_2 + NO_2 \rightarrow MNO_3 + NO \qquad (29)$$

The oxide produced in Reaction (26) may also react[47,49] with NO_2 to form nitrate and nitrite:

$$M_2O + 2NO_2 \rightarrow MNO_2 + MNO_3 \qquad (30)$$

At higher temperatures (above 873 for $NaNO_2$ and 1073 for KNO_2) the nitrites decompose completely to oxide according to Reaction (27). Bearing in mind that nitrate and nitrite can interconvert according to Reaction (1), it becomes very difficult to discriminate between oxide formation from nitrates or from nitrites.

At still higher temperatures, the nitrites being more unstable than the nitrates will appear only as an unstable intermediate product as the nitrates decompose according to reactions such as (2) or

$$2MNO_3 \rightarrow M_2O + 2NO_2 + (1/2)O_2 \ . \qquad (31)$$

Bond and Jacobs[50] studied $NaNO_3$ decomposition from 743 K to 1033 K and observed that the decomposition proceeds in two overlapping and consecutive steps which are: decomposition to $NaNO_2$ and decomposition of the nitrite to sodium oxide. They observed an inflection in their weight loss curves from their isothermal thermogravimetric experiments. The inflection corresponded to the weight loss at which complete transformation of nitrate to nitrite would have occurred. Their weight loss curves were empirically fit to

$$-\ln(1-\alpha)^{1/3} = kt \qquad (32)$$

where α is the fraction of the sample decomposed. Freeman performed dynamic (changing temperature) thermogravimetric experiments with $NaNO_3$[34] and KNO_3[42]. In his experiments, Freeman did not observe decomposition of $NaNO_3$ to oxide below 973 K and his weight losses arrested at a weight corresponding to complete oxide formation.

Freeman[34] analyzed the gaseous products of $NaNO_2$ which was decomposed in argon. Nitrogen was the first gas evolved and it appeared at 733 K. As decomposition proceeded and at higher temperature, O_2 was evolved in increasing proportions. Freeman did not observe N_xO_y gas species from $NaNO_2$ from 723 - 1053 K which contrasts with the observations of Pêneloux and Joliot[51] and Buchler and Stauffer[52] who identified N_2 and NO as the decomposition products of $NaNO_2$ from 578 - 827 K.

The gaseous products of decomposition of $NaNO_3$[34,53] and KNO_3[42] in argon have been studied. From 673 to 873 K, O_2 and N_2 were the products of decomposition.[53] In another study[34], oxygen was the principle decomposition product and N_2 was a minor species from $NaNO_3$ at 923 K. At 973 K and higher temperatures, O_2 and a larger proportion of N_2 were evolved.[34] Nitrogen dioxide was evolved from $NaNO_3$ above 973 K. Freeman[34] noted that NO may actually have been evolved from $NaNO_3$ and subsequently reacted with evolved O_2 to form NO_2, per Eq. (13). Bartos and Margrave[53] did observe NO above 973 K and minor amounts of NO_2 and N_2O above 1073 K.

Few studies have been made of the gaseous products of sodium or potassium nitrate decomposing in vacuum.[21,54] In one Knudsen cell-mass spectrometer experiment, decomposition of $NaNO_3$ in vacuum commenced at 570 K when NO and N_2O gas species were observed.[21] Above 670 K, N_2 and O_2 were also observed from $NaNO_3$.[21] Nitric oxide was also evolved from KNO_3 above 823 K in vacuum.[54]

The thermodynamic tendency for Reaction (2) and (27) to occur was evaluated by performing some thermodynamic calculations of the free energies of these reactions. I used the values for the nitrate and nitrite free energies of formation listed in Table 3 and the

thermodynamic data for N_2 and O_2 in Reference 32 to calculate the free energies of Reactions (2) and (27) (see Figures 16 and 17).

The free energy for Reaction (2) is positive over the temperature range 600-1000 K for both $NaNO_3$ and KNO_3. The free energy of decomposition for KNO_3 is about 25 kcal greater than for $NaNO_3$ from 600 - 1000 K because of free-energy differences between the nitrates. The free energies of decomposition for the nitrites are about 30 kcal less than for the nitrate salts. The free energy of decomposition for $NaNO_2$ is negative above 930 K. Thus, KNO_3 is thermodynamically most stable with respect to decomposition, and $NaNO_2$ is the least stable.

The activities of the condensed phases (a_{M_2O}, a_{MNO_3}, and a_{MNO_2}) and the partial pressures of the gases are related to the equilibrium constants. The equilibrium constants for Reactions (2) and (27) are

$$K_{eq} = \frac{a_{M_2O} \; P_{N_2} \; P_{O_2}^{5/2}}{a_{MNO_3}^2} \tag{33}$$

and

$$K_{eq} = \frac{a_{M_2O} \; P_{N_2} \; P_{O_2}^{3/2}}{a_{MNO_2}^2} \quad , \tag{34}$$

respectively. The gaseous atmosphere over the salt samples can have a considerable effect on the activities of the condensed phases and their ratios at a given temperature. As a hypothetical situation, I considered $NaNO_3$ at 600 K where ΔG = 46 kcal. The value of K_{eq} calculated from Eq (33) is 1.8×10^{-17}. If decomposition is occurring in air, P_{O_2} = 0.2 atm and P_{N_2} = 0.8 atm. The ratio $a_{Na_2O}/a_{NaNO_3}^2$ is therefore 1.2×10^{-15}, indicating that an insignificant amount of Na_2O is formed. At 900 K for $NaNO_3$ the ratio $a_{Na_2O}/a_{NaNO_3}^2$ is 0.08. If $NaNO_3$ is saturated with dissolved Na_2O, a_{Na_2O} is 1. Thus, the activity

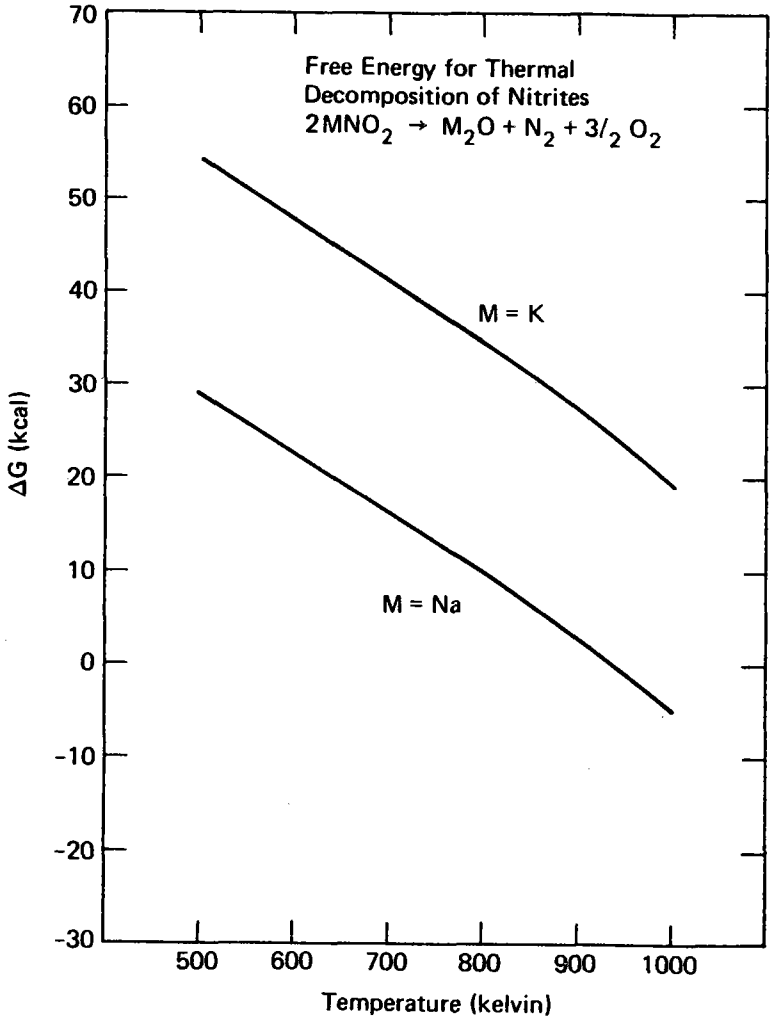

Figure 16. Free Energy for Thermal Decomposition of Nitrates

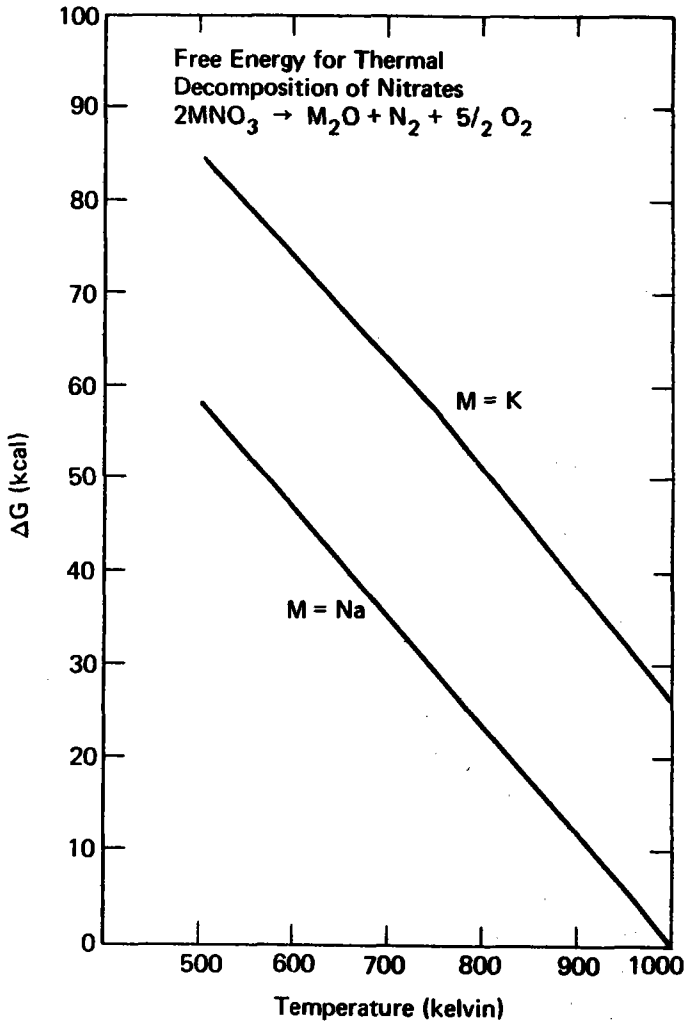

Figure 17. Free Energy for Thermal Decomposition of Nitrites

of $NaNO_3$ is 0.28, indicating that Na_2O is a significant constituent of the molten mixture of $NaNO_3$ and Na_2O. Estimates such as these, indicate the tendency of decomposition to occur.

If decomposition occurs in vacuum, the ratio of the activities of the condensed phases are changed by many orders of magnitude. A conservative estimate of the partial pressure of N_2 or O_2 in vacuum is 10^{-6} atm. The product $P_{N_2} \times P_{O_2}^{5/2}$ is 0.014 in air whereas it is 10^{-21} in vacuum. Therefore $a_{Na_2O}/a^2_{NaNO_3}$ (in eq. 33) will be $K_{eq}/0.014$ in air and $K_{eq}/10^{-21}$ in vacuum. Thus at lower temperatures, decomposition (the amount of oxide formed) will be more significant in vacuum than in air.

Decomposition reactions to oxide are complicated by N_xO_y species. As was calculated in Section IIA, the free energy difference between N_2 compared to O_2 and NO_2 is 15 kcal at 500 K. If one considers Reaction (31) (which is the sum of Reaction (2) and twice Reaction (8)), the free energy will be approximately 30 kcal greater than that of Reaction (2). The tendency to form K_2O by Reaction (31) can be evaluated from the equilibrium constant,

$$K_{eq} = \frac{a_{K_2O}\, P^2_{NO_2}\, P^{1/2}_{O_2}}{a^2_{KNO_3}} \qquad (35)$$

Stern[31] calculated this equilibrium constant to be 2×10^{-40} at 600 K and 2×10^{-18} at 1000 K. However, if P_{NO_2} is very low the ratio $a_{M_2O}/a^2_{MNO_3}$ may be much higher than it is in Equation (33) for MNO_3 at the same temperature. The N_XO_Y gas species provide additional decomposition paths that may contribute to decomposition of the nitrates. These paths are less favorable thermodynamically but may be important in the kinetics of decomposition.

II D. Reactions of the Melt Species

The decomposition of the nitrates and nitrites to oxide is clouded with the controversy concerning the basic species that exist in the melt.[55,56] In particular the chemistry of oxygen and oxygen ions in nitrates is obscure and conflicting.[57-60] Originally it was believed that oxide ions (M_2O or O^{-2}) were stable in the nitrate and nitrite melts. More recently electrochemical research has shown that only peroxide ions (M_2O_2 or O_2^{-2}) and superoxide ions (MO_2 or O^{-2}) are soluble and stable in the melt.[61-64]

Oxide ions that are introduced into nitrate melts undergo the following reaction in the absence of oxygen[56,61,64,65]:

$$O^{-2} + NO_3^- \rightarrow O_2^{-2} + NO_2^- \qquad (36)$$

Yurinskii[56] reported that amount of peroxide present at equilibrium in $NaNO_3$, KNO_3 or $(Na/K)NO_3$ (from 653 - 673 K) was 10 times greater than the amount of oxide. The peroxide is also reactive in nitrate melts and forms superoxide[61,64,65] via the reaction

$$O_2^{-2} + 2NO_3^- \rightarrow 2O_2^- + 2NO_2^- \qquad (37)$$

In these reactions nitrite, peroxide, and superoxide are formed from oxide ions in nitrates and nitrites.

If oxygen is present, oxygen and oxide ion may react[61] as

$$O^{-2} + (1/2)\ O_2 \rightarrow O_2^{-2} \qquad (38)$$

to form peroxide. The peroxide product may also react with oxygen to form superoxide by[65,66]

$$O_2^{-2} + O_2 \rightarrow 2O_2^- \qquad (39)$$

Thus, because of Reactions (36) - (40), oxide ions resulting from nitrate or nitrite decomposition will not remain in the molten salt under any conditions.

In contrast to these electrochemical observations, the literature on nitrate decomposition considers nitrate to decompose primarily to oxides.[31,34,42,50] Freeman's[34] evidence for decomposition to oxide was this: his weight loss experiment with $NaNO_3$ and $NaNO_2$ arrested at the weight corresponding to Na_2O. Peroxide[50,67] and superoxide[34] have been considered only as intermediate ions formed as the nitrates and nitrites decompose.

To enhance our understanding of the equilibrium of various species in molten nitrates. I calculated the free energies of Reactions (36) - (40). Thermodynamic data were taken from Reference 32. At high temperatures (to 1000 K) where values of the free energy of formation of several oxygen ion species were not available, I extrapolated the low temperature data. The free energies for Reactions (36) - (39) are shown in Figures 18 - 21. The values that used the extrapolated oxygen ion data are shown with dashed lines.

The free energy of Reaction (36) is negative for potassium species as seen in Figure 18. From 600 - 1000 K, the free energy decreases from -6 to -9 kcal/mole. Thus, the thermodynamic tendency is for K_2O to react to form K_2O_2 in KNO_3. The free energy for sodium species in Reaction (36) is less negative. The stability of sodium oxide in sodium nitrate is greater than potassium oxide in potassium nitrate[62] as has been experimentally observed.[56,62]

The calculated free energy of Reaction (37) is graphed in Figure 19. Over the entire temperature range, the free energies for both

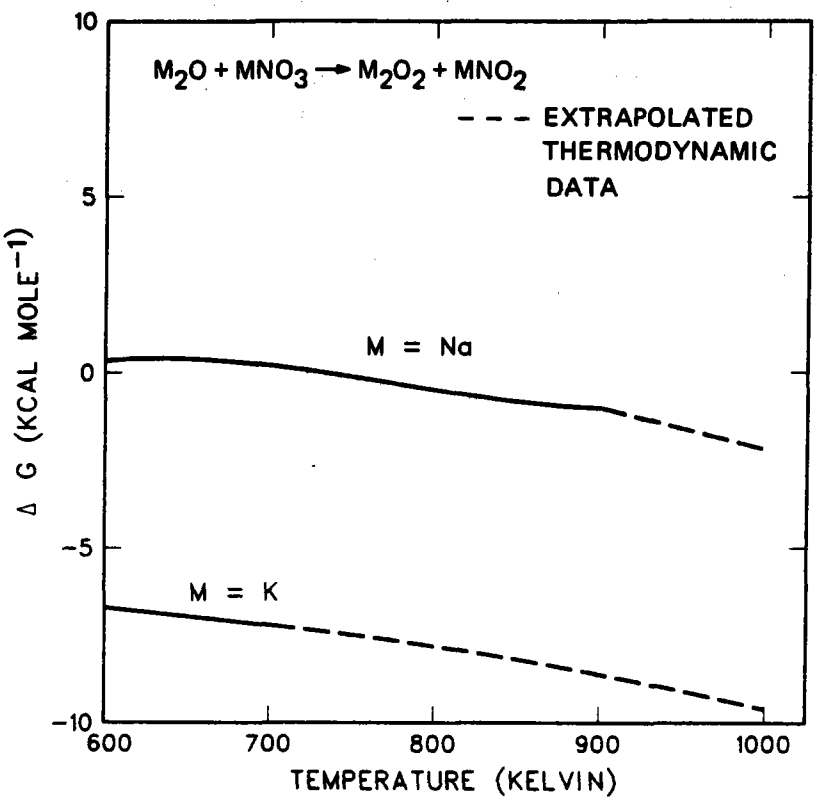

Figure 18. Free Energy of Reaction of Alkali Oxides with Nitrates

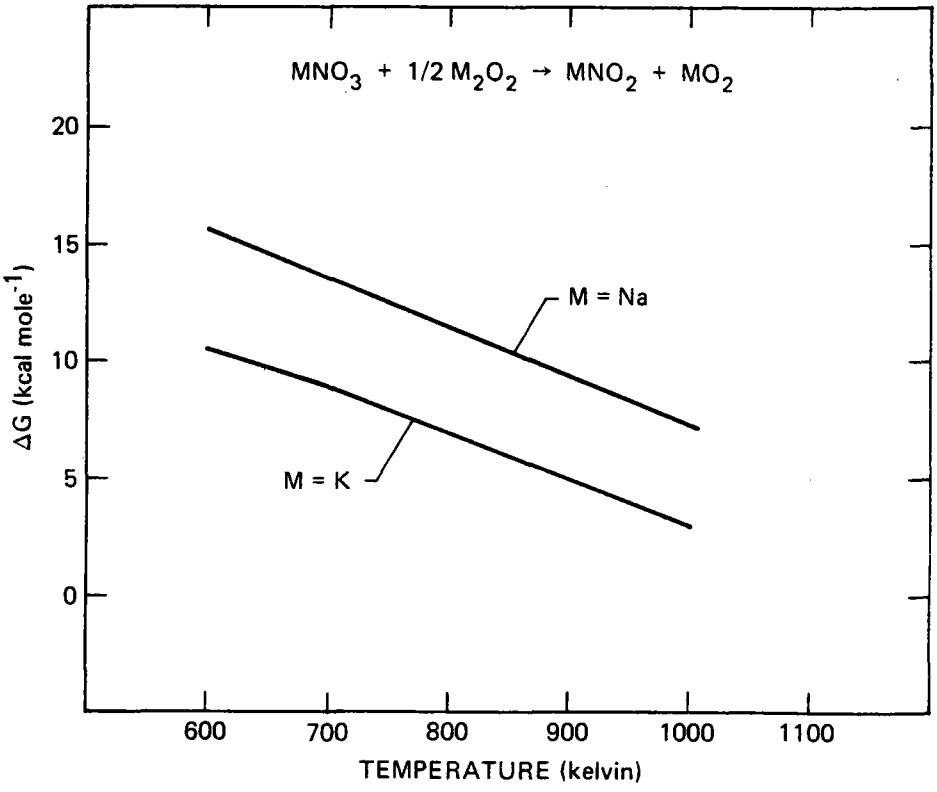

Figure 19. Free Energy of Reaction of Peroxides with Nitrates

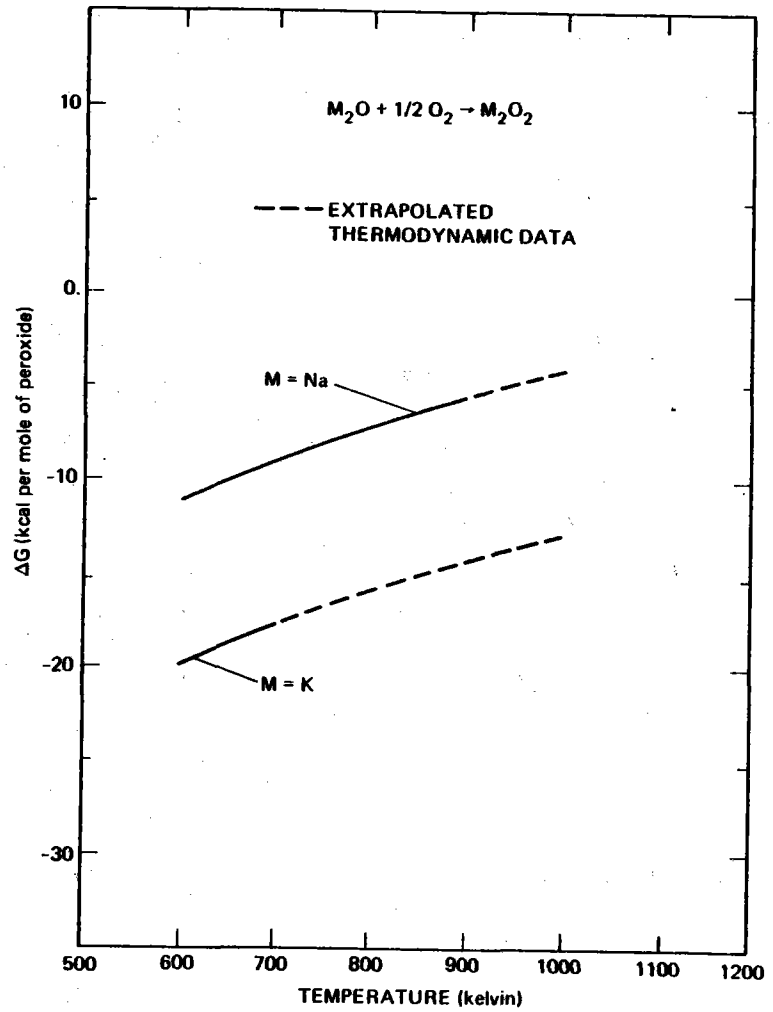

Figure 20. Free Energy of Reaction of Alkali Oxides with Oxygen

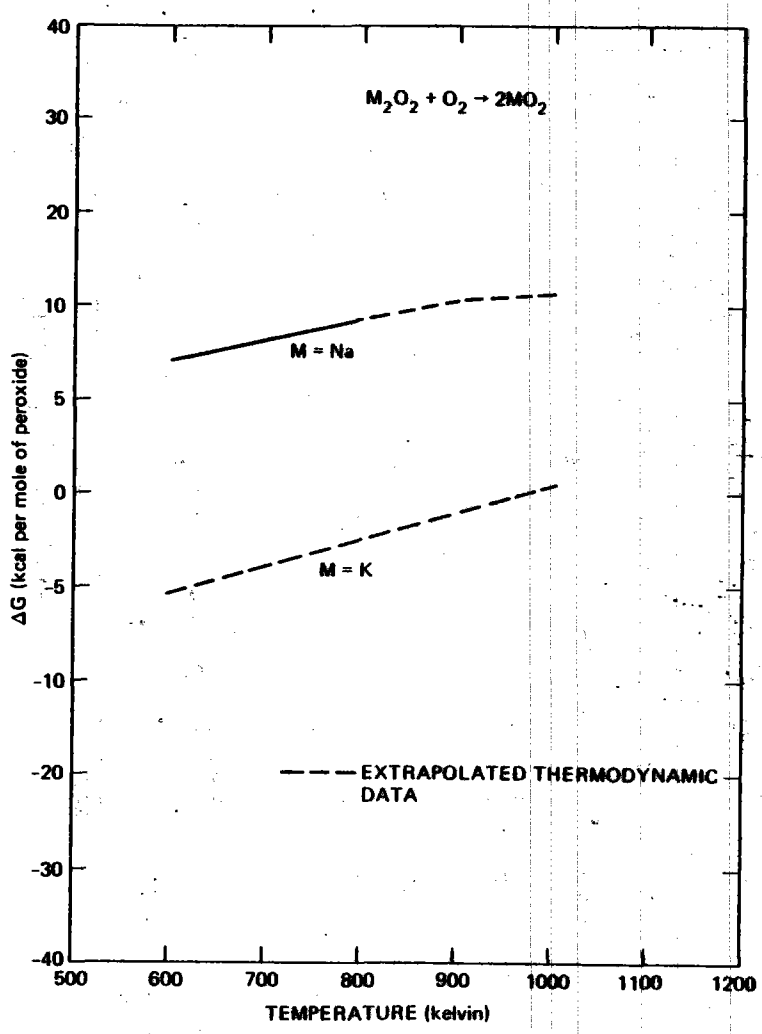

Figure 21. Free Energy of Reaction of Peroxides with Oxygen

sodium and potassium versions of Reaction (37) are positive. Because the free energies are positive, only a small fraction of peroxide will react with the nitrates to form nitrite and superoxide. However, more superoxide and nitrite will be formed in KNO_3 than in $NaNO_3$ via Reaction (37). The exact amounts are dependent on the activities of each species in nitrates.

If sodium or potassium oxide is allowed to react with oxygen (Reaction (38)), peroxides will be formed because the free energies are negative. See Figure 20. The driving force for peroxide formation is smaller (by approximately 10 kcal) for Na_2O than for K_2O to react with oxygen. As the temperature is increased, however, the driving force decreases (greater oxide stability in oxygen) but is never zero for either Na or K species.

The last reaction of the melt species to consider is (39), where peroxide reacts with oxygen to form superoxide. The free energy, shown in Figure 21, is negative for K_2O_2 and positive for Na_2O_2; therefore the stability of NaO_2 in $NaNO_3$ less than the stability of KO_2 in KNO_3. The driving force to form NaO_2 or KO_2 is diminished as the temperature is increased.

In summary, the oxygen ion equilibria are numerous and complex. Oxide, peroxide, and superoxide species may coexist in sodium and potassium nitrate. Superoxide ions are more stable in KNO_3 than in $NaNO_3$. Oxide ions are more stable in $NaNO_3$ than in KNO_3 although they are a minor species in either nitrate.

II E. Reaction with CO_2

Reactions of the nitrates and nitrites with CO_2 in air has been observed in commerical uses of these salts.[11,15] The formation of

carbonates has three deleterious effects for nitrates as a heat transfer fluid. One effect is that carbonates dissolved in nitrates elevate the melting point over pure nitrates.[15,24] Secondly, carbonates have very low solubility in sodium and potassium nitrates[68] and may precipitate out of the molten salt in cooler portions of a system. The solubility is reported to be less than 0.3% at 673 K in HTS.[15] Precipitation occurring in critical areas such as small diameter pipes in a heat exchanger may cause clogging and system failure. Thirdly, carbonate formation in the nitrates will increase the fluid's viscosity, which requires more energy to pump the fluid.

Carbonates may form by two processes: direct reaction with the salt as shown in Eq. (3), or by reaction with the basic (oxygen ion species) products of decomposition from a reaction such as (2). It is known, for example, that CO_2 is readily absorbed by alkali oxides to form carbonate.[15] To examine the thermodynamic tendency for direct reaction of CO_2 and nitrates to occur (and analogous reactions for the nitrites) I calculated the free energies of carbonate formation. I used the free energies of formation from Reference 27 and those calculated for the nitrates and nitrites in Section IIB. The free energies are plotted in Figures 22 and 23 respectively.

The free energy of formation of Na_2CO_3 according to Reaction (2) or the reaction

$$2NaNO_2 + CO_2 \rightarrow Na_2CO_3 + N_2 + (3/2)\ O_2 \qquad (40)$$

is always negative. In other words if CO_2 is present, there is a thermodynamic driving force to form Na_2CO_3 from $NaNO_3$ or $NaNO_2$. With regard to K_2CO_3 formation, the driving forces are not as large as for

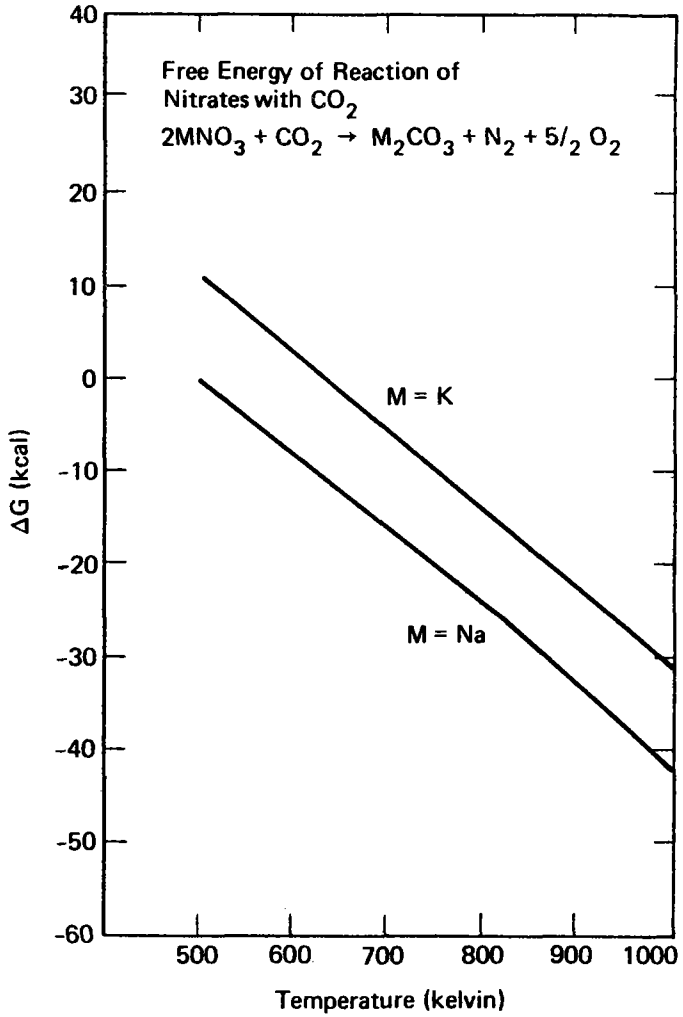

Figure 22. Free Energy of Reaction of Nitrates with CO_2

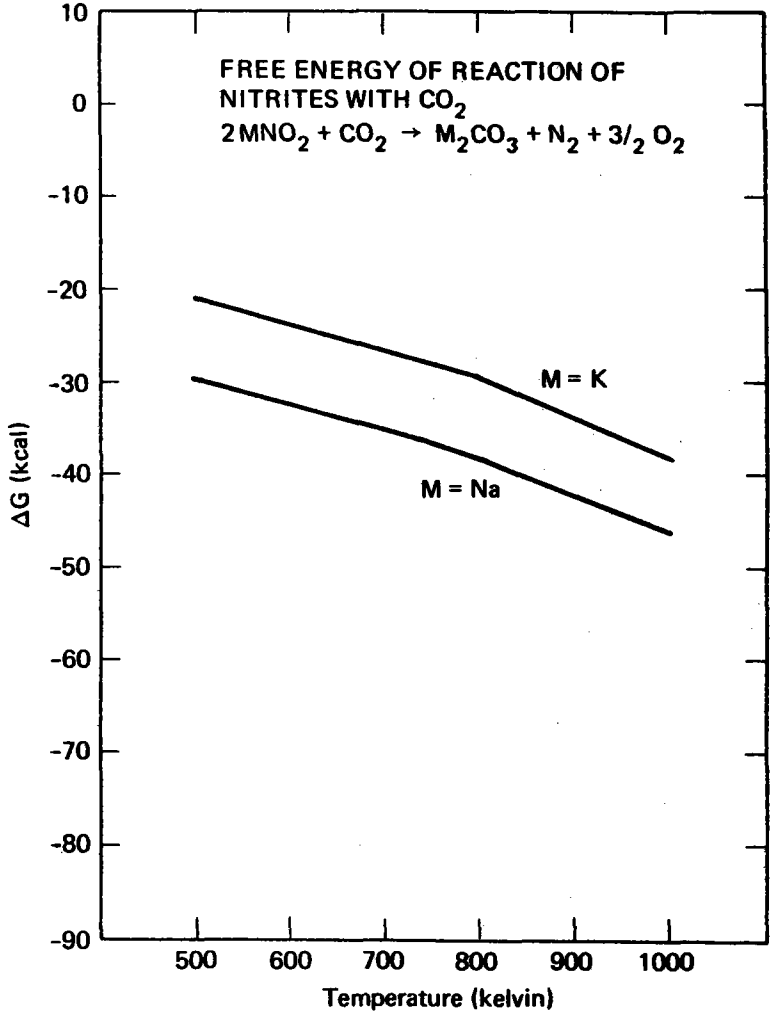

Figure 23. Free Energy of Reaction of Nitrites with CO_2

Na_2CO_3 formation. The free energy for potassium nitrite in a reaction like (40) is negative from 600-1000 K. The free energy of reaction to form K_2CO_3 from a direct reaction of CO_2 with KNO_3 is negative above 630 K. Therefore, at temperatures greater than 630 K, carbonate formation is thermodynamically favored. Sodium or potassium carbonate may form by direct reaction of CO_2 with either nitrates or nitrites or by reaction with Na_2O or K_2O.

II F. Hydrolysis

The reaction of the nitrates and nitrites with water to form hydroxide-salt mixtures has (as for the carbonates) been observed in practical applications.[11,15] Water alters the reactions observed in electrochemical experiments with nitrates.[65,69-71] Water vapor influences the decomposition and the corrosive nature of HTS in stainless steel.[72] Like the carbonates, hydroxides dissolved in molten nitrates may elevate the melting point[24] and may form amorphous precipitates.[15] Furthermore, hydroxides are particularly corrosive to conventional containment materials such as plain carbon and low-alloy steels.

Using the free energies calculated in IIB and the data in Reference 32, I calculated the free energies for the reactions (4) and

$$2NaNO_2 + H_2O \rightarrow 2NaOH + N_2 + 3/2\ O_2 \qquad (41)$$

as a function of temperature. The results are shown in Figures 24 and 25 for the nitrates and nitrites, respectively. The free energies of hydroxide formation from nitrates are negative above 790 K for $NaNO_3$ and above 910 K for KNO_3. The nitrites are thermodynamically more susceptible to hydrolysis than the nitrates. The free energy of

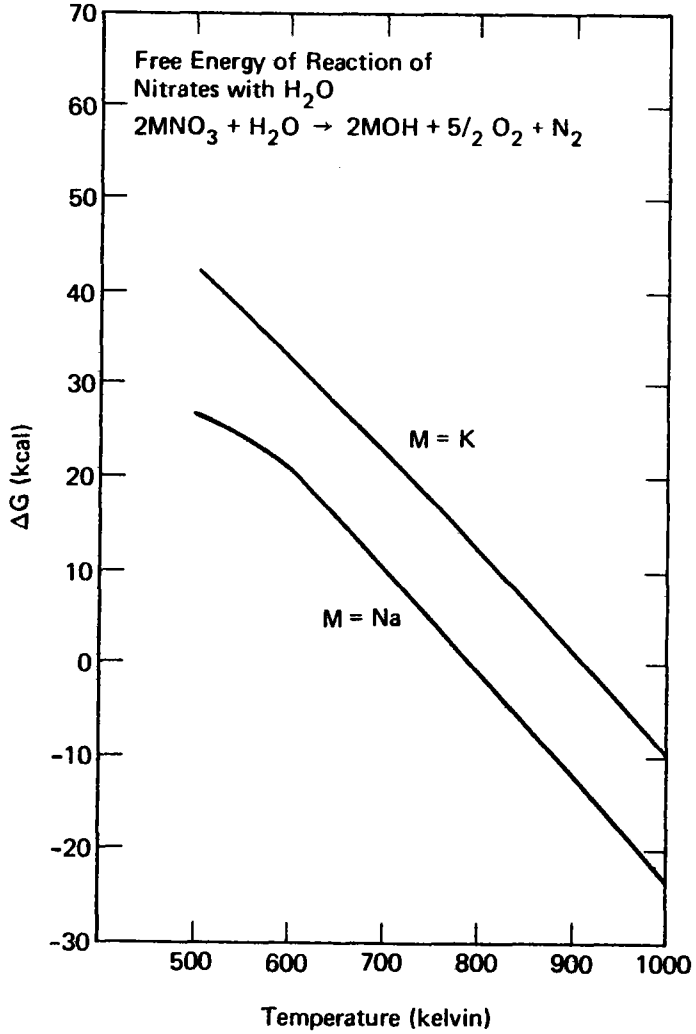

Figure 24. Free Energy of Reaction of Nitrates with H_2O

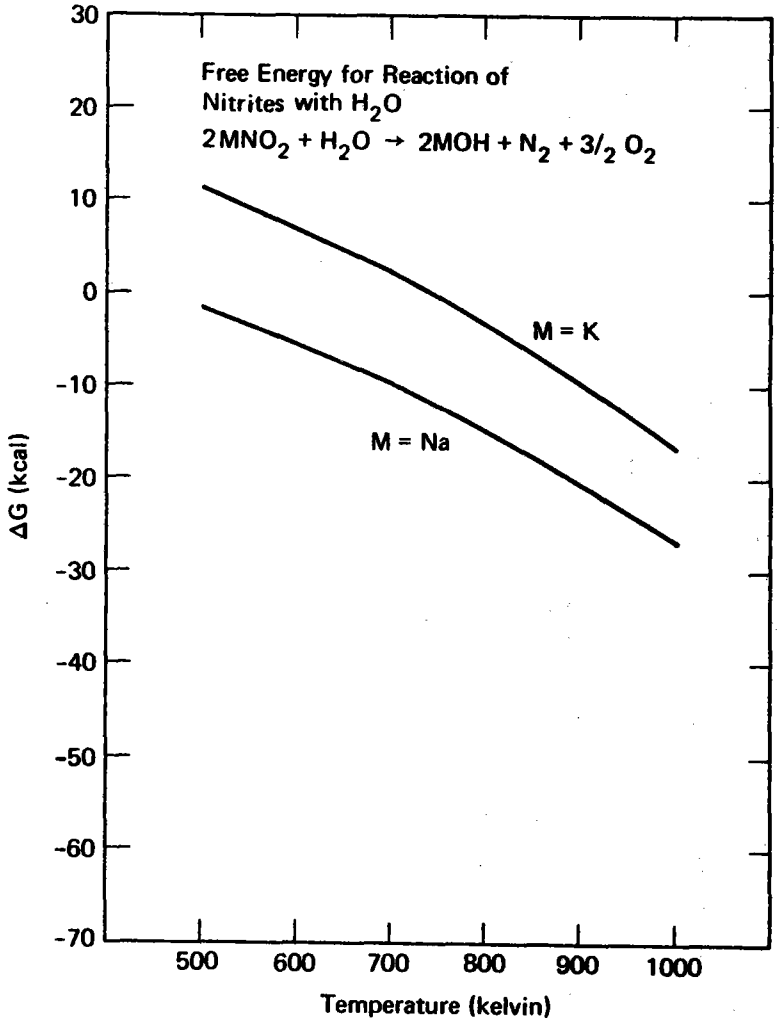

Figure 25. Free Energy of Reaction of Nitrites with H_2O

Reaction (42) is negative above 500 K for $NaNO_2$ and above 750 K for KNO_2. Although the driving forces for nitrates or nitrites to react with H_2O are not as large as those for the corresponding reactions with CO_2, hydroxide formation is thermodynamically favored. Depending on the experimental conditions and the activities of the species, hydroxide formation may occur above 500 K.

II G. Vaporization of Nitrates and Nitrites

The congruent vaporization of the nitrates and nitrites of sodium and potassium was first recognized by Hardy and Field,[54] who distilled $NaNO_2$, $NaNO_3$, and KNO_3 at 623 K and KNO_2 at 743 K. They[54] and others[73,74] observed that the nitrates and nitrites may vaporize without substantial decomposition as low as 50 K above the melting point of the salt.[73,74] For example, only a minor amount of nitrite (0.1%) was observed by Hardy and Field[54] in their potassium nitrate condensate.

The work of Hardy and Field was followed by that of Buchler and Stauffer[52], who performed mass spectrometric studies of $NaNO_3$ (750 K) and $NaNO_2$ (690 K) vapors (whose spectra are listed in Table 4). During Buchler and Stauffer's experiments, O_2, N_2, and NO evolved in addition to monomers and dimers of sodium nitrate and nitrite.

The thermodynamics of the vaporization of $NaNO_3$ and KNO_3 were investigated more recently.[75,76] The mass spectra observed in these vaporization studies are listed in Table 4. Over the temperature ranges studied (647-709 K for $NaNO_3$, 649-688 K for KNO_3) monomers and dimers were observed for both salts.[52,75,76] Researchers using matrix isolation techniques[73] established that just above the salts' melting points, nitrate monomers are more abundant. An expression for the vapor pressure

Table 4

Mass Spectra and Relative Intensities of Na and K Nitrates and Nitrites

Ion Species[d]	$NaNO_3$[a] (700K)	$NaNO_3$[b] (750 K)	KNO_3[c] (680 K)	$NaNO_2$[b] (690 K)
M^+	100	4.6	100	5.2
MO^+	4.07	--	3.48	--
MNO^+	0.07	--	--	--
MNO_2^+	1.84	0.06	0.45	0.1
MNO_3^+	8.24	0.18	0.40	--
M_2O^+	0.17	--	0.57	--
$M_2NO_2^+$	0.10	0.06	0.10	0.3
$M_2NO_3^+$	3.65	0.11	4.24	--
O_2^+	--	300	--	--
NO^+	--	15	--	~50
N_2^+	--	--	--	~50
NO_2^+	--	--	--	--
M_2^+	--	0.6	0.03	--

a Ref 76

b Ref 52

c Ref 75

d M = Na or K

of each species was determined as listed in Table 5. The form of the equations for the vapor pressure, P, of the monomer or dimer is

$$\ln(K) = \ln(P) = -\Delta H_v^\circ/RT + \Delta S_v^\circ/R \qquad (42)$$

where R is the universal gas constant and ΔH_v and ΔS_v are the standard enthalpy and entropy of vaporization, respectively, of the species whose vapor pressure was measured.

Table 5

Vapor Pressure Expressions for KNO_3 and $NaNO_3$ Species

Vapor Species	ΔH_v (kcal/mole^{-1})	ΔH_v (kJ mole^{-1})	ΔS_v (cal/mole)	ΔS_v (J-mole^{-1})	Reference
$NaNO_3$	41.03 ± 0.75	172.	49.19	206.	76
$(NaNO_3)_2$	49.40 ± 1.2	207.	56.97	238.	76
KNO_3	41.77 ± 0.32	175.	50.34	211.	75
$(KNO_3)_2$	48.03 ± 0.92	201.	52.81	221.	75

To calculate the vapor pressures of the nitrates for temperatures of 600-1000 K, I used Equation (42) and the values in Table 5. The results are tabulated in Table 6 and illustrated in Figures 26 and 27. The vapor consists mostly of nitrate monomers below 800 K. The vapor pressures of $NaNO_3$ and KNO_3 monomers are similar over the temperature range 600-1000 K. The vapor pressures of the dimers, particularly $(KNO_3)_2$, are lower than those of the monomers. Above 700 K the total vapor pressures are greater than 10^{-3} Torr.

To estimate the maximum rate of vaporization of the nitrates, I used the Hertz-Langmuir equation[77]

Table 6

Vapor Pressures of the Nitrates (Torr)[a]

	$NaNO_3$			KNO_3		
Temperature (K)	Monomer	Dimer	Total	Monomer	Dimer	Total
600	$6.41(10^{-5})$	$2.90(10^{-6})$	$6.70(10^{-5})$	$6.12(10^{-5})$	$1.11(10^{-10})$	$6.23(10^{-5})$
700	$8.74(10^{-3})$	$1.08(10^{-3})$	$9.82(10^{-3})$	$9.12(10^{-3})$	$3.51(10^{-4})$	$9.47(10^{-3})$
800	0.349	0.091	0.44	0.389	0.0263	0.4153
900	6.13	2.87	9.0	7.21	0.755	7.965
1000	60.81	45.39	106.2	74.47	11.06	85.53

[a]Values calculated using thermodynamic data from Ref. 75 and 76.

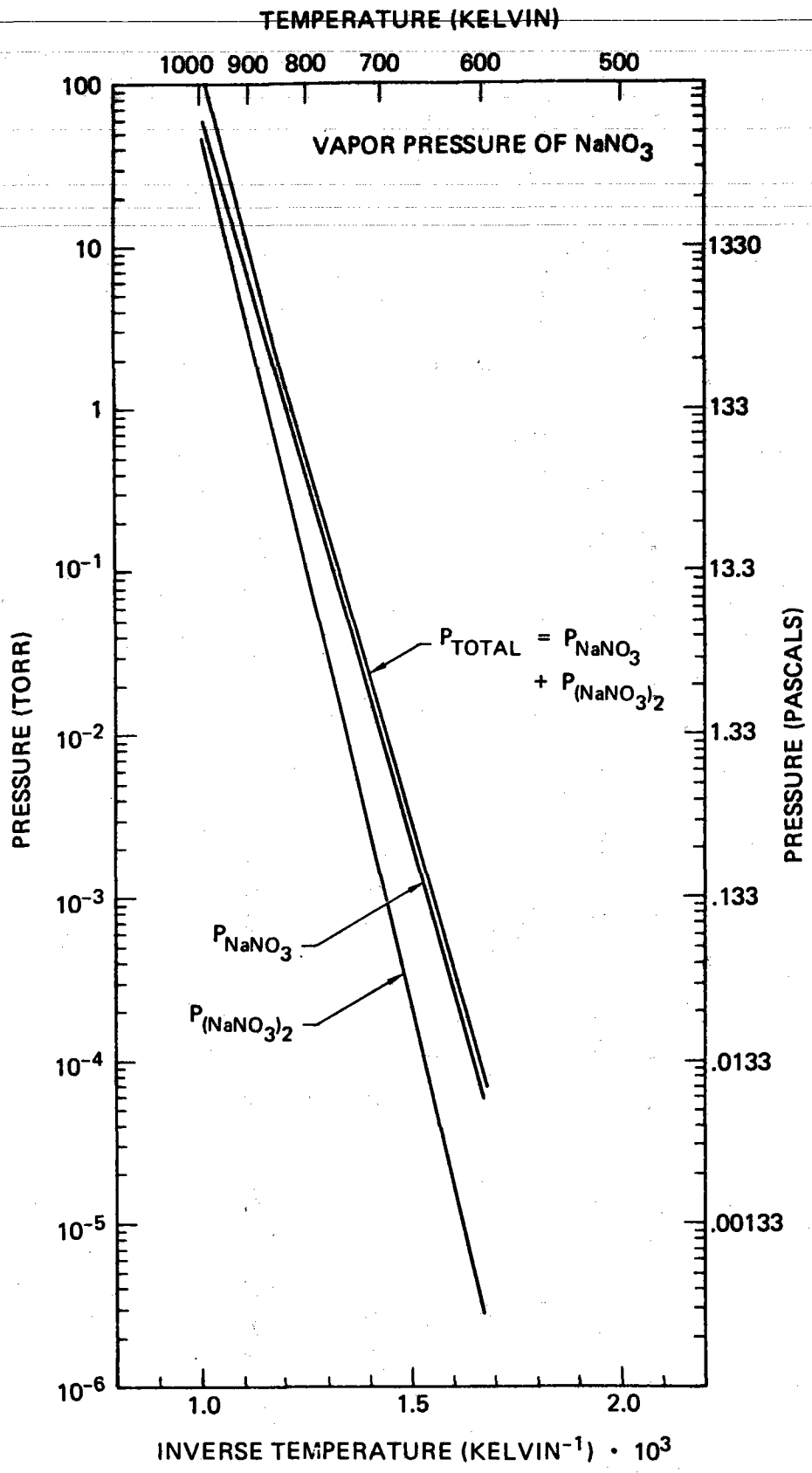

Figure 26. Vapor Pressure of $NaNO_3$

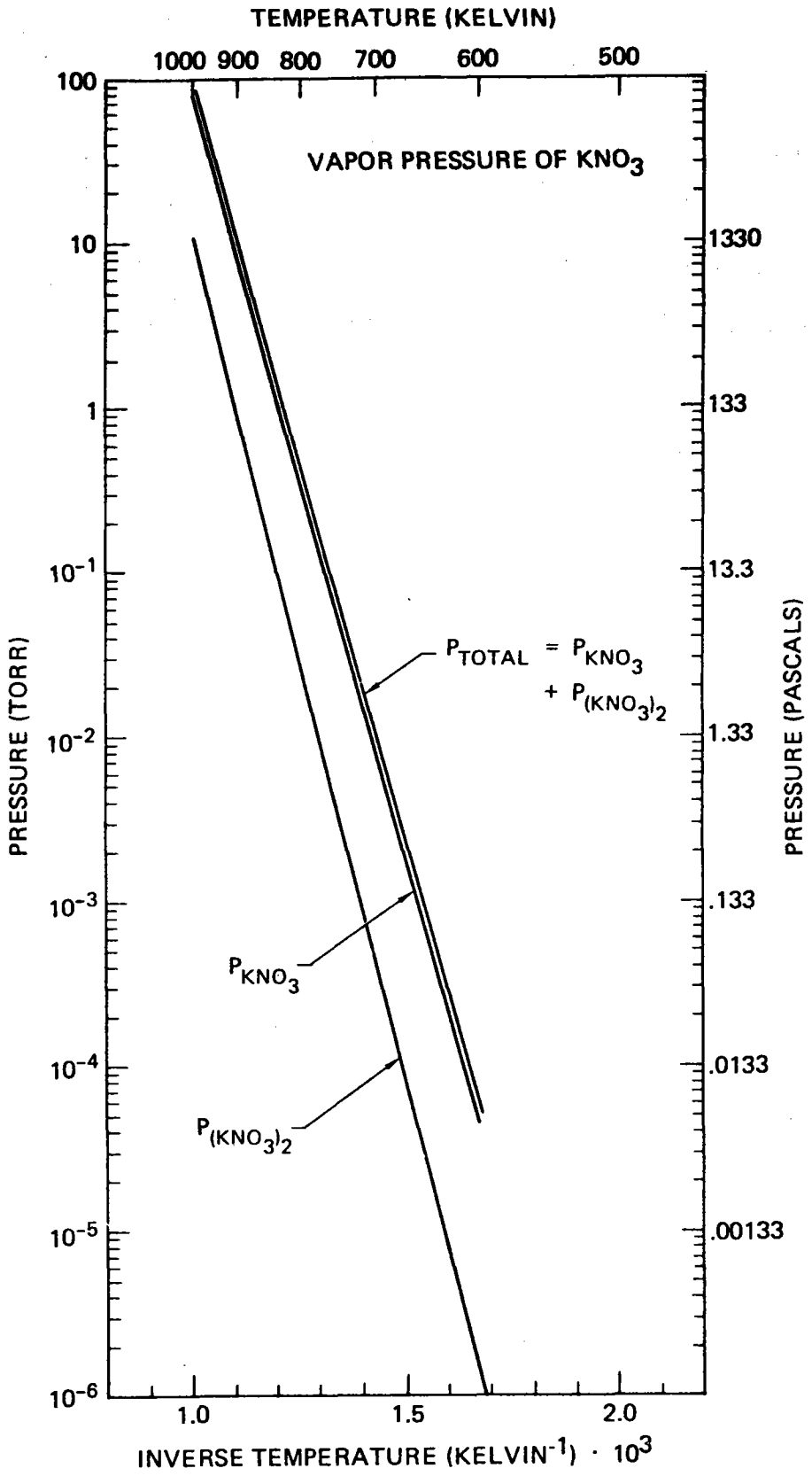

Figure 27. Vapor Pressure of KNO_3

$$J_{Max} = P/(2\pi MRT)^{1/2} \quad , \tag{43}$$

where J_{Max} is the maximum flux (in moles per unit area per unit time), P is the equilibrium vapor pressure, and M is the molecular weight of the vapor molecule. Combining this expression with (43) leads to a relationship between the thermodynamic quantities for vaporization and the maximum flux:

$$J_{Max} = [\exp(\frac{\Delta S_v}{R} - \frac{\Delta H_v}{RT})]/(2\pi MRT)^{1/2} \tag{44}$$

I calculated the maximum fluxes for $NaNO_3$ and KNO_3, and the results are shown in Table 7 and Figures 28 and 29. At 800 K the fluxes are greater than 1 g cm^{-2} min^{-1}. Of course, these are the unimpeded rates (i.e., vacuum), which will be considerably decreased by gaseous collisions if the vaporization takes place in 1 atm pressure. Nevertheless, these rates may be useful for comparison with fluxes measured in thermogravimetric experiments, particularly those conducted in vacuum (described in subsequent sections).

Knudsen recognized that some substances vaporize at less than the equilibrium rate and introduced a vaporization coefficient α into the flux equation:[77,78]

$$J = \alpha J_{Max} \quad . \tag{45}$$

The vaporization coefficients for $NaNO_3$[76] and KNO_3[75] are approximately 1. and 0.7, respectively.

Table 7

Maximum Vaporization Rates for $NaNO_3$ and KNO_3[a]
($g\ cm^{-2}\ min^{-1}$)

	$NaNO_3$			KNO_3		
Temperature (K)	Monomer	Dimer	Total	Monomer	Dimer	Total
600	$7.78(10^{-4})$	$6.52(10^{-5})$	$8.33(10^{-4})$	$8.84(10^{-4})$	$3.21(10^{-5})$	$8.72(10^{-4})$
700	$9.83(10^{-2})$	$2.43(10^{-2})$	0.123	0.122	$9.39(10^{-3})$	0.131
800	3.67	1.91	5.58	4.87	0.658	5.53
900	60.79	56.92	117.71	85.02	17.81	102.85
1000	572.	854.	1426.	833.	247.51	1080.

[a]Values calculated using thermodynamic data from Ref. 75 and 76.

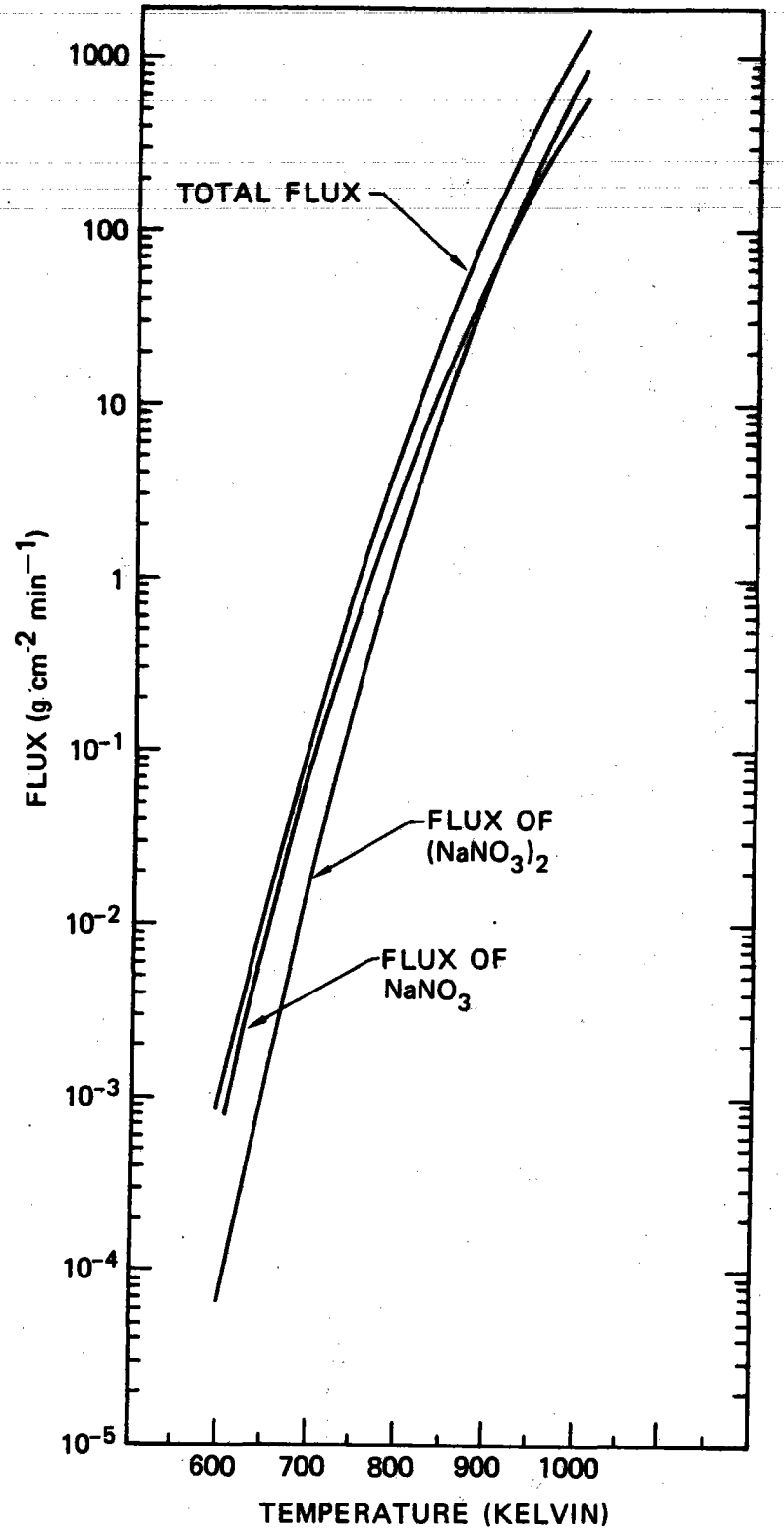

Figure 28. Maximum Flux of Vapor Species from $NaNO_3$

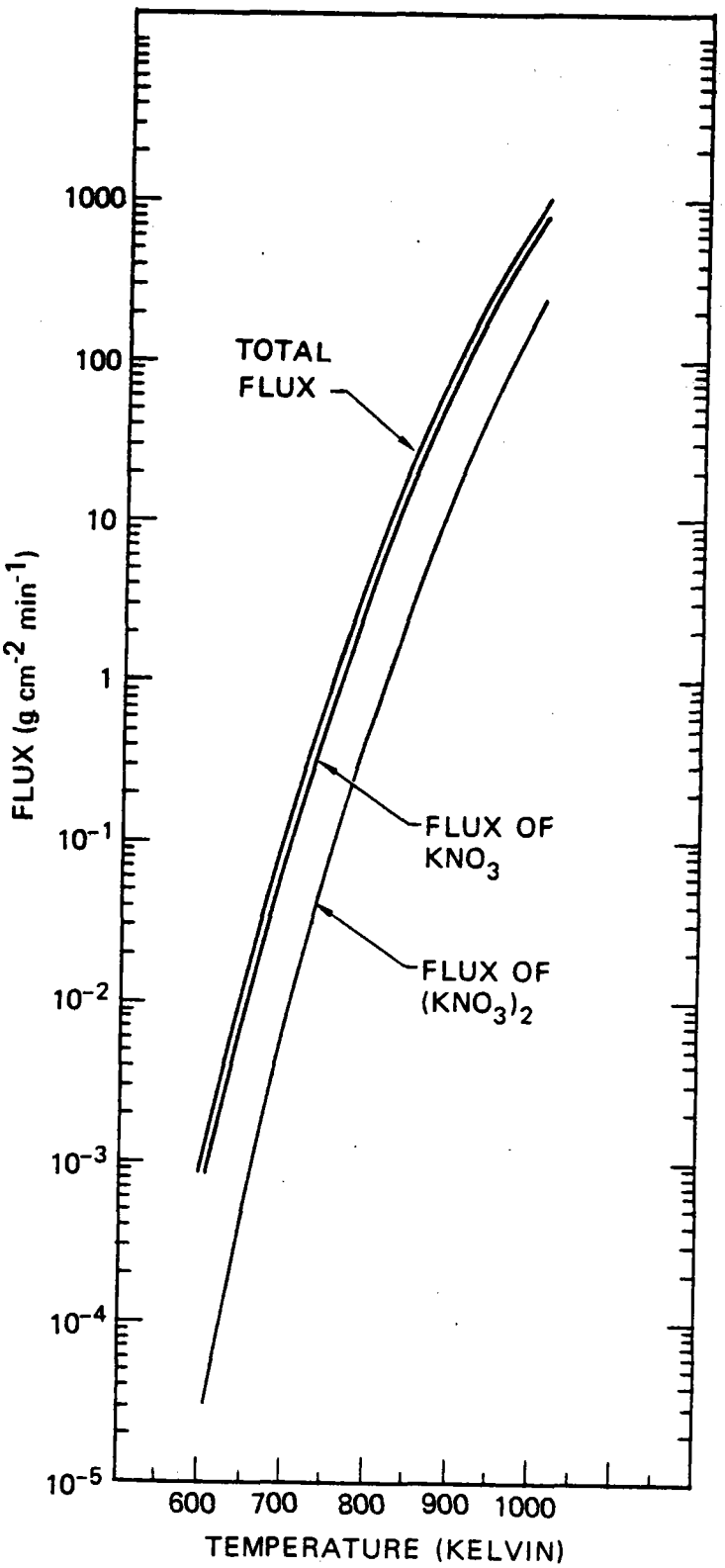

Figure 29. Maximum Flux of Vapor Species from KNO_3

III. EXPERIMENTAL TECHNIQUES AND ANALYSIS

There are many techniques that can be used to study the decomposition reactions that molten sodium and potassium nitrate undergo. Electrochemistry[61], evolved gas analysis,[53] spectroscopic analysis of the gases[53,62,73,74] or salts,[79-81] electrical conductivity, x-ray analysis,[80] and differential thermal analysis[36] are just some of the methods that have been applied to chemical kinetic studies of molten nitrates.

For the study of the chemical behavior of $NaNO_3$ and KNO_3 I performed 5 kinds of experiments:

1. Differential scanning calorimetry (DSC)
2. Plackett-Burman screening tests at 1 atmosphere pressure
3. Decomposition tests in argon
4. Thermogravimetry (TG) at 1 atm
5. Thermogravimetry and mass spectrometry (TG/MS) under vacuum conditions

Of common concern throughout the experiments was the choice of an appropriate container material for the salts. The problem of choosing a nonreactive container for nitrate and nitrite experiments has plagued many experimenters. Although many of the earliest studies were performed in silicate glass containers, it was soon recognized that SiO_2 could react and contribute oxide ions to the molten salts.[79,82] Silica can also react with oxide ions to form superoxide by[79]

$$SiO_2 + 2O^{-2} \rightarrow SiO_3^{-2} + O^{-2} \qquad (46)$$

Other workers claim to have successfully worked with stainless steel containers. However, stainless steel is oxidized by the nitrates and

nitrites.[11] Researchers have found that Cr_2O_3, which protects stainless steel from oxidation, catalyzes the decomposition of KNO_3[83] or HTS[14] by forming chromates and dichromates.

I performed several experiments to find a nonreactive container. Gold, zirconia, and alumina did not react with the salts as determined by visual examination and an atomic absorption test which showed that neither Al, Zr, nor Au had been dissolved into the salt. Gold has been used without reaction by Bagarat'yan et al.[75] These materials are not the only suitable materials for nitrate decomposition studies. For instance, silver has been used without reaction.[37,72].

Although other researchers have used Pt vessels for their experiments without reaction[61], I found that Pt was darkened and dissolved into salts that had been decomposed in air. Corrosive attack and formation of black particles on Pt was also observed by Miles and Fletcher.[62] Platinum is attacked by hydroxides, which I believe to have formed in the salt during decomposition in air.

Another perplexing issue regarding these salts is their unbridled propensity to spread and wet any ceramic or metal surface. Therefore, it was difficult both to contain the salts and to characterize their gas-liquid surface areas. No material could be found that was not wetted by the salt. Several other researchers have observed the phenomenon of spreading.[14,36,84] The tendency of the nitrates to spread and wet surfaces may be understood if one considers the surface energies acting at a liquid-solid-vapor interface. Such an idealized interface situation is that of a sessile drop of liquid on a rigid solid substrate shown in Figure 30. The equilibrium of the surface energies (γ_{LV}, γ_{SV}, γ_{SL}) between the solid, liquid and vapor phases is given by

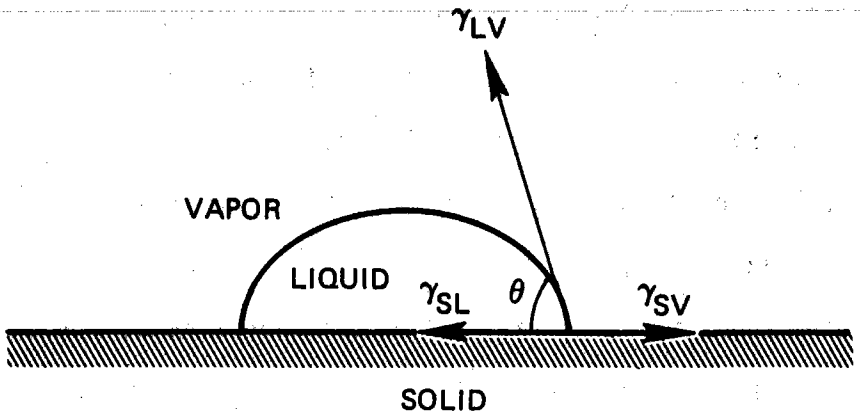

CREEP OR WETTING OCCURS WHEN

$$\cos\theta = \frac{\gamma_{SV} - \gamma_{SL}}{LV} \geq 1, \cos\theta \text{ FORCED TO } 0^\circ$$

Figure 30. A Sessile Drop

$$\frac{\gamma_{SV} - \gamma_{SL}}{\gamma_{LV}} = \cos\theta \qquad (47)$$

The contact angle, θ, is determined by (47). If $(\gamma_{SV} - \gamma_{SL})/\gamma_{LV}$ is greater than 1, θ is forced to 0°, which is the condition called wetting. Wetting occurs when the surface energies of the solid or vapor in contact with the liquid are less than the difference between the solid-vapor and the solid liquid surface energies[85], as they appear to be for the nitrates and nitrites.

III A. Differential Scanning Calorimetry Experiments

When materials are heated, they may undergo physical or chemical changes that are endothermic or exothermic. Differential thermal analysis (DTA) and differential scanning calorimetry (DSC) are thermal analysis techniques that measure these endothermic and exothermic reactions. Both DTA and DSC are reviewed in Reference 86 and the DSC technique is discussed in detail in References 87 and 88.

Both DSC and DTA are simple and rapid methods of elucidating the temperature range over which reactions occur. DTA is a technique in which the temperature of the material undergoing a change is compared with that of an inert sample. For the DSC technique, a differential heat flow is measured. When endothermic or exothermic thermal transitions occur, a difference is recorded in the power needed to maintain the heating rate or temperature of two identical furnaces, one of which has the sample material and the other the inert reference material. The temperatures of transitions found by DTA should be the same as those found by DSC.

Several authors have used DTA to study the alkali nitrates[36,89] and rare earth nitrites.[90] Differential scanning calorimetry has been

successfully applied to the study of the $NaNO_3$-KNO_3 phase diagram,[91] the melting and solidification of salt hydrates,[92] and solid-solid transitions in $NaNO_2$[93] and $NaNO_3$.[94]

A Perkin-Elmer differential scanning calorimeter (DSC-2) was employed to obtain thermal spectra of $NaNO_3$, KNO_3, $(Na,K)NO_3$, $NaNO_2$, and KNO_2 from 300 to 990 K the upper temperature limit of the DSC-2. The DSC was calibrated with In and K_2CrO_4, whose temperatures of fusion and solid-solid transition are well known. The samples were made from reagent-grade powders that were dried at 380 K under vacuum for at least 12 hours. Small (<30 mg) samples were encapsulated in high-pressure stainless steel and gold plated stainless steel DSC pans and heated at a constant rate of 10 K/min from 300 to 900 K. The reference pan was always an empty pan.

III B. Plackett Burman Screening Tests

The object of this series of experiments was to identify which independent variables were most important to nitrate and nitrite decomposition in air. This information was intended to be useful in planning and controlling other experiments by knowing what variables caused what reactions.

Ten variables were selected for study: temperature, N_2, O_2, H_2O, CO_2, K/Na, purity, gas flow rate, salt sample size, and salt surface area. It was expected that N_2, O_2, H_2O, and CO_2 would affect the salts because these are the gases involved in Reactions (1)-(4). Both the rate and the extent of reaction depend on temperature. Purity was included as a variable because one would like to know if the commercial grade of the nitrates will behave differently than reagent grade. I included the alkali metal ratio (K/Na) in order to determine if the

mixtures of $NaNO_3$ and KNO_3 were much more stable than $NaNO_3$. Lee and Johnson[95] found that the gas flow rate influenced which reaction dominated the decomposition of $LiNO_2$. The gas flow rate was included as a variable. Furthermore, in Lee and Johnson's studies[95] and in Freeman's[34,42] the surface area of the salt exposed to the ambient gas affected the reactions observed with the nitrates and nitrites; therefore the surface area was also chosen to be a variable. As for sample size, I wanted to see if changing it markedly altered the chemical reactions we observed in our experiments.

A classical approach to the problem of identifying the important variables affecting nitrates would have led to a series of experiments which examined only one factor (independent variable) at a time. Because of the number of independent variables, the number of experiments would be large. Thus I took advantage of a statistical screening design, which maximizes the information about the effects of many variables with a minimum number of experiments.[96-98]

A 20-experiment Plackett-Burman[96-98] design was chosen for the screening. A Plackett-Burman test matrix allows identification of the primary factors affecting the experimental responses. A 20-run matrix with 10 independent variables can estimate main effects (which variables cause a certain experimental response), but its chief limitation is that the matrix cannot provide information on the statistical interactions of variables.

A Plackett-Burman test matrix is run with each variable or factor set at one of two possible levels, either high or low.[96,98] As an example, the purity is set as either reagent or commercial grade. The levels for each continuous variable are chosen to be extremes so that a

TABLE 8

THERMAL DECOMPOSITION VARIABLES

Factor	Actual Spread in Levels	
	High	Low
Temperature (K)	869 - 923	576 - 640
Oxygen[a]	19.5 - 21.0	< 0.01
Nitrogen[a]	68.3 - 70.1	< 0.01
Carbon Dioxide[a]	9.7 - 10.6	< 0.001
Flow Rate (ℓ-sec^{-1})	0.017 - 0.023	0.0008 - 0.0017
Surface Area[b] (cm^2)	0.77 - 0.84	0.079 - 0.28
$KNO_3/NaNO_3$[c]	0.56 - 1.0	0 - 0.3
Sample Size (g)	2.3 - 4.6	0.64 - 0.97
Relative Humidity	~100% at Room Temperature	Gas Dried with $CaSO_4$
Purity	Reagent Grade	Partherm 430[d] or Reagent Grade + 3% Cl + 1% $NaNO_2$

[a]Weight Percentages of premixed gases.

[b]Of crucible; does not include salt spreading.

[c]Molar ratio; for nitrate matrix only.

[d]Park Chemical Co.

factor's influence can be easily identified in the statistical analysis. The two levels for each of the variables are listed in Table 8. Note the spread in the high and low levels of some factors, in particular temperature, K/Na, sample size, and surface area. This spread contributes to the experimental noise. However, because extremes were chosen, the two levels do not overlap. The high levels of N_2, O_2, K/Na, and temperature are the expected operating conditions of a thermal storage system[4], as are the low levels of CO_2, H_2O, purity, and temperature. The high CO_2 level was a dramatic overtest of the effect of CO_2 because this level is about 300 times greater than CO_2 found in air. The surface areas, the sizes of the samples, and their ratios (surface area to volume ratio) did not approach actual operating conditions of a thermal storage system, but those convenient for bench top experiments.

Two Plackett-Burman series of experiments were performed concurrently, one series with $NaNO_3$ and KNO_3 and the other with $NaNO_2$. The nitrite experiments were identical to the nitrate experiments with the exception that the variables K/Na and purity were excluded; very pure $NaNO_2$ was used in every experiment.

Salt samples in high-purity alumina crucibles were placed in a horizontal 6.3 cm diameter tube furnace. The furnace was evacuated and backfilled twice with the premixed gases (Matheson Gas Products) for each experiment, and the gas flow rate was adjusted with a calibrated flowmeter. For some of the Plackett-Burman experiments the sum of the weight percentages of CO_2, N_2, and O_2 was less than 100%; the balance was made up with Ar, which was mixed with the other gases. The salts were rapidly heated (10 K/min) to the temperature required, held for 10 hours, and then rapidly cooled by turning the furnace off. To subject samples to

high humidity the premixed gases were bubbled through a container filled with water and glass beads. By a separate test the gases were found to be saturated with water at room temperature using this technique. To remove water vapor from the incoming gas, the gases were passed through $CaSO_4$. The gases exited through a bubbler containing vacuum pump oil.

During the course of the experiments three physical responses occurred: mass transport, degree of spreading, and color of the salt. The degree of mass transport was judged by the amount of salt that was deposited downstream at the cool end of the furnace. Spreading was measured by the salt's propensity to crawl out of its container. Color (white to chartreuse) was noted visually. These three responses were assigned quantitative values based on visual observations. Table 9 describes the values qualitatively.

Samples of the salts were submitted for chemical analyses. The analyses included testing for NO_3^-, NO_2^-, Na^+, K^+, $CO_3^=$, Cl^-, and pH, according to the tests described in "Standard Methods for the Examination of Water and Waste Water," published by the American Public Health Association. Our confidence level in the chemical analysis depended on the type of analysis. For example, the minimum carbonate level determined by chemical analysis for any experiment was 0.1%, which simply was the minimum level of detection for the chemical analysis for $CO_3^=$. Spreading of the salt caused some difficulty in this regard because in some instances less than 100 mg samples were available. Measurements of the pH (performed by dissolving the salt samples in water) include the contributions of hydroxide, carbonate, and oxide ions from Reactions (4), (3), and (2), respectively. Oxide ions are completely converted to hydroxide in the presence of water.[63,99,100]

TABLE 9

DESCRIPTION OF PHYSICAL RESPONSES

Response	Assigned Value 0	1	2	3
Color	White	Yellowish	Very Pale Chartreuse	Pale Chartreuse
Mass* Transfer	No Deposit	Very Slight Deposit	Slight Deposit	Filmy Deposit
Spreading	No Spreading	Some salt crept on outside of crucible	Almost all of the salt crept outside of crucible	Not assigned

*Deposit refers to salt deposit observed on the flange at the end of the furnace.

The statistical analysis described in References 96 and 98 was applied to the following responses: NO_3^-, NO_2^-, Na/K, pH, $CO_3^=$, color, degree of spreading, and the extent of mass transport. From the results the primary variables affecting all the responses were identified. A description of the statistical analysis technique is given in Appendix B.

III C. Decomposition in Argon

Two experiments were performed with nitrates and nitrites in argon. The objective of these experiments was to determine the gaseous products and chemical changes of the nitrates and nitrites in argon. To this end, 10 gram samples of $NaNO_3$, KNO_3, $(Na,K)NO_3$, $NaNO_2$ and KNO_2 were decomposed at 624 K and 736 K for 100 hours. The salts were reagent grade. The sample containers were long, closed-end tubes of stainless steel which had a valve welded onto the cap of the tube (to facilitate mass spectrometer analysis of the ullage gases). Stainless steel was used becuse oxidation and reaction with the salts in stainless was anticipated to be slow, and gas-tight containers could be easily and inexpensively made. The salts were placed in the tubes and the tops were loosely screwed onto the tubes and placed in a fluidized bath at 390 K. The fluidized bath had a 20 cm long zone of uniform heating. The tops of the tubes extended out of the bath to protect the seals from heat. The salts were hygroscopic therefore they were heated at 390 K for 72 hours to remove water. The KNO_2 was particularly hygroscopic. After the bakeout, the tubes were sealed with Cu or Al gaskets, evacuated and backfilled 3 times with argon at 1 atmosphere pressure. The argon was passed through magnesium perchlorate to remove any CO_2 or H_2O. The argon-filled containers were reimmersed in the fluidized bath and heated at 624 $\pm$ (3) or 736 ($\pm$ 16) K for 100 hours.

After the experiments were over, the ullage gas was analyzed by a magnetic sector mass spectrometer capable of quantitative gas analysis. Next the containers were opened and the salts were dissolved in hot water and submitted for chemical analysis. The analysis included testing for NO_3^-, NO_2^-, Na^+, K^+, $CO_3^=$, OH^- according to the tests described in "Standard Methods for the Examination of Water and Waste Water," published by the American Public Health Association. Trace metals were analyzed spectrographically.

III D. Thermogravimetry

Thermogravimetry is a record of a sample's weight during the course of an experiment. Thermogravimetry (TG) is a widely used technique to study decomposition reactions[101] and chemical kinetics.[102,103] Many articles have been written on the applicability of TG and the factors affecting TG experiments.[102,103,104-109]

Many of the reactions discussed in Section II are associated with the evolution of gaseous products; therefore the degradation of nitrate can be studied with the thermogravimetric (TG) technique of thermal analysis. Specific advantages led me to choose thermogravimetry as the primary experimental technique for the study of the high-temperature studies of $NaNO_3$ and KNO_3. Among these advantages are: the availability of sensitive microbalances for TG that provided continuous measurements of the sample's weight[110], the ability to add an evolved gas analysis system to the microbalance[111-113], the existing theoretical back ground on TG kinetics[114,115], and the variety of experimental conditions possible with the microbalance.[116] The experimental conditions for the available TG apparatus may range from operation at 1 atm

or 10^{-8} Torr; 25 K to 1273 K; isothermal or dynamic heating (changing temperature); sample sizes from 1 mg to 10 grams; sensitivities as high as .01 mg; ability to use samples that are liquid or solid.[116]

Kinetic expressions have been used to describe decomposition reactions and specifically TG kinetics.[103,114,115,117-127] The preponderence of these expressions rely on solid state diffusion equations and crystal growth.[117,128-131] Diffusion may be important in the decomposition of these salts but because they are liquid, convection may also influence the kinetics.[103]

First order kinetics to describe the decomposition of the nitrates[34,42] and nitrites.[38] Bond and Jacobs[50] used an empirically determined expression (equation (32)) to describe the kinetics of decomposition. In photochemical[132] and gamma radiolysis[133] decomposition of nitrate to nitrite, constant (zero order kinetic) rates of decomposition were observed. In preliminary experiments I observed that the rates of salt decomposition slowly and smoothly decreased with time. Many reactions (described in the Introduction) may occur in TG experiments with nitrates, therefore the dominant kinetic rate law may vary during the experiment.

To analyze the TG data I wrote a computer program to perform a least-squares analysis for the weight (wt), the weight per unit surface area (wt/sa), the fractional weight loss (wt/wt_0), and the natural logarithm of the weight loss ($\ln (wt/wt_0)$), all as a function of time. The equations which were fitted to the data are:

$$\frac{wt}{sa} = a + bt + ct^2 \tag{48}$$

$$wt = a' + b't + c't^2 \tag{49}$$

$$\ln\left(\frac{wt}{wt_o}\right) = a'' + b''t \tag{50}$$

$$\frac{wt}{wt_o} = a''' + b'''t + c'''t^2 \tag{51}$$

The computer program calculated the best values of the constants a, b, c, a', b', c', a", b", c", a"', b"' and c"' for each experiment. The values of b and b' are the initial fluxes for the experiments in terms of mg-cm^{-2}-min^{-1} and mg-min^{-1}, respectively. The rate constant b" is the first order rate constant and b'" is the initial rate of the fractional weight loss.

I assumed that these rate constants had an Arrhenius dependence on temperature[120,121], in other words

$$b_i = \exp(\Delta S^*/R)\ \exp(-\Delta H^*/RT)\ . \tag{52}$$

where ΔS^* and ΔH^* are the entropy and enthalpy of activation for a reaction. To investigate the temperature dependences, the computer was also programmed to plot ln(b), ln(b'), ln(b"), and ln (b'") versus 1/T for a series of experiments. The best linear least squares fit of $\ln(b_i)$ versus 1/T was determined. The slope and intercept of the b_i versus 1/T were used to calculate ΔS^* and ΔH^* for each experiment series.

The computer program also plotted the data for each experiment. One of the computer plots is shown in Figure 31. The data sets for each experiment are shown in Appendix C. For each experiment there are 4 graphs which show 1) the weight and the weight per unit surface area versus time on one graph (in the upper left-hand corner), 2) the natural logarithm of the fraction of the sample remaining versus time (in the upper right-hand corner), 3) the temperature profile during the experiment (in the lower left-hand corner), and 4) the percent weight loss versus time (in the lower right-hand corner). Graphs 1, 2, and 4 also

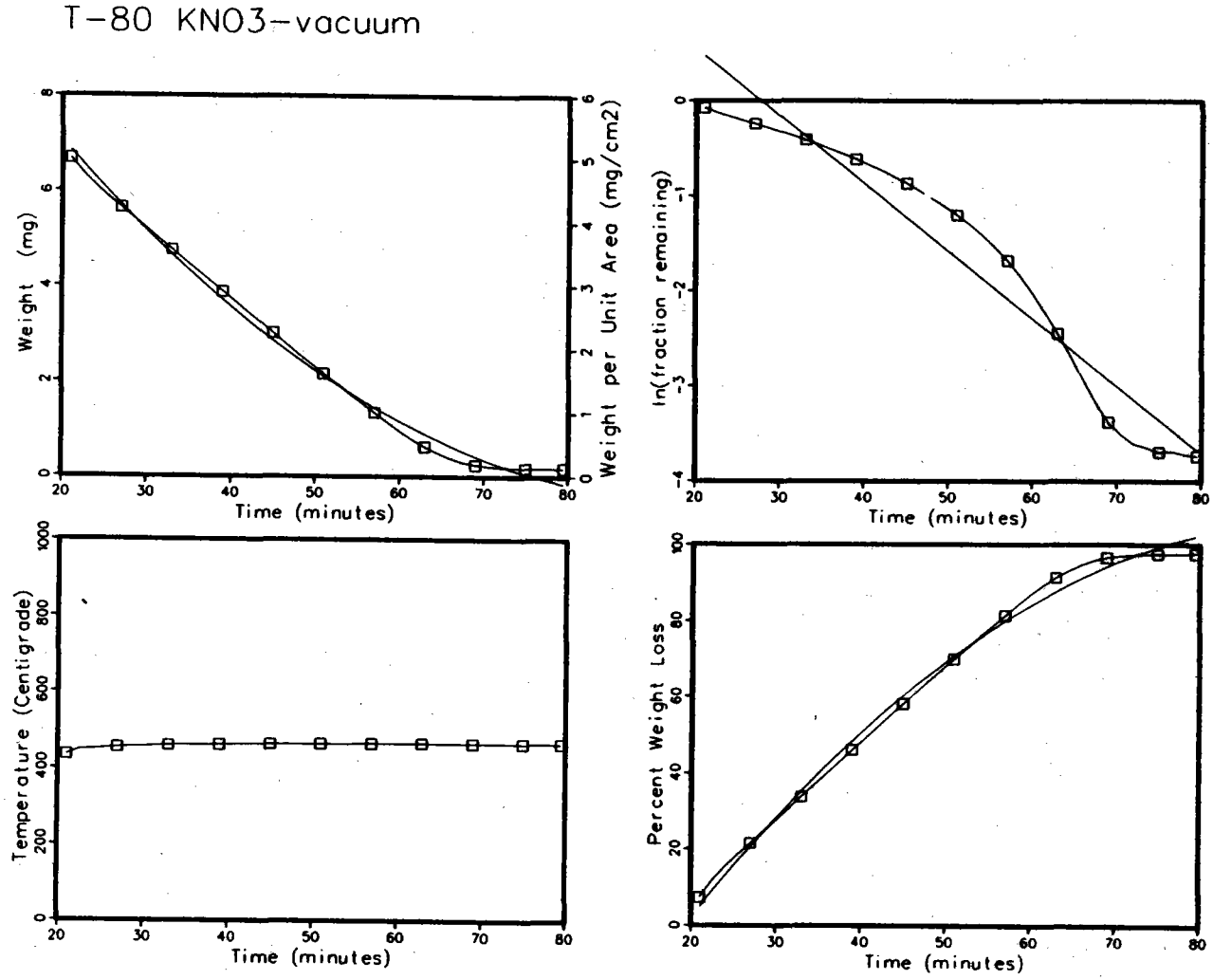

Figure 31. An Example of TG Kinetic Data

have the best linear least-squares fit to the data plotted with the experimental data in accordance with Eqs. (48), (50), and (51), respectively. The experimental data points are simply connected by straight lines with periodic markers (not for each data point). The least-squares fits have no markers. The plots do not show the low temperature data (before the isothermal temperature was reached).

For the experiments performed in air, the temperature and weight of the samples were recorded on a strip chart recorder. The data from strip chart records was manually digitized. The temperature profiles for the experiments performed at 1 atmosphere pressure are not accurate because they simply show the nominal temperature at which the experiment was performed and do not illustrate the drift or the temperature instability. This detail was changed when a data acquisition system became available as is described in Section III D2. All the temperature profiles of the experiments run in vacuum show the actual sample temperature.

III D1. Thermogravimetry Under Atmospheric Pressure

A series of TG decomposition experiments were done with nitrates at one atmosphere gas pressure. Three series of experiments were performed: $NaNO_3$ decomposition in air, mixtures of $NaNO_3$ and KNO_3 in air, and mixtures of $NaNO_3$ and KNO_3 in argon. The conditions of these series of experiments are described in Tables 10, 11, and 12. These experiments represent a wide range of experimental configurations which trace my evolving technique of working with nitrates. All the experiments were isothermal; the temperatures are noted in Tables 10-12.

As a result of the learning process involved in these experiments the sample size ranged from 10 to 200 mg. Both Cahn RG and R-100 microbalances were used and the minimum detectable weight change ranged from

Table 10

Thermogravimetry Experiments with $NaNO_3$ in Air[c]

Trial[a]	Temperature (K)	Container	Surface Area cm^2	Starting Weight mg	Percent Total Weight Lost	Duration min	Comments
25G	799.	Pt	0.28	39.30	3.25	1000.	Static Air
5R	848.	Al_2O_3	0.238	158.00	2.67	1000.	Static Dry Air
6R	875.	Al_2O_3	0.238	170.38	1.54	1000.	Static Dry Air
8R	873.	Al_2O_3	0.24	143.80	4.44	345.	b
10R	833.	Al_2O_3	0.24	152.00	3.00	280.	b
11R	941.	Al_2O_3	0.24	167.47	0.85	11.7	b
12R	833.	Al_2O_3	0.24	162.35	0.75	120.	b

[a]The suffix R refers to the Cahn R-100 balance in which the experiments were performed. Likewise G refers to the RG balance.

[b]Sample chamber was evacuated and backfilled with dry air; dry air flowed continuously during experiments.

[c]All experiments were performed with reagent grade $NaNO_3$.

Table 11

Thermogravimetry Experiments with $NaNO_3$ and KNO_3 Mixtures in Air[a] or N_2

Trial[b]	Temperature (K)	Container	Surface Area cm^2	Purity[c]	Starting Weight mg	Percent Total Weight Lost	Duration min
15	793.	Pt	0.28	C	48.06	2.83	550.
16	805.	Pt	0.28	C	42.44	5.51	1008.
18	840.	Pt	0.28	R	46.06	3.26	462.
20	805.	Pt	0.28	R	41.50	3.40	1120.
21[d]	833.	Pt	0.28	R	46.90	7.99	423.

[a]All the experiments in air were run with a static air environment with the exception of 21G.

[b]The suffix G on the trial number refers to experiments performed with the Cahn RG balance. Likewise, the suffix R refers to those experiments performed with the Cahn R-100 balance.

[c]R = reagent grade mixtures of 50/50 (Na/K)NO_3; C = commercial grade purity (Partherm 430 from Park Chemical Co.).

[d]This experiment was run with a <.001 l/min flow of N_2 during the experiment. No prior evacuation or purging of the air was performed.

Table 12

Thermogravimetry Experiments with $(Na/K)NO_3$ in Argon[a]

Trial[b]	Temperature (K)	Container	Surface Area cm^2	Starting Weight mg	Percent Total Weight Lost	Duration min
15R	897.	Sapphire	0.84	2902.0	0.94	190.
16R	1073.	"	0.84	2392.0	7.26	60.
17R	869.	"	0.84	2157.7	7.23	540.

[a]All samples were reagent grade mixtures of 50/50 $(Na/K)NO_3$.

[b]The suffix R refers to the Cahn R-100 balance in which the experiments were performed.

0.01 mg to 0.1 mg depending on the experiment. Some of the eperiments were performed in ambient air, while others were performed in carefully dried air or argon. The first experiments were performed in static air and later the flow of gas was carefully controlled. At first Pt crucibles were used, and later sapphire crucibles were substituted because the Pt was darkened and dissolved by reaction with the salts. The surface area of the crucible was also varied. Commercial grade draw salt, pure draw salt, and pure $NaNO_3$ were used for the experiments. Some experiments lasted a few minutes and others were continued for 2-3 days; not all samples were completely decomposed.

Various furnace and thermocouple configurations were used during the course of these experiments. The furnaces were either Pyrex or quartz glass tubes which I wound externally with a kanthal heater. The furnace heater was loosely wrapped with a fibrous ceramic blanket insulation. The diameters of the glass tubes were approximately 12 mm to reduce convective currents in the furnace.[134,135] The overall lengths of the furnaces varied from 10 - 30 cm. The isothermal heating zones in the furnaces were determined to be 25 mm or more, which was significantly larger than the 5 mm long sample containers. A proportional controller was used to regulate the furnace temperature. The tip of the chromel-alumel thermocouple (for the temperature controller) was placed next to one of the central kanthal coils on the glass tube. All temperature changes were made manually. During the course of the experiments the sample temperature frequently drifted 10 K above the starting temperature. A chromel-alumel thermocouple placed within 3 mm of the bottom of the sample crucible was assumed to measure the sample temperature. This thermocouple was inserted into the furnace through the

bottom of the furnace tube. In some cases the thermocouple was sealed into the furnace with a wax seal. In other cases it was unsealed or placed in a thermocouple well.

III D2. Thermogravimetry and Mass Spectrometry in Vacuum

To gain more insight into the intrinsic decomposition of the nitrates, we constructed a combined system of a mass spectrometer and a microbalance to detect gases as they were evolving from the salts and weight losses as they were occurring. These techniques have been combined successfully to study decomposition reactions[107,113,136-138] and pyrolysis.[112,140-144] The system itself is described in a later section and the experiments are described here.

Five salts were studied with the TG/MS system described in Section III D2.1. These salts are: 1) $NaNO_3$, 2) $NaNO_3$ and KNO_3 mixtures, and 3) $NaNO_2$ 4) KNO_3, and 5) $LiNO_3$. Primarily isothermal experiments were performed in vacuum. However, in addition to the isothermal experiments, three dynamic heating experiments were performed with $NaNO_3$, KNO_3 and $LiNO_3$ in vacuum and are described after the isothermal experiments. All the experiments are described in Tables 13-19.

Preliminary experiments were performed with $NaNO_3$ and KNO_3 mixtures in crucibles which had a variety of diameters and depths. (See Table 14.) Decomposition studies of solids are commonly performed with similar crucibles for substances such as carbonate[136,145] and sulfate[146,148] decompositions or vapor pressure determinations.[147] It was during these experiments that we found that the wetting and spreading problem could not be alleviated therefore, we decided to take advantage of wetting. The crucibles to contain the salt were abandoned. Instead, the salt was applied to small gold "flags" or thin rectangular substrates

Table 13

Thermogravimetry Experiments with $NaNO_3$ in Vacuum

Trial[a]	Temperature (K)	Surface Area[b] cm^2	Purity[c]	Starting Weight mg	Percent Total Weight Lost	Duration min.
26	677.	2.89	R	27.84	12.5	65.
29	716.	1.489	R	9.80	98.6	80.
30	737.	1.489	R	8.46	100.0	55.
33	723.	1.489	R	7.70	99.4	75.
38	726.	1.489	R	13.3	99.8	177.
40	774.	1.489	U	8.72	99.4	59.
41	726.	1.489	U	10.43	99.9	169.
44	784.	1.489	U	5.15	97.7	25.5
47	655.	1.489	U	7.68	27.9	208.5

[a]All experiments performed with the Cahn R-H balance.

[b]All samples were placed on a Au flag substrate with the given surface area. For Trials 27-47, the same Au flag was used.

[c]R = reagent grade $NaNO_3$; U = ultra high purity $NaNO_3$ from SPEX Co.

Table 14

Thermogravimetry Experiments with $NaNO_3$ and KNO_3 Mixtures in Vacuum

Trial[a]	Temperature (K)	Container	Surface Area cm^2	Purity[b]	Starting Weight mg	Percent Total Weight Lost	Duration min.
5	817.	Sapphire	0.79	R	67.43	87.5	90.
6	810.	"	0.79	R	68.62	22.0	27.
7	795.	"	0.79	R	73.55	70.8	110.
13	898.	Au	0.20	R	64.28	80.9	195.

[a]These experiments were performed with Cahn R-H balance.

[b]R = reagent grade 50/50 (Na/K)NO_3 mixtures.

Table 15

Thermogravimetry and Mass Spectrometry Experiments with $NaNO_3$ in Vacuum[a]

Trial	Temperature (K)	Weight (mg) Initial	Final	NO/N_2	O_2/N_2	O_2/NO
50[d]	752.	7.03	0.00	<0.85	<0.23	<0.28
55[d]	745.	6.43	0.00	<0.52	<0.08	0.15
56[d]	744.	7.50	0.00	0.31	0.15	0.49
49[d]	636.	4.88	4.57	0.52	0.0	0.0
54[d]	627.	6.88	6.28	0.086	0.0	0.0
55[d]	631.	6.61	5.90	0.066	0.0	0.0
74	676.	6.98	c	0.91	0.057	0.063
75	650.	9.16	c	0.51	0.042	0.12
76	715.	5.03	c	0.77	0.27	0.35

[a]All samples were crystallized on a Au flag with 1.489 cm^2 surface area.

[b]When the ratio is indicated to be less than the value shown, the mass spectrometer was saturated during peak production of the gases.

[c]Not available.

[d]Experiments in 3x2 statistical design.

Table 16

Thermogravimetry and Mass Spectrometry Experiments with $NaNO_2$ in Vacuum[a]

Trial	Temperature (K)	Weight (mg) Initial	Final	NO/N_2	O_2/N_2	O_2/NO
51[d]	745.	2.18	0.00	0.82	<0.016	<0.020
53[d]	743.	7.93	0.80	0.86	<0.052	<0.060
54[d]	753.	7.45	0.00	0.70	<0.018	<0.026
48[d]	627.	4.33	1.14	0.48	0.0042	0.0089
52[d]	623.	6.35	3.62	0.62	0.0	0.0
57[d]	627.	3.29	0.71	0.42	0.0	0.0
65	671.	9.68	c	0.49	0.0	0.0
77	717.	7.48	c	0.24	0.0	0.0
78	663.	5.12	c	0.52	0.0	0.0

[a]All samples were crystallized on a Au flag with 1.489 cm^2 surface area.

[b]When the ratio is indicated to be less than the value shown, the mass spectrometer was saturated during peak production of the gases.

[c]Not available.

[d]Experiments in 3x2 statistical design.

Table 17

Thermogravimetry and Mass Spectrometry Experiments with KNO_3 in Vacuum[a]

Trial	Temperature (K)	Initial Weight, mg	NO/N_2	O_2/N_2	O_2/NO
66	747.	7.37	b	b	b
72[c]	743.	6.62	0.56	0.062	0.11
80[c]	737.	8.03	0.27	0.16	0.58
81	717.	7.64	b	b	b
82	671.	7.70	0.21	0.086	0.041
83[c]	741.	8.05	0.42	0.189	0.45
84	650.	7.81	0.087	0.0	0.0
85[c]	624.	8.07	0.047	0.0	0.0
86[c]	623.	8.29	0.035	0.0	0.0
87[c]	621.	7.24	0.025	0.090	0.11

[a]All samples were crystallized on a Au flag with 1.489 cm^2 surface area.

[b]Not available.

[c]Experiments in 3x2 statistical design.

Table 18

Thermogravimetry and Mass Spectrometry Experiments with $LiNO_3$ in Vacuum[a]

Trial	Temperature (K)	Initial Weight, mg	NO/N_2	O_2/N_2	O_2/NO
73	745.	82.56	0.88	0.37	0.42
88	723.	2.26	0.81	0.091	0.11
89	730.	2.74	1.14	0.17	0.15

[a]All samples were crystallized on a Au flag with 1.489 cm^2 surface area.

Table 19

Dynamic Thermogravimetry and Mass Spectrometry Experiments in Vacuum[a]

Trial	Salt	Initial Weight, mg	10% Weight Loss[b]
69	$NaNO_3$	7.38	747 K
70	KNO_3	7.82	731 K
71	$LiNO_3$	4.53	674 K

[a]All samples were crystallized on a Au flag with 1.489 cm^2 surface area.

[b]Temperature at which 10% welight loss had occurred.

whose area was easy to measure. The flags were suspended in the furnace by thin Au wires that were welded to the flags. When melted, the salt samples tended to cover the entire substrate. The samples of salt were small (< 10 mg) and did not form pendant drops on the substrate, so that the salt thickness was approximately uniform over the surface of the flag. The form of sample preparation is the Langmuir method.[77]

The salts were applied to the substrates by dipping the flag into a hot saturated solution of salt and distilled water. As the solution cooled, the salt precipitated onto the substrate. The sample was then dried with a hot air gun but the salt was not melted. To ensure that salts were unchanged by this procedure, precipitated salt samples were submitted to infrared absorption analysis. Indeed, the $NaNO_3$, KNO_3, $NaNO_2$ and $LiNO_3$ samples were unchanged by precipitation from the salt water solutions. The success of this precipitation technique is not surprising because anhydrous alkali metal nitrates and nitrites have been prepared in this manner by several researchers.[33,79,149-151]

Using this sample configuration with Au flags having 1.49 cm^2 surface area had its limitations, however. Experiments could not be performed above 750 K because the flux from the salts was too high. Above 750 K the pressure rose above 5×10^{-5} torr, the upper pressure limit for safe operation of the mass spectrometer, and the ion pump became saturated, overheated, and lost significant pumping speed.

The experimental details are these. The sample size varied from 3 - 8 mg and the same gold substrate was used in every case. The $NaNO_3$ and KNO_3 were ultra high purity and the $NaNO_2$ and the $LiNO_3$

were reagent grade purity. Infrared absorption showed that the $NaNO_2$ traces of $NaNO_3$. The nitrates had no detectable nitrite.

The heating schedule for the isothermal experiments in vacuum was as follows: 1) heat the sample from room temperature to 330 K in 3 minutes, 2) hold the sample at 330 K for 180 minutes, 3) heat the sample at approximately 27 K per minute to the chosen temperature, 4) hold the furnace at the chosen temperature for 360 minutes, 5) cool to room temperature by cutting the power to the furnace. Because there was no convection in the vacuum to aid heating, and the temperatures were too low for efficient radiant heat conduction, the sample temperature lagged behind the furnace temperature. Therefore, the rate of sample temperature rise was not exactly linear. Minimal weight loss (< 2%) occurred before the test temperature was reached.

The data acquisition system was programmed to collect data for the duration of each experiment. These data are plotted in Appendix C. The kinetic data were edited in this fashion: The data were ignored at temperatures below the isothermal temperature and the weights were corrected for the buoyancy difference between air and vacuum. To make this correction, 0.21 mg was added to each weight reading, which had been determined to be the difference between the balance's null point in air (where it was calibrated) and the balance's zero in vacuum (the condition in which the data was taken).

In the experiments denoted T-48 and higher, a unique method of comparing the evolved gases was employed that was not used before T-48. From preliminary experiments it was observed that masses 28, 30 and 32 (N_2, NO, and O_2) were the only gases evolved from $NaNO_2$, KNO_3, and $NaNO_3$. To compare the amounts of each gas that was evolved in each experiment,

the mass range 27-33 was quickly and repeatedly scanned with the mass spectrometer. The mass spectra was recorded on a strip chart recorder that was advancing very slowly (10 cm/hr). The resulting record gives discrete peaks that form an envelope for each mass. A photograph of such a record is shown in Figure 32. After the experiment was finished, I used a planimeter to measure the area under each envelope for each mass which is simply converted into volt-minutes knowing the vertical scale and speed of the chart recorder. This technique gives relative amounts of the gases, not absolute ones. The planimetry results are given in Tables 15-18 for each salt.

The intensity of each peak is proportional to the partial pressure of that gas[152,153], that is

$$I_i = S_i P_i \qquad (53)$$

where S_i is the sensitivity of the instrument to that gas. Therefore the areas measured with a planimeter are proportional to the amount of that gas that was evolved.[154] The sensitivities of the quadrupole mass spectrometer to N_2, NO, and O_2 may be very similar because the molecules are all diatomic and close to one another in mass.[154] Attempts to calibrate the mass spectrometer with a mixture of N_2 and NO produced erratic results. The height of the N_2 peak compared to the NO peak changed with time and the volume of the sample chamber. I believe that NO has peculiar surface adsorption properties which contributed to the erratic behavior. Therefore in comparing the relative amounts of each gas, trends were sought in the ratios of the amounts of the gases (recorded under constant conditions) and not their absolute amounts.

A statistical 3x2 series of experiments with $NaNO_2$, KNO_3 and $NaNO_3$ was performed to achieve the following objectives: 1) to compare the rates

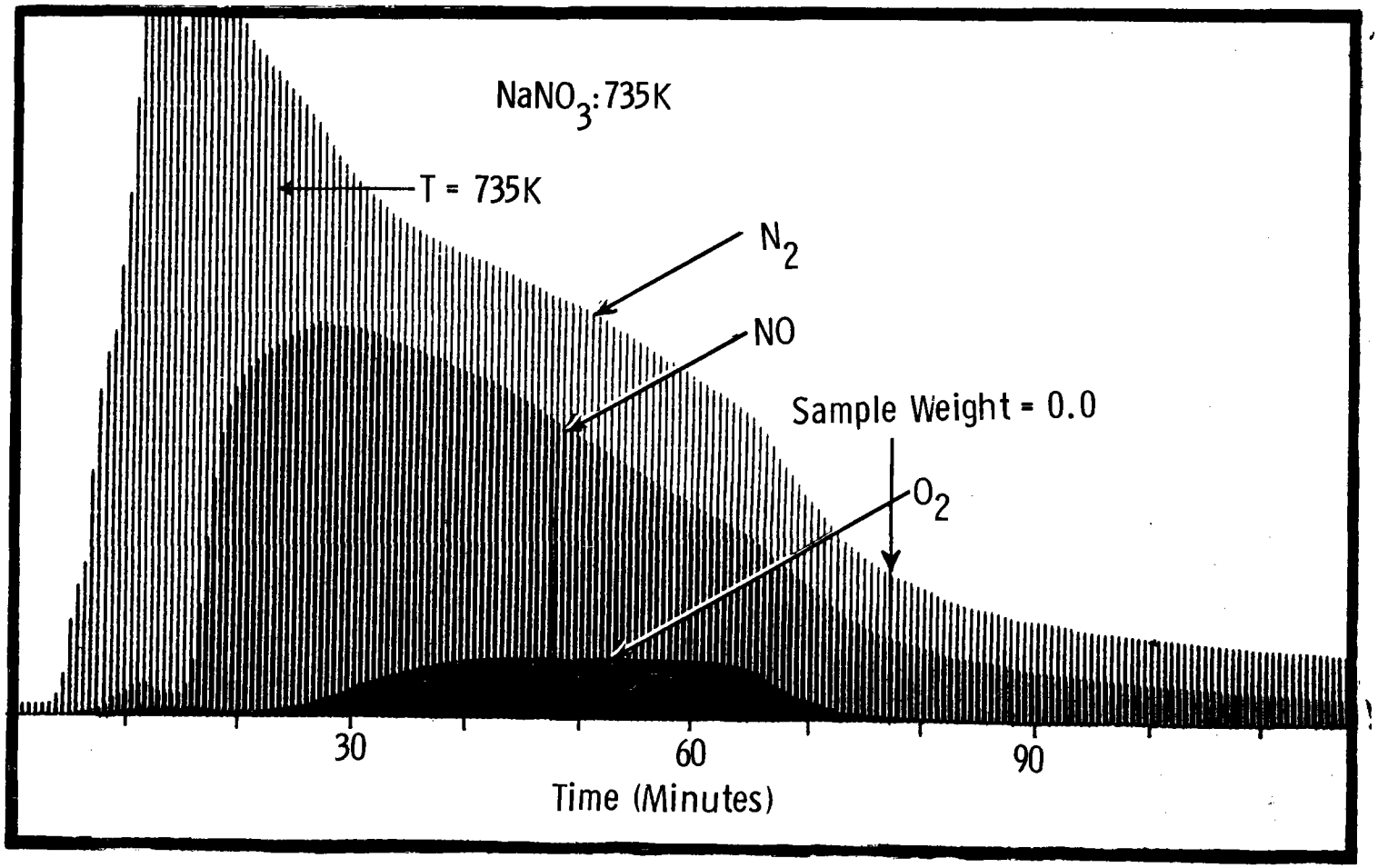

Figure 32. Mass Spectrum of Gases from $NaNO_3$ at 747 K

of decomposition, 2) to compare the gaseous products of decomposition, 3) to compare the behavior of the salts at 620 K and 740 K, 4) to see how reproducible the experiments would be, and 5) to use these comparisons to gain insight into the mechanism of decomposition of $NaNO_3$, KNO_3, and $NaNO_2$ in vacuum. The series consisted of eighteen experiments indicated in Tables 15-17. Six experiments were performed with each salt; three experiments were performed at 740 K and three at 630 K. The $NaNO_3$ and $NaNO_2$ statistical experiments were randomized to reduce any systematic error. The KNO_3 statistical experiments were performed after the $NaNO_3$ and $NaNO_2$ experiments. In addition, three isothermal $LiNO_3$ experiments were performed to compare to the other high temperature isothermal experiments. Several graphs are given in the Results and Discussion section that compare and contrast the salts at two temperatures.

In addition to the 3x2 matrix of experiments, other TG/MS experiments with $NaNO_3$, KNO_3, and $NaNO_2$ were performed at intermediate temperatures (between 630 and 740 K). These experiments are also summarized in Tables 15-17. The same experimental techniques and procedure were used for the experiments performed at intermediate temperatures. Also several experiments were performed with $NaNO_3$ prior to the statistical series. (See Table 13.) In these $NaNO_3$ experiments, the proportional temperature controller was used and no planimetry was performed (because the mass spectrometer scanning technique designed above was not used).

The three dynamic heating experiments with $NaNO_3$, KNO_3, and $LiNO_3$ were performed as follows. The samples were prepared and baked out at 330 K for 180 minutes (in vacuum) as for the isothermal experiments.

The furnace was programmed to heat at 25 K per minute to 1000 K and the weight and the sample temperature was recorded every 30 seconds. As in the isothermal experiments, the sample temperature lagged the furnace temperature, therefore the sample temperature rise was not precisely linear; however, the temperature profiles from each of the three dynamic heating experiments were identical. The evolved gases were also recorded in the same manner as for the isothermal experiments. The dynamic heating experiments are also plotted in Appendix C.

The rates of decomposition of the three nitrates were calculated from the dynamic heating experiments data. The average rate of weight change over each 30 second interval was calculated. This rate was assigned to the average sample temperature of that same time interval. Because of electronic fluctuations in the balance output, the minimum detectable rate was .006 mg-min^{-1}.

III D3. TG/MS System

The TG/MS system is shown in Figure 33. The essential elements of the TG/MS system are: the microbalance, the furnace, the gas inlet system, the mass spectrometer, the vacuum system, the data acquisition system, and the control console. These elements are described separately below.

Microbalance

A Cahn R-H microbalance was installed in a stainless steel vacuum-tight housing (Figure 34). As with the Cahn R-G and R-100 balances, its principle of operation is null-balance and electromagnetic compensation for changes in weight. A schematic representation of the microbalance elements is shown in Figure 35. The sample is suspended from one end of

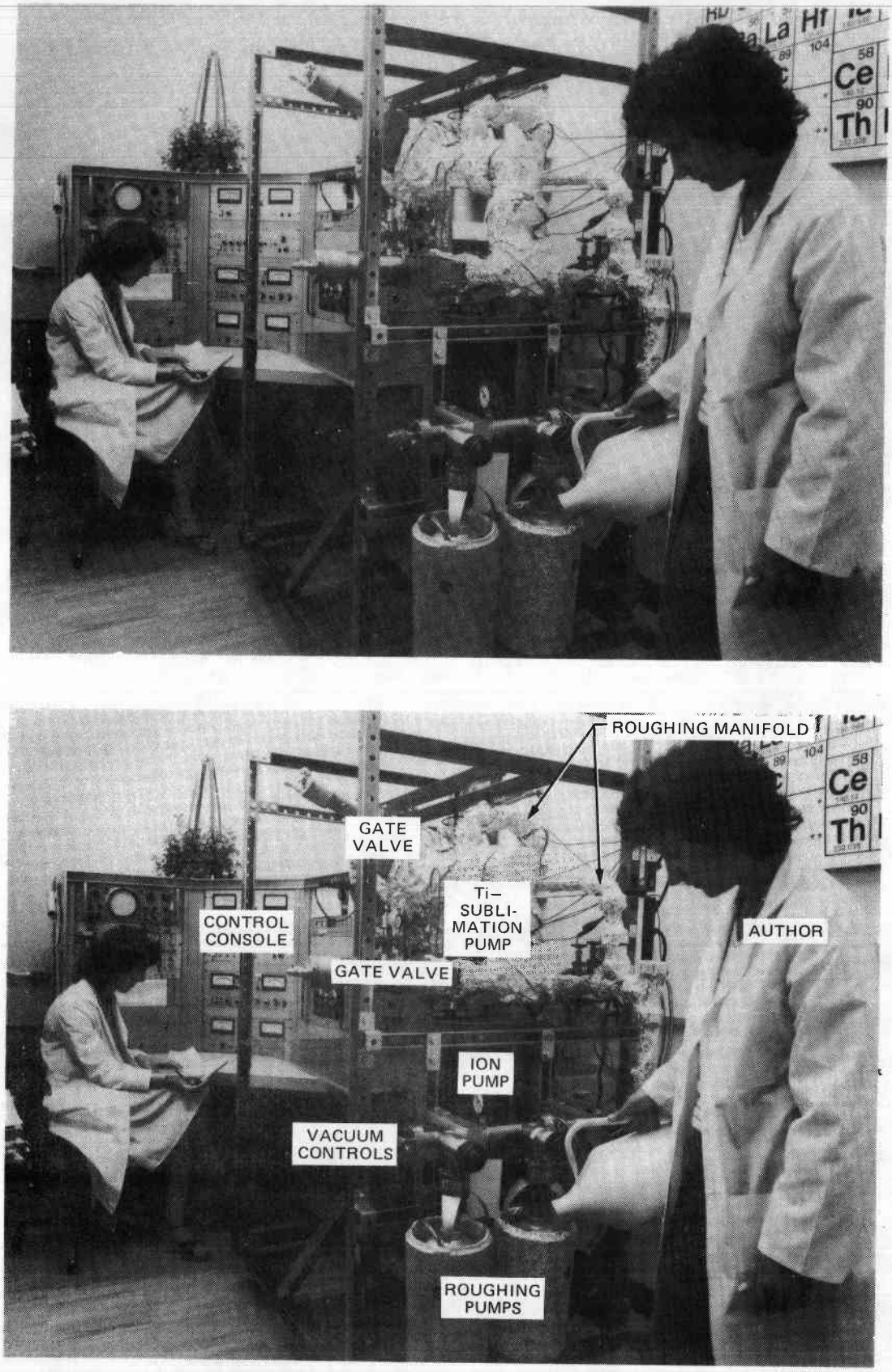

Figure 33. TG/MS System

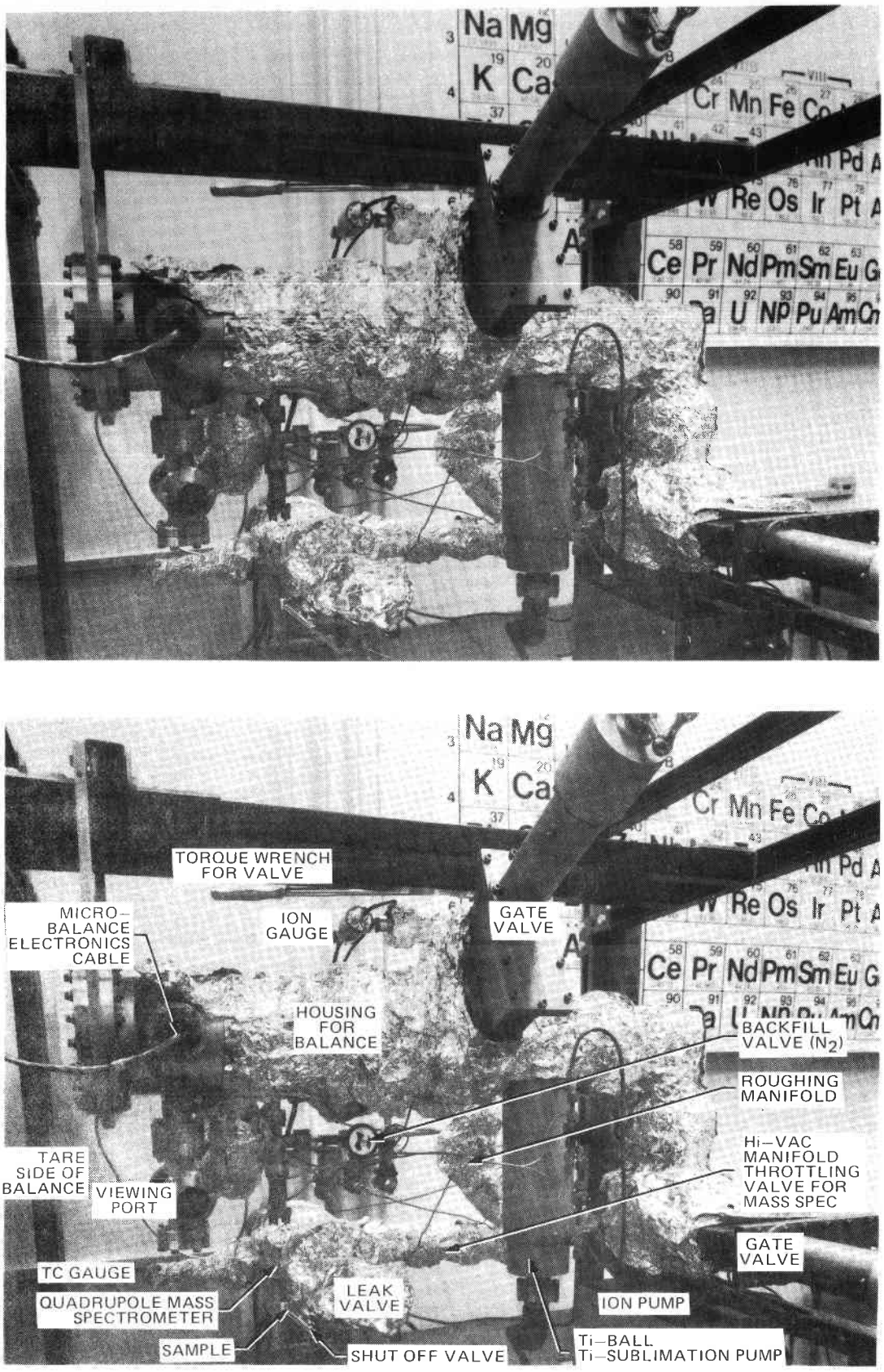

Figure 34. TG/MS Microbalance

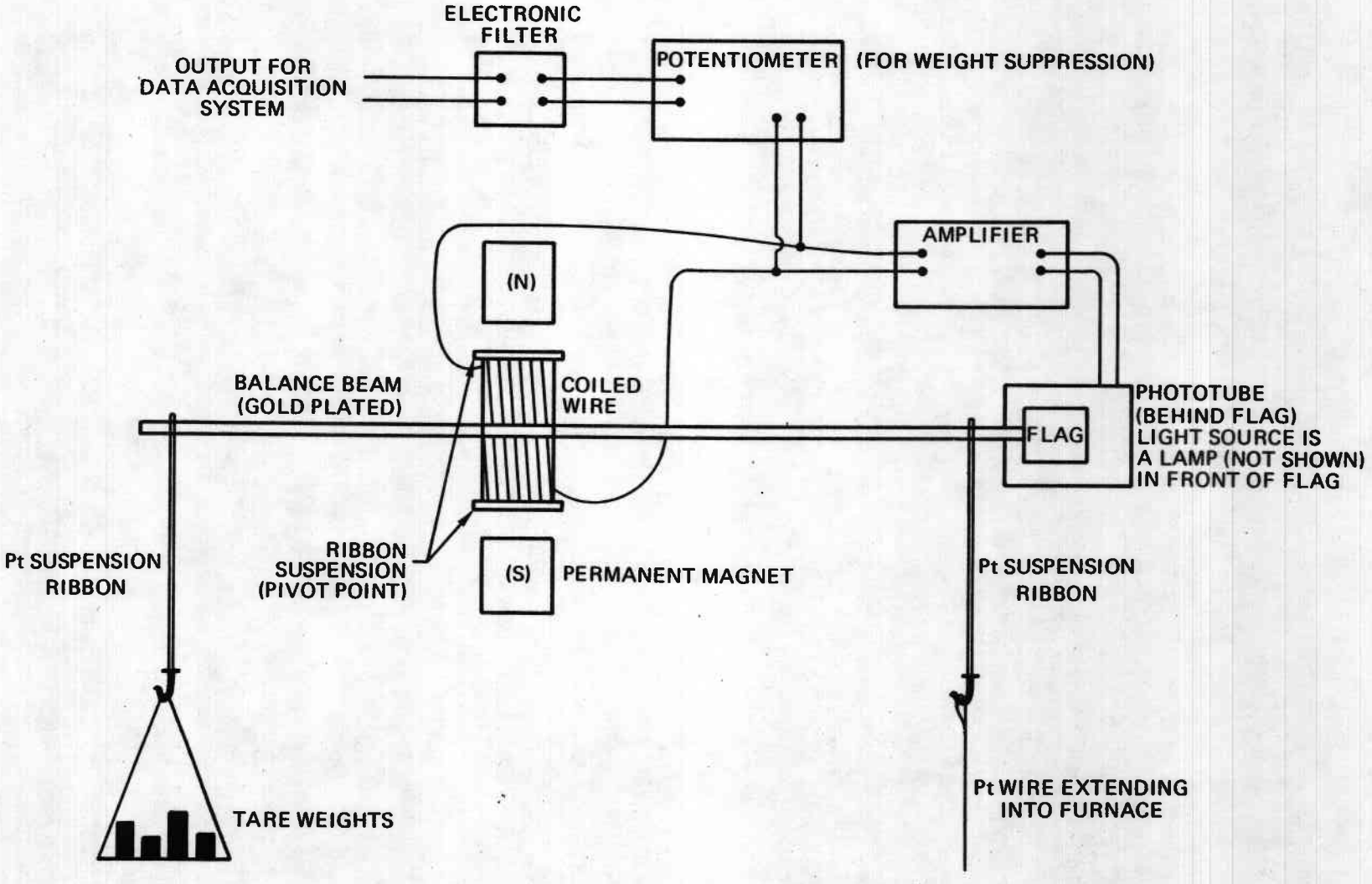

Figure 35. Schematic of Cahn R-H Microbalance

the balance beam and tare weights from the other. A weight change is sensed by the balance when the balance beam pivots which allows light from a lamp to impinge upon a phototube. The phototube is normally shielded by a flag that is mounted at one end of the balance beam. The intensity of the light falling on the phototube causes a proportional restoring force which is amplified and applied to the coil in Figure 35 (which is a magnetic field). The current in the coil (in the magnetic field) exerts a force on the balance beam to restore it to the null position. Additional features of the balance are a potentiometer to change the null output point of the balance (weight suppression) and an electronic filter than smoothes the noise in the voltage ouptut. The voltage output is proportional to the weight. The minimum detectable weight change is 10 μg and the maximum detectable weight change is 10 g. The maximum sample size is 100 g.

The tare weight and the sample hang in tubes that extend from the bottom of the balance chamber. The sample is suspended by a thin wire that extends into the furnace.

Furnace

The furnace is a 19 mm diameter stainless steel tube that is heated externally by a kanthal heater. The furnace design is shown in Figures 36. To protect the balance mechanism from heat, copper cooling coils (in which water was circulated) were silver soldered onto the stainless steel tube above the furnace and below the balance chamber. The furnace can be operated as high as 1273 K and is limited by the oxidation of the stainless steel tube.

For the earlier experiments with the TG/MS system, the furnace temperature was regulated with a non-programmable proportional band

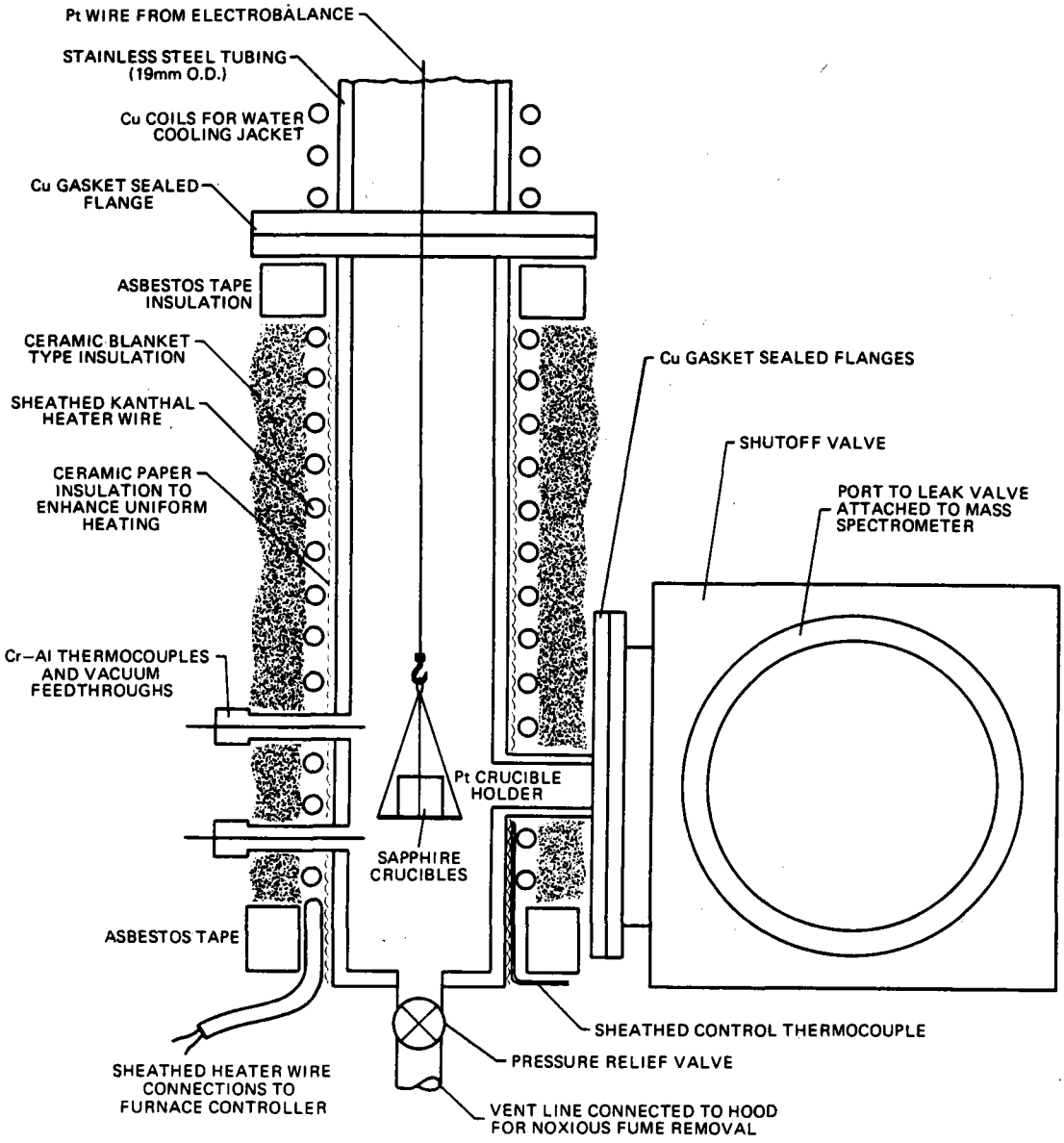

Figure 36. TG/MS Furnace Schematic

controller. For the experiments designated T-45 and higher, a programmable temperature controller was used. This new controller had seven variable length time intervals. Eight temperatures could be specified which were the temperatures the controller would achieve at the beginning (and end) of each time interval. For instance, when the interval for time segment 1 was 2 hours and temperatures 1 and 2 were 298 and 373 K, the temperature is linearly ramped from 298 K to 373 K in 2 hours. Isothermal experiments were achieved by setting two successive temperatures to the same value. In addition to the programming features, the controller had a variable reset rate, variable proportional band, adjustable maximum power output level, and an integrating rate of approach to temperature control. These features vastly improved the performance and contollability compared to the proportional controller of the furnace. Temperature drift greater than 3 K and overshooting the desired temperature were eliminated.

Some experiments were performed to characterize the furnace's behavior. In one test the furnace temperature was determined to be uniform within 5 K over approximately 5 cm in the central heating zone where the sample was suspended. Another experiment was performed to measure the temperature of the salt more precisely. For this test a thermocouple was inserted through the bottom of the furnace and positioned in a $NaNO_3$ sample (which prevented the balance from operating properly). The temperature of the salt was recorded along with the temperatures of the two other thermocouples in the furnace shown in Figure 36 and 37. The system was equilibrated at many different furnace temperatures and the three thermocuple readings were recorded. The thermocouple readings from the side of the furnace were compared to the temperature of the salt sample.

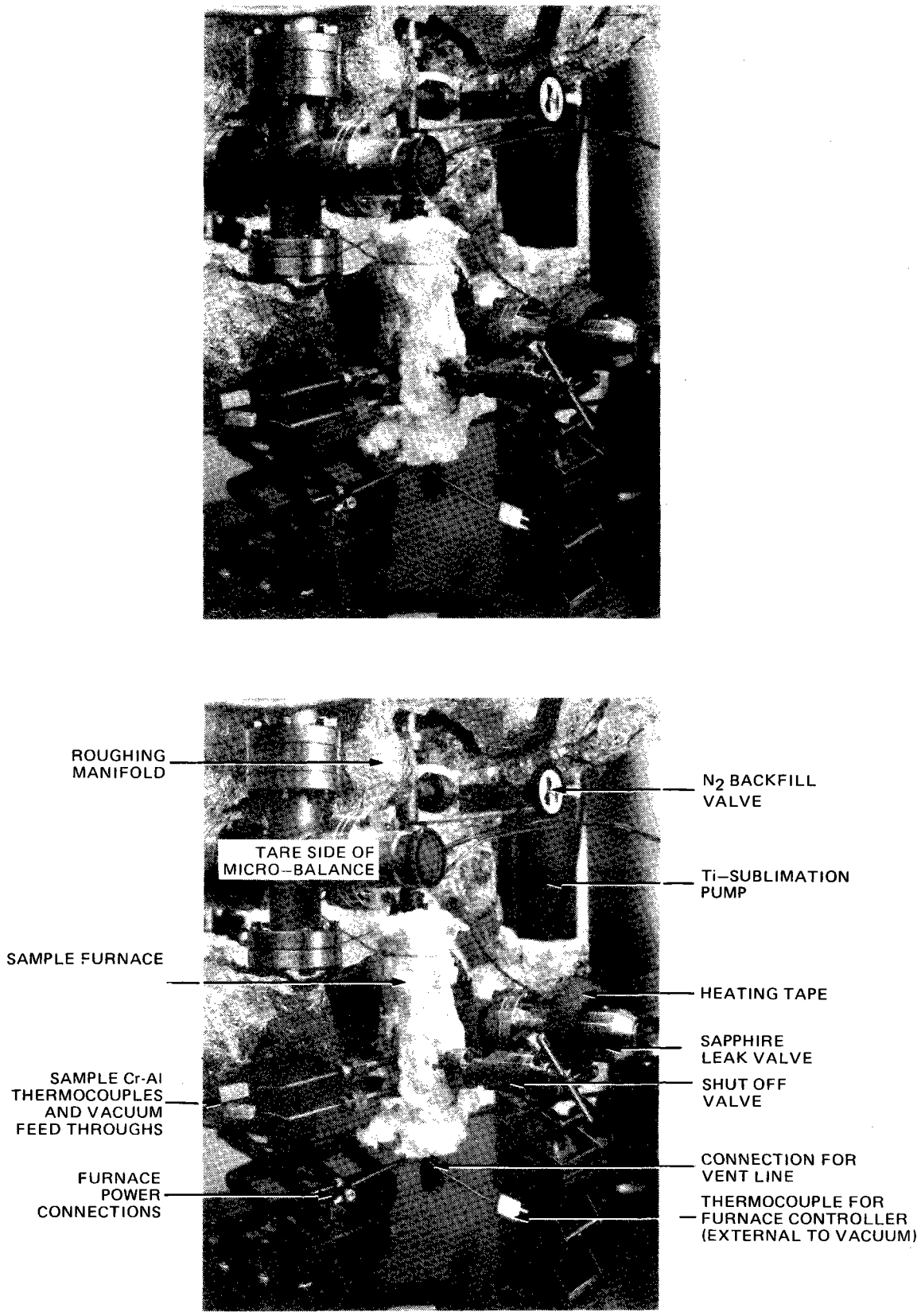

Figure 37. TG/MS Furnace and Gas Inlet System

Other researchers have been concerned that the endothermic reactions their samples undergo may cause erroneous temperature readings during their experiments.[155] To address this problem I compared the thermocouple readings from the salt temperature calibration experiment that was described above. A linear least squares fit of the temperature of lower side thermocouple (T_{side}) versus the actual salt temperature (T_{salt}) for temperatures greater than 400 K was made. The equation that describes the relationship between the two thermocouple measurements is:

$$T_{salt} = 1.025\ T_{side} + 39.91 \qquad (54)$$

Because the slope (1.025) is nearly 1, the two thermocouples differ in temperature by a constant. If the salt decomposition reactions caused a change in the sample's temperature, the thermocouple temperatures would not be displaced by a constant for all temperatures. Also, I carefully examined the salt temperature trace as the temperature was elevated through the melting point of the salt. No inflection was observed in the salt temperature versus time curve at the melting point. This lack of an inflection and the constant temperature difference between the two thermocouples led me to conclude that the enthalpic changes that occur as the salt decomposes did not influence the salt temperature.

The salt temperature experiment provided me with insight into the heat transfer characteristics of the furnace. The observed salt temperature was always much higher than the temperatures of the thermocouples that were inserted through the side wall. See Equation (54). It appeared to me that the vacuum feedthroughs in the side of the furnace caused sufficient heat conduction to alter the furnace temperature locally. As a result, the location of the thermocouples was changed.

The lower thermocouple was moved from the side position, where it extended underneath the sample, to the bottom of the furnace. In this bottom position the thermocouple extended to within 3 mm of the bottom of the sample. All temperatures recorded prior to this thermocouple modification were corrected by using Equation (54) for the kinetic data analysis.

Gas Inlet System

A unique feature of this TG/MS system is that the sample may be decomposed in vacuum or at any pressure up to 1 atm and mass spectrometry of the evolved gases may be studied in either case. A gas sampling system had to be devised to couple the vacuum chamber for the mass spectrometer (which must be kept at less than 10^{-4} torr) to the sample chamber, which may be at 760 torr.[156] To achieve this pressure drop, a small (6 mm) tube was welded in the furnace wall at the upper edge of the sample crucible. This tube was connected to a shutoff valve bolted to a sapphire (sapphire-copper seal) leak valve. The leak valve provides a variable but reproducible control of the gas flow into the mass spectrometer.[101] This system allows time-resolved detection of decomposition processes, which apparently has not been applied to the nitrates before. Figures 37 and 38 are photos of the two valves of the inlet system.

In the later experiments the 6-mm tube from the furnace to the leak valve was replaced by flexible stainless steel tubing approximately 8 cm longer than the other design. The connections were much more convenient and the gas inlet and mass spectrometer behaved the same as with the shorter inlet.

Tests were made to see how rapidly evolved sample gases could be detected by the mass spectrometer. The results of these tests indicated

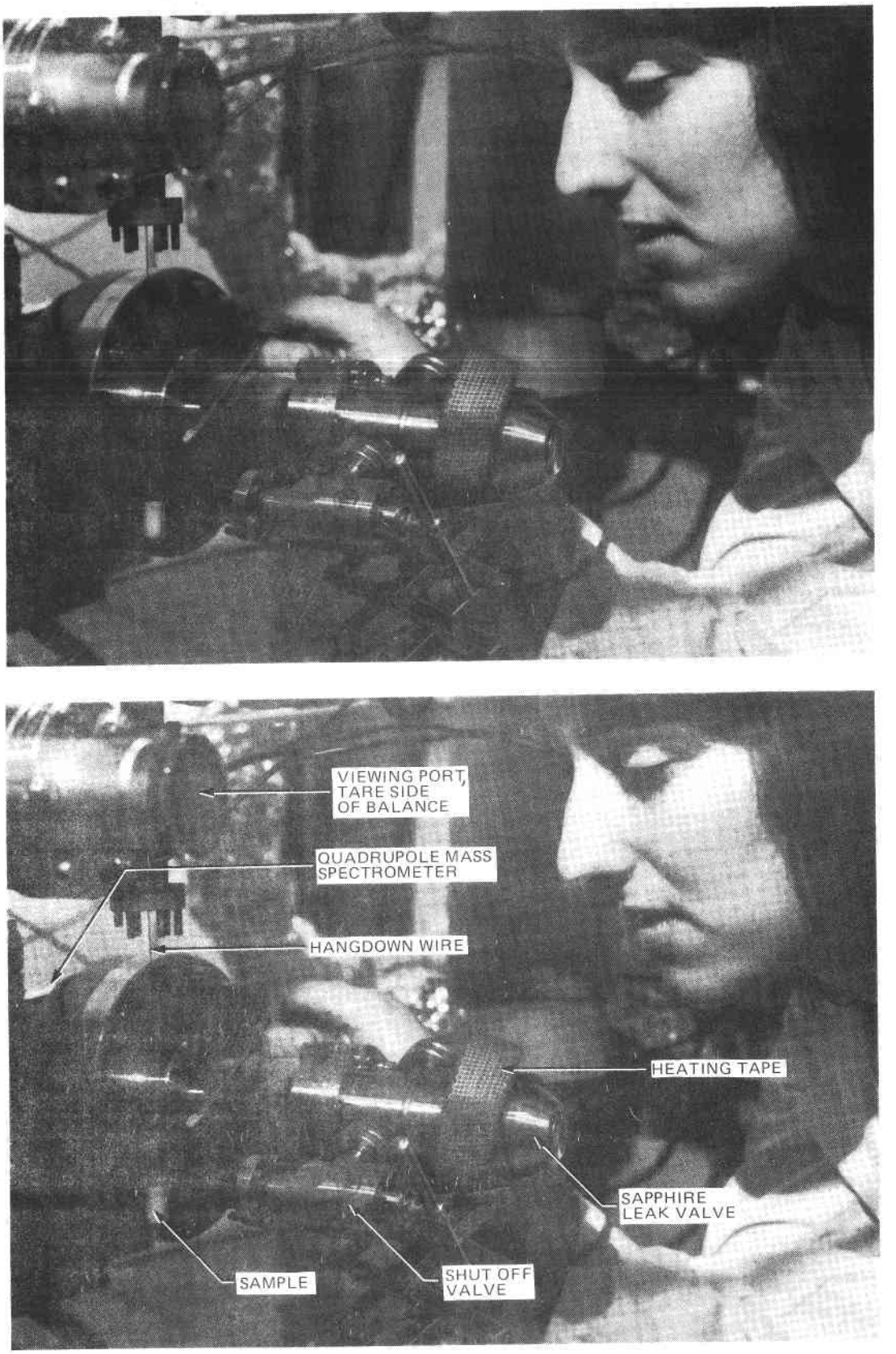

Figure 38. TG/MS Gas Inlet System

that the mass spectrometer detected gases from the sample chamber in less than 30 seconds at 1 atmosphere and in less than 1 second for samples in vacuum.

A disadvantage of this gas sampling arrangement is that vapor species that are condensible at room temperature could not be detected. These vapors condense on the circuitous and relatively cold route to the mass spectrometer. Although systems have been built that can sample and detect condensible species from 1 atmosphere[21,113,156-158], the cost and design difficulties were prohibitive for this work.

Mass Spectrometer

The mass spectrometer (see Figures 38 and 39) is an Extranuclear Laboratories quadrupole mass spectrometer. A quadrupole mass spectrometer is a relatively compact unit which does not use magnetic fields (that may interfere with other instruments), and can be used at relatively high pressures ($\leq 5 \times (10^{-5})$ Torr) because ion velocity and collisions are unimportant to its operation. The incoming gases are partially ionized by electron impact from a hot filament. The chemical species of positive ions are unique in kind and in amount for the gas and are discriminated by the quadrupole mass filter. The reader is referred to References 152 and 159 for discussions of the principles of mass spectrometer operation. A brief description of the quadrupole mass filtering principles as first described by Paul[160-162] are given below.

The mass filter has four cylindrical rods arranged in a rectangular array, between which ions are injected longitudinally (the ions are accelerated by an extractor lens into this region). The four rods are subjected to superimposed direct current and radio frequency voltages (U

and V cos ωt, respectively). One pair of rods (at opposite corners of the rectangle) is at a positive potential while the other pair is at a negative potential. The voltages create a combination alternating and direct current potential to form fields of hyperbolic geometry in the region between the rods where the ions are injected. The potential ϕ in the analyzing region is

$$\phi = (U + V \cos \omega t) \frac{x^2 - y^2}{r_o^2} \tag{55}$$

where the centers of the rods are separated by $2r_o$. The distances x and y are measured in the plane perpendicular to the axes of the rods.

Paul[160-162] conceived the idea for the mass separation by this form of the potential by recognizing that the equations of motion of the ions in between the rods will conform to Mathieu's differential equations,

$$m\ddot{x} + 2q(U + V \cos \omega t) \frac{x}{r_o^2} = 0 \tag{56}$$

$$m\ddot{y} + 2q(U + V \cos \omega t) \frac{y}{r_o^2} = 0 \tag{57}$$

$$m\ddot{z} = 0 \tag{58}$$

where q is the ion's charge and m is the ion's mass. Stable solutions to these equations, where the ions resonate between the rods (where x,y remain finite) are possible for given values of U, V, w, q, and r_o for a range of masses. Stable solutions mean that the ions proceed down the axis of the mass filter and are detected by the multiplier at the end of the rods. Commercial instruments vary both U and V (but not U/V or ω) to scan a spectrum of masses.

The mass spectra obtained from a quadrupole mass spectrometer may be qualitatively and quantitatively analyzed by standard techniques.[152,159] In analyzing the spectra one makes these assumptions: 1) Each gas molecule gives a constant and characteristic spectrum, 2) the spectrum of a gas mixture is a superposition of the individual species, 3) the ion current is proportional to the partial pressure of the gas.

The Extranuclear mass spectrometer I used had an axial ionizer and a 14-stage Cu-Be multiplier-detector. The quadrupole rods were 9.52 mm in diameter and could detect masses in the range 1-208 amu. To facilitate comparisons of experiments, the electron optics were adjusted so that the ion intensities were insensitive to small changes in the lenses. The ionizing energy was 100 ev and the multiplier voltage was 2400 V.

Vacuum System

A vacuum system was built to house the mass spectrometer and create the vacuum conditions for certain TG/MS experiments. The components were made entirely of stainless steel and are shown schematically in Figure 39. A rough vacuum (approximately 10 μm) was created by an air aspirator and cryogenic pumps (Varian Vacsorb pumps). High vacuum conditions were possible by using the ion pump (220 l/sec) and a titanium sublimation pump. Several valves were strategically placed in the system to allow various chambers to be isolated. The balance chamber could not be heated with heating tape to bake out water (because the balance mechanism was sensitive to heat); however, the sample chamber could be pumped down to 10^{-7} torr. The rest of the vacuum system could be isolated and baked out so the pressure in the mass spectrometer was as low as 1×10^{-9} Torr.

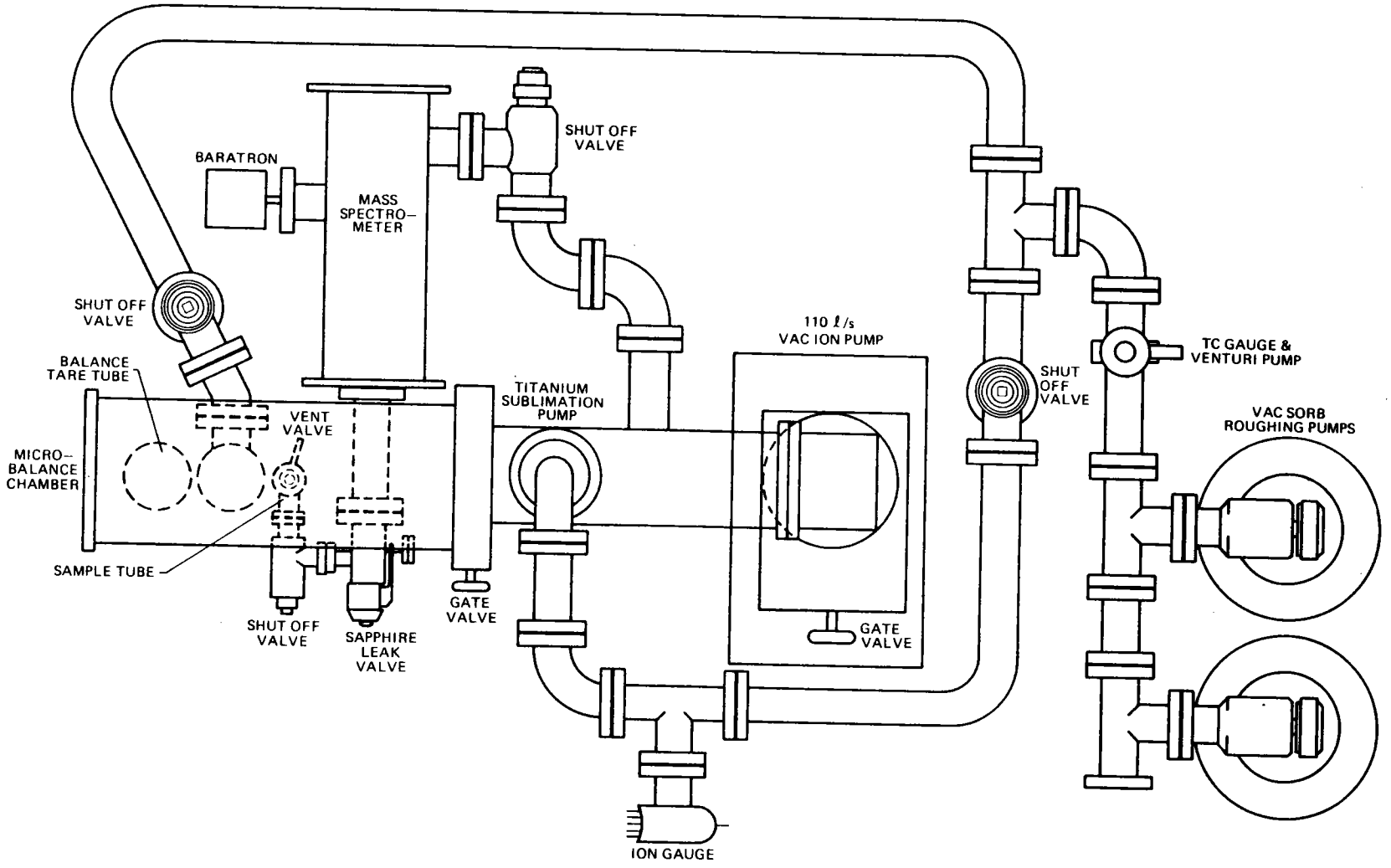

Figure 39. Schematic of TG/MS Vacuum System

The residual gases in the system were predominantly water vapor, nitrogen, and carbon monoxide. Carbon dioxide, hydrogen, and argon (argon is poorly pumped by ion pumps) were minor species in the background. No oxygen or any other species were present in the background. Because CO, H_2O, and CO_2 peaks were always elevated as the mass spectrometer was warming up, the mass spectrometer was allowed to operate for one hour before an experiment and create a stable background spectrum. Gases emanating from the hot furnace walls entered the mass spectrometer because the gas inlet system was not a line of sight system over the sample. The kind and the amounts of the gases were determined by operating the furnace without a sample in it. Masses 28, 18 and 44 (N_2 and CO, H_2O and CO_2) intensities temporarily increased when the furnace was heated. These peaks quickly (in less than five minutes) fell to equilibrium values. Several empty runs at high and low temperatures (750 K and 630 K) were performed to establish background levels for these gases.

Data Acquisition System

A data acquisition system was incorporated into the TG/MS system to make it easier to analyze the thermogravimetric data. Data analysis systems have been attached to thermogravimetric units[163] and TG/MS systems.[138] Some systems have computers programmed to gather and plot the thermogravimetric data.[163,164] In the present system, (described in Reference 165) the balance output voltage was fed into a 5-digit digital voltmeter. A microprocesser unit was assembled to read the digital voltmeter and two digital chromel-alumel thermocouples at intervals determined for each experiment. At the start of each experiment the test duration at the interval between data points was chosen,

which was 30 - 120 sec. The thermocouple readings (in degrees Celsius) and the voltmeter output were printed on a teletype. These data were digitized and read into the CDC 6600 computer for the kinetic analysis that was described at the beginning of Section III D.

Control Console

The electronics for the vacuum system, the mass spectrometer, the furnace, and the data analysis system were all mounted in the control console shown in Figure 40. In this arrangement the experiments were easily monitored and controlled.

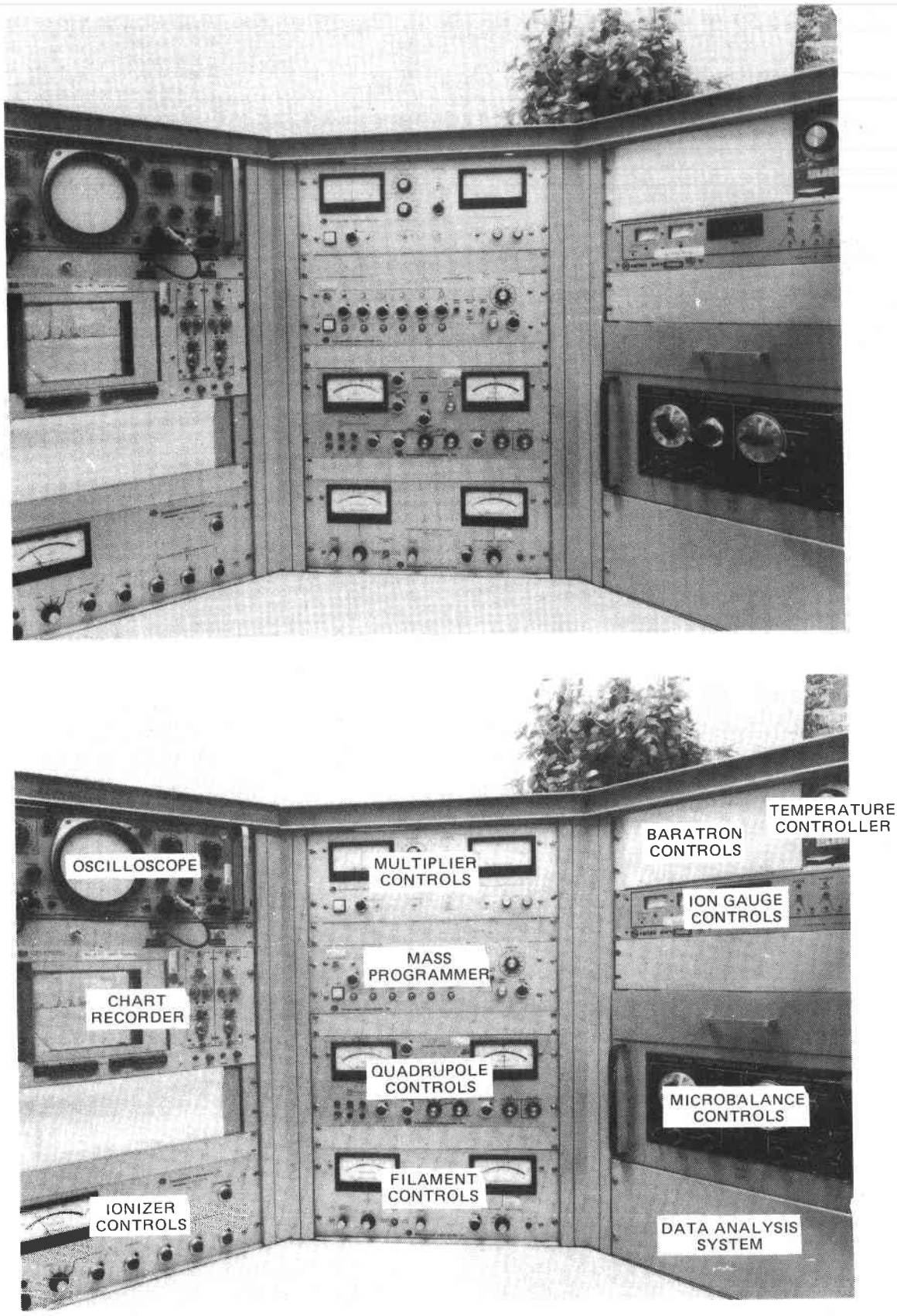

Figure 40. TG/MS Control Console

IV. RESULTS AND DISCUSSION

IV A. Differential Scanning Calorimetry Results and Discussion

Thermal spectra were made of $NaNO_3$, KNO_3, $(Na,K)NO_3$, $NaNO_2$ and KNO_2 using the DSC technique. Large endothermic peaks were observed for each salt at the temperatures corresponding to the reported melting point of each salt. Above the melting point of each salt, the DSC traces became noisey, a behavior that is uncharacteristic of the DSC. Furthermore, above the melting point of each salt endothermic reactions occurred. Sometimes the DSC trace very abruptly went off-scale (> 10 mcal-sec displacement) indicating an endothermic reaction. However the temperatures at which these abrupt endotherms occurred was not reproducible. Usually, the salts were observed to be leaking out of their pans when these abrupt endotherms occurred. If abrupt endothermic reactions did not occur, gradual endothermic reactions occurred. In other words, the differential energy required to heat the sample relative to the empty pan slowly increased, indicative of an endothermic reaction at elevated temperatures. The melting points and the temperature at which either abrupt or gradual endothermic reactions began are given in Table 20. These are the results of 2-10 experiments with each salt. Also included in Table 20 are the DTA endothermic decomposition peaks reported in the literature.[36,89]

The DSC thermal spectra obtained from the gold plated stainless steel and the stainless steel pans differed slightly. Some of the DSC traces where stainless steel pans were used had small exotherms. This indicated that the Cr_2O_3 on the surface of the stainless steel was reacting with the salt since chromium oxide has been observed to react with KNO_3.[14,83] Also decomposition of the nitrates is endothermic

Table 20

DSC and DTA Studies of Nitrates and Nitrites

Sample	Onset of Decomposition Endotherm	Melting Point	Reference
$NaNO_3$-Al_2O_3[a]	1006 K	589 K	36
$NaNO_3$-MgO[a]	1029 K	610 K	36
$NaNO_3$	793 K	579 K	89
$NaNO_3$	840 ± 10 K	579 K	This Work
KNO_3-Al_2O_3[a]	958 K	610 K	36
KNO_3-MgO[a]	1027 K	642 K	36
KNO_3	901 K	610 K	89
KNO_3	820 ± 20 K	609 K	This Work
$(Na,K)NO_3$	900 ± 10 K	498 K	This Work
$NaNO_2$	800 ± 10 K	558 K	This Work
KNO_2	800 ± 10 K	704 K	This Work

[a]Salt was mixed with oxide powder.

according to the calculations presented in Section IC. The exothermic peaks were not present in the spectra of samples in Au-plated stainless steel pans.

From these results I drew several conclusions. The onset of decomposition endotherms reported by DTA and DSC techniques depended on the technique, its sensitivity and the container material. The decomposition reactions gradually accelerated above the melting point of the salts. The DSC results showed that sodium nitrite and potassium nitrite begin to decompose at 800 K ($\pm$ 10 K). Sodium nitrate, potassium nitrate, and a 50/50 molar mixture of the two nitrates had endothermic reactions in the DSC beginning at approximately 840, 820 and 900 K, respectively. The nitrates were slightly more stable than the nitrites and a mixture of $NaNO_3$ and KNO_3 was more stable with respect to decomposition than the salts were separately.

IV.B. Plackett-Burman Screening Tests' Results

The significant variables are the ones whose statistical effect exceeds the value of the minimum significant effect ("min") calculated for that experimental response. The experimental responses are tabulated in Tables 21 and 22. The effect of each variable is tabulated in Table 23 for the nitrate matrix and Table 24 for the $NaNO_2$ experimental matrix along with the "min" for each response.

The important variables causing a specific response can be ranked by the absolute values of their effects. The sign of the effect indicates their coding. For instance, the positive effect of temperature on carbonate response means that as temperature increases (from its low

Table 21

Placket Burman Responses for Nitrate Experiments[a]

Trial	NO_3^-	NO_2^-	$CO_3^=$	pH	Na/K	Spreading	Color	Mass Transport
1	51.5	10.1	5.23	11.7	0.444	0	2	3
2	0.85	0.21	62.6	11.5	88.4	2	2	3
3	63.3	0.42	0.1	6.2	0.337	0	0	0
4	64.1	1.37	0.1	8.0	86.8	0	0	0
5	6.60	1.86	60.2	11.2	164.	2	0	3
6	38.2	17.2	20.1	12.0	58.8	1	3	3
7	4.41	0.79	63.4	11.5	289.	2	0	3
8	31.7	20.5	23.5	12.2	488.	1	3	0
9	68.8	0.26	0.1	6.4	2430.	0	0	0
10	35.8	11.7	22.7	11.2	1.58	1	2	3
11	66.9	2.08	0.1	6.0	0.432	0	1	0
12	34.3	30.3	1.75	10.7	253.	0	2	2
13	56.5	0.24	0.1	8.0	0.777	0	0	1
14	69.4	5.19	0.1	6.8	0.977	0	0	0
15	67.0	0.18	0.1	6.6	1200.	0	0	0
16	70.8	0.37	0.1	6.0	12400.	0	0	0
17	51.1	12.9	2.94	10.1	0.240	0	0	3
18	39.0	8.20	1.74	9.7	0.551	1	0	0
19	64.6	0.69	0.1	7.8	0.841	0	0	0
20	60.4	0.47	0.1	6.9	111.6	0	0	0

[a] NO_3^-, NO_2^-, $CO_3^=$ are weight percentages and Na/K is a ratio of weight percentages.

Table 22

Placket Burman Responses for $NaNO_2$ Experiments[a]

Trial	NO_3^-	NO_2^-	$CO_3^=$	pH	Na/K	Spreading	Color	Mass Transport
1	52.7	12.1	14.7	12.1	97.9	0	2	3
2	0.05	1.76	64.5	11.4	393.	2	2	3
3	25.5	60.5	2.46	10.1	60.6	0	0	0
4	1.20	70.0	0.10	9.2	1010.	1	0	0
5	12.10	3.38	50.5	10.5	1.72	2	0	3
6	40.6	18.3	16.5	12.3	281.	1	3	3
7	0.95	0.06	62.5	11.3	377.	2	0	3
8	20.4	21.1	50.7	12.3	4910.	1	3	0
9	10.1	53.1	0.26	10.0	65.6	0	0	0
10	35.4	12.1	29.7	11.9	70.6	1	2	3
11	16.7	58.4	0.10	8.2	105.	0	1	0
12	15.3	20.5	29.3	12.2	141.	0	2	2
13	3.00	60.3	0.23	9.2	102.	0	0	1
14	15.7	51.1	3.96	10.3	215.	0	0	0
15	17.7	51.2	2.14	10.2	497.	0	0	0
16	22.6	52.1	0.13	10.7	6520.	0	0	0
17	52.5	15.1	4.42	10.6	125.	0	0	3
18	22.4	1.20	26.8	10.8	370.	1	0	0
19	34.1	38.0	0.10	8.7	80.3	0	0	0
20	3.76	57.1	0.10	8.6	2270.	0	0	0

[a] NO_3^-, NO_2^-, $CO_3^=$ are weight percentages and Na/K is a ratio of weight percentages.

Table 23

Effects of Experimental Variable sin the Nitrate Screening Experiments[a]

Response	Minimum Level of Significance	Effects of Experimental Variables[a]									
		Temp.	Oxygen	Nitrogen	Carbon Dioxide	Relative Humidity	Flow Rate	Surface Area	K/Na	Size	Purity
$CO_3^=$	11.4	26.3	(3.96)	(-.77)	11.8	(-3.5)	12.2	(-8.13)	(-7.85)	(-8.07)	-19.4
NO_2^-	5.30	10.2	(-2.98)	(-.005)	(-6.23)	(1.20)	(3.47)	(2.6)	(-1.83)	(0.75)	?4.56
NO_3^-	8.32	-35.8	(2.88)	(1.69)	-7.61	(5.0)	-10.6	(0.36)	(6.4)	(2.6)	14.4
pH	0.55	4.31	(0.09)	(0.13)	-0.45	0.45	(0.19)	(0.11)	(-0.31)	(-0.17)	-0.93
Na/K	2100.	(-1480)	(1320.)	(1120.)	(-900.)	(860.)	(-1120.)	(-1400.)	-1700.	(1290.)	(1590.)
Spreading	0.40	1.0	(0.0)	(0.04)	(0.16)	(0.04)	(0.04)	(0.04)	(0.04)	(0.04)	(0.36)
Color	0.55	1.3	(-0.3)	(0.01)	- 1.1	0.5	(-0.3)	0.5	-0.5	(-0.3)	(0.1)
Mass Transport	0.66	2.2	0.6	-0.6	(0.0)	0.6	0.6	(-0.2)	(0.2)	(0.0)	-0.8

[a]Those effects in parentheses were not considered to be significant. A question mark indicates a questionable influence of the variable. These effects are dimensionless numbers determined by the statistical analysis described in Appendix B.

Table 24

Effects of Experimental Variables in the $NaNO_2$ Screening Experiments[a]

Response	Minimum Level of Significance	Effects of Experimental Variables[a]							
		Temp.	Oxygen	Nitrogen	Carbon Dioxide	Relative Humidity	Flow Rate	Surface Area	Size
$CO_3^=$	12.6	34.0	(-6.06)	(-0.094)	(7.61)	(-4.38)	9.34	(-4.28)	(-4.81)
NO_2^-	6.61	-44.6	(-1.63)	(-0.16)	(-4.26)	6.73	-5.76	(-1.23)	(-0.91)
NO_3^-	13.6	10.3	(8.4)	(6.1)	(-8.6)	(6.5)	(-3.5)	(3.1)	(-1.)
pH	0.684	2.0	(-0.34)	(0.28)	(-0.18)	?0.58	(0.22)	(-0.2)	(-0.2)
Spreading	0.54	0.9	(0.1)	(0.3)	0.5	(-0.1)	(0.1)	(-0.1)	(-0.1)
Color	0.56	1.3	(-0.3)	(0.1)	-1.1	0.5	(-0.3)	0.5	(-0.3)
Mass Transport	0.73	2.2	0.6	-0.6	(0.0)	0.6	0.6	(-0.2)	(0.0)

[a]Those effects in parentheses were not considered to be significant. A question mark indicates a questionable influence of the variable. These effects are dimensionless numbers determined by the statistical analysis described in Appendix B.

level to its high level), carbonate ion content increases. The negative effect of temperature on the nitrate response in Table 23 means that as temperature increases, the nitrate ion content decreases.

The Plackett-Burman test matrix can also be separated into high- and low-temperature experiments without destroying the balance of the matrix. Although balanced, the separate experiments are not orthogonal and do not have the good mathematical properties of the Plackett-Burman-experiment. The same type of statistical analysis was separately applied to the high- and low-temperature experiments. Because the high- and low-temperature matrices are not orthogonal, the apparent importance of variables in the separate analysis may be spurious where the overall analysis does not indicate importance. Nevertheless, the separate temperature analyses are useful to point out which responses occur only at high or low temperature or which variables influence a response only at high or low temperature. The results of the high- and low-temperature analyses are given in Tables 25 - 28.

The remainder of the results section is divided into specific discussions of each of the responses.

Mass Transport

The mass transport response is an estimate of the amount of material carried downstream in vapor to the end of the furnace where the gases exit. It is a combined effect from the nitrate and nitrite matrices because the nitrate and nitrite experiments were run concurrently. The estimated amount of transported material in an experiment was less than 1%. The dominant variable enhancing mass transport is temperature, which has a positive effect. No mass transport occurred in the low temperature experiments. The purity also affected mass transport, but with a

TABLE 25

HIGH TEMPERATURE EFFECTS ON NITRATES

Response	Minimum Level of Significance	Independent Variables[a] O2	N2	CO2	Relative Humidity	Flow Rate	Surface Area	K/Na	Size	Purity
Mass Transport	1.4	1.4(1)	-1.0	0.2	0.2	1.0	-0.2	0.2	-0.2	-1.4(1)
Na/K	206.	-64.	16.	-52.	-15.	49.	-108.	-202.(1)	-131.	28
Spreading	0.8	0.0	0.4	0.8(2)	-0.4	0.4	-0.4	-0.4	-0.4	-1.2(-1)
Color	1.0	-0.8	-0.4	-2.0(-1)	1.2(2)	-0.4	0.8	-1.2(-2)	-0.4	0.
$CO_3^=$	22.3	7.9	-1.5	23.5(3)	-7.1	24.4(2)	-16.3	-15.7	-16.1	-38.8(-1)
pH	0.69	0.24	0.16	-0.76(-3)	0.63(?4)	0.28	-0.12	-0.8(-2)	-1.08(-1)	0.6(?-5)
NO_3^-	17.31	2.0	1.8	-17.9(-3)	10.6	-19.6(-2)	6.8	14.9	5.7	24.4(1)
NO_2^-	(0.0)	-5.6	1.0	-13.2(-1)	1.6	-5.4)	3.6	-4.8	2.6	10.0(2)

[a]The significant variables are rank ordered by importance and this rank order is given in parentheses. The + or - indicates if the effect was positive or negative. A question mark indicates the variable was marginally significant. These effects are dimensionless numbers determined by the statistical analysis described in Appendix B.

TABLE 26

LOW TEMPERATURE EFFECTS ON NITRATES

Response	Minimum Level of Significance	O2	N2	CO2	Relative Humidity	Flow Rate	Surface Area	K/Na	Size	Purity
Mass Transport	0.4	-0.2	-0.2	-0.2	-0.2	-0.2	-0.2	0.2	-0.2	-0.2
Na/K	4260.	2700.	2200.	-1700.	1700.	2200.	-2700.	3230.(-1)	2700.	3140.(2)
Spreading	-	0.	0.	0.	0.	0.	0.	0.	0.	0.
Color	0.4	0.2	-0.2	-0.2	-0.2	-0.2	0.2	0.2	-0.2	0.2
$CO_3^=$	-	0.	0.	0.	0.	0.	0.	0.	0.	0.
pH	0.9	-0.06	0.1	-0.1	0.3	0.1	0.3	0.2	0.7(?2)	-1.3(-1)
NO_3^-	5.5	3.7	1.6	2.7	0.7	1.5	2.4	2.0	0.4	4.4(1)
NO_2^-	1.6	-0.4	-1.0	0.7	0.8	-1.5(?-2)	1.6(1)	1.2	-1.1	-0.9

[a]The significant variables are rank ordered by importance and this rank order is given in parentheses. The + or - indicates if the effect was positive or negative. A question mark indicates the variable was marginally significant. These effects are dimensionless numbers determined by the statistical analysis described in Appendix B.

TABLE 27

HIGH-TEMPERATURE EFFECTS ON $NaNO_2$

Response	Minimum Level of Significance	O2	N2	CO2	Relative Humidity	Flow Rate	Surface Area	Size
Mass Transport	1.4	1.4(1)	-1.0	0.2	0.2	1.0	-0.2	-0.2
Spreading	1.0	0.0	0.4	0.8(1?)	-0.4	0.4	-0.4	-0.4
Color	1.0	-0.8	0.4	-2.0(-1)	1.2(2)	-0.4	0.8	-0.4
$CO_3^=$	23.2	-10.5	-0.2	13.6(2)	-9.6	18.7(1)	-9.2	-8.0
pH	0.6	-0.4	0.04	-1.2(-1)	0.4	-0.08	0.4	-0.3
NO_3^-	19.8	13.1	1.2	-15.3	-16.0	-18.0(?-1)	1.9	-0.2
NO_2^-	8.4	-1.5	1.3	-12.5(-1)	6.2	-6.0	0.4	-0.9

[a]The significant variables are rank ordered by importance and this rank order is given in parentheses. The + or - indicates if the effect was positive or negative. A question mark indicates the variable was marginally significant. These effects are dimensionless numbers determined by the statistical analysis described in Appendix B.

TABLE 28

LOW-TEMPERATURE EFFECTS ON $NaNO_2$

Response	Minimum Level of Significance	O2	N2	CO2	Relative Humidity	Flow Rate	Surface Area	Size
Mass Transport	0.4	-0.2	-0.2	-0.2	0.2	0.2	-0.2	0.2
Spreading	0.2	0.1	0.1	0.1	0.1	-0.1	-0.1	-0.1
Color	0.4	0.2	-0.2	-0.2	-0.2	-0.2	-0.2	-0.2
$CO_3^=$	1.2	-1.64(-2)	0.86	1.65(1)	0.8	0.1	0.6	-1.59(-3)
pH	0.9	-0.3	0.5	0.9(1)	0.7(2?)	0.5	-0.4	-0.08
NO_3^-	12.4	3.7	10.3	-1.9	-3.0	11.0(?1)	4.2	-1.8
NO_2^-	11.7	-1.7	-1.6	4.0	7.2	-5.5	-2.9	-1.0

[a]The significant variables are rank ordered by importance and this rank order is given in parentheses. The + or - indicates if the effect was positive or negative. A question mark indicates the variable was marginally significant. These effects are dimensionless numbers determined by the statistical analysis described in Appendix B.

negative effect. Oxygen, nitrogen, the relative humidity, and the flow rate had only borderline importance. The nitrogen content, too, had a negative effect, meaning that a greater N_2 partial pressure reduces mass transport. No explanation was found for either of the negative effects.

At high temperatures the O_2 content and purity were above the minimum significant effect level. The relative humidity was far below the significance level in contrast to the overall analysis. The flow rate and the nitrogen content were close to the minimum level of significance but slightly below the "min" in the high temperature analysis, as was observed in the overall analysis.

Samples of the white deposit that resulted from mass transport were analyzed by X-ray diffraction and identified as $NaNO_3$. The gas flow during the experiments probably caused transpiration of the nitrate vapors. That the gas flow rate appears to enhance mass transport supports this conclusion. Congruent vaporization (see Reaction (5)) of monomers and dimers of $NaNO_3$ and KNO_3 has been observed as low as 623 K for $NaNO_3$ and KNO_3. The equilibrium vapor pressures for $NaNO_3$ and KNO_3 at 600 K are approximately 6×10^{-5} Torr.[75,76] However, since the rates of vaporization are unknown, the significance of these vapor pressures cannot be assessed. Other investigators have observed losses in excess of those calculated for redox or thermal decomposition reactions.[36] The losses were observed to be greater for $NaNO_3$ than for KNO_3 and may be due to the same mass transport processes observed in these experiments.

Na/K

The spread in the high level of the K/Na variable was very large (0.56 - 1.0) because reagent grade mixtures and commercial grade salts

were used. As a result, the Na/K response had such a high minimum level of significance that not even the K/Na variable emerged as significant (see Table 8), although it did have the greatest statistical effect. The Na/K results show the limitations of the experimental matrix.

Since only $NaNO_3$ was identified by X-ray diffraction of the material deposited downstream in the furnace, it was thought that the Na/K ratio in the salts remaining in the crucibles could be correlated with this selective deposit. However, preferential loss of Na from the samples was difficult to detect because the amount of mass transport was small.

Spreading

Excessive spreading of the salts was observed at high temperatures. The salts tended to cover the entire crucible, leaving little salt in the bottom. The spreading phenomena distorts the surface area, particularly of small samples, and surface area may be important to many of the phenomena occurring in nitrate salts, such as Reactions (1) or (5). Spreading is a problem that has interfered with other investigations of the nitrates and nitrites.[36,84]

As in the mass transport phenomena, the primary factor that enhances spreading of the nitrates or nitrites is high temperature. It was observed that creep did not occur in the low-temperature experiments. At high temperatures, CO_2 and the salt purity influence spreading. Purer salts tended to spread less, suggesting that impurities influence the surface energies. Higher CO_2 percentages also enhanced spreading. That the CO_2 content affected several chemical phenomena may be reflected by greater spreading of the salts as CO_2 content increased.

Color

Some of the salt samples developed a pale chartreuse color. Temperature was the dominant variable causing coloration of the melt. No change in color of the samples from the low-temperature experiments was observed. Carbon dioxide was the second most significant factor. At high temperatures the relative humidity, surface area, and the K/Na ratio also influenced the salt color. No correlation of the color with trace metals was found.

Carbonate Formation

Carbonate present in the salt samples indicates, among other things, reaction of the salts with CO_2. Carbonates could also be formed by reaction of oxide or hydroxide from a reaction such as (2) or (4) and subsequent reaction with carbon dioxide in the air after the experiment. Therefore the amount of $CO_3^=$ in the samples was a combined response due to Reactions (2), (3) and (4).

The levels of carbonate observed in nitrates were in some instances very large (up to 64%). The variables that affect the amount of $CO_3^=$ found in the nitrate salts samples are, in order of decreasing magnitude; temperature, purity, gas flow rate, and CO_2. Purity has a negative effect on carbonate formation. It is interesting that, of these variables, CO_2 has the smallest effect. This suggests that rates of carbonate formation are not determined by reaction steps involving CO_2 interaction, such as (3). It is possible that carbonates are formed by a sequence of reactions, including

$$Na_2O + CO_2 \rightarrow Na_2CO_3 \qquad (59)$$

but that Reaction (2) is the slow step. For the nitrate salts at high

temperature the dominant variables are (in decreasing order) purity, flow rate, and CO_2, as determined in the overall analyses. At low temperatures the carbonate levels were very low (0.1%).

Hydroxides also rapidly react with CO_2 in air to form Na_2CO_3. Since the relative humidity is not a significant variable, sodium hydroxide formation may not be a necessary step to forming the carbonates. These conclusions are supported by Alexander and Hinden,[5] who comment on the independence of hydroxide and carbonate formation in the nitrate salts studies.

The overall analysis of factors affecting carbonate formation in nitrites showed that high temperature and possibly high flow rates encouraged carbonate formation. This suggests that thermal decomposition of the nitrites to oxides (and subsequent reaction with CO_2) is the primary source of carbonate formation in the nitrites. The nitrite experiments at high temperature had no significant variables causing carbonate formation although the carbonate levels were rather high (4-64%). At low temperature the carbonate contents were 0.1-4%. The low-temperature analysis of the nitrite experiments showed that CO_2, O_2 (negative effect), and sample size (also negative) affected the carbonate formation. These results indicate that at high temperatures, nitrite decomposition to oxides is prevalent (since CO_2 was not a significant variable) and at low temperatures, reaction of the nitrites with CO_2 dominates the accumulation of carbonate in the salts. Comparing the levels of carbonate in the nitrate and nitrite samples shows that the nitrites are most susceptible to reaction with carbon dioxide and thermal decomposition, as found in the literature.[8,11]

Furthermore, these results indicate that in the nitrite salts, reactions forming carbonate (positive effect of CO_2) are competing with reactions forming nitrate (attested to by the negative effect of O_2 due to occurrence of Reaction 1 in reverse). The ranges in the amounts of NO_3^- and $CO_3^=$ in the nitrites samples were large (0.05-53% and 0.1-64% respectively), perhaps because several reactions are occurring to a significant extent simultaneously. That size has a negative effect on $CO_3^=$ formation leads us to believe that diffusion of CO_2 into the nitrite salt was controlling carbonate formation.

pH

The pure nitrate and nitrite salts have neutral pH (7) when dissolved in water. The overall analysis of the experiments showed that the pH usually went up, or the salts became more basic, as the temperature went up. The lower-purity nitrate samples also had higher pH values. The high-temperature experiments had pH values from 9.7 to 12.3 while the low-temperature samples had pH values from 6.0 - 10.7. The effect of the relative humidity is marginal for both the nitrates and nitrites. The carbon dioxide content has a marginal and negative effect on the pH of the nitrate samples (in other words, CO_2 tended to keep the pH closer to 7) and no effect on the nitrites.

At high temperatures the basicity of the nitrates is minimized by large samples, high potassium nitrate contents, and high CO_2 percentages. High relative humidity or low purity had marginal statistical effects and may enhance basicity in the nitrates at high temperatures. Because size and the potassium content are influential variables, a diffusion-controlled process--such as gas diffusion into the melt to react with

the sodium species--is suggested. At low temperatures the pH of the nitrates is only influenced by purity. The low-temperature nitrate sample had pH values that were the closest on the average to 7. (It is interesting that these samples also have the lowest carbonate contents.) Therefore the effect of salt purity on pH may be due to basic impurities present in the starting commercial grade salts such as hydroxide ion.

The pH of the nitrite salts at low temperature were not significantly influenced by any variable, although carbon dioxide and the relative humidity were marginal in their effects. Thus, in contrast to the nitrates, size is not an influential variable. (Purity and the K/Na ratio were not variables in the nitrite experimental matrix.) At high temperature, the nitrites were influenced by CO_2 only, which tended to reduce the pH. The negative influence of CO_2 on the pH may be understood if one considers the products of Reactions (2) and (3), oxide and carbonate, respectively. The oxide becomes hydroxide when dissolved in water for the pH titration. Hydroxide is a very strong base compared with carbonates. Therefore, increasing the CO_2 content of the gas, which causes increased carbonate formation during, or after the experiment, will tend to detract from the available salt for oxide or hydroxide formation during or after the experiments, and thereby lower the pH. The negative effect of CO_2 on the pH, which appears beneficial, is in fact due to another deleterious effect that CO_2 causes, namely, carbonate formation. Relative humidity does not seem to be an important factor for the pH of the nitrites.

It appeared there was a positive correlation of the color and the pH. We plotted the pH and the color responses are plotted in Fig. 41. Such a simple way to evaluate the salts' pH may prove useful.

Nitrate Content

The factors affecting nitrate content are the same as those that affect the carbonate content of the nitrate samples. However, the signs of the effects are opposite. The ranking of the important variables (in order of increasing effect: CO_2, flow rate, purity, and temperature) is also the same for the nitrate and carbonate responses in the nitrate samples. Thus it appears that carbonate is developed at the expense of nitrate. Because nitrites are less stable than the nitrates, it was expected that the correlation of $CO_3^=$ content would be related to the NO_2^- content or be influenced by the same variables as the NO_2^- content. The correlation of NO_3^- and $CO_3^=$ indicates that NO_3^- decomposes or reacts directly without first decomposing to NO_2^-. To demonstrate this inverse relationship Figure 42 was constructed, which plots the nitrate content versus the carbonate content for each nitrate salt sample.

The high-temperature nitrate experiments were influenced by the variables identified in the overall analysis. However, at low temperatures the nitrate content was unchanged and unaffected by any variable, indicating nitrate salt stability at 600-650 K with respect to decomposition to oxide or reaction with CO_2. These are the same results found for the carbonate formation response in nitrates.

The nitrite experiments contrast with the nitrate results because temperature was the variable that had the largest effect on nitrate formation in nitrites; however, it was still less than the minimum level of significance. No additional variables were revealed by the separate

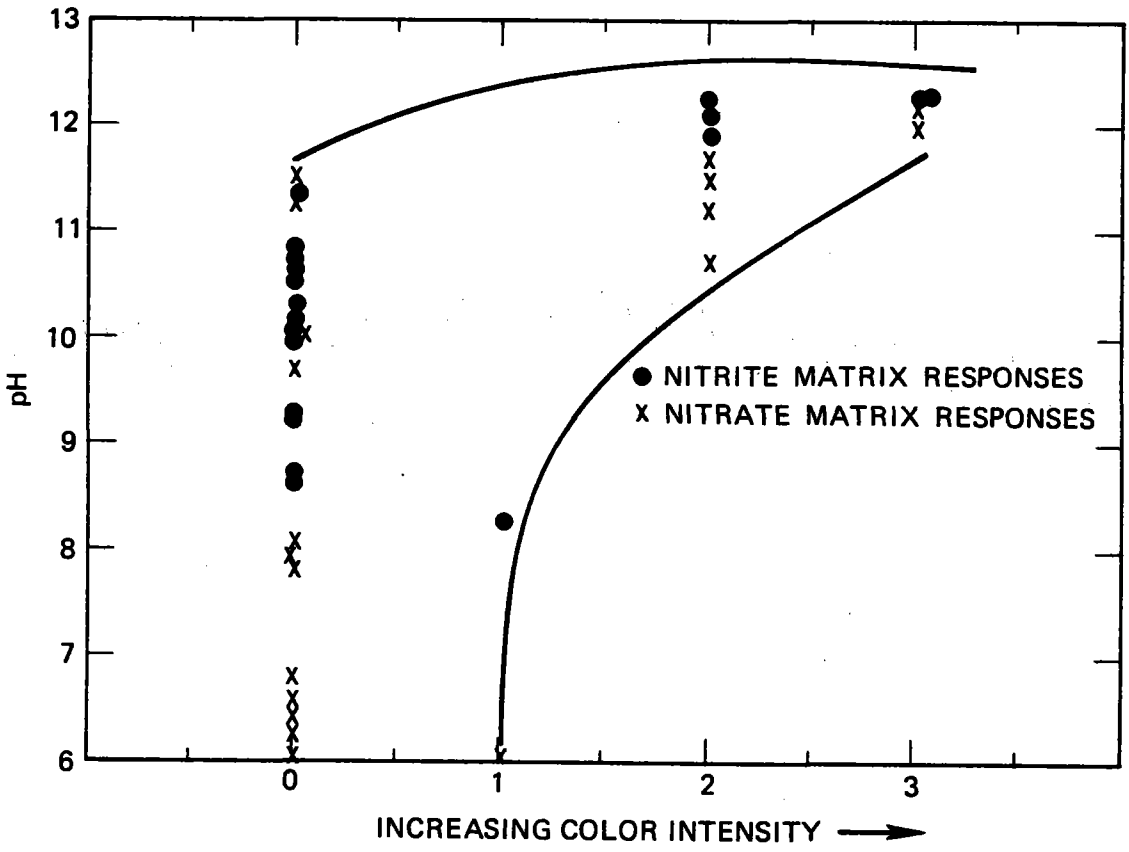

Figure 41. Correlation of pH Response and the Color of the Salts

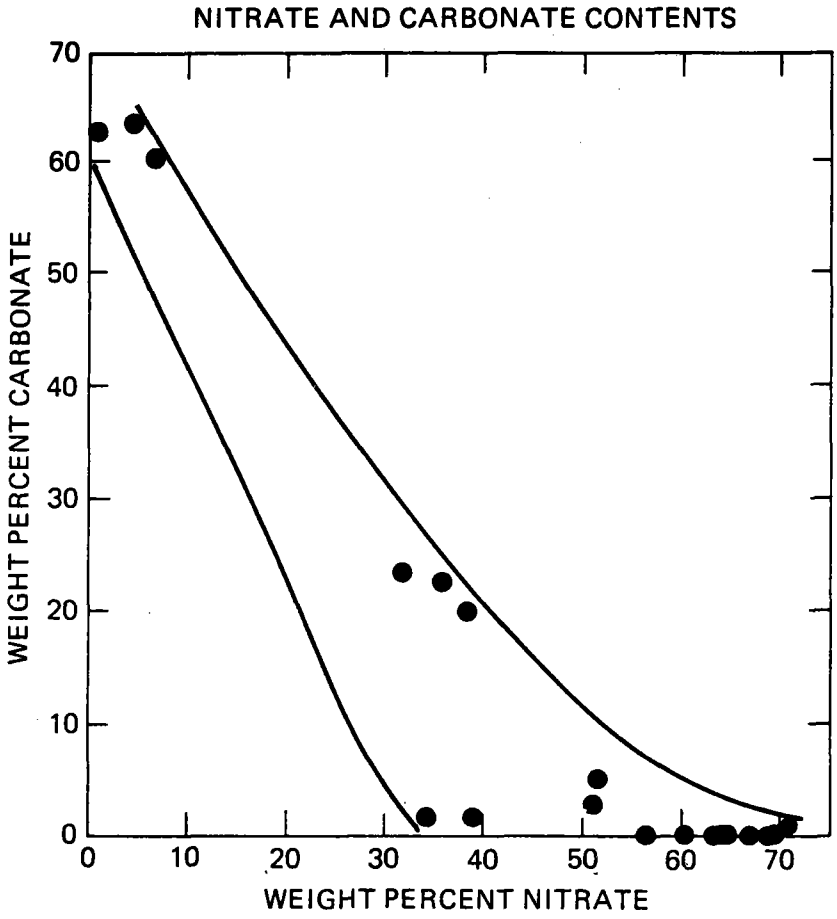

Figure 42. Nitrate and Carbonate Contents

temperature analyses. The flow rate had the largest effect in the separate high- and low-temperature analyses, although it was also below the minimum level of significance. The range of the nitrate contents in the nitrite samples was large (.05-53%), and it is curious that there was no variable identified as causing the spread in values.

It had been anticipated that oxygen, the surface area, and the gas flow rate would influence the nitrate content in nitrite salts (as others have observed[34]) because of their effect on the reverse of Reaction (1). Oxygen had the second highest effect in the overall analysis of the nitrite response to form nitrate but was still below the minimum level of significance for NO_3^-. The effect of surface area was observed by the salts' spreading. The gas flow rate was clearly not influential in the statistical analysis.

Nitrite Content

The nitrite content found in the nitrate experiments was enhanced by high temperatures, low carbon dioxide contents, and perhaps high purity. The temperature effects correlate with the shift to higher equilibrium nitrite contents that are present at higher temperatures. The amount of nitrite in the nitrites, however, was greater at low temperatures, high relative humidities, and perhaps high flow rates (the flow rate had a marginally significant effect). In this case the negative temperature effect reflects the slower reaction rates at lower temperatures. Freeman[34] noted that the oxidation rate of $NaNO_2$ increased with increasing temperature while the extent of oxidation decreased.

At high temperatures carbon dioxide influenced the nitrite contents in the nitrates and nitrites, tending to decrease the nitrite contents as the carbon dioxide level was raised, which correlates with the $CO_3^=$ results

for $NaNO_2$. At low temperatures no factors were observed to influence the nitrite content. Oxygen was not found to influence the nitrite content. Thus, because O_2 did not significantly affect the NO_2^- or NO_3^- content of the salts, it appears that the redox reaction (1) cannot be viewed as an isolated reaction. The nitrate and nitrite contents seem to be intertwined with other reactions occurring in air.

For each experiment I calculated the ratio of nitrite to nitrate. Dividing the experiments into high and low temperature groups, we averaged the nitrite-to-nitrate ratios and compare them in Table 29 with the values calculated for equilibrium conditions. Taking the NO_2^- to NO_3^- ratios and averaging the values neglects that other reactions were observed besides Reaction (1) but is a useful screening test. From Table 29 it is clear that the equilibrium values of the nitrite-to-nitrate ratio were not reached by the nitrites after 10 hours. The ratio of $X_{NO_2^-}/X_{NO_3^-}$ in the nitrite samples was greater than the calculated equilibrium value at low and high temperatures. However, the average ratio was much less at high temperature, indicating more complete conversion to nitrate. At low temperatures, the nitrate samples had an average nitrite/ nitrate ratio that was close to the equilibrium values. At high temperature, however, the average ratio exceeded the equilibrium values. KNO_3 decomposing to KNO_2 has been observed to reach equilibrium in 5 hours at 873 K.[42] However, the reaction of KNO_2 with O_2 did <u>not</u> equilibrate in 5 hours, consistent with our results. The excess nitrite in nitrates at high temperatures seems to indicate that (a) other reactions are occurring which consume nitrate and (b) nitrate-consuming reactions are more rapid than Reaction (1). To test this supposition the gases emanating from the furnaces were sampled with a device (used to

TABLE 29

NITRATE-TO-NITRITE RATIOS

	Low-Temperature[a] Experiments	/ Equilibrium[b] $NaNO_2/NaNO_3$	KNO_2/KNO_3	High-Temperature[a] Experiments	/ Equilibrium NO_2^-/NO_3^-[b] $NaNO_2/NaNO_3$	KNO_2/KNO_3
Nitrates	0.0168	$5.2(10^{-4})$	$1.4(10^{-4})$	0.367	0.32	0.17
Nitrites	11.5	$5.2(10^{-4})$	$1.4(10^{-4})$	3.97	0.32	0.17

[a]Average NO_2^- based on weight percent.

[b]Ratios calculated at 623 and 923 K, weight percent.

assess air pollution) that was sensitive to NO and NO_2 gas. Both gases were present downstream of the samples at high and low temperatures. The presence of traces of nitrogen oxide indicates that other thermal decomposition reactions are occurring.

Summary of Plackett-Burman Results

Of all the variables studied, temperature had the largest effect on nitrate decomposition. Increasing the temperature caused increased nitrite formation, increased carbonate formation, higher pH values and decreased nitrite levels. When the experiments were separated into high and low temperature experiments we observed that these phenomena occurred only in the high temperature experiments: pH > 7.0, $CO_3^=$ > 0.1%, NO_2^-/NO_3^- > 1%.

Oxygen and nitrogen had no measurable effects on salt stability over the range of concentrations studied (0-20% and 0-80%, respectively). Varying the O_2 and N_2 levels from zero to values found in air caused no significant decomposition. Since a correlation was not observed, between O_2 and N_2 and decomposition, controlling the O_2 or N_2 content of the ullage gas in a thermal storage system is not important. The lack of correlation of O_2 and N_2 with salt stability appears to conflict with the literature.[34,42] However, it may simply reflect that the reactions which occur with nitrates in air are complex and several occur concurrently. Furthermore, Bond and Jacobs[50] found that the kinetics of $NaNO_3$ decomposition were not dependent on the O_2 and N_2 partial pressures.

Carbon dioxide increased carbonate formation, decreased nitrate and nitrite levels decreased the pH of the salts. These interactions are deleterious and indicate that CO_2 in the ullage gas of a thermal

storage will cause salt decomposition and may have to be controlled to insure a 30 year lifetime of the salt. Water vapor increased the pH of the salts. The relative humidity of the ullage gas is much less influential than CO_2, and, in our opinion, need not be controlled in a thermal storage system. Neither the CO_2 nor the water vapor have statistical effects as large as temperature does on decomposition of nitrates.

The gas flow rate salt surface area and sample size are factors that we expected to influence the kinetics of decomposition. High gas flow rates increased carbonate formation and decreased to nitrate content, which correlates with the effects of CO_2. Surface area did not affect decomposition, however, in these experiments it was uncontrolled due to creep. Neither did our range of sample sizes affect the responses.

The spread in the high level of the K/Na variable was very large (0.56 - 1.0), but the two levels did not overlap. None of the responses were influenced by the ratio of KNO_3 to $NaNO_3$. Therefore decomposition is insensitive to the ratio of KNO_3 to $NaNO_3$.

Next to temperature, purity was the most significant variable. As the salt purity increased, carbonate formation decreased, nitrate contents increased and the pH level decreased. The salt purity was varied from reagent grade to commercial purity. Unfortunately we cannot correlate any aspect of the purity with the phenomena we observed. The purity of the salt may be important to control to prevent decomposition. We feel that further tests are necessary to identify what aspect of the purity affects decomposition.

IV C. Decomposition in Argon - Results and Discussion

Table 30 summarizes the results of the decomposition tests performed in argon. These results are blemished because two of the containers leaked to the air ($NaNO_3$ at 624 K and $NaNO_2$ at 736 K). Unfortunately these experiments could not be repeated because the heating elements of the fluidized bath failed and replacement parts were not available.

Another problem was that interaction between the salt and the container occurred, especially at 736 K. Specifically, $NaNO_2$ and KNO_2 corroded the stainless steel containers in the 736 K experiment and Fe_3O_4 was precipitated in the bottom of the tubes. At 736 K all the salts contained Fe, Cr and Ni (see Table 30), indicative of reaction with the container. Despite these two problems (leaking and corrosion), some interesting observations may be made.

The amount of NO_2^- was much greater than the amount of NO_3^- present at the end of the two experiments for every salt. This indicates that the nitrite samples were oxidized to a small extent and that the nitrate samples decomposed to a large extent to NO_2^-. The ratios of NO_2^- to NO_3^- were unexpectedly high for the nitrate samples. The high NO_2^-/NO_3^- may indicate that when Reaction (1) occurs and oxygen is released, the oxygen was consumed by another reaction, such as corrosion of the stainless steel container or the Cu gaskets. As expected from the discussion in the Introduction, higher NO_2^-/NO_3^- were measured at 736 K than at 624 K.

At 736 K the NO_2^-/NO_3^- ratio for the nitrate samples decreased from $NaNO_3$ to KNO_3 to $(Na/K)NO_3$. At 624 K the opposite rank ordering was observed for the NO_2^-/NO_3^- ratios ($(Na/K)NO_3 > KNO_3 > NaNO_3$).

TABLE 30

DECOMPOSITION RESULTS IN ARGON AT 736 K

	NO_2^-/NO_3^-[a]	Total Alkalinity[b] ($mg\text{-}l^{-1}$)	N_2[d]	O_2[d]	N_2O[d]	NO[d]	Fe($mg\text{-}l^{-1}$)	Cr($mg\text{-}l^{-1}$)	Ni($mg\text{-}l^{-1}$)
$NaNO_3$	45.	11	7.7	17.1	0.0	0.0	2.3	3.1	0.0
KNO_3	29.	8	12.4	9.5	1.6	0.1	1.2	3.5	0.0
$(Na/K)NO_3$	20.	11	2.7	10.3	2.2	0.0	2.7	7.3	0.0
$NaNO_2$	180.	4400	c.	c.	c.	c.	640.	290.	30.
KNO_2	260.	2200	46.1	0.0	0.0	0.0	46.	35.	9.3

DECOMPOSITION RESULTS IN ARGON AT 624 K

$NaNO_3$	7.4	15	c.	c.	c.	c.	0.9	0.9	0.0
KNO_3	9.3	8	15.3	0.0	4.4	1.3	0.0	0.0	0.0
$(Na/K)NO_3$	26.	11	3.7	0.9	1.0	0.2	0.0	1.0	0.0
$NaNO_2$	415.	2200	30.6	0.0	0.0	0.0	1.0	9.8	0.0
KNO_2	160.	94	6.9	0.0	0.0	0.0	1.5	0.0	0.0

a Molar Ratio

b Sum of weight % of OH^-, CO_3, and HCO_3^-

c Container Leaked

d Mole or Volume percent; Argon = balance, Accuracy = $\pm$ 0.1%

As in the Plackett-Burman tests, the total alkalinity is a measure of all the oxygen anions, carbonate and hydroxide in the salts. The total alkalinity of the nitrites was much higher than the nitrates. Of course, the nitrites are less stable than the nitrates with regard to any decomposition reaction or interaction with either CO_2 or H_2O. Sodium nitrite had the highest alkalinity and KNO_2 had the second highest. The alkalinity of the nitrates was much lower (2000 $mg\text{-}l^{-1}$ versus 10 $mg\text{-}l^{-1}$). No substantial differences between the three nitrates with respect to alkalinity were observed.

Nitrogen was the primary gaseous decomposition product we observed at 604 K. The percentage of N_2 was largest for $NaNO_2$ at 624 K, which also had the highest alkalinity. The other salts had substantially the same N_2 in the ullage gas.

Because of the high NO_2^-/NO_3^-, we expected to observe O_2 in the ullage gas at 624 K, however, $\leq$ 0.5% was observed. The lack of O_2 also indicates (as does the high NO_2^-/NO_3^-) that, if Reaction (1) occurs, the O_2 is being consumed in other reactions.

The amounts of N_2 and O_2 were higher at 736 K. Oxygen was found in the gases above the nitrates but not the nitrites. Minor amounts of N_2O and NO were observed; however, no NO_2 was observed in any sample. These gas analyses may be indicative of a series of reactions that occurred in the experiment including (1), and (26)-(30).

IV D1. Thermogravimetry Results and Discussion Under Atmospheric Pressure

The rates of weight loss at one atmosphere varied widely; however, the rates of weight loss per unit surface area had several interesting trends. These rates are given in Tables 31-33 and are plotted in Figure 43 versus inverse temperature. One important observation is that a flowing dynamic atmosphere enhances the weight losses compared to static atmospheres. The rates of weight loss from $(Na,K)NO_3$ are higher in either flowing argon or N_2 compared to static air. For comparison, four experiments performed with $(Na,K)NO_3$ in vacuum are also included in Figure 43. The rates in vacuum, the most dynamic kind of atmosphere, are approximately 100 times greater than those observed in static air. The same trend was observed for $NaNO_3$ in static air (lower rates) compared to $NaNO_3$ in dry, flowing air (higher rates). The influence of gas flow rate is probably due to the removal of gaseous decomposition products which enhances the rate of reaction.[84] The gas flow rate was an influential variable identified in the Plackett Burman tests causing increased $CO_3^{=}$ formation, lesser nitrate percentages, and enhanced mass transport.

Secondly, the rates of $NaNO_3$ decomposition in Table 31 are not significantly different from the rates of $(Na,K)NO_3$ decomposition (Table 32) at the same temperatures. The lack of influence of the Na to K ratio on decomposition was observed in the Plackett-Burman screening tests. However, the commercial mixture of $NaNO_3$ and KNO_3 denoted as Partherm (Park Chemical Co.), decomposed more rapidly than the reagent grade salts at the same temperature. The lower purity samples decomposed more in the Plackett-Burman tests also.

Table 31

Kinetic Thermogravimetric Data for $NaNO_3$ in Air

Trial	Temperature (K)	Weight Lost, %	b(mg cm^{-2} min^{-1})[a]	c(mg cm^{-2} min^{-2})[a]	b'(mg min^{-1})[b]	c'(mg min^{-2})[b]	b"(min^{-1})[c]	b"'(% min^{-1})[d]	c"'(% min^{-2})[d]
25G	799.	3.25	$-5.036(10^{-3})$	$9.056(10^{-7})$	$-1.420(10^{-3})$	$2.554(10^{-7})$	$-3.012(10^{-5})$	$3.613(10^{-3})$	$-6.498(10^{-7})$
5R	848.	2.67	$-2.112(10^{-2})$	$4.614(10^{-6})$	$-5.028(10^{-3})$	$1.098(10^{-6})$	$-2.514(10^{-5})$	$3.182(10^{-3})$	$-6.951(10^{-7})$
6R	875.	1.54	$-1.431(10^{-2})$	$3.674(10^{-6})$	$-3.405(10^{-3})$	$8.744(10^{-7})$	$-1.491(10^{-5})$	$1.998(10^{-3})$	$-5.132(10^{-7})$
8R	873.	4.44	$-9.322(10^{-2})$	$5.966(10^{-5})$	$-2.219(10^{-2})$	$1.420(10^{-5})$	$-1.252(10^{-4})$	$1.543(10^{-2})$	$-9.875(10^{-6})$
10R	833.	3.00	$-9.065(10^{-2})$	$7.951(10^{-5})$	$-2.158(10^{-2})$	$1.892(10^{-5})$	$-1.112(10^{-4})$	$1.419(10^{-2})$	$-1.245(10^{-5})$
11R	941.	0.85	$-8.548(10^{-1})$	$3.634(10^{-2})$	$-2.032(10^{-1})$	$8.648(10^{-3})$	$-5.262(10^{-4})$	$1.214(10^{-1})$	$-5.164(10^{-3})$
12R	833.	0.75	$-6.384(10^{-2})$	$1.835(10^{-4})$	$-1.519(10^{-2})$	$4.367(10^{-5})$	$-6.351(10^{-5})$	$9.358(10^{-3})$	$-2.690(10^{-5})$

[a]Rates of sample weight change per unit area: rate = b + ct.

[b]Rate of sample weight change = b' + c't.

[c]First order kinetic rate of weight change = b".

[d]Rate of weight change in percent of starting weight = b"' + c"'t.

Table 32

Kinetic Thermogravimetric Data for $NaNO_3$ and KNO_3 Mixtures in Air or N_2

Trial	Temperature (K)	Weight Lost, %	b(mg cm^{-2} min^{-1})[a]	c(mg cm^{-2} min^{-2})[a]	b'(mg min^{-1})[b]	c'(mg min^{-2})[b]	b"(min^{-1})[c]	b"'(% min^{-1})[d]	c"'(% min^{-2})[d]
15G	793.	2.83	$-1.144(10^{-2})$	$4.196(10^{-6})$	$-3.226(10^{-3})$	$1.183(10^{-6})$	$-5.419(10^{-5})$	$6.714(10^{-3})$	$-2.462(10^{-6})$
16G	805.	5.51	$-1.185(10^{-2})$	$4.418(10^{-6})$	$-3.341(10^{-3})$	$1.246(10^{-6})$	$-5.366(10^{-5})$	$7.872(10^{-3})$	$-2.936(10^{-6})$
18G	840.	3.26	$-1.589(10^{-2})$	$1.175(10^{-5})$	$-4.480(10^{-3})$	$3.314(10^{-6})$	$-6.621(10^{-5})$	$7.727(10^{-3})$	$-7.196(10^{-6})$
20G	805.	3.40	$-5.149(10^{-3})$	$9.056(10^{-7})$	$-1.452(10^{-3})$	$2.554(10^{-7})$	$-2.856(10^{-5})$	$3.499(10^{-3})$	$-6.154(10^{-7})$
21G	833.	7.99	$-3.289(10^{-2})$	$7.363(10^{-6})$	$-9.274(10^{-3})$	$2.076(10^{-6})$	$-1.871(10^{-4})$	$1.977(10^{-2})$	$-4.427(10^{-6})$
22G	800.	15.43	$-1.478(10^{-2})$	$3.143(10^{-7})$	$-4.167(10^{-3})$	$8.863(10^{-7})$	$-1.663(10^{-4})$	$1.911(10^{-2})$	$-4.064(10^{-6})$

[a]Rates of sample weight change per unit area: rate = b + ct.

[b]Rate of sample weight change = b' + c't.

[c]First order kinetic rate of weight change = b".

[d]Rate of weight change in percent of starting weight = b"' + c"'t.

Table 33

Kinetic Thermogravimetric Data for $NaNO_3$ and KNO_3 Mixtures in Argon

Trial	Temperature (K)	Weight Lost, %	b(mg cm^{-2} min^{-1})[a]	c(mg cm^{-2} min^{-2})[a]	b'(mg min^{-1})[b]	c'(mg min^{-2})[b]	b"(min^{-1})[c]	b"'(% min^{-1})[d]	c"'(% min^{-2})[d]
15R	897.	0.94	-0.1763	$3.404(10^{-4})$	-0.1481	$2.859(10^{-4})$	$-3.211(10^{-5})$	$5.102(10^{-3})$	$-9.852(10^{-6})$
16R	1073.	7.26	-4.704	$3.187(10^{-2})$	-3.9510	$2.677(10^{-2})$	$-1.021(10^{-3})$	$1.697(10^{-1})$	$-1.149(10^{-3})$
17R	869.	7.23	-0.4059	$1.261(10^{-4})$	-0.3410	$1.059(10^{-4})$	$-1.361(10^{-4})$	$1.580(10^{-2})$	$-4.910(10^{-6})$

[a]Rates of sample weight change per unit area: rate = b + ct.

[b]Rate of sample weight change = b' + c't.

[c]First order kinetic rate of weight change = b".

[d]Rate of weight change in percent of starting weight = b"' + c"'t.

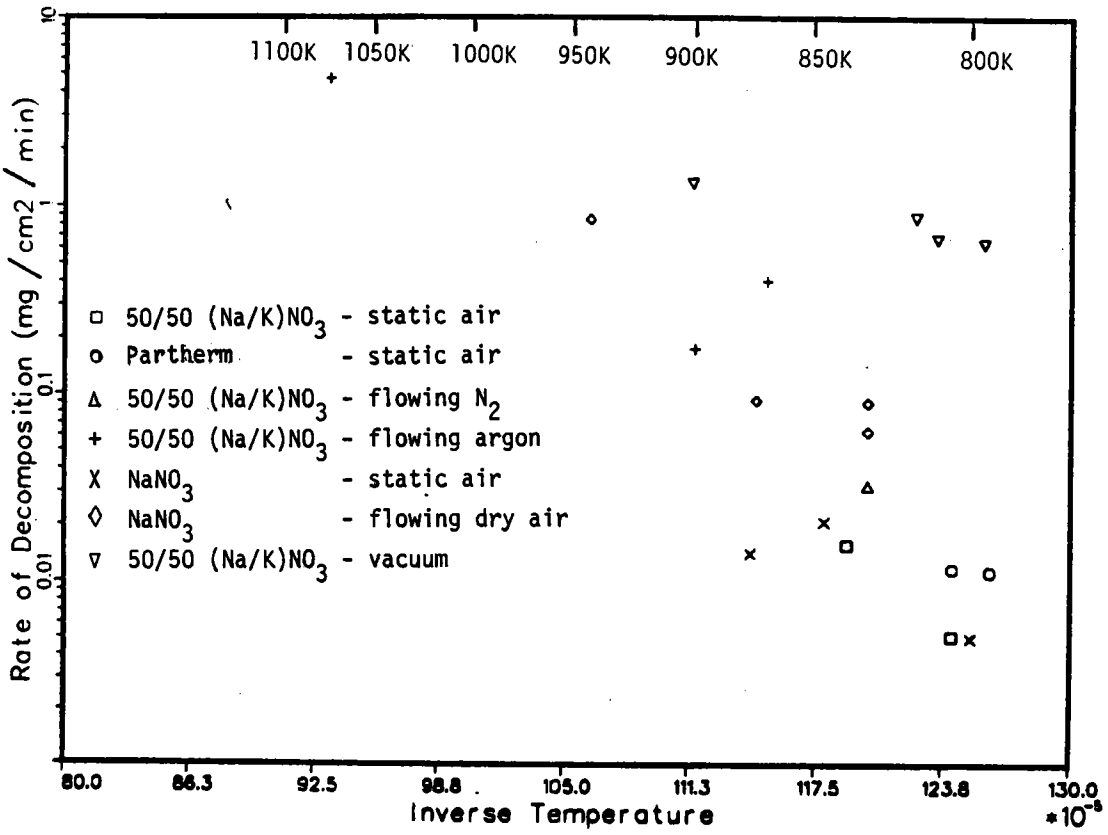

Figure 43. Decomposition of Nitrates at 1 atm

Another interesting observation that is not reflected in Figure 43 is this. In contrast to Freeman's[34,42], and Bond and Jacobs'[50] TG experiments, no arrests and no inflections were observed in the weight loss curves. The rates slowly and smoothly decreased with time. Freeman observed that his TG weight losses arrested at weights corresponding to oxide whereas I observed weight losses in excess of complete decomposition to oxide. Chun[35] also observed weight losses from $NaNO_3$ in excess of decomposition to oxide who suggested that vaporization of nitrates and nitrites occurs. In fact, the nitrates could be completely decomposed so that no sample remained. Vaporization occurred in the Plackett-Burman tests and the TG tests. I concluded that several processes are occurring which are: vaporization of the salts, decomposition to some oxygen ion species (not necessarily oxide), and vaporization of that oxide ion species.

IV D2. Thermogravimetry and Mass Spectrometry in Vacuum Results and Discussion

Isothermal Experiments

In the TG experiments with nitrates in air I observed that the entire sample weight could be lost. I also observed this phenomena in vacuum. The 5-10 mg samples of nitrates and nitrites were completely decomposed and vaporized in vacuum in less than 100 minutes at 750 K. At 630 K the nitrates lost less than 11% of their initial weight in 360 minutes whereas $NaNO_2$ samples lost 25-75% of their initial weight in this time. As discussed in the Introduction, decomposition of the nitrates and nitrites has been believed to proceed to oxide formation with a weight loss arrest corresponding to 100% oxide formation.[34,42,50] The present TG results in air and in vacuum indicate that other processes

occur simultaneously. The mass transport observed in the Plackett-Burman tests and the continuous weight loss profiles in the TG experiments suggest that vaporization of the nitrates and nitrites occur concurrently with decomposition and that the products of decomposition also vaporize. In this section I will discuss what I learned about these three phenomena (salt vaporization, salt decomposition and decomposition product vaporization) from the TG/MS experiments. Specifically, I'll discuss the time resolved profile of the evolved gases and the weight loss kinetics.

In discussing these results it's important to be aware of what distinguishes these experiments from other decomposition studies of the nitrates. Most nitrate decomposition experiments have been performed at 1 atmosphere pressure whereas these were performed in vacuum. In a vacuum the products of decomposition are continuously removed and prevented from reacting with the remaining salt. Secondly, the evolved gases were analyzed as the experiment proceeds and were unlikely to interact because they were at such a low density in the vacuum. As a result, the essential nature or the intrinsic decomposition of the salts was studied.

As mentioned in the Experimental Techniques section, only N_2, NO and O_2 were evolved from the salts we studied. These gases have very low solubilities (10^{-4} mole-mole^{-1}) in nitrates, therefore they are not dissolved gases that were rejected on heating the salts.[166] Of course condensible vapor species could not be monitored in the present experimental set-up. The amounts of each gas depended on time, the temperature of the experiment, and the salt. No salt evolved NO_2 although this has been reported in the literature.[34,42] These results are not inconsistent with the earlier data because the reported NO_2 was

probably oxidized NO released from the nitrates or nitrites in the presence of O_2.[34,53]

Two characteristic gas spectra were obtained from the salts and are shown in Figures 32 and 44. The spectrum in Figure 32 shows N_2, NO, and O_2 being released. This spectrum was characteristic of the nitrates. Figure 44 has the gas spectrum of $NaNO_2$ from which no O_2 gas was evolved. This spectrum is also characteristic of the nitrates at 630 K. Between 630 K and 750 K, the gas spectrum from nitrates gradually changed from one like Fig. 44 to the one shown in Fig. 32.

The amount of O_2 evolved from the salts varied with temperature. To assess this change I calculated the ratios of O_2 to N_2 and O_2 to NO. These ratios are the ratios of the total areas under each intensity-time curve measured with a planimeter. Figures 45 and 46 show the ratios have O_2/N_2 and O_2/NO, respectively, plotted for $NaNO_2$, KNO_3 and $NaNO_3$ at 740 K and 630 K and $LiNO_3$ at 730 K. Figures 47 and 48 show the O_2/N_2 and O_2/NO versus inverse temperature for the same four salts. From these figures it is obvious that at higher temperatures more O_2 (relative to N_2 and NO) is evolved. Very little O_2 is released from $NaNO_2$ at any temperature Although there is some scatter in the results, the trend is the amount of oxygen relative to NO increases from $NaNO_2$ to $LiNO_3$ to $NaNO_3$ to KNO_3.

Another important phenomena to consider is that oxygen evolution was always delayed relative to N_2 and NO evolution (see Figure 32). This contrasts with Freeman's gas analysis[34,42] who observed that O_2 was the first decomposition product; however, his analyses were periodic and not continuous. But delayed oxygen evolution agrees with the decomposition study of $NaNO_3$ performed in vacuum where only NO and N_2 were evolved

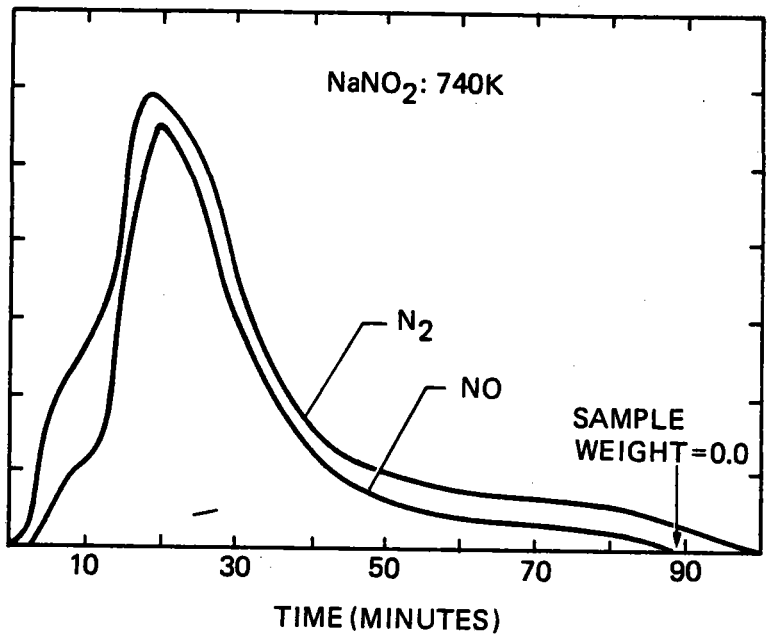

Figure 44. Mass Spectrum of Gases from $NaNO_2$ at 740 K

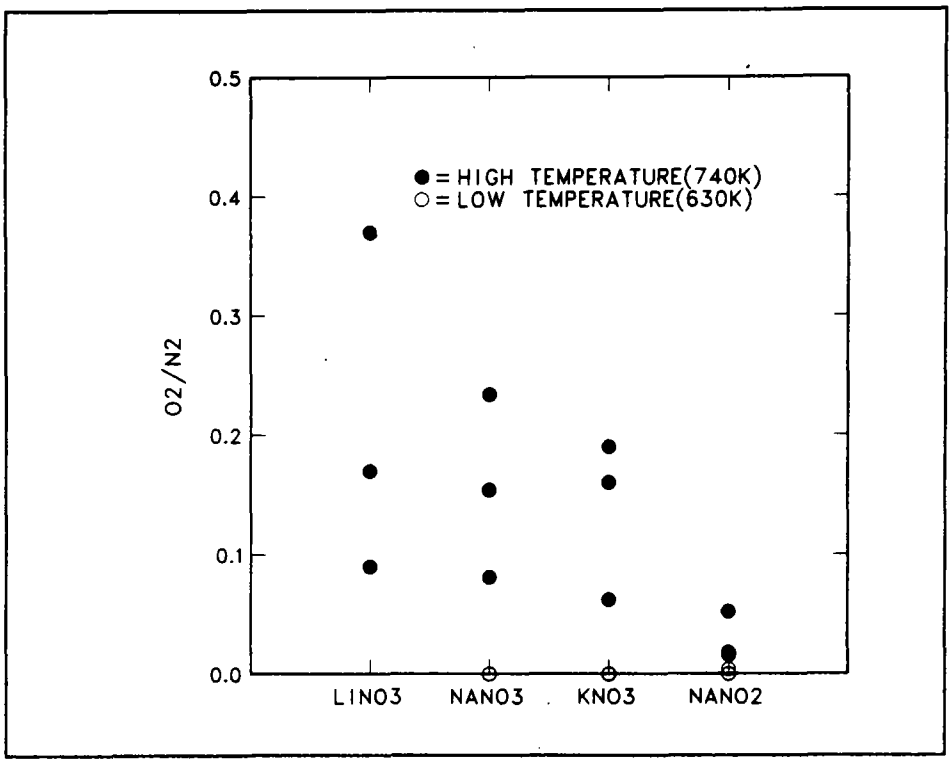

Figure 45. Decomposition Gases - O_2/N_2

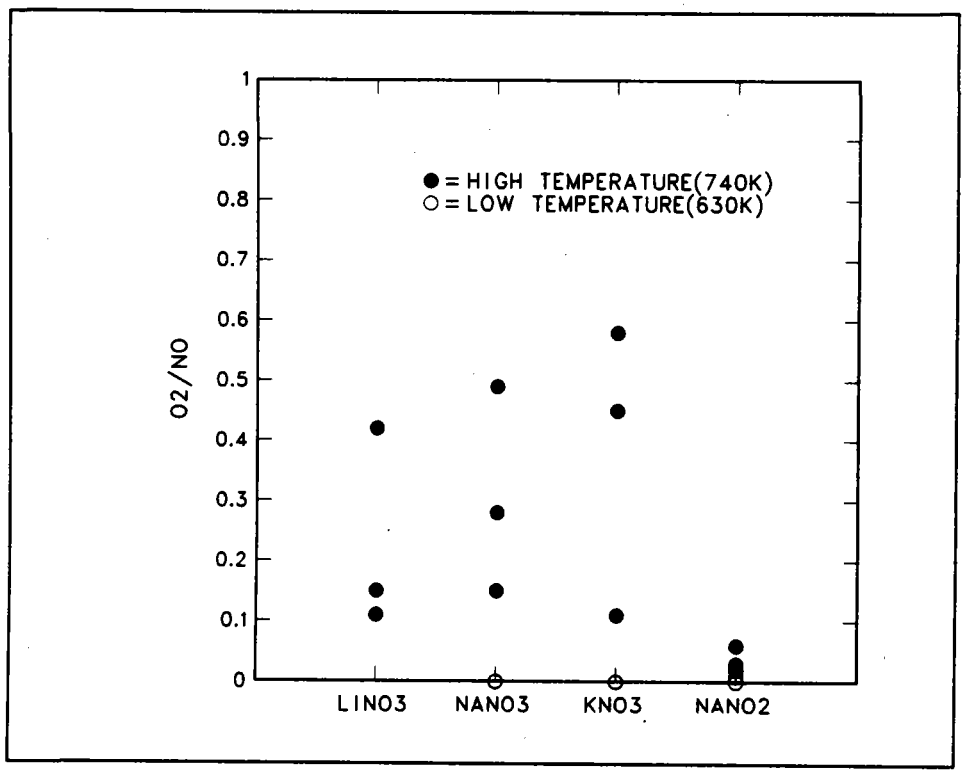

Figure 46. Decomposition Gases - O_2/NO

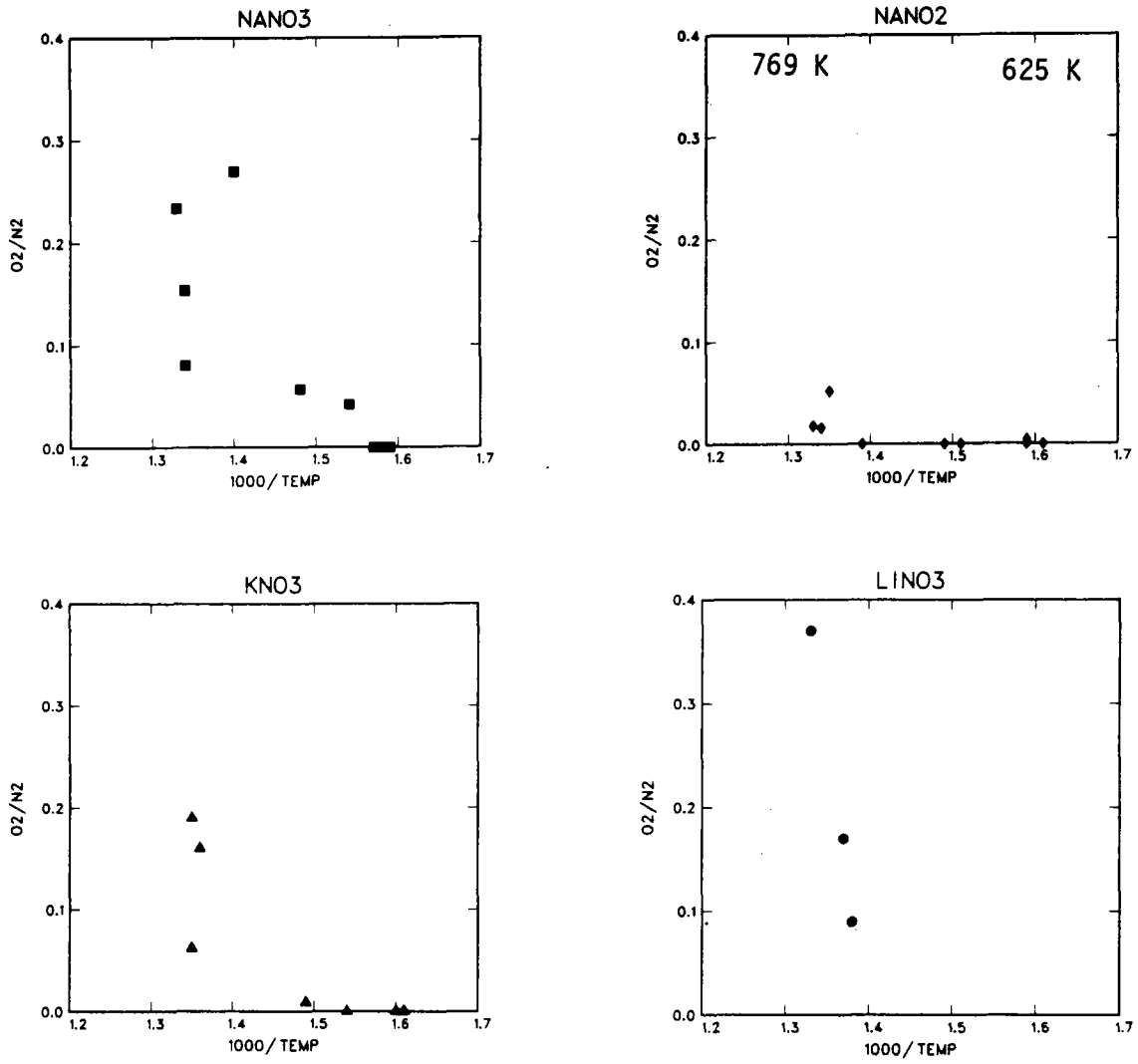

Figure 47. Decomposition Gases - O_2/N_2 as a Function of Temperature

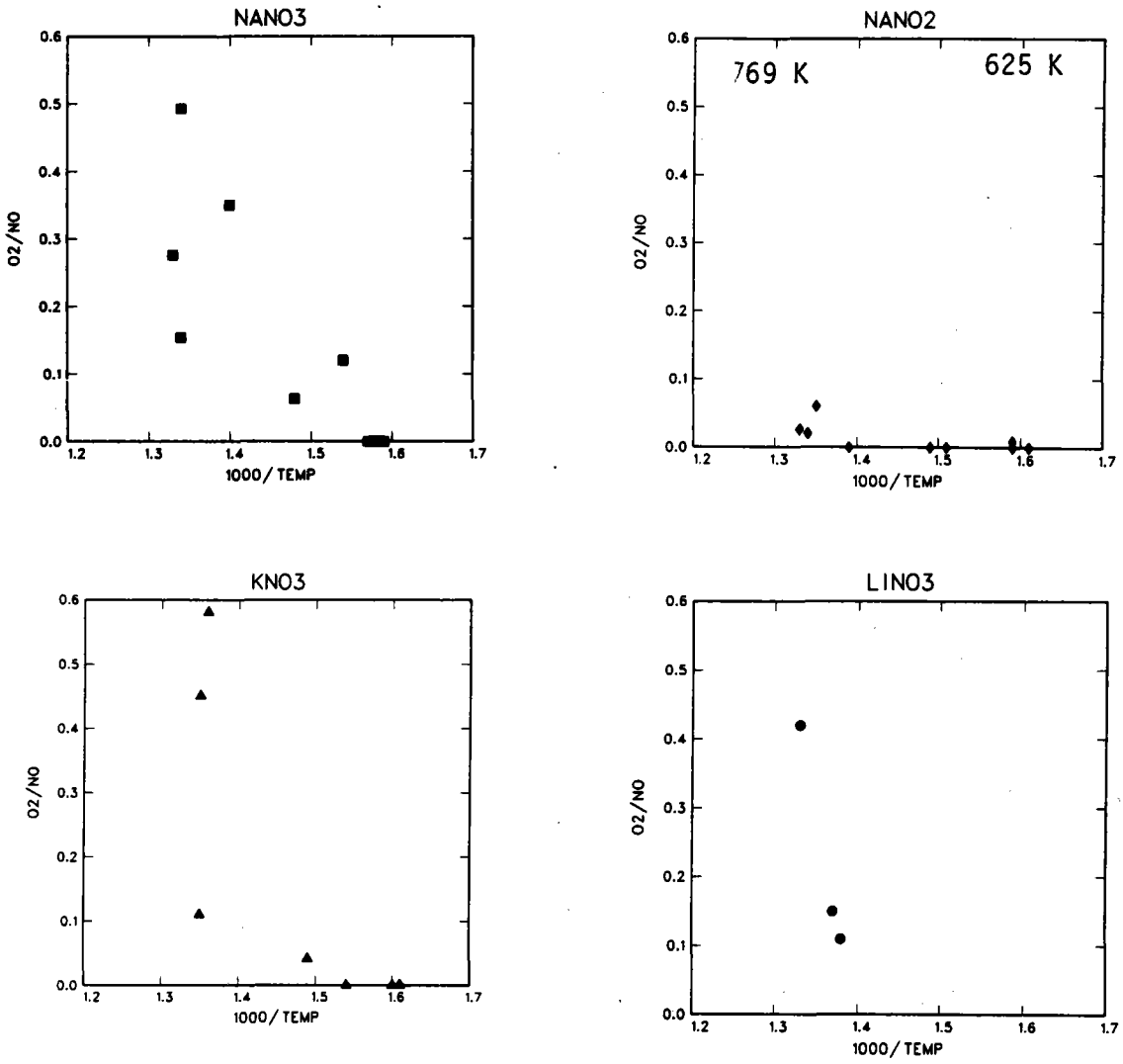

Figure 48. Decomposition Gases - O_2/NO as a Function of Temperature

at 570 K.[21] In a study in which $LiNO_3$ was decomposed, it was observed that the maximum rates of evolution N_2 and NO occurred at lower temperatures than for O_2.[167]

Several experiments were performed to assess the background of gases when no sample was in the furnace. No nitric oxide and no oxygen were observed in these empty runs; however, mass 28 (N_2 and CO) was observed. The amount of mass 28 observed in the empty experiments was significantly less than the amounts observed with salt samples and I neglected the background of mass 28.

From these gaseous profiles I deduced a sequence of reactions that explain the observed phenomena. First, consider the profile of gases evolved from $NaNO_2$ where N_2 and NO are almost exclusively released (Fig. 44). I believe that nitrogen is released from $NaNO_2$ due to the decomposition of the anions according to[168]

$$NO_2^- \rightarrow O_2^- + N \qquad (60)$$

and

$$N + N \rightarrow N_2 \qquad (61)$$

where superoxide (O_2^-) is a product. Nitric oxide may be released by a parallel path such as

$$NO_2^- \rightarrow O^- + NO \qquad (62)$$

and

$$2O^- \rightarrow O_2^{-2} \qquad (63)$$

where peroxide (O_2^{-2}) is also a product. There is potentiometric evidence for O^- formation in nitrates.[169] Reaction (63) is very fast, according to Zambonin[66] who described mechanisms of oxygen ion interactions in nitrates. As discussed in the Introduction, peroxide (O_2^{-2}) and superoxide (O_2^{-2}) are considered to be stable species in the nitrates.

Next, let us consider the more complex profile where O_2 is evolved from the nitrates as in Figure 32. The nitrates in vacuum will have significant fractions of nitrite present at equilibrium. To illustrate this point I calculated the equilibrium molar ratios of $NaNO_2$ to $NaNO_3$ from 500 - 1000 K at three partial pressures of oxygen; 10^{-4}, 10^{-7}, and 10^{-9} atm. The results depicted in Figure 49 show that at 10^{-7} atm of oxygen, approximately the P_{O_2} under which the experiments were run, the amount of nitrite will exceed the amount of nitrate present at equilibrium above 650 K. Therefore, the nitrate samples decomposed in vacuum had a large driving force to form nitrite.

Nitrate decomposition to nitrite has been previously explained by this two step sequence[34,42,168]

$$NO_3^- \rightarrow NO_2^- + O \qquad (64)$$

$$O + NO_3^- \rightarrow NO_2^- + O_2 \ . \qquad (65)$$

Oxygen evolution did not occur at the beginning of the nitrate decomposition experiments. Initially N_2 and NO were evolved as in the decomposition of the nitrites. Reaction (64) may occur so that nitrite is formed and decomposes, but Reaction (65) may not occur. Instead of Reaction (65) the oxygen atoms released by Reaction (64), being highly reactive, may combine with peroxide (O_2^{-2}), a product of nitrite ion decomposition, to form superoxide (O_2^-) as below.

$$O + O_2^{-2} \rightarrow O_3^{-2} \qquad (66)$$

$$O + O_3^{-2} \rightarrow 2O_2^- \qquad (67)$$

Peroxide ion would be available for Reactions (66) and (67) as the nitrate ions decompose because the inevitably present residual nitrite would be decomposing.[44,70] As the superoxide builds up in the nitrate sample it may decompose to peroxide and oxygen according to this reaction

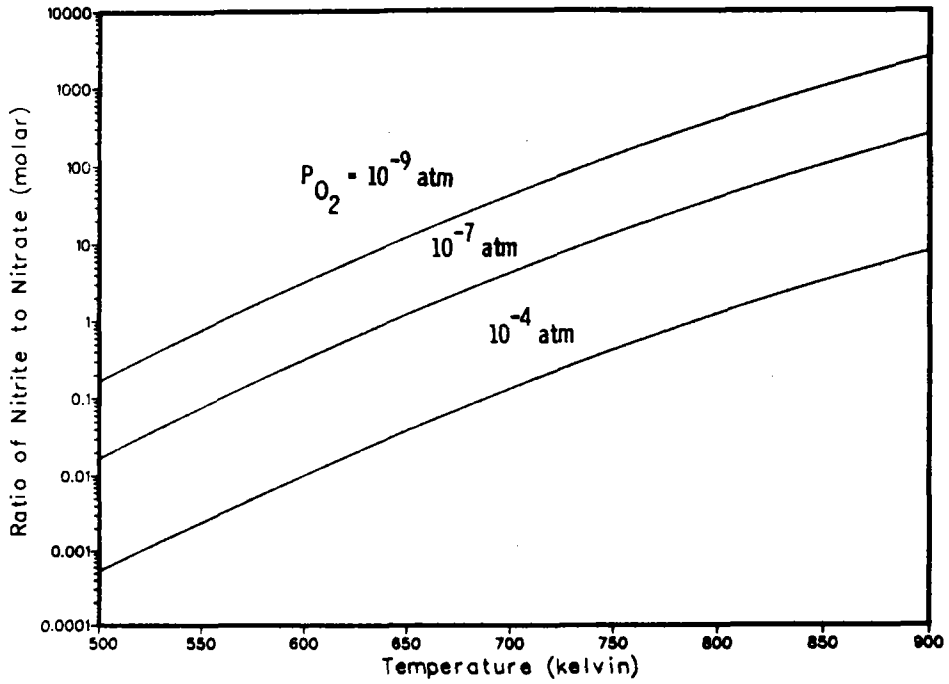

Figure 49. Equilibrium of Nitrates and Nitrites in Vacuum

$$2O_2^- \rightarrow O_2^{-2} + O_2 \qquad (68)$$

The decomposition of superoxide to peroxide and oxygen in a vacuum (Reaction (68)) was observed by Zambonin.[66] This sequence of reactions, predicated on the high reactivity of oxygen atoms released from nitrate decomposing to nitrite, explains the delayed oxygen evolution from nitrates in vacuum.

One may wonder why very little O_2 is released from $NaNO_2$ decomposition. It is the equilibrium expressed in Reaction (37) that prevents O_2 formation from $NaNO_2$. In Reaction (37), ($O_2^{-2} + 2NO_3^- \rightleftarrows 2O_2^- + 2NO_2^-$) peroxide and nitrate react to form superoxide and nitrite, or vice versa. The free energy for this reaction to form sodium superoxide and nitrite, plotted in Figure 19, is only 13 - 15 kcal from 630 - 750 K; therefore only a small amount of superoxide and nitrite may be present at equilibrium. Conversely, if nitrite and superoxide are present, there is a large driving force for them to react and form nitrate and peroxide. Superoxide ion in nitrite samples is consumed by reaction with nitrites, so no superoxide is available for Reaction (68) and oxygen is not evolved. At higher temperatures, the driving force to consume the superoxide in nitrites is decreased, therefore the amount of O_2 evolved from $NaNO_2$ should be greater at elevated temperatures. The amount of O_2 evolved from $NaNO_2$ was slightly greater at 750 K compared to 630 K.

According to this reaction scheme involving Reaction (37), $NaNO_2$ should contain increasing amounts of $NaNO_3$ as it decomposes, even in the absence of oxygen. To test this hypothesis $NaNO_2$ was decomposed at 673 K in vacuum in the TG/MS apparatus until 50% of the initial weight was lost. The sample chamber was opened to air and submitted the residual salt was submitted for infrared absorption (IRA) analysis. The IRA

results showed that Na_2CO_3, $NaNO_2$ and $NaNO_3$ were present. The Na_2CO_3 is indicative of a Na-oxygen ion species which had reacted with CO_2 in the air before the analysis was performed. Therefore Na_2O, Na_2O_2 and/or NaO_2 was present in the residual salt. Traces of $NaNO_3$ were present in the $NaNO_2$ starting material; however, the amount of $NaNO_3$ present in the half decomposed $NaNO_2$ sample was greater (by approximately a factor of 2) than the amount present in the starting salt. Therefore, $NaNO_2$ did self-oxidize in vacuum which is evidence that Reaction (37) occurs.

Infrared absorption analysis was also performed on two partially decomposed $NaNO_3$ samples. One sample came from $NaNO_3$ that had been decomposed a few percent in vacuum and no O_2 had been observed in the gases evolved from this sample. Another $NaNO_3$ sample was analyzed from an experiment in which a large portion of O_2 had been evolved. In both $NaNO_3$ samples $NaNO_3$, $NaNO_2$ and Na_2CO_3 were found in the IRA spectra. The amounts of $NaNO_2$ and Na_2CO_3 were much smaller in the sample which had undergone less decomposition.

The reaction scheme described above does not include oxide ion (O^-_2). A balanced reaction cannot be written to include oxide ion, N_2 and NO formation that does not also include oxygen. Superoxide and peroxide ion are considered to be stable in the nitrates whereas oxide is not, as discussed in the Introduction. These two observations indicate that nitrites and nitrates do not intrinsically decompose to oxide ion.

According to the described reaction scheme, N_2 is indicative of superoxide formation and NO is indicative of peroxide formation. I calculated the ratios of NO to N_2 for each experiment and they are plotted in Figure 50 versus inverse temperature for $NaNO_2$, $LiNO_3$, $NaNO_3$ and KNO_3. In Figure 51 NO/N_2 is plotted for $NaNO_2$, KNO_3 and $NaNO_3$

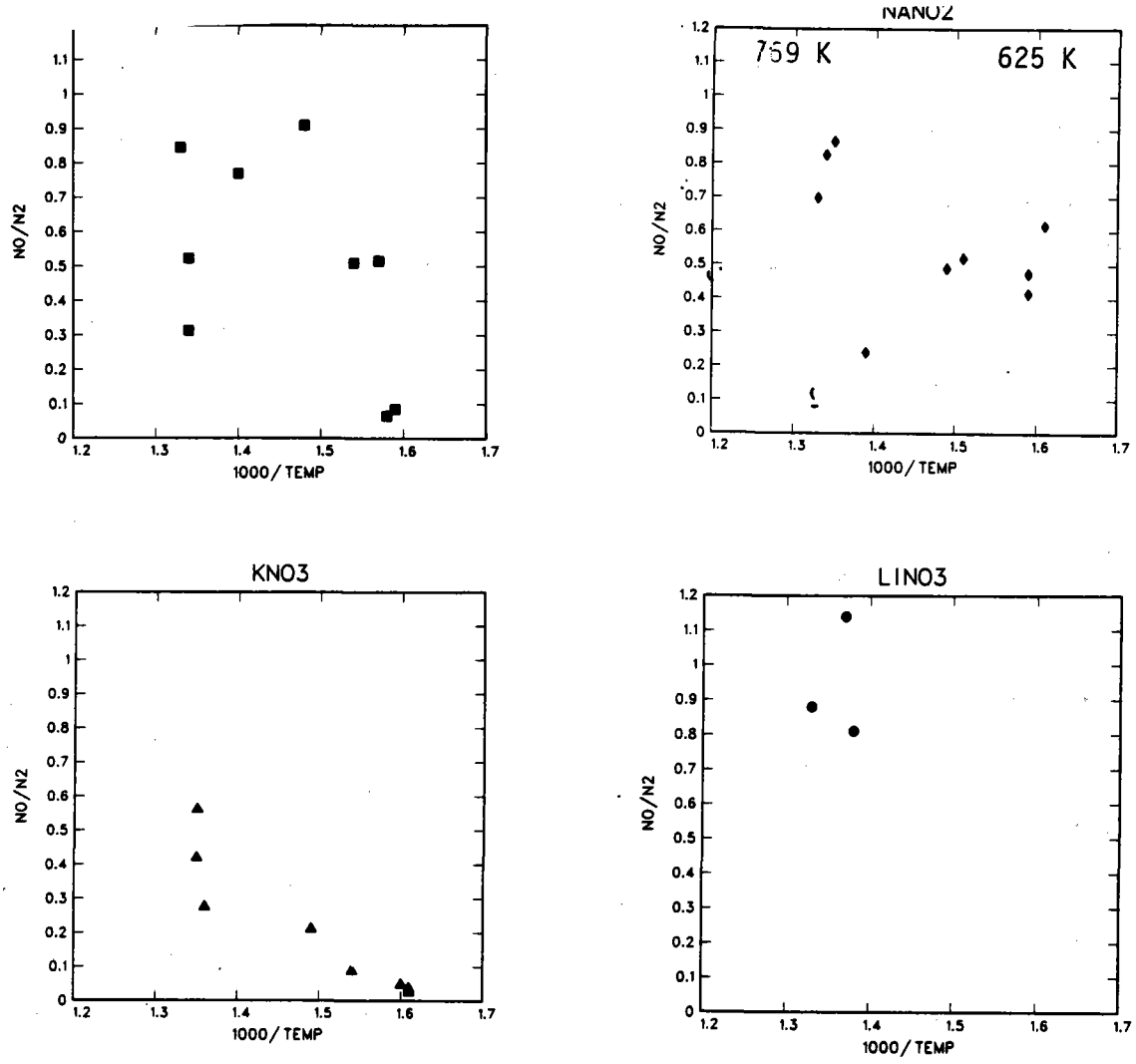

Figure 50. Decomposition Gases - NO/N_2 as a Function of Temperature

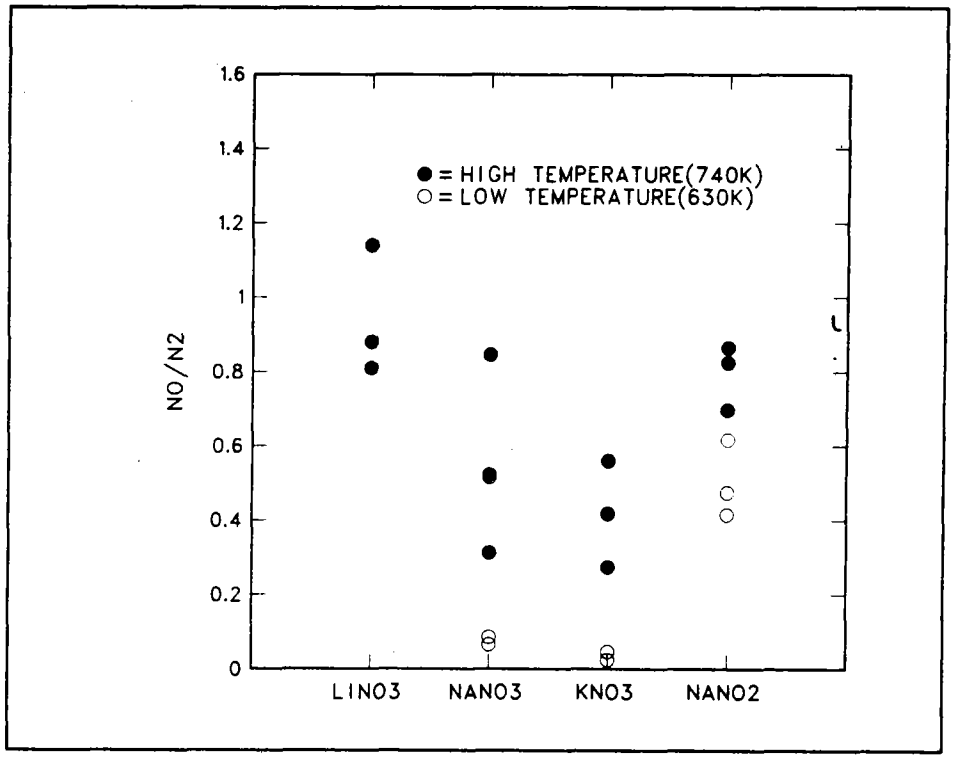

Figure 51. Decomposition Gases - NO/N_2 for Several Salts

at 740 K and 630 K and $LiNO_3$ at 730 K. The ratio, NO/N_2 decreases from $LiNO_3$ to $NaNO_2$ to $NaNO_3$ to KNO_3. A decrease in NO/N_2 indicates, according to the present reaction scheme, that more superoxide is formed in KNO_3 than in $NaNO_3$ than in $NaNO_2$ than in $LiNO_3$. This trend is the same at either high (740 K) or low (630 K) temperatures. This trend in superoxide formation agrees with the thermodynamic calculations of superoxide stability discussed in the Introduction and the literature.[94,171] The free energy of Reaction (39), the reaction of peroxide with oxygen to form superoxide is graphed in Figure 21 and shows that potassium superoxide is more stable (relative to its peroxide) than is sodium superoxide. Lithium superoxide in nitrates has been observed to be even less stable than NaO_2. As discussed earlier, peroxide formation is favored over superoxide in $NaNO_2$ due to the driving force of Reaction (37). Therefore the observed trend in NO/N_2 and its implication on the present reaction scheme are consistent with the thermodynamics of peroxide and superoxide formation in these salts.

The weight loss kinetics of isothermal decomposition of $NaNO_3$, KNO_3, $NaNO_2$ and $LiNO_3$ were also analyzed. As described in the experimental section, the weight measurements were plotted and fitted to four kinetic expressions which are illustrated for each experiment in Appendix C. The rate constants for Equations (48)-(51) are tabulated in Tables 34-38. The first order fit to the data was the poorest. The graphs of the ln (fraction remaining) are linear in the first stage of decomposition but are inadequate to describe the entire decomposition process, indicating that as decomposition proceeds, the dominant reaction changes. The first order kinetic expression is satisfactory for experiments where less than 50% of the initial weight was lost.

Table 34

Kinetic Thermogravimetry Data for $NaNO_3$ and KNO_3 Mixtures in Vacuum

Trial	Salt[e]	Temperature (K)	Total Weight Lost,%	b(mg cm^{-2} min^{-1})[a]	c(mg cm^{-2} min^{-2})[a]	b'(mg min^{-1})[b]	c'(mg min^{-2})[b]	b"(min^{-1})[c]	b"'(% min^{-1})[d]	c"'(% min^{-2})[d]
5	R	817.	87.5	$-8.780(10^{-1})$	$-8.605(10^{-4})$	$-6.936(10^{-1})$	$-6.798(10^{-4})$	$-2.434(10^{-2})$	$1.029(10^{0})$	$1.008(10^{-3})$
6	R	810.	22.0	$-6.752(10^{-4})$	$-7.990(10^{-4})$	$-5.334(10^{-1})$	$-6.312(10^{-4})$	$-9.132(10^{-3})$	$7.773(10^{-1})$	$9.199(10^{-4})$
7	R	795.	70.8	$-6.393(10^{-1})$	$-5.014(10^{-4})$	$-5.050(10^{-1})$	$-3.961(10^{-4})$	$-1.208(10^{-2})$	$6.866(10^{-1})$	$5.385(10^{-4})$
13	R	897.	80.9	$-1.329(10^{0})$	$-4.108(10^{-4})$	$-2.606(10^{-1})$	$-8.052(10^{-5})$	$-8.248(10^{-3})$	$4.054(10^{-1})$	$1.253(10^{-4})$

[a]Rate of sample weight change per unit surface area: rate = b + ct.

[b]Rate of sample weight change = b' + c't.

[c]First order kinetic rate of weight change = b".

[d]Rate of weight change in percent of starting weight = b"' + c"'t.

[e]R = reagent grade, equimolar $NaNO_3$ and KNO_3; C = Partherm 430, Park Chemical Co.

Table 35

Kinetic Thermogravimetry Data for $NaNO_3$ in Vacuum

Trace	Temperature (K)	b(mg cm^{-2} min^{-1})[a]	c(mg cm^{-2} min^{-2})[a]	b'(mg min^{-1})[b]	c'(mg min^{-2})[b]	b"(min^{-1})[c]	b"'(% min^{-1})[d]	c"'(% min^{-2})[d]
26	677.	$-1.883(10^{-2})$	$2.332(10^{-5})$	$-5.437(10^{-2})$	$6.733(10^{-5})$	$-1.922(10^{-3})$	$1.953(10^{-1})$	$-2.419(10^{-4})$
29	716.	$-1.082(10^{-1})$	$1.787(10^{-4})$	$-1.612(10^{-1})$	$2.661(10^{-4})$	$-4.844(10^{-2})$	$1.644(10^{0})$	$-2.714(10^{-3})$
30	737.	$-1.798(10^{-1})$	$1.181(10^{-3})$	$-2.676(10^{-1})$	$1.759(10^{-4})$	$-1.212(10^{-1})$	$3.165(10^{0})$	$-2.080(10^{-2})$
33	723.	$-7.957(10^{-2})$	$2.548(10^{-5})$	$-1.185(10^{-1})$	$3.794(10^{-5})$	$-4.565(10^{-2})$	$1.539(10^{0})$	$-4.927(10^{-4})$
38	726.	$-9.342(10^{-2})$	$1.710(10^{-4})$	$-1.391(10^{-1})$	$2.546(10^{-4})$	$-3.008(10^{-2})$	$1.046(10^{0})$	$-1.915(10^{-3})$
40	774.	$-4.010(10^{-1})$	$3.019(10^{-3})$	$-5.971(10^{-1})$	$4.496(10^{-3})$	$-1.039(10^{-1})$	$6.849(10^{0})$	$-5.157(10^{-2})$
41	726.	$-6.620(10^{-2})$	$6.503(10^{-5})$	$-9.857(10^{-2})$	$9.684(10^{-5})$	$-2.401(10^{-2})$	$9.451(10^{-1})$	$-9.284(10^{-4})$
44	784.	$-3.116(10^{-1})$	$4.078(10^{-3})$	$-4.640(10^{-1})$	$6.072(10^{-3})$	$-1.874(10^{-1})$	$9.010(10^{0})$	$-1.179(10^{-1})$
47	655.	$-7.203(10^{-3})$	$1.426(10^{-6})$	$-1.072(10^{-2})$	$2.124(10^{-6})$	$-1.568(10^{-3})$	$1.396(10^{-1})$	$-2.766(10^{-5})$
50	752.	$-1.628(10^{-1})$	$-6.263(10^{-4})$	$-2.424(10^{-1})$	$9.326(10^{-4})$	$-1.030(10^{-1})$	$3.446(10^{0})$	$-1.326(10^{-2})$
55	745.	$-1.171(10^{-1})$	$3.608(10^{-4})$	$-1.744(10^{-1})$	$5.372(10^{-4})$	$-8.425(10^{-2})$	$2.626(10^{0})$	$-8.090(10^{-3})$
56	744.	$-1.198(10^{-1})$	$3.692(10^{-4})$	$-1.784(10^{-1})$	$5.497(10^{-4})$	$-8.141(10^{-2})$	$2.312(10^{0})$	$-7.127(10^{-3})$
49	636.	$-1.105(10^{-3})$	$-3.282(10^{-8})$	$-1.645(10^{-3})$	$-4.887(10^{-8})$	$-3.437(10^{-4})$	$3.235(10^{-2})$	$9.609(10^{-7})$
54	627.	$-1.765(10^{-3})$	$4.182(10^{-7})$	$-2.628(10^{-3})$	$6.227(10^{-7})$	$-3.600(10^{-4})$	$3.705(10^{-2})$	$-8.778(10^{-6})$
58	631.	$-1.721(10^{-3})$	$4.350(10^{-7})$	$-2.563(10^{-3})$	$6.477(10^{-7})$	$-3.636(10^{-4})$	$3.758(10^{-2})$	$-9.497(10^{-6})$
74	676.	$-5.572(10^{-3})$	$6.79(10^{-8})$	$-8.297(10^{-3})$	$1.011(10^{-7})$	$-1.068(10^{-3})$	$9.058(10^{-2})$	$-1.104(10^{-6})$
75	650.	$-2.884(10^{-3})$	$5.823(10^{-7})$	$-4.294(10^{-3})$	$8.670(10^{-7})$	$-4.294(10^{-3})$	$6.149(10^{-2})$	$-1.241(10^{-5})$
76	715.	$-3.045(10^{-2})$	$4.104(10^{-5})$	$-4.533(10^{-2})$	$6.111(10^{-5})$	$-3.060(10^{-2})$	$9.013(10^{-1})$	$-1.215(10^{-3})$

[a]Sample weight/surface area = $a + bt + ct^2$; surface area = 1.489 cm^2 for every experiment.

[b]Sample weight = $a' + b't \quad c't^2$.

[c]First order kinetics: ln(sample weight/initial weight) = $a" + b"t$.

[d]Percent weight loss: (sample weight/initial weight) · 100 = $a"' + b"'t + c"'t^2$.

Table 36

Kinetic Thermogravimetry Data for $NaNO_2$ in Vacuum

Trace	Temperature (K)	b(mg cm^{-2} min^{-1})[a]	c(mg cm^{-2} min^{-2})[a]	b'(mg min^{-1})[b]	c'(mg min^{-2})[b]	b"(min^{-1})[c]	b"'(% min^{-1})[d]	c"'(% min^{-2})[d]
51	745.	$-7.118(10^{-1})$	$1.279(10^{-2})$	$1.060(10^{0})$	$1.904(10^{-2})$	$-5.417(10^{-1})$	$4.857(10^{1})$	$-8.727(10^{-1})$
53	743.	$-4.307(10^{-1})$	$2.998(10^{-3})$	$-6.413(10^{-1})$	$4.464(10^{-3})$	$1.905(10^{-1})$	$8.091(10^{0})$	$-5.632(10^{-2})$
64	753.	$-4.868(10^{-1})$	$5.397(10^{-3})$	$7.249(10^{-1})$	$8.036(10^{-3})$	$-1.445(10^{-1})$	$9.730(10^{0})$	$-1.079(10^{-1})$
48[e]	627.	$-9.646(10^{-3})$	$1.303(10^{-5})$	$-1.436(10^{-2})$	$1.941(10^{-5})$	$3.014(10^{-3})$	$3.391(10^{-1})$	$-4.582(10^{-4})$
52	623.	$-6.818(10^{-3})$	$3.103(10^{-6})$	$-1.015(10^{-2})$	$4.621(10^{-6})$	$-1.736(10^{-3})$	$1.599(10^{-1})$	$-7.277(10^{-5})$
57	627.	$-7.329(10^{-3})$	$5.662(10^{-6})$	$-1.091(10^{-2})$	$8.431(10^{-6})$	$-4.084(10^{-3})$	$2.777(10^{-1})$	$-2.145(10^{-4})$
65	671.	$-2.994(10^{-2})$	$3.331(10^{-5})$	$-4.385(10^{-2})$	$4.960(10^{-5})$	$-5.054(10^{-3})$	$4.530(10^{-1})$	$-5.124(10^{-3})$
77	717.	$-1.024(10^{-1})$	$3.513(10^{-4})$	$-1.524(10^{-1})$	$5.230(10^{-4})$	$-5.614(10^{-2})$	$2.038(10^{0})$	$-6.993(10^{-3})$
78	663.	$-1.327(10^{-2})$	$1.050(10^{-5})$	$-1.975(10^{-2})$	$1.564(10^{-5})$	$-6.602(10^{-3})$	$3.861(10^{-1})$	$-3.058(10^{-4})$

[a]Sample weight/surface area = $a + bt + ct^2$; surface area = 1.489 cm^2 for every experiment.

[b]Sample weight = $a' + b't$ $c't^2$.

[c]First order kinetics: ln(sample weight/initial weight) = $a" + b"t$.

[d]Percent weight loss: (sample weight/initial weight) · 100 = $a"' + b"'t + c"'t^2$.

[e]During this experiment the teletype failed and the kinetic data for the last 135 minutes was lost.

Table 37

Kinetic Thermogravimetry Data for KNO_3 in Vacuum

Trace	Temperature (K)	b(mg cm^{-2} min^{-1})[a]	c(mg cm^{-2} min^{-2})[a]	b'(mg min^{-1})[b]	c'(mg min^{-2})[b]	b"(min^{-1})[c]	b"'(% min^{-1})[d]	c"'(% min^{-2})[d]
66	747.	$-1.938(10^{-1})$	$9.845(10^{-4})$	$-2.885(10^{-1})$	$1.466(10^{-3})$	$-8.364(10^{-2})$	$3.914(10^{0})$	$-1.989(10^{-2})$
72	743.	$-1.924(10^{-1})$	$9.438(10^{-4})$	$-2.865(10^{-1})$	$1.405(10^{-3})$	$-1.081(10^{-1})$	$4.328(10^{0})$	$-2.123(10^{-2})$
80	737.	$-1.908(10^{-1})$	$1.006(10^{-3})$	$-2.842(10^{-1})$	$1.497(10^{-3})$	$-7.102(10^{-2})$	$3.539(10^{0})$	$-1.865(10^{-2})$
81	717.	$-3.994(10^{-2})$	$7.699(10^{-5})$	$-5.947(10^{-2})$	$1.146(10^{-4})$	$-1.801(10^{-2})$	$7.784(10^{-1})$	$-1.500(10^{-3})$
82	671.	$-9.742(10^{-3})$	$2.236(10^{-6})$	$-1.451(10^{-2})$	$3.329(10^{-6})$	$-2.569(10^{-3})$	$1.884(10^{-1})$	$-4.323(10^{-5})$
83	741.	$-2.3817(10^{-1})$	$1.349(10^{-3})$	$-3.546(10^{-1})$	$2.009(10^{-3})$	$-1.103(10^{-1})$	$4.405(10^{0})$	$-2.495410^{-2})$
84	650.	$-4.981(10^{-3})$	$2.074(10^{-6})$	$-7.416(10^{-3})$	$3.088(10^{-6})$	$-9.396(10^{-4})$	$9.496(10^{-2})$	$-3.954(10^{-5})$
85	624.	$-1.950(10^{-3})$	$8.724(10^{-7})$	$-2.903(10^{-1})$	$1.299(10^{-6})$	$-3.147(10^{-4})$	$3.600(10^{-2})$	$-1.610(10^{-5})$
86	623.	$-1.863(10^{-3})$	$9.152(10^{-7})$	$2.773(10^{-3})$	$1.363(10^{-6})$	$-2.851(10^{-4})$	$3.345(10^{-2})$	$-1.644(10^{-5})$
87	621.	$-2.455(10^{-3})$	$2.231(10^{-6})$	$3.655(10^{-3})$	$3.322(10^{-6})$	$-3.489(10^{-4})$	$5.049(10^{-2})$	$-4.589(10^{-5})$

[a]Rate of sample weight change per unit surface area: rate = b + ct.

[b]Rate of sample weight change = b' + c't.

[c]First order kinetic rate of weight change = b".

[d]Rate of weight change in percent of starting weight = b"' + c"'t.

Table 38

Kinetic Thermogravimetry Data for $LiNO_3$ in Vacuum

Trace	Temperature (K)	b(mg cm^{-2} min^{-1})[a]	c(mg cm^{-2} min^{-2})[a]	b'(mg min^{-1})[b]	c'(mg min^{-2})[b]	b"(min^{-1})[c]	b"'(% min^{-1})[d]	c"'(% min^{-2})[d]
73	745.	$-1.680(10^{-1})$	$2.535(10^{-4})$	$-2.502(10^{-1})$	$3.774(10^{-4})$	$-2.502(10^{-1})$	$3.030(10^{-1})$	$-4.572(10^{-4})$
88	723.	$-1.273(10^{-1})$	$-2.943(10^{-4})$	$-1.896(10^{-1})$	$-4.382(10^{-4})$	$-2.896(10^{-1})$	$8.389(10^{0})$	$1.939(10^{-2})$
89	730.	$-3.252(10^{-1})$	$2.974(10^{-3})$	$-4.843(10^{-1})$	$4.429(10^{-3})$	$-3.713(10^{-1})$	$1.769(10^{1})$	$-1.617(10^{-1})$

[a]Rate of sample weight change per unit surface area: rate = b + ct.

[b]Rate of sample weight change = b' + c't.

[c]First order kinetic rate of weight change = b".

[d]Rate of weight change in percent of starting weight = b"' + c"'t.

The kinetic expressions for the weight, weight per unit area and the percent weight remaining all satisfactorily describe the decomposition experiments. In the decomposition experiments in air, I observed that the weight loss per unit area was the most useful way to compare experiments performed with vastly different sample crucibles and sample sizes. The same is true in vacuum. Three $LiNO_3$ experiments were performed which were identical except that one sample was much larger (75 mg versus 8 mg starting weight). When these three experiments were compared, the rates of weight loss and weight loss per unit area were comparable although the percent weight loss rates differed significantly. Based on the kinetic results in air and vacuum, I concluded that the most significant rates to consider were the weight losses per unit area per unit time ($mg\text{-}cm^{-2}\text{-}min^{-1}$).

The rates of weight loss per unit area are

$$r(T) = b(T) + 2 \cdot c(T) \cdot t \qquad (69)$$

where r is the rate, b and c are the rate constants from Eq. (48), t is time. Here r, c, and b are functions of temperature.

The initial rates, b, from the high (730 - 750 K) and low (620 - 630 K) temperature experiments are plotted for each salt in Figure 52. This figure illustrates that the rates depend on temperature and the salt. The rates of decomposition of $NaNO_3$ and $NaNO_2$ at 630 K are 0.002 and 0.01 mg cm^{-2} min^{-1}, respectively. At 740 K the rates are 0.15 and 0.07 mg cm^{-2} min^{-1} for $NaNO_3$ and $NaNO_2$.

The values of b also illustrated in Figure 53 for the individual salts and Figure 54 for all the salts together. The data are plotted with the best linear least squares fit of ln (b) versus 1/T. The rate data conform to this (Arrhenius) analysis, therefore the temperature

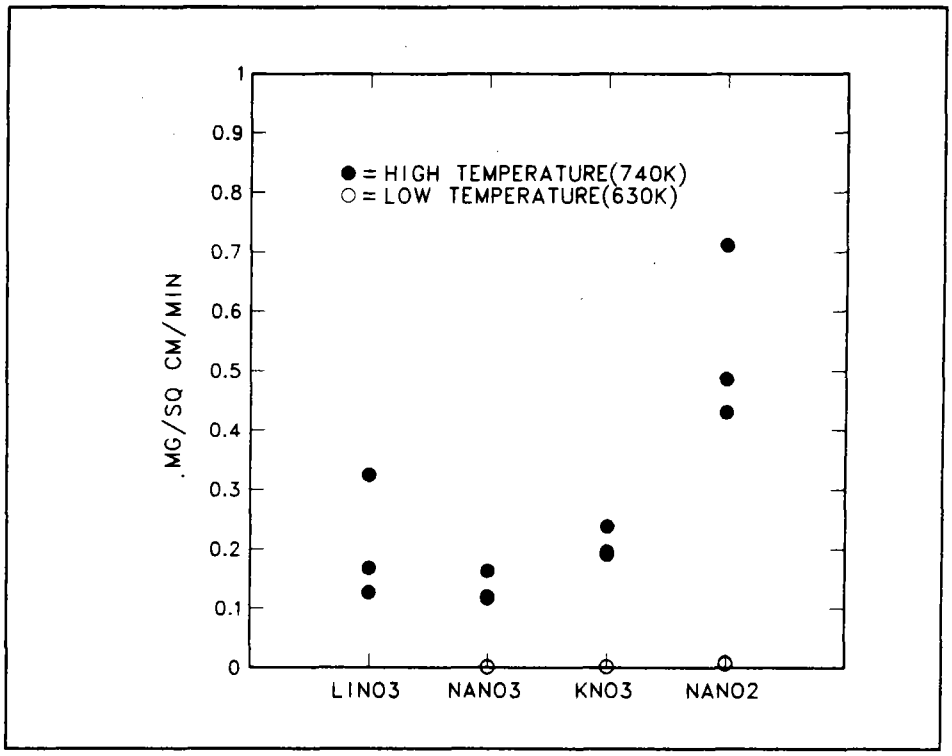

Figure 52. Rates of Weight Loss for Several Salts

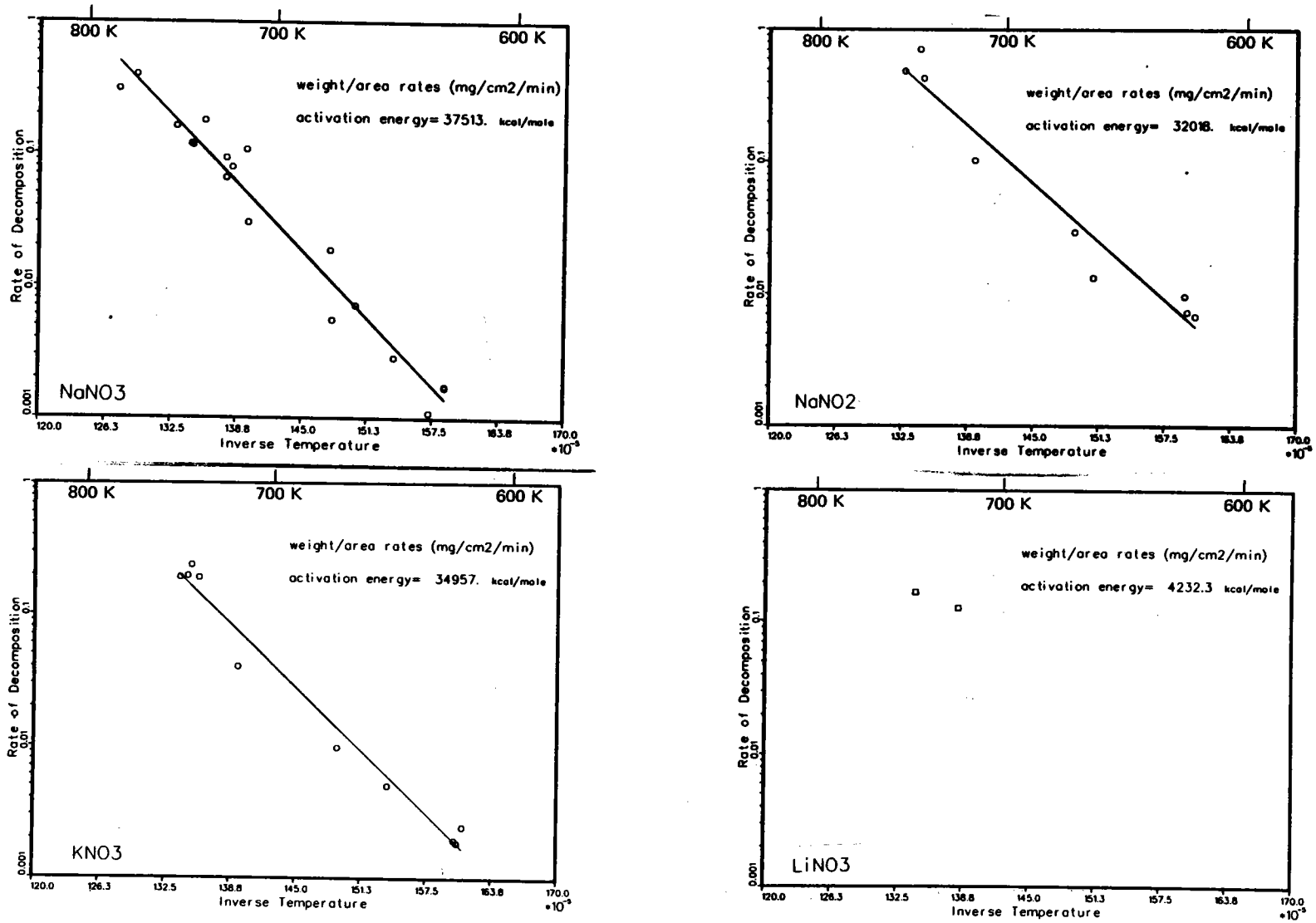

Figure 53. Rates of Weight Loss as a Function of Temperature

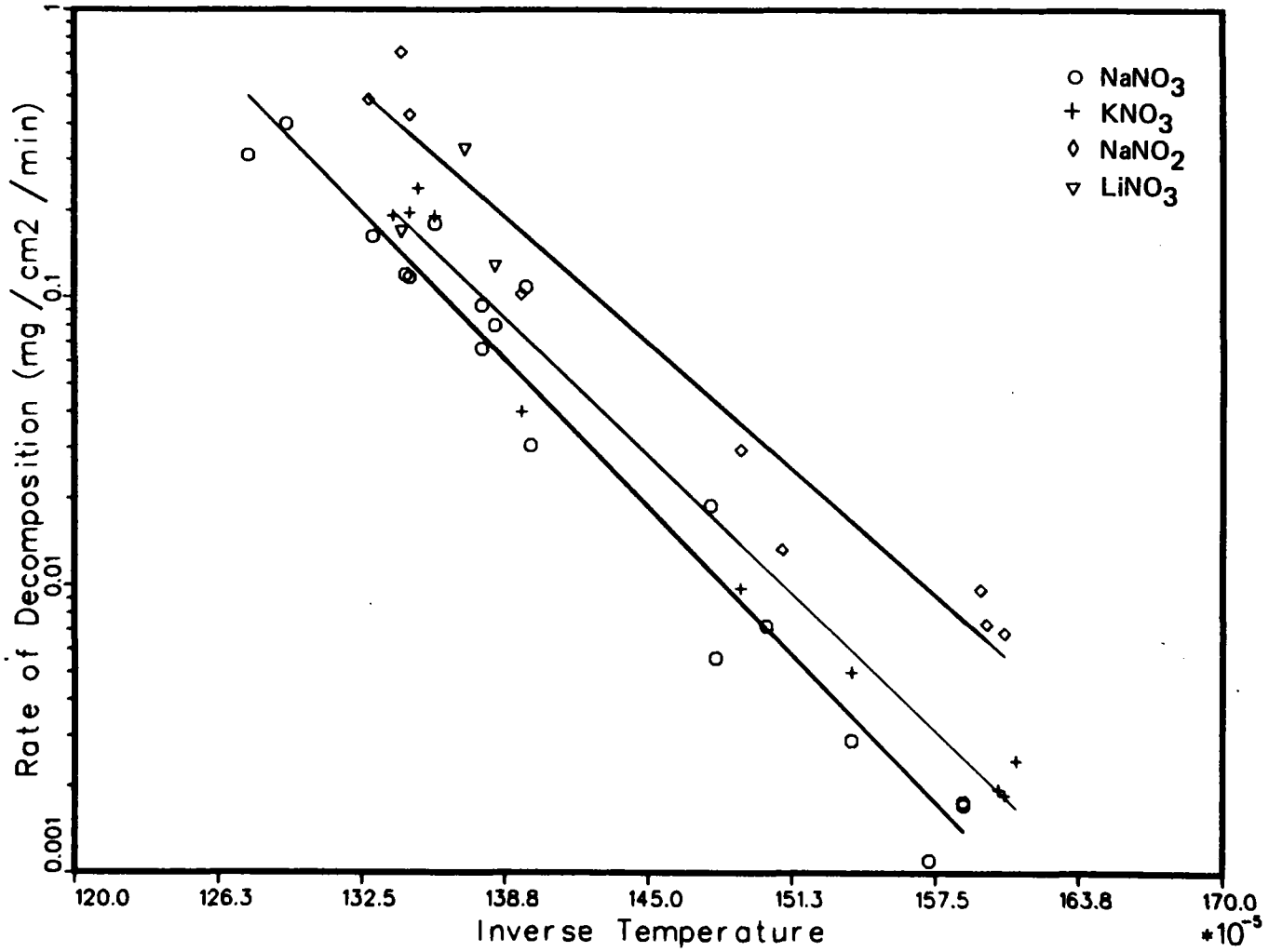

Figure 54. Rates of Weight Loss in Vacuum

dependence of the initial rate of decomposition of $NaNO_3$, $NaNO_2$ and KNO_3 may be described by Equation (52). The enthalpies and entropies of activation are given in Table 39.

Several observations may be made about the relative magnitudes of the rates and the temperature dependencies of the rates of each salt. The rates of weight loss per unit area decrease in this order: $NaNO_2$, $LiNO_3$, KNO_3 and $NaNO_3$. The temperature dependencies of the initial rates of weight loss per unit area for $NaNO_2$, KNO_3 and $NaNO_3$ are similar as judged by the values of ΔH^* and ΔS^* (see Table 39), ranging from 32 - 36 kcal $mole^{-1}$ (134 - 151 KJ-$mole^{-1}$). These values of ΔH^* are much lower than the previously reported activation energies or enthalpies for either decomposition or vaporization processes (see Table 40). The ΔH^* values determined in this work were determined under much different conditions than the previous decomposition studies, notably high vacuum and lower temperatures; therefore the lower values ΔH^* in this work are not surprising.[77] The temperature dependencies determined in this work are lower than vaporization studies. The vaporization studies do not include decomposition whereas the ΔH^* values reported here reflect the combined temperature dependencies of the initial rates of decomposition and salt vaporization.

As decompositon proceeds, increasing contributions to the rate arise from the term $2 \cdot c(T) \cdot t$; of Eq. (69) therefore the values of c(T) are of interest to compare as in Figures 55 and 56. The values of c from all the isothermal experiments were negative (with 2 exceptions). Negative values of c mean that the rate decreases with time. Decomposition rates that decreased with time were also observed by Voskrenskaya and Berul[14] with HTS. The values of c were much smaller (10^{-7} to 10^{-5} mg-cm^{-2}-min^{-2}) at

Table 39

Temperature Dependence of Salt Decomposition[a]

Experimental Series	Weight Loss per Unit Area				Weight Loss			
	ΔH*		ΔS*		ΔH*		ΔS*	
	kcal-mole^{-1}	kJ-mole^{-1}	cal-mole^{-1}	J-mole^{-1}	kcal-mole^{-1}	kJ-mole^{-1}	cal-mole^{-1}	J-mole^{-1}
$NaNO_3$ and KNO_3 in Vacuum	30.29	120.7	37.23	155.8	28.32	118.5	31.23	130.7
$NaNO_3$ in Vacuum	36.55	152.9	44.93	188.0	36.55	152.9	45.72	191.3
$NaNO_2$ in Vacuum	32.11	134.3	41.72	174.6	32.11	134.3	42.51	177.9
KNO_3 in Vacuum	34.93	146.1	43.55	182.2	34.93	146.1	44.34	185.5

Experimental Series	Percent Weight Lost				First Order Kinetics			
	ΔH*		ΔS*		ΔH*		ΔS*	
	kcal-mole^{-1}	kJ-mole^{-1}	cal-mole^{-1}	J-mole^{-1}	kcal-mole^{-1}	kJ-mole^{-1}	cal-mole^{-1}	J-mole^{-1}
$NaNO_3$ and KNO_3 in Vacuum	22.03	92.17	24.70	103.3	21.15	88.49	15.88	66.44
$NaNO_3$ in Vacuum	35.58	148.7	49.68	207.9	45.17	189.0	55.70	233.0
$NaNO_2$ in Vacuum	31.58	132.1	47.73	199.7	34.09	142.6	42.84	179.2
KNO_3 in Vacuum	35.30	147.7	49.98	209.1	43.61	182.5	53.74	224.8

[a] ΔH* = enthalpy of activation; ΔS* = entropy of activation.
ΔH are ± 4.9 kcal/mole and ΔS are ± 2 cal/mole for a 90% confidence limit.

Table 40

Temperature Dependence of Salt Evaporation

Reaction	H^* kcal-mole^{-1}	H^* kJ-mole^{-1}	Reference
$KNO_3 \rightarrow KNO_2 + 1/2\ O_2$	65.6	274.	42
KNO_3 evaporation[a]	34.9	146.	This Work
$KNO_3(\ell) \rightarrow KNO_3$ (g)	41.8	175.	75
$2KNO_3(\ell) \rightarrow (KNO_3)_2$ (g)	48.0	201.	75
$NaNO_3 \rightarrow NaNO_2 + 1/2\ O_2$	44.7	187.	34
$NaNO_3 \rightarrow NaNO_2 + 1/2\ O_2$	40.3	169.	50
$NaNO_3$ evaporation[a]	36.6	153.	This Work
$NaNO_3(\ell) \rightarrow NaNO_3$ (g)	41.0	172.	76
$2NaNO_3(\ell) \rightarrow (NaNO_3)_2$ (g)	49.4	207.	76
$2NaNO_2 \rightarrow Na_2O + N_2 + 3/2\ O_2$	42.8	179.	50
$NaNO_2$ evaporation[a]	32.1	134.	This Work
$(Na/K)NO_3$ evaporation[a]	30.3	127.	This Work

[a]Evaporation = vaporization + decomposition.

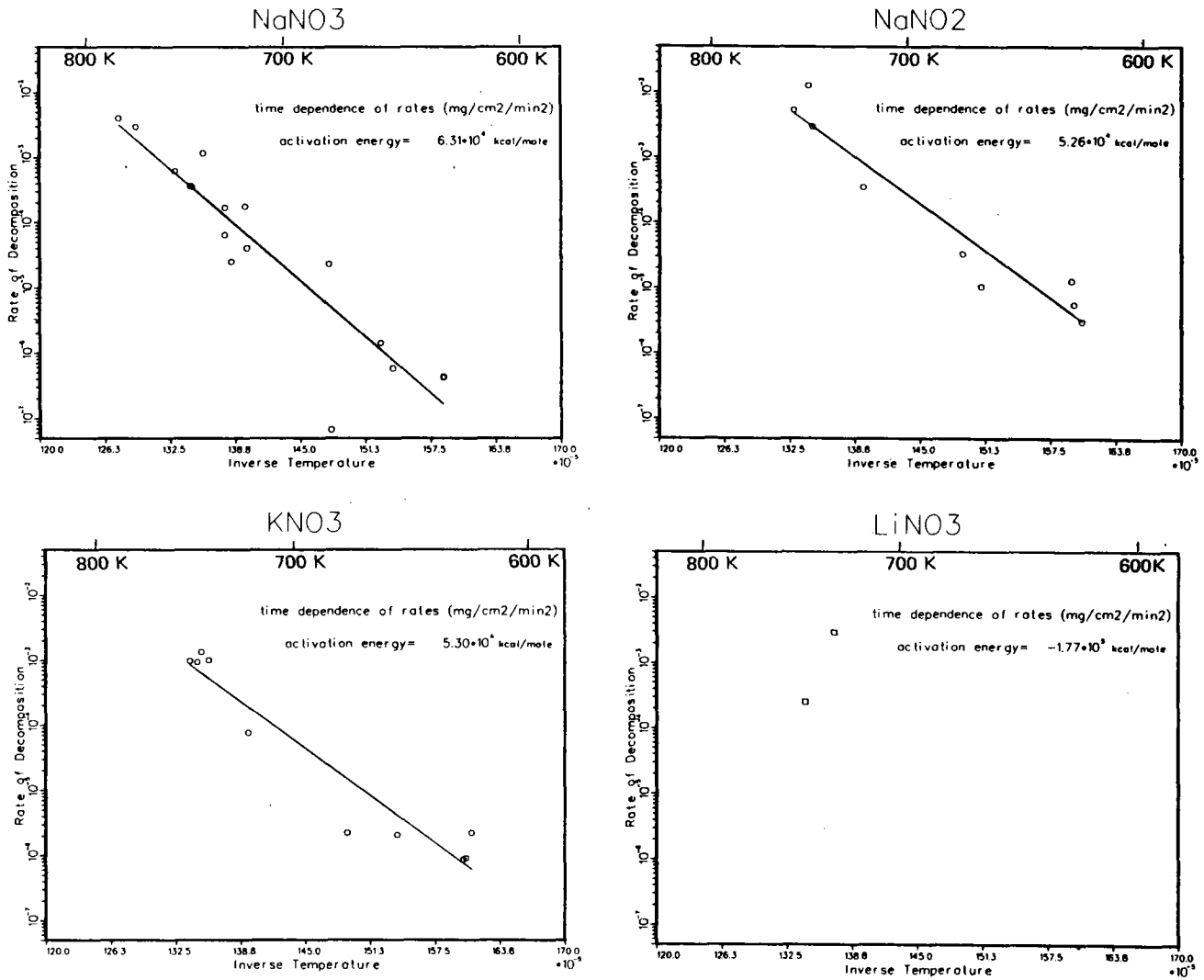

Figure 55. Time Dependence of Rates of Weight Loss for Several Salts

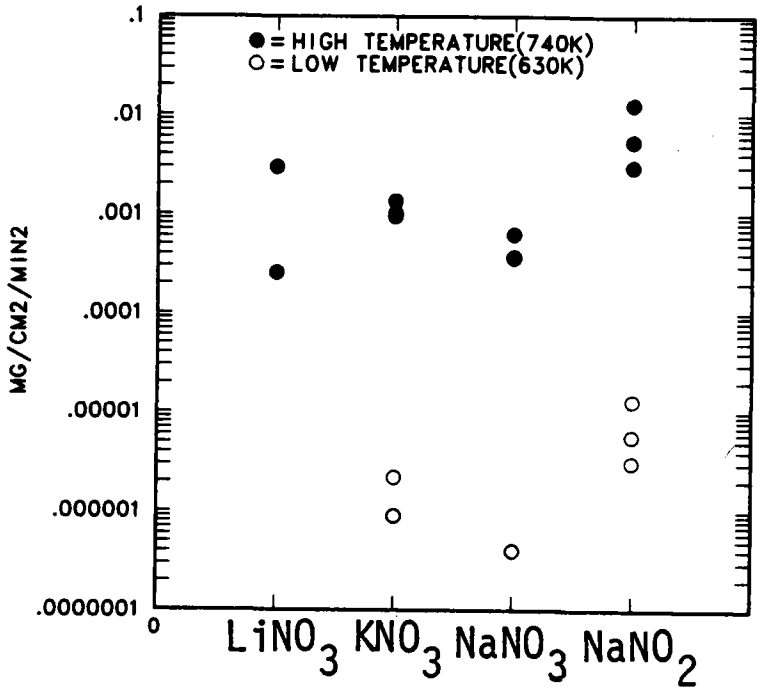

Figure 56. Time Dependence of Rates of Weight Loss as a Function of Temperature

630 K than at 740 K (10^{-4} - 10^{-2} mg-cm^{-2}-min^{-2}) and were also a function of the salt. The change in the rate of weight loss that is represented by c is due to several overlapping simultaneous processes. The rate constant of a secondary reaction such as vaporization of the decomposition product, or superoxide decomposition contributes to c. The activation enthalpies of c for $NaNO_2$, KNO_3 and $NaNO_3$ are 52.6, 53.0, and 63.1 Kcal-mole^{-1}, respectively. These activation enthalpies are much higher than those observed for the initial rates.

In the Introduction the maximum vaporization rates were calculated based on vapor pressure data. The fluxes measured from the TG experiments are approximately 0.1% of the fluxes predicted from vaporization which is surprisingly low. There are several explanations for this. The value of α (see Equation (45)) may be 0.001 for these salts. Values of α equal to 0.009 or 0.001 have been reported[172,173], however low values of α are expected for solids[185] and α is reported to be 0.7 and 1.0 for liquid $NaNO_3$[76] and KNO_3[75] respectively. Possibly, the kinetics of vaporization and decomposition are controlled by different activation complexes in the thin layers used here compared to the bulk samples or equilibrium conditions used in other studies.[77] Or, most likely, the vapor pressures may be wrong because there was unobserved decomposition that interfered with the accuracy of the vapor pressure measurements.

As mentioned earlier, the rates of weight loss per unit area in vacuum are higher for KNO_3 than for $NaNO_3$ from 630 - 750 K. Potassium nitrate is more stable than $NaNO_3$ with respect to decomposition.[34,37,42,54,169] Contributions from nitrate vaporization may account for this. Although the vapor pressure of KNO_3 is less than that of $NaNO_3$, the maximum

flux from KNO_3 is slightly higher than that of $NaNO_3$ because of its larger molecular weight. Therefore, the rates of decomposition of KNO_3 may be less than those of $NaNO_3$ but the total flux from KNO_3 may exceed that of $NaNO_3$ due to vaporization of the heavier KNO_3 or $(KNO_3)_2$ molecules.

Lastly, since the sample is entirely vaporized and decomposed in an experiment, the decomposition products must be vaporizing. A study has been made of the vaporization of potassium oxides and in the temperature range of interest (630 K - 750 K), both KO and K_2O_2 vaporize.[174] No determinations of the vapor species are possible with the TG/MS apparatus. The products of decomposition according to the proposed reaction scheme are superoxide and peroxide. The peroxide may vaporize to peroxide or monoxide. The superoxide may be consumed by Reaction (37) or decompose to peroxide and oxygen or vaporize.

Dynamic Heating Experiments

The dynamic heating experiments confirm many of the results obtained in the isothermal experiments. One of these results is that the gases that are evolved and the sequence in which they are evolved is N_2, NO, and O_2. All three gases are evolved at lower temperatures from $LiNO_3$ than from $NaNO_3$ or KNO_3. The temperatures at which gases evolve from $NaNO_3$ are the same as from KNO_3.

To compare the 3 salts I determined the temperatures at which a 10% weight loss has occurred. The temperatures at which 10% weight loss had occurred are 673, 746 and 736 K respectively for $LiNO_3$, $NaNO_3$ and KNO_3. This comparison is illustrated in Figure 57 where the sample weight versus sample temperature is plotted for the three salts. Figure 58 shows the rates calculated from the dynamic heating experiments. The rates of weight loss from KNO_3 exceed the rates for $NaNO_3$ as in

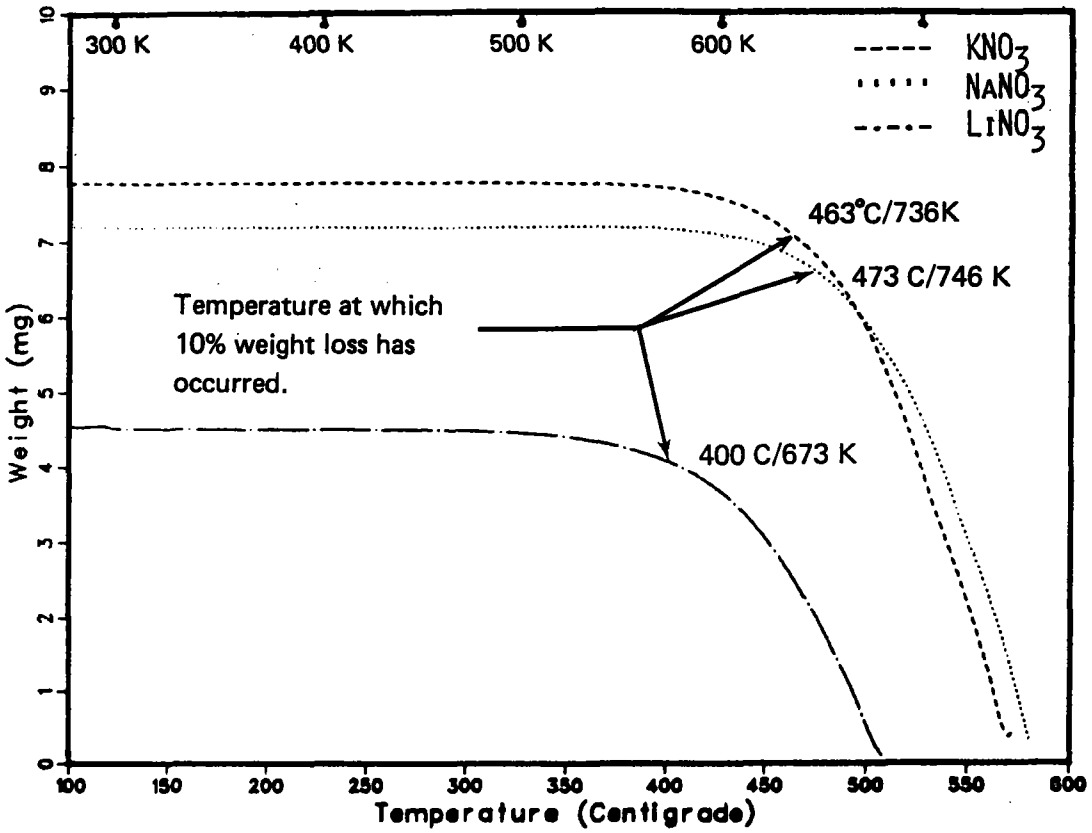

Figure 57. Dynamic TG Experiments

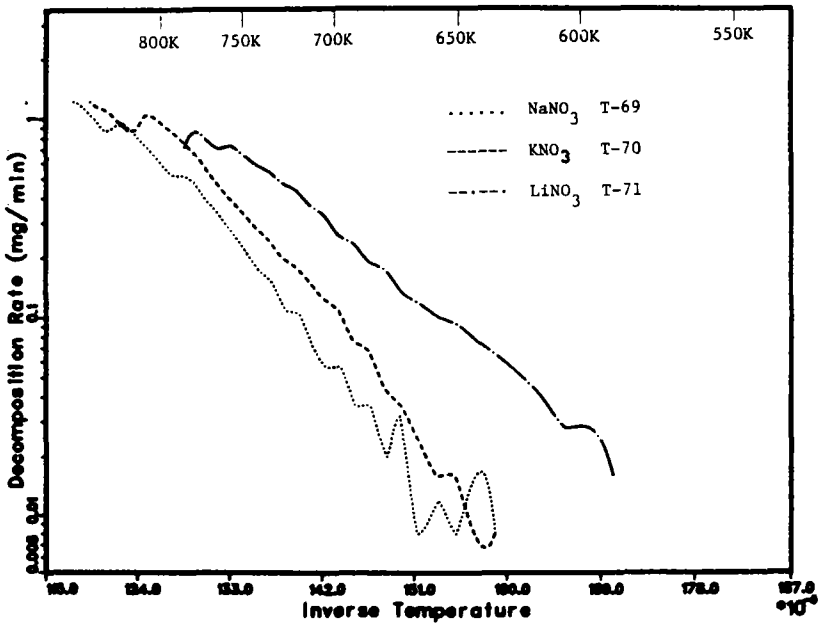

Figure 58. Dynamic TG Rates of Weight Loss

the isothermal experiment. The $LiNO_3$ rates of weight loss are always greater than the KNO_3 or $NaNO_3$ rates in either isothermal or dynamic heating experiments. Lithium nitrate has been observed to be less stable than $NaNO_3$ or KNO_3.[33,37,167] Furthermore, the dynamic rates of weight loss for $LiNO_3$ increase more slowly than the $NaNO_3$ or KNO_3 rates as the temperature is raised.

The values of the isothermal rates of weight loss are comapred with the dynamic rates of weight loss for $LiNO_3$, KNO_3 and $NaNO_3$ in Figure 59. The agreement between the isothermal rates and the dynamic rates is good. The isothermal rates below 700 K are lower than the dynamic rates. The isothermal rates were determined by a least squares fit to several hundred weight readings whereas the dynamic rates were determined from two successive weight readings; therefore the isothermal rates at low weight loss rates (temperatures below 700 K) are more accurate than the dynamic rates. Dynamic TG techniques are generally considered to be less accurate than the isothermal TG techniques.[122,175]

In the isothermal experiments I observed that as the temperature increases and the reaction proceeds, the magnitude and the contribution of the constant c to the rates of weight loss (rate = b+2ct) increases. Because the dynamic heating experiments increase in temperature as the samples decompose, the dynamic rates have contributions from b(T) and c(T). Therefore, the dynamic rates (b+2ct) and the isothermal rates only) cannot be strictly compared.

Furthermore one can see in Figure 58 that the dynamic rates are not amenable to a linear least squares Arrhenius analysis as the initial rates are. The graph of ln(dynamic rates) versus 1/T has a distinct curvature for all 3 nitrates. The curvature or deviation from

Arrhenius behavior arises both from the increasing contribution of 2·c·t to the rate as the temperature rises.

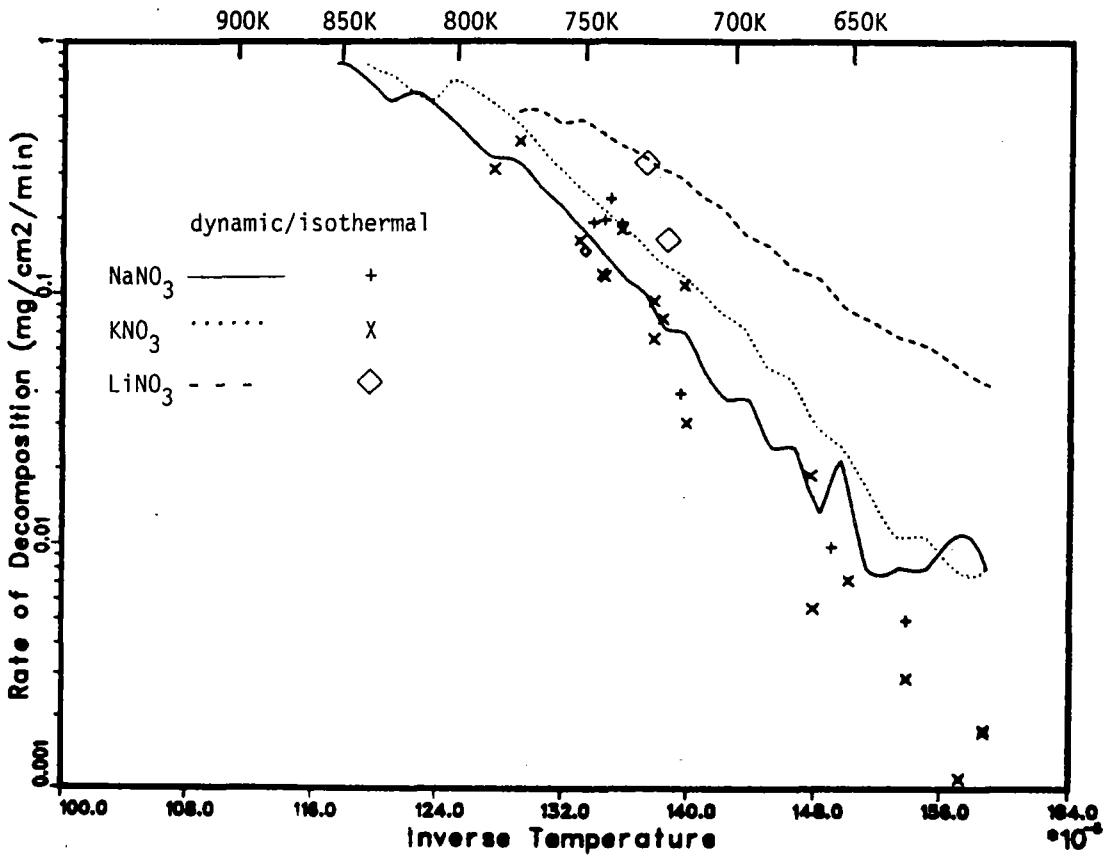

Figure 59. Dynamic and Isothermal TG Rates of Weight Loss

V. SUMMARY AND CONCLUSIONS

Five series of experiments have been performed to elucidate the decomposition of sodium and potassium nitrate. Decomposition was studied in air, argon and vacuum. The experimental techniques were differential scanning calorimetry (DSC), thermogravimetry (TG), mass spectrometry (MS) and chemical analysis.

Decomposition of sodium and potassium nitrate and nitrite in air was studied using DSC where it was observed that endothermic decomposition reactions began at 840 $\pm$ 10 K and 820 $\pm$ 20 K for $NaNO_3$ and KNO_3 respectively and above 800 $\pm$ 10 K for both $NaNO_2$ and KNO_2. Decomposition reactions of nitrates and nitrites in air were also studied using a statistical screening technique in conjunction with chemical analysis. Ten variables were evaluated which were: temperature, N_2, O_2, CO_2, H_2O, gas flow rate, salt surface area, salt purity, K to Na ratio, and sample size. In this series of screening experiments the salts underwent many reactions including carbonate formation, increased alkalinity, vaporization, nitrite formation in nitrates, and nitrate formation in $NaNO_2$. The salts also spread and wetted their containers and discolored (turned green). High temperatures had the most significant influence in enhancing these processes. Higher CO_2 contents, higher gas flows, higher humidity, and lesser salt purity also significantly enhanced the complex decomposition processes. The O_2 and N_2 over the salts, the Na to K ratio and the sample size did not have significant influences on the multiple reactions that occurred.

Experiments were also conducted in argon using sealed stainless steel containers in which salt samples were kept for 100 hours at either 624 K or 736 K. Sodium and potassium nitrate were decomposed almost

completely to nitrite and a small fraction of oxygen ion (oxide, peroxide or superoxide). The nitrite samples decomposed more extensively to oxygen ions. The nitrates and especially the nitrites reacted with the stainless steel containers.

The kinetics of decomposition were studied using TG in air and in vacuum. The rates of weight loss in the TG experiments were proportional to the surface area of the salt in air and in vacuum. The rates slowly decreased with time. High gas flow rates, the presence of inert gas or dry air, low salt purity, and high temperatures increased the rates of weight loss in air. The kinetics were the same for either $NaNO_3$ or $(Na/K)NO_3$ in air. In vacuum, the weight loss rate per unit area was greatest for $NaNO_2$, lesser for KNO_3 and least for $NaNO_3$. The activation energies for these three salts in vacuum were not statistically different over the temperature range studied (630 K - 750 K) although they ranged from 32 to 37 kcal-mole^{-1}. Over this temperature range the rates of weight loss in vacuum varied from 0.001 to 1.0 mg-cm^{-2}-min^{-1}. These rates include contributions from vaporization of the nitrates, decomposition of the nitrates and vaporization of the oxygen ion decomposition products. The rates of weight loss in vacuum were approximately 100 times greater than those observed in static air.

In the TG/MS experiments performed in vacuum, the intrinsic (non-condensible) gaseous decomposition products of $NaNO_2$ were nitrogen and nitric oxide. Sodium and potassium nitrate decompose and initially give off N_2 and NO at 630 K; however oxygen is released from the nitrates at higher temperatures and later in the decomposition process. Evidence was

presented for a sequence of reactions occurring in the nitrates and nitrites which includes superoxide, peroxide, N_2, NO and O_2.

VI. REFERENCES

1. A. Villiers, The Way of a Ship, Charles Scribner & Sons, New York, 1970.
2. L. N. Tallerico, "A Description and Assessment of Large Solar Power Systems Technology," Sandia Laboratories Report SAND79-8015 (1979).
3. T. D. Brumleve, "Status Report on the Direct Absorption Receiver," Sandia Laboratories Report SAND78-8702 (1978).
4. W. D. Drotning, Solar Energy 20, 313 (1978).
5. L. Radosevich, "Thermal Energy Storage for Advanced Solar Central Receiver Power Systems," Sandia Laboratories Report SAND78-8821 (1978).
6. A. Borucka, "Survey and Selection of Inorganic Salts for Application to Thermal Energy Storage," ERDA-59 (1975).
7. H. P. Voznick and V. W. Uhl, Chem. Eng. 70, 135 (1963).
8. B. W. Watt and D. H. Kerridge, Chem. in Brit 15, 78 (1979).
9. A. Bonomi and C. Gentaz in Proc. of the Conference Molten Salts: Technology and Future Trends, (Frankfurt, Germ.) 1975.
10. D. E. Etter and J. C. Wiedenheft, Solar Energy Materials 2, 423 (1980).
11. R. Lalchandani and P. D. Grover, Ind. Chem. Eng 14, 34 (1972).
12. M. D. Silverman and J. R. Engle, "Survey of Technology for Storage of Thermal Energy in Heat Transfer Salt," Oak Ridge National Laboratories report ORNL/TM-5682 (1977).
13. A. C. Skinrood, "High-Temperature Solar Options for Electric Utilities and Users of Process Heat," Sandia Labortories Report SAND80-8695 (1980).

    A. C. Skinrood, Solar Age 5 (8), 84 (1980).

14. N. K. Voskresenskaya and S. I. Berul, Zh. Neorg. Khim 1 (8), 180 (1956).

15. J. Alexander and S. G. Hindin, Ind. Eng. Chem 39 (8), 1044 (1947).

16. W. H. Smyrl, "Corrosion in Molten Salts Used for Solar Thermal Storage Applications," Sandia Laboratories Report, SAND79-0246C.

17. J. A. Plambeck in Ency. of Electrochem. of the Elements, Fused Salt Systems, 10, edited by A. J. Bard (Marcel Dekker, NY 1976).

18. M. H. Miles, A. N. Fletcher, J. Appl. Electrochem. 10, 251 (1980).

19. S. D. Stookey, J. S. Olcott, H. M. Garfinkel, and D. L. Rothermel, in Advances in Glass Technology (Plenum Press, NY 1962), 397.

20. R. N. Kust, J. Electrochem. Soc., 116 (8), 1137 (1969).

21. R. W. Brown, J. H. Lippiatt, D. Price and D. C. A. Izod, Int'l J. Mass Spect. and Ion Phys. 16, 101 (1975).

22. P. Lloyd and E. A. C. Chamberlain, J. Irn Steel Inst. 142, (2), 141 (1940).

23. R. J. Box and B. A. Middleton, J. Irn Steel Inst. 151 (1), 71 (1945).

24. E. G. Bohlmann, "Heat Transfer Salt for High Temperature Steam Generation," Oak Ridge National Laboratories report ORNL-TM-3777 (1972).

25. H. W. Hoffman and S. I. Cohen, "Fused Salt Heat Transfer - Part III: Forced Convection Heat Transfer in Circular Tubes Containing the Salt Mixture $NaNO_2$ - $NaNO_3$-KNO_3," Oak Ridge National Laboratories report ORNL-2433 (1960).

26. Partherm Heat Transfer Salt Bulletin, Park Chemical Co., 8074 Military Avenue, Detroit, MI 48204.

27. N. K. Voskresenskaya and S. I. Berul, Zh. Neorg. Khim 1 (8), 1867 (1956).

28. W. E. Kirst, W. M. Nagle, and J. B. Castner, AIChe. Trans. 36, 371 (1941).

29. "Hitec Heat Transfer Salt," E. I. DuPont de Nemours and Co., Inc. Bulletin, Wilmington, DE 19898.

30. H. P. Voznick and V. W. Uhl, Chem. Eng. 70, 129 (May 27, 1963).

31. K. H. Stern, J. Phys. Chem. Ref. Data 1 (3), 747 (1972).

32. I. Barin and O. Knacke, Thermochemical Properties of Inorganic Substances (Springer-Verlag, Berlin 1973).

33. C. C. Addison and N. Logan in Advances in Inorganic and Radiochemistry, 6, edited by H. J. Emeleus and A. G. Sharpe (Academic Press, New York 1964).

34. E. S. Freeman, J. Phys. Chem. 60, 1487 (1956).

35. K. S. Chun, "Studies on the Thermal Decomposition of Nitrates Found in Highly Active Waste and of Chemicals used to Convert the Waste to Glass," AERE-R 8735 (1977).

36. M. Sweeney, Thermochimica Acta 11, 409 (1975).

37. E. A. Bordyushkova, P. I. Protsenko, and L. N. Venerovskaya, J. Appl. Chem USSR 40, 1386 (1967).

38. P. I. Protsenko and E. A. Bordyushkova, Russ. J. Inorg. Chem. 10 (5), 657 (1965).

39. R. J. Kee, J. A. Miller, T. H. Jefferson, "CHEMKIN: A General Purpose, Problem-Independent, Transportable, Fortran Chemical Kinetics Code Package," Sandia Laboratories, SAND80-8003 (1980).

40. J. A. Miller, M. C. Branch, and R. J. Kee, "A Chemical Kinetic Model for the Selective Reduction of Nitric Oxide by Ammonia," Sandia Laboratories, SAND80-8635 (1980).

41. R. F. Bartholomew, J. Phys. Chem. 70 (11), 3442 (1966).

42. E. S. Freeman, J. Amer. Chem. Soc. 79, 838 (1957).

43. G. D. Sirotkin, Russ. J. Inorg. Chem. 4 (11) 1180 (1959).

44. R. N. Kust and J. D. Burke, Inorg. Nucl. Chem. Letters 6, 333 (1970).

45. F. Paniccia and P. G. Zambonin, Chem Soc. Lon., Farad. Trans. I 72, 1512 (1976).

46. T. M. Oza, J. Ind. Chem. Soc. 22, 173 (1945).

47. T. M. Oza, and B. R. Walawalkar, J. Ind. Chem. Soc. 22, 243 (1945).

48. V. J. Szper and K. Fiszman, Z. Anorg. Allgem. Chem. 206, 257 (1932).

49. T. M. Oza and S. A. Patel, J. Ind. Chem. Soc. 31, (7) 520 (1954).

50. B. D. Bond and P. W. M. Jacobs, J. Chem. Soc. Lon. A (9), 1265 (1966).

51. M. A. Peneloux and M. F. Joliot, Bull. Franc. Acad. Sci. 23, 1082 (1953).

52. A. Buchler and J. L. Stauffer, J. Phys. Chem. 70 (12), 4092 (1966).

53. H. R. Bartos and J. L. Margrave, J. Phys. Chem. 160, 256 (1956).

54. C. J. Hardy and B. O. Field, Chem. Soc. J. Pt 4-5, 5131 (1963).

55. S. S. Al Omer and D. H. Kerridge, J. Inorg. Nucl. Chem. 40, 975 (1978).

56. V. P. Yurkinskii, N. B. Vorobeva, E. G. Firsova and A. G. Morachevskii, J. App. Chem. of USSR, 52 (1) 60 (1979).

57. L. E. Topol, R. A. Osteryoung, and J. H. Christie, J. Phys. Chem. 70, 2857 (1966).

58. R. N. Kust and F. R. Duke, J. Amer. Chem. Soc. 85, 3338 (1963).

59. A. A. El Hosary and A. M. Shams El Din, Electrochimica Acta 16, 143 (1971).

60. R. A. Graham and H. S. Johnston, Amer. Chem. Soc. 82 (3), 254 (1978).

61. D. R. Flinn and K. H. Stern, J. Electroanalyt. Chem. 63, 39 (1975).

62. M. H. Miles and A. N. Fletcher, J. Electrochem. Soc.127 (8), 1761 (1980).

63. J. Jordan, W. B. McCarthy and P. G. Zambonin, in Characterization and Analysis in Materials Science, edited by G. Mamantov, (Marcel Dekker, NY, 1969).

64. P. G. Zambonin and J. Jordan, J. Amer. Chem. Soc. 91 (9), 2225 (1969).

65. P. G. Zambonin and J. Jordan, J. Amer. Chem. Soc. 89 (24), 6365 (1967).

66. F. Paniccia and P. G. Zambonin, J. Phys. Chem. 78 (17), 1693 (1974).

67. K. Leschewski, Deut. Chem. Ges. Ber. Chem. Ber. 72B, 1763 (1939).

68. R. B. Temple and C. J. Lockyer, Aust. J. Chem. 32, 1849 (1979).

69. E. Desimoni, F. Palmisano, and P. G. Zambonin, J. Electroanal. Chem. 84, 315 (1977).

70. P. G. Zambonin and G. Signorile, J. Electroanal. Chem. 35, 251 (1972).

71. P. G. Zambonin, Electroanal. Interfac. Chem. 33, 243 (1971).

72. N. K. Voskresenskaya and S. I. Berul, Russ. J. Inorg. Chem. 5, (3), 315 (1960).

73. D. Smith, D. W. James, and J. P. Devlin, J. Chem. Phys. 54 (10), 4437 (1971).

74. N. Smyrl and J. P. Devlin, J. Phys. Chem 77 (26), 3067 (1963).

75. N. V. Bagaratiyan, M. K. Il'in and O. T. Nikitin, Mosc. Univ. Chem. Bull 32 (1), 10 (1977).

76. N. V. Bagaratiyan and O. T. Nikitin, Mosc. Univ. Chem. Bull 32 (4), 8 (1977).

77. A. W. Searcy and D. Beruto, J. Phys. Chem. 78 (13), 1298 (1974).

78. C. T. Ewing and K. H. Stern, J. Phys. Chem. 78 (20), 1998 (1974).

79. M. H. Brooker, J. Electrochem. Soc. 126 (12), 2095 (1979).

80. S. Hata and K. Sekido, Memoirs of the Def. Acad. Jap. 12 (1), (1972).

81. J. J. Bates and G. E. Boyd, App. Spectro. 27 (3), 204 (1973).

82. V. P. Burolla, J. J. Bartel, "The High Temperature Compatibility of Nitrate Salts, Granite Rock and Pelletized Iron Ore," Sandia Laboratories Report SAND79-8634 (1979).

83. M. R. Udupa, Themochimica Acta, 16, 231 (1976).

84. A. K. K. Lee, "Kinetics and Mechanism of the Thermal Decomposition of Molten Anhydrous Lithium Nitrite," Ph.D. thesis, Princeton Univ., 1968.

85. I. A. Aksay, C. E. Hoge and J. A. Pask, J. Phys. Chem. 78, 1178 (1974).

86. A. P. Gray in Analytical Chemistry, edited by R. S. Porter and J. F. Johnson (Plenum Press, NY 1968).

87. J. L. McLaughton and C. T. Mortimer, IRS: Physical Chemistry Series 2 10, (Butterworths, London 1975).

88. W. P. Brennan, in Analytical Calorimetry 3, edited by R. S. Porter and J. F. Johnson (Plenum Press NY).

89. S. Gordon and C. Campbell, Analytical Chem. 27, 1102 (1955).

90. P. I. Protsenko and E. A. Bordyushkova, Russ. J. of Phys. Chem. 39 (8), 1049 (1965).

91. C. M. Kramer and C. J. Wilson, "The Phase Diagram of $NaNO_3/KNO_3$," Sandia Laboratories, SAND80-8502 (1980); accepted for publication in Thermochimica Acta.

92. S. Cantor, "DSC Study of Melting and Solidification of Salt Hydrates," CONF-781078-3, (1978).

93. W. Klement, A. Balboa and P. Ruiz, Themochimica Acta 9, 289 (1974).

94. K. E. Johnson, P. S. Zacharias and J. Matthews, in Proceedings of the International Symposium on Molten Salts, edited by J. P. Pemsler, J. Braunstein, D. R. Morris, K. Nobe, and N. E. Richards, (The Electrochemical Society Inc., Princeton, NJ 1976).

95. A. K. K Lee and E. F. Johnson, Inorg. Chem. 11 (4), 782 (1972).

96. J. W. Dini and H. R. Johnson, "Use of Strategy of Experimentation in Gold Plating Studies," Sandia Laboratories, SAND78-8043 (1979).

97. A. Hald, Statistical Theory with Engineering Applications (Wiley, New York 1952).

98. R. L. Plackett and J. P. Burman, Biometrika 33, 305 (1946).

99. P. G. Zambonin, F. Paniccia, and A. Bufo, J. Phys. Chem. 76 (3), 122 (1972).

100. J. Jordan, Electroanalyt. Interfac. Electrochem. 29, 127 (1971).

101. H. G. Wiedemann, E. Sturzenegger, G. Bayer, in Thermal Analysis: Proceedings of Fourth ICTA 1, 1964.

102. A. W. Coats and J. P. Redfern, Analyst. 88, 906 (1963).

103. C. J. Keattch and D. Dollimore, An Introduction to Thermogravimetry, 2nd ed., (Heyden, London 1975).

104. A. E. Newkirk, Analytical Chem. 32, 1558 (1960).

105. S. P. Ray, Rev. Sci. Instrum. 48 (6), 693 (1977).

106. M. J. Kennedy and S. C. Bevan in Progress in Vacuum Microbalance Techniques 2, edited by S. C. Bevan et al. (Plenum Press, NY, 1973) 91.

107. H. G. Wiedemann in Vacuum Microbalance Techniques 7 (Plenum Press, NY, 1970) 217.

108. A. Berlin and R. J. Robinson, Anal. Chim. Acta 27, 50 (1962).

109. A. Blazek, Thermal Analysis (Van Nostrand Reinhold Co., London, 1972) Chapter 2.

110. W. S. Bradley and W. W. Wendlandt, Anal. Chem. 43 (2), 223 (1971).

111. ASTM Standard Recommended Practices E472-73, E474-73.

112. G. J. Mol, Thermochimica Acta 10, 259 (1974).

113. E. Kaiserberger, Thermochimica Acta 29, 215 (1979).

114. G. M. Lukaszewski and J. P. Redfern, Lab. Practice 10, 721 (1961).

115. A. Marini, V. Berbenni and G. Flor, Z. Natur. 34 (5), 661 (1979).

116. E. Pedersen, J. Sci. Instru. (J. Phys. E), Series 2, 1, 1013 (1968).

117. T. A. Clarke and J. M. Thomas, Nature 219, 1149 (1968).

118. J. B. Dawson, M. Finch, and S. J. Gregg in Progress in Vacuum Microbalance Techniques 2, edited by S. C. Bevan et al. (Plenum Press, NY, 1973) 201.

119. V. Satava, Thermochimica Acta 2, 423 (1971).

120. E. S. Freeman and B. Carroll, J. Phys. Chem 62, 394 (1958).

121. V. Satava and F. Skvara, J. Amer. Ceramic Soc. 52, 591 (1969).

122. D. W. Johnson and P. K. Gallager, J. Phys. Chem 76, (10) 1474 (1972).

123. D. W. Johnson and P. K. Gallagher, Thermochimica Acta 5, 455 (1973).

124. R. M. Fuoss, I. O. Slyer, and H. S. Wilson, J. Polymer Sci., A 2, 3147 (1964).

125. J. H. Flynn and L. A. Wall, J. Res. 70A (6), 487 (1966).

126. B. Carroll, Thermochimica Acta 3, 449 (1972).

127. H. Briscall, "Kinetic Analysis of Thermogravimetric Data Computer Program TGA2," AWRE O 56/78 (1979).

128. F. C. Tompkin, Pure App. Chem. 9, 387 (1964).

129. A. R. Allnatt and P. W. M. Jacobs, Canad. J. Chem. 46, 111 (1968).

130. P. W. M. Jacobs and F. C. Tompkin in Chemistry of the Solid States, edited by W. E. Garner (Academic Press, NY 1955) 184.

131. J. Zsako, J. Phys. Chem. 72, (7) 2406 (1968).

132. J. Kalecinski, Bull. de l'acad. Polon des Sci 20, (3) 279 (1972).

133. J. Kalecinski, Int. J. Radiat. Phys. Chem. 4, 171 (1972).

134. L. Cahn and H. Schultz, Anal. Chem 35, (11), 1729 (1963).

135. L. Cahn and N. C. Peterson, Anal. Chem. 39 (3), 403 (1967).

136. P. K. Gallagher, Thermochimica Acta 26, 175 (1978).

137. H. A. Papazian, P. J. Pizzolato, and R. R. Orrell, Thermochimica Acta 4, 97 (1972).

138. L. W. Collins, E. K. Gibson and W. W. Wendlandt, Thermochimica Acta 9, 15 (1974).

139. J. Chiu and A. J. Beattie, Thermochimica Acta 40, 251 (1980).

140. J. G. Brown, J. Dollimore, C. M. Freedman and B. H. Harrison in Vacuum Microbalance Techniques 8, edited by A. W. Czanderna, (Plenum Press, NY 1971) 17.

141. W. W. Wedlandt, and T. M. Southern, Anal. Chimica Acta 2, 495 (1965).

142. K. W. Smalldon, R. E. Ardrey and L. R. Mullings, Anal. Chimica Acta 107 (1), 327 (1979).

143. S. Morisaki, Thermochimica Acta 25, 171 (1978).

144. R. F. Schwenker and P. D. Garn, Thermal Analysis, (Academic Press, New York 1969), 281.

145. K. Motzfeldt, J. Amer. Chem. Soc. 59, 139 (1955).

146. J. C. Halle and K. H. Stern, J. Phys. Chem. 84 (13), 1699 (1980).

147. H. G. Wiedemann, Thermochimica Acta 3, 355 (1972).

148. K. H. Lau, D. Cubicciotti, and D. L. Hildenbrand, J. Chem. Phys. 66 (10), 4532 (1977).

149. C. C. Addison and N. Logan, Prep. Inorg. Reactions 1, 141 (1964).

150. L. V. Puchkov, V. G. Matashkin and R. P. Matveeva, J. Appl. Chem. USSR 52 (5), 967 (1979).

151. P. C. Ray, J. Chem. Soc. London 87, 177 (1905).

152. R. T. Grimley in High Temperature Vapors, edited by J. L. Margrave, Chapter 8.

153. P. K. Raychaudhuri and P. E. Stafford, Matl. Sci. and Eng. 20, (1975).

154. J. H. Lippiatt and D. Price, First European Symp. on Thermal Analysis, 280 (1976).

155. C. T. Ewing and K. H. Stern, J. Phys. Chem. 77, 1442 (1973).

156. H. Eppler and H. Selhofer, Thermochimica Acta 20, 45 (1977).

157. W. J. McLean and R. F. Sawyer, Acta Astron. 1, 523 (1974).

158. C. A. Stearns, F. J. Kohl, G. C. Fryburg, and R. A. Miller, Industrial Research/Development, (1) 116 (1980).

159. J. Vac. Sci. Technol. 9 (5), 1260 (1972).

160. W. Paul and Steinweder, Z. Naturforsch 8A, 449 (1953).

161. W. Paul and M. Raether, Z. Physik 140, 262 (1955).

162. W. Paul, H. P. Reinhad and U. Vonzahn, Z. Physik 152, 143 (1958).

163. D. Amstutz in Proceedings of the Third ICTA, Thermal Analysis 1, (Birkauser-Verlag, Basel, 1971) 415.

164. A. R. Doelman, A. R. Gregges and E. M. Barall, J. Res. Develop. 22 (1), 81 (1978).

165. K. Burris, "Automation of a Repetitive Experiment Applied to a Thermogravimetric Analyzer," Sandia Laboratories, SAND80-8010 (March 1980).

166. J. P. Frame, E. Rhodes, and A. R. Ubbelohde, Trans. Farad. Soc. 57, 1075 (1960).

167. V. A. Krasnovskaya and S. N. Ganz, J. Appl. Chem. USSR 50 (7), 1397 (1977).

168. F. Paniccia and P. G. Zambonin, J. Phys. Chem 77 (14), 1810 (1973).

169. A. N. Fletcher, M. H. Miles and M. L. Chan, J. Electrochem. Soc. 126 (9), 1496 (1979).

170. H. S. Swofford and P. G. McCormick, Anal. Chem. 37 (8), 970 (1965).

171. J. M. de Johng and G. H. J. Broers, Electrochimica Acta 22, 565 (1977).

172. E. Kaldis, J. Cryst. Growth 17, 3 (1972).

173. R. J. Galluzzo and A. W. Searcy, High Temp. Sci. 3, 491 (1971).

174. H. J. Byker, I. Eliezer, R. C. Howard, and T. C. Ehlert, High Temp. Sci. 11, 153 (1979).

175. J. Sestak, Talanta 13, 567 (1966).

ACKNOWLEDGMENTS

I have some special friends that have enriched my life during the time I've been working on and writing this dissertation. I doubt that I could have survived to finish this project without you. I hope to thank you in a more unique and individual way but I'd like to mention your names because you have helped me change

from this: to this:

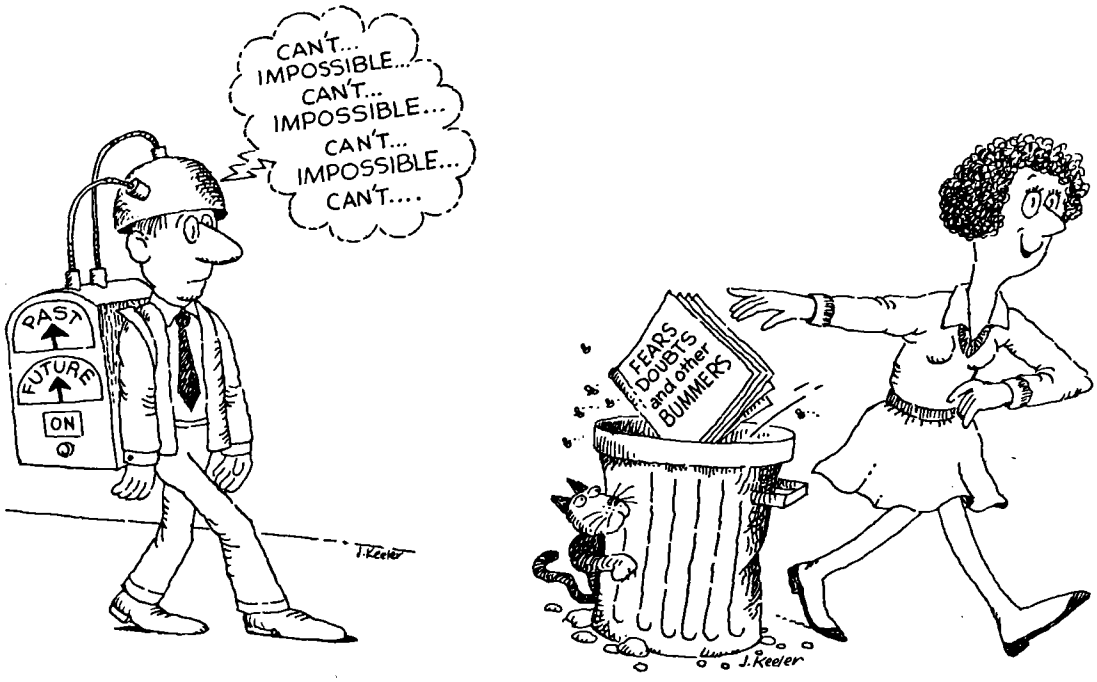

Thank you so very much Gwendolyn Dunn, Bill Flower, Alyce Joyce, Doris Lee, Joe Millard, Karen Pashman, Larry Petro, Hugh Pierson, Sue Roche, Dot Schroepfer, Ray Smith, Joanne Volponi, Sherry White and Christine Wilson.

So many other people have helped me throughout this project. I am indebted to Joanne Volponi who made enormous contributions to this project. Joanne performed many of the experimental tasks cheerfully and enthusiastically. Paul Coronado launched Joanne and I into vacuum technology and was always there to bail us out and to cheer us onward. Paul, Steve Guthrie and Carl Schoenfelder "lent" us a large number of essential items for which I am very grateful. Bob Tucker transformed an ugly duckling rough draft into a PhD thesis and made writing palletable for me. Michael Schalit, Susan Coniglio and Doris Pouard retrieved the references cited here. I'm grateful to Charles de Carli for his statistical analysis and to Chris Imler for her extra-sensory perception with my handwriting.

I also appreciate the advice and services of Belva Mayfield, Dona Crawford, Dale Boehme, Cal Feemster, Miles Clift, Diane Atwood, Ray Leri, Carol Flores, Bob Freeze, Don Beard, Sherry Bowen, Doris Brown, Jim Bartel, Hazel Willyard, George Uveges, Michelle Silver and all the people in the Photo Lab and the Joining Lab.

I'd like to thank Ray Mar, David Schuster and Byron Murphey for their support of this work, and Professor Munir for his guidance. Dianne Martin made it possible for me to meet the University guidelines from a remote location for which I am incredibly grateful. And I thank my committee for the time and thought put into reviewing this work: Professors Zuhair Munir, James Schackelford and Amiya Mukherjee. This work was supported under the USDOE Contract DOE-AC04-76DP00789.

APPENDIX A

The values of the ratios of the activities (a_{MNO_2}/a_{MNO_3}) of nitrate and nitrite mixtures are tabulated for temperatures from 500-1000 K. Three oxygen pressures have been considered: 1., .2, and .0001 atm. The columns are labeled according to the cation whose ratio is represented.

OXYGEN PRESSURE = .2 atm

T (k)	sodium	potassium
500.	.1182E-04	.4614E-06
501.	.1219E-04	.4876E-06
502.	.1258E-04	.5152E-06
503.	.1298E-04	.5442E-06
504.	.1339E-04	.5747E-06
505.	.1381E-04	.6068E-06
506.	.1424E-04	.6405E-06
507.	.1469E-04	.6760E-06
508.	.1516E-04	.7133E-06
509.	.1563E-04	.7525E-06
510.	.1612E-04	.7937E-06
511.	.1663E-04	.8369E-06
512.	.1716E-04	.8824E-06
513.	.1768E-04	.9301E-06
514.	.1824E-04	.9802E-06
515.	.1881E-04	.1033E-05
516.	.1939E-04	.1088E-05
517.	.2000E-04	.1146E-05
518.	.2062E-04	.1207E-05
519.	.2126E-04	.1270E-05
520.	.2192E-04	.1337E-05
521.	.2260E-04	.1407E-05
522.	.2330E-04	.1480E-05
523.	.2402E-04	.1557E-05
524.	.2476E-04	.1638E-05
525.	.2552E-04	.1722E-05
526.	.2631E-04	.1811E-05
527.	.2712E-04	.1904E-05
528.	.2795E-04	.2001E-05
529.	.2881E-04	.2102E-05
530.	.2969E-04	.2208E-05
531.	.3060E-04	.2320E-05
532.	.3153E-04	.2438E-05
533.	.3250E-04	.2562E-05
534.	.3349E-04	.2695E-05
535.	.3451E-04	.2818E-05
536.	.3556E-04	.2958E-05
537.	.3664E-04	.3103E-05
538.	.3775E-04	.3255E-05
539.	.3889E-04	.3414E-05
540.	.4007E-04	.3580E-05
541.	.4128E-04	.3754E-05
542.	.4253E-04	.3936E-05
543.	.4381E-04	.4125E-05
544.	.4513E-04	.4328E-05
545.	.4649E-04	.4529E-05
546.	.4789E-04	.4744E-05
547.	.4933E-04	.4969E-05
548.	.5080E-04	.5204E-05
549.	.5233E-04	.5449E-05
550.	.5389E-04	.5704E-05
551.	.5550E-04	.5970E-05
552.	.5716E-04	.6248E-05
553.	.5886E-04	.6538E-05
554.	.6061E-04	.6839E-05
555.	.6241E-04	.7154E-05
556.	.6426E-04	.7482E-05
557.	.6617E-04	.7824E-05
558.	.6813E-04	.8180E-05
559.	.7014E-04	.8551E-05
560.	.7221E-04	.8937E-05
561.	.7434E-04	.9338E-05
562.	.7653E-04	.9758E-05
563.	.7879E-04	.1019E-04
564.	.8110E-04	.1065E-04
565.	.8348E-04	.1112E-04
566.	.8593E-04	.1161E-04
567.	.8844E-04	.1212E-04
568.	.9103E-04	.1265E-04
569.	.9369E-04	.1321E-04
570.	.9642E-04	.1378E-04
571.	.9923E-04	.1438E-04
572.	.1021E-03	.1500E-04
573.	.1051E-03	.1565E-04
574.	.1081E-03	.1632E-04
575.	.1113E-03	.1702E-04
576.	.1145E-03	.1776E-04
577.	.1178E-03	.1850E-04
578.	.1212E-03	.1928E-04
579.	.1247E-03	.2010E-04
580.	.1283E-03	.2094E-04
581.	.1320E-03	.2182E-04
582.	.1358E-03	.2273E-04
583.	.1396E-03	.2368E-04
584.	.1436E-03	.2466E-04
585.	.1478E-03	.2568E-04
586.	.1520E-03	.2673E-04
587.	.1563E-03	.2783E-04
588.	.1608E-03	.2897E-04
589.	.1653E-03	.3015E-04
590.	.1700E-03	.3137E-04
591.	.1749E-03	.3264E-04
592.	.1798E-03	.3396E-04
593.	.1849E-03	.3532E-04
594.	.1901E-03	.3674E-04
595.	.1955E-03	.3820E-04
596.	.2010E-03	.3972E-04
597.	.2067E-03	.4130E-04
598.	.2125E-03	.4293E-04
599.	.2185E-03	.4462E-04
600.	.2246E-03	.4637E-04
601.	.2309E-03	.4818E-04
602.	.2373E-03	.5006E-04
603.	.2440E-03	.5200E-04
604.	.2508E-03	.5402E-04
605.	.2578E-03	.5610E-04
606.	.2649E-03	.5826E-04
607.	.2723E-03	.6049E-04
608.	.2799E-03	.6280E-04
609.	.2876E-03	.6519E-04
610.	.2956E-03	.6766E-04
611.	.3038E-03	.7022E-04
612.	.3121E-03	.7287E-04
613.	.3207E-03	.7560E-04
614.	.3295E-03	.7843E-04
615.	.3386E-03	.8136E-04
616.	.3479E-03	.8438E-04
617.	.3575E-03	.8751E-04
618.	.3673E-03	.9074E-04
619.	.3773E-03	.9408E-04
620.	.3876E-03	.9753E-04
621.	.3982E-03	.1011E-03

T (k)	sodium	potassium
622.	.4006E-03	.1048E-03
623.	.4088E-03	.1086E-03
624.	.4316E-03	.1125E-03
625.	.4433E-03	.1166E-03
626.	.4553E-03	.1208E-03
627.	.4676E-03	.1251E-03
628.	.4802E-03	.1296E-03
629.	.4932E-03	.1342E-03
630.	.5065E-03	.1390E-03
631.	.5201E-03	.1439E-03
632.	.5341E-03	.1490E-03
633.	.5484E-03	.1543E-03
634.	.5631E-03	.1598E-03
635.	.5781E-03	.1655E-03
636.	.5936E-03	.1716E-03
637.	.6094E-03	.1769E-03
638.	.6257E-03	.1836E-03
639.	.6423E-03	.1893E-03
640.	.6594E-03	.1958E-03
641.	.6769E-03	.2026E-03
642.	.6948E-03	.2096E-03
643.	.7132E-03	.2166E-03
644.	.7320E-03	.2240E-03
645.	.7513E-03	.2316E-03
646.	.7711E-03	.2394E-03
647.	.7914E-03	.2474E-03
648.	.8122E-03	.2557E-03
649.	.8335E-03	.2643E-03
650.	.8554E-03	.2731E-03
651.	.8777E-03	.2821E-03
652.	.9007E-03	.2915E-03
653.	.9242E-03	.3011E-03
654.	.9483E-03	.3110E-03
655.	.9729E-03	.3212E-03
656.	.9982E-03	.3317E-03
657.	.1024E-02	.3426E-03
658.	.1051E-02	.3537E-03
659.	.1078E-02	.3652E-03
660.	.1106E-02	.3770E-03
661.	.1134E-02	.3891E-03
662.	.1163E-02	.4016E-03
663.	.1193E-02	.4145E-03
664.	.1224E-02	.4277E-03
665.	.1255E-02	.4413E-03
666.	.1287E-02	.4553E-03
667.	.1320E-02	.4697E-03
668.	.1354E-02	.4846E-03
669.	.1389E-02	.4997E-03
670.	.1424E-02	.5154E-03
671.	.1460E-02	.5315E-03
672.	.1497E-02	.5480E-03
673.	.1536E-02	.5650E-03
674.	.1574E-02	.5825E-03
675.	.1614E-02	.6006E-03
676.	.1655E-02	.6190E-03
677.	.1696E-02	.6380E-03
678.	.1739E-02	.6575E-03
679.	.1783E-02	.6776E-03
680.	.1827E-02	.6982E-03
681.	.1873E-02	.7193E-03
682.	.1920E-02	.7411E-03
683.	.1968E-02	.7634E-03

T (k)	sodium	potassium
684.	.2017E-02	.7863E-03
685.	.2067E-02	.8099E-03
686.	.2119E-02	.8341E-03
687.	.2171E-02	.8589E-03
688.	.2225E-02	.8844E-03
689.	.2280E-02	.9106E-03
690.	.2337E-02	.9375E-03
691.	.2394E-02	.9651E-03
692.	.2453E-02	.9934E-03
693.	.2514E-02	.1022E-02
694.	.2576E-02	.1052E-02
695.	.2639E-02	.1083E-02
696.	.2703E-02	.1114E-02
697.	.2769E-02	.1147E-02
698.	.2837E-02	.1180E-02
699.	.2906E-02	.1214E-02
700.	.2977E-02	.1248E-02
701.	.3049E-02	.1284E-02
702.	.3123E-02	.1321E-02
703.	.3199E-02	.1358E-02
704.	.3278E-02	.1397E-02
705.	.3358E-02	.1436E-02
706.	.3437E-02	.1477E-02
707.	.3519E-02	.1518E-02
708.	.3604E-02	.1561E-02
709.	.3691E-02	.1604E-02
710.	.3779E-02	.1649E-02
711.	.3870E-02	.1695E-02
712.	.3962E-02	.1742E-02
713.	.4057E-02	.1790E-02
714.	.4153E-02	.1839E-02
715.	.4252E-02	.1889E-02
716.	.4353E-02	.1941E-02
717.	.4457E-02	.1994E-02
718.	.4562E-02	.2049E-02
719.	.4670E-02	.2104E-02
720.	.4780E-02	.2161E-02
721.	.4893E-02	.2219E-02
722.	.5008E-02	.2279E-02
723.	.5126E-02	.2340E-02
724.	.5246E-02	.2403E-02
725.	.5369E-02	.2467E-02
726.	.5495E-02	.2533E-02
727.	.5623E-02	.2600E-02
728.	.5754E-02	.2669E-02
729.	.5888E-02	.2739E-02
730.	.6025E-02	.2812E-02
731.	.6165E-02	.2885E-02
732.	.6307E-02	.2961E-02
733.	.6453E-02	.3038E-02
734.	.6602E-02	.3117E-02
735.	.6755E-02	.3198E-02
736.	.6910E-02	.3281E-02
737.	.7069E-02	.3366E-02
738.	.7231E-02	.3453E-02
739.	.7397E-02	.3541E-02
740.	.7566E-02	.3632E-02
741.	.7739E-02	.3725E-02
742.	.7915E-02	.3820E-02
743.	.8096E-02	.3917E-02
744.	.8280E-02	.4016E-02
745.	.8467E-02	.4117E-02
746.	.8659E-02	.4221E-02
747.	.8855E-02	.4327E-02

T (k)	sodium	potassium
748.	.9655E-02	.4438E-02
749.	.9859E-02	.4546E-02
750.	.9467E-02	.4660E-02
751.	.9680E-02	.4776E-02
752.	.9897E-02	.4894E-02
753.	.1012E-01	.5015E-02
754.	.1035E-01	.5139E-02
755.	.1058E-01	.5265E-02
756.	.1081E-01	.5394E-02
757.	.1106E-01	.5526E-02
758.	.1130E-01	.5661E-02
759.	.1155E-01	.5799E-02
760.	.1180E-01	.5939E-02
761.	.1206E-01	.6083E-02
762.	.1233E-01	.6230E-02
763.	.1260E-01	.6380E-02
764.	.1288E-01	.6533E-02
765.	.1316E-01	.6690E-02
766.	.1345E-01	.6849E-02
767.	.1375E-01	.7012E-02
768.	.1405E-01	.7179E-02
769.	.1435E-01	.7349E-02
770.	.1466E-01	.7523E-02
771.	.1498E-01	.7700E-02
772.	.1531E-01	.7881E-02
773.	.1564E-01	.8066E-02
774.	.1598E-01	.8255E-02
775.	.1632E-01	.8447E-02
776.	.1667E-01	.8644E-02
777.	.1703E-01	.8844E-02
778.	.1740E-01	.9049E-02
779.	.1777E-01	.9258E-02
780.	.1815E-01	.9471E-02
781.	.1854E-01	.9688E-02
782.	.1894E-01	.9910E-02
783.	.1934E-01	.1014E-01
784.	.1975E-01	.1037E-01
785.	.2017E-01	.1060E-01
786.	.2060E-01	.1084E-01
787.	.2103E-01	.1109E-01
788.	.2148E-01	.1134E-01
789.	.2193E-01	.1159E-01
790.	.2239E-01	.1185E-01
791.	.2286E-01	.1212E-01
792.	.2334E-01	.1239E-01
793.	.2383E-01	.1267E-01
794.	.2432E-01	.1295E-01
795.	.2483E-01	.1323E-01
796.	.2536E-01	.1353E-01
797.	.2587E-01	.1382E-01
798.	.2641E-01	.1413E-01
799.	.2696E-01	.1444E-01
800.	.2751E-01	.1475E-01
801.	.2808E-01	.1508E-01
802.	.2866E-01	.1540E-01
803.	.2925E-01	.1574E-01
804.	.2985E-01	.1608E-01
805.	.3048E-01	.1643E-01
806.	.3108E-01	.1678E-01
807.	.3172E-01	.1714E-01
808.	.3236E-01	.1751E-01
809.	.3302E-01	.1788E-01

T (k)	sodium	potassium
810.	.3369E-01	.1826E-01
811.	.3438E-01	.1865E-01
812.	.3507E-01	.1905E-01
813.	.3578E-01	.1945E-01
814.	.3650E-01	.1986E-01
815.	.3723E-01	.2028E-01
816.	.3798E-01	.2071E-01
817.	.3874E-01	.2114E-01
818.	.3952E-01	.2158E-01
819.	.4031E-01	.2203E-01
820.	.4111E-01	.2249E-01
821.	.4193E-01	.2296E-01
822.	.4276E-01	.2343E-01
823.	.4361E-01	.2392E-01
824.	.4447E-01	.2441E-01
825.	.4535E-01	.2491E-01
826.	.4624E-01	.2542E-01
827.	.4715E-01	.2594E-01
828.	.4808E-01	.2647E-01
829.	.4902E-01	.2701E-01
830.	.4998E-01	.2756E-01
831.	.5095E-01	.2812E-01
832.	.5196E-01	.2869E-01
833.	.5296E-01	.2926E-01
834.	.5398E-01	.2985E-01
835.	.5503E-01	.3045E-01
836.	.5610E-01	.3106E-01
837.	.5718E-01	.3168E-01
838.	.5828E-01	.3231E-01
839.	.5940E-01	.3295E-01
840.	.6054E-01	.3361E-01
841.	.6170E-01	.3427E-01
842.	.6288E-01	.3495E-01
843.	.6408E-01	.3563E-01
844.	.6530E-01	.3633E-01
845.	.6654E-01	.3705E-01
846.	.6780E-01	.3777E-01
847.	.6909E-01	.3851E-01
848.	.7039E-01	.3925E-01
849.	.7172E-01	.4002E-01
850.	.7307E-01	.4079E-01
851.	.7445E-01	.4158E-01
852.	.7584E-01	.4238E-01
853.	.7726E-01	.4319E-01
854.	.7870E-01	.4402E-01
855.	.8017E-01	.4486E-01
856.	.8166E-01	.4572E-01
857.	.8318E-01	.4659E-01
858.	.8472E-01	.4747E-01
859.	.8629E-01	.4837E-01
860.	.8788E-01	.4928E-01
861.	.8950E-01	.5021E-01
862.	.9115E-01	.5116E-01
863.	.9282E-01	.5212E-01
864.	.9452E-01	.5309E-01
865.	.9625E-01	.5409E-01
866.	.9800E-01	.5509E-01
867.	.9978E-01	.5612E-01
868.	.1016E+00	.5716E-01
869.	.1034E+00	.5822E-01
870.	.1053E+00	.5929E-01
871.	.1072E+00	.6038E-01
872.	.1091E+00	.6149E-01
873.	.1111E+00	.6262E-01

T (k)	sodium	potassium
874.	.1131E+00	.6377E-01
875.	.1151E+00	.6493E-01
876.	.1172E+00	.6611E-01
877.	.1193E+00	.6731E-01
878.	.1214E+00	.6853E-01
879.	.1236E+00	.6977E-01
880.	.1257E+00	.7103E-01
881.	.1280E+00	.7231E-01
882.	.1302E+00	.7361E-01
883.	.1325E+00	.7493E-01
884.	.1348E+00	.7627E-01
885.	.1372E+00	.7763E-01
886.	.1396E+00	.7901E-01
887.	.1421E+00	.8041E-01
888.	.1445E+00	.8183E-01
889.	.1470E+00	.8328E-01
890.	.1496E+00	.8475E-01
891.	.1522E+00	.8624E-01
892.	.1548E+00	.8775E-01
893.	.1575E+00	.8929E-01
894.	.1602E+00	.9085E-01
895.	.1630E+00	.9244E-01
896.	.1657E+00	.9404E-01
897.	.1686E+00	.9568E-01
898.	.1715E+00	.9733E-01
899.	.1744E+00	.9901E-01
900.	.1773E+00	.1007E+00
901.	.1803E+00	.1025E+00
902.	.1834E+00	.1042E+00
903.	.1865E+00	.1060E+00
904.	.1896E+00	.1078E+00
905.	.1928E+00	.1096E+00
906.	.1961E+00	.1115E+00
907.	.1993E+00	.1134E+00
908.	.2027E+00	.1153E+00
909.	.2060E+00	.1173E+00
910.	.2095E+00	.1193E+00
911.	.2129E+00	.1213E+00
912.	.2165E+00	.1233E+00
913.	.2200E+00	.1254E+00
914.	.2237E+00	.1276E+00
915.	.2273E+00	.1296E+00
916.	.2311E+00	.1317E+00
917.	.2349E+00	.1339E+00
918.	.2387E+00	.1361E+00
919.	.2426E+00	.1384E+00
920.	.2465E+00	.1407E+00
921.	.2505E+00	.1430E+00
922.	.2546E+00	.1453E+00
923.	.2587E+00	.1477E+00
924.	.2629E+00	.1501E+00
925.	.2671E+00	.1526E+00
926.	.2714E+00	.1551E+00
927.	.2757E+00	.1576E+00
928.	.2801E+00	.1601E+00
929.	.2846E+00	.1627E+00
930.	.2891E+00	.1654E+00
931.	.2937E+00	.1680E+00
932.	.2983E+00	.1707E+00
933.	.3030E+00	.1734E+00
934.	.3078E+00	.1762E+00
935.	.3126E+00	.1790E+00

T (k)	sodium	potassium
936.	.3175E+00	.1819E+00
937.	.3225E+00	.1848E+00
938.	.3275E+00	.1877E+00
939.	.3326E+00	.1907E+00
940.	.3378E+00	.1937E+00
941.	.3430E+00	.1967E+00
942.	.3483E+00	.1998E+00
943.	.3537E+00	.2030E+00
944.	.3591E+00	.2062E+00
945.	.3647E+00	.2094E+00
946.	.3702E+00	.2126E+00
947.	.3759E+00	.2159E+00
948.	.3816E+00	.2193E+00
949.	.3874E+00	.2227E+00
950.	.3933E+00	.2261E+00
951.	.3992E+00	.2296E+00
952.	.4053E+00	.2332E+00
953.	.4114E+00	.2367E+00
954.	.4175E+00	.2404E+00
955.	.4238E+00	.2440E+00
956.	.4301E+00	.2478E+00
957.	.4365E+00	.2515E+00
958.	.4430E+00	.2554E+00
959.	.4496E+00	.2592E+00
960.	.4562E+00	.2632E+00
961.	.4630E+00	.2671E+00
962.	.4698E+00	.2712E+00
963.	.4767E+00	.2752E+00
964.	.4837E+00	.2794E+00
965.	.4907E+00	.2836E+00
966.	.4979E+00	.2878E+00
967.	.5051E+00	.2921E+00
968.	.5125E+00	.2964E+00
969.	.5199E+00	.3008E+00
970.	.5274E+00	.3053E+00
971.	.5350E+00	.3098E+00
972.	.5426E+00	.3144E+00
973.	.5504E+00	.3190E+00
974.	.5583E+00	.3237E+00
975.	.5662E+00	.3285E+00
976.	.5743E+00	.3333E+00
977.	.5824E+00	.3381E+00
978.	.5906E+00	.3431E+00
979.	.5990E+00	.3481E+00
980.	.6074E+00	.3531E+00
981.	.6159E+00	.3582E+00
982.	.6245E+00	.3634E+00
983.	.6332E+00	.3687E+00
984.	.6421E+00	.3740E+00
985.	.6510E+00	.3793E+00
986.	.6600E+00	.3848E+00
987.	.6691E+00	.3903E+00
988.	.6783E+00	.3959E+00
989.	.6876E+00	.4015E+00
990.	.6970E+00	.4072E+00
991.	.7066E+00	.4130E+00
992.	.7162E+00	.4189E+00
993.	.7259E+00	.4248E+00
994.	.7358E+00	.4308E+00
995.	.7457E+00	.4368E+00
996.	.7558E+00	.4430E+00
997.	.7659E+00	.4492E+00
998.	.7762E+00	.4555E+00
999.	.7866E+00	.4618E+00

OXYGEN PRESSURE = .0001 atm

T (k)	sodium	potassium
500.	.5284E-03	.2064E-04
501.	.5452E-03	.2181E-04
502.	.5625E-03	.2304E-04
503.	.5803E-03	.2434E-04
504.	.5986E-03	.2570E-04
505.	.6175E-03	.2714E-04
506.	.6370E-03	.2866E-04
507.	.6571E-03	.3023E-04
508.	.6778E-03	.3190E-04
509.	.6991E-03	.3366E-04
510.	.7210E-03	.3549E-04
511.	.7436E-03	.3743E-04
512.	.7669E-03	.3946E-04
513.	.7909E-03	.4159E-04
514.	.8156E-03	.4383E-04
515.	.8410E-03	.4619E-04
516.	.8673E-03	.4865E-04
517.	.8943E-03	.5124E-04
518.	.9221E-03	.5396E-04
519.	.9507E-03	.5681E-04
520.	.9802E-03	.5979E-04
521.	.1011E-02	.6292E-04
522.	.1042E-02	.6621E-04
523.	.1074E-02	.6965E-04
524.	.1107E-02	.7325E-04
525.	.1141E-02	.7703E-04
526.	.1176E-02	.8098E-04
527.	.1213E-02	.8513E-04
528.	.1250E-02	.8947E-04
529.	.1288E-02	.9401E-04
530.	.1328E-02	.9876E-04
531.	.1368E-02	.1037E-03
532.	.1410E-02	.1089E-03
533.	.1453E-02	.1144E-03
534.	.1498E-02	.1201E-03
535.	.1543E-02	.1260E-03
536.	.1590E-02	.1323E-03
537.	.1639E-02	.1388E-03
538.	.1688E-02	.1456E-03
539.	.1739E-02	.1527E-03
540.	.1792E-02	.1601E-03
541.	.1846E-02	.1679E-03
542.	.1902E-02	.1760E-03
543.	.1959E-02	.1845E-03
544.	.2018E-02	.1933E-03
545.	.2079E-02	.2025E-03
546.	.2142E-02	.2122E-03
547.	.2206E-02	.2222E-03
548.	.2272E-02	.2327E-03
549.	.2340E-02	.2437E-03
550.	.2410E-02	.2551E-03
551.	.2482E-02	.2670E-03
552.	.2556E-02	.2794E-03
553.	.2632E-02	.2924E-03
554.	.2711E-02	.3059E-03
555.	.2791E-02	.3199E-03
556.	.2874E-02	.3346E-03
557.	.2958E-02	.3498E-03

T (k)	sodium	potassium
558.	.3047E-02	.3658E-03
559.	.3137E-02	.3824E-03
560.	.3230E-02	.3997E-03
561.	.3325E-02	.4177E-03
562.	.3423E-02	.4364E-03
563.	.3523E-02	.4559E-03
564.	.3627E-02	.4762E-03
565.	.3733E-02	.4973E-03
566.	.3843E-02	.5193E-03
567.	.3955E-02	.5421E-03
568.	.4071E-02	.5659E-03
569.	.4190E-02	.5907E-03
570.	.4312E-02	.6164E-03
571.	.4438E-02	.6432E-03
572.	.4567E-02	.6710E-03
573.	.4698E-02	.6999E-03
574.	.4836E-02	.7300E-03
575.	.4976E-02	.7612E-03
576.	.5120E-02	.7937E-03
577.	.5268E-02	.8274E-03
578.	.5420E-02	.8624E-03
579.	.5576E-02	.8988E-03
580.	.5737E-02	.9366E-03
581.	.5902E-02	.9758E-03
582.	.6071E-02	.1017E-02
583.	.6245E-02	.1059E-02
584.	.6424E-02	.1103E-02
585.	.6608E-02	.1148E-02
586.	.6797E-02	.1196E-02
587.	.6991E-02	.1245E-02
588.	.7190E-02	.1296E-02
589.	.7394E-02	.1348E-02
590.	.7605E-02	.1403E-02
591.	.7820E-02	.1460E-02
592.	.8042E-02	.1519E-02
593.	.8270E-02	.1580E-02
594.	.8504E-02	.1643E-02
595.	.8744E-02	.1709E-02
596.	.8990E-02	.1776E-02
597.	.9243E-02	.1847E-02
598.	.9503E-02	.1920E-02
599.	.9770E-02	.1995E-02
600.	.1004E-01	.2074E-02
601.	.1033E-01	.2155E-02
602.	.1061E-01	.2239E-02
603.	.1091E-01	.2328E-02
604.	.1122E-01	.2416E-02
605.	.1153E-01	.2509E-02
606.	.1185E-01	.2606E-02
607.	.1218E-01	.2705E-02
608.	.1252E-01	.2808E-02
609.	.1286E-01	.2915E-02
610.	.1322E-01	.3026E-02
611.	.1358E-01	.3140E-02
612.	.1396E-01	.3259E-02
613.	.1434E-01	.3381E-02
614.	.1474E-01	.3508E-02
615.	.1514E-01	.3638E-02
616.	.1556E-01	.3774E-02
617.	.1599E-01	.3914E-02
618.	.1642E-01	.4058E-02
619.	.1687E-01	.4207E-02
620.	.1733E-01	.4362E-02
621.	.1781E-01	.4521E-02

T (k)	sodium	potassium
622.	.1829E-01	.4686E-02
623.	.1879E-01	.4856E-02
624.	.1930E-01	.5032E-02
625.	.1982E-01	.5214E-02
626.	.2036E-01	.5402E-02
627.	.2091E-01	.5596E-02
628.	.2148E-01	.5795E-02
629.	.2206E-01	.6000E-02
630.	.2265E-01	.6215E-02
631.	.2326E-01	.6435E-02
632.	.2388E-01	.6662E-02
633.	.2452E-01	.6897E-02
634.	.2518E-01	.7138E-02
635.	.2586E-01	.7388E-02
636.	.2655E-01	.7645E-02
637.	.2725E-01	.7911E-02
638.	.2798E-01	.8185E-02
639.	.2873E-01	.8467E-02
640.	.2949E-01	.8758E-02
641.	.3027E-01	.9058E-02
642.	.3107E-01	.9368E-02
643.	.3189E-01	.9687E-02
644.	.3274E-01	.1002E-01
645.	.3360E-01	.1036E-01
646.	.3449E-01	.1070E-01
647.	.3539E-01	.1107E-01
648.	.3632E-01	.1144E-01
649.	.3728E-01	.1182E-01
650.	.3825E-01	.1221E-01
651.	.3925E-01	.1262E-01
652.	.4028E-01	.1304E-01
653.	.4133E-01	.1347E-01
654.	.4241E-01	.1391E-01
655.	.4351E-01	.1437E-01
656.	.4464E-01	.1484E-01
657.	.4580E-01	.1532E-01
658.	.4698E-01	.1582E-01
659.	.4820E-01	.1633E-01
660.	.4945E-01	.1686E-01
661.	.5072E-01	.1740E-01
662.	.5203E-01	.1796E-01
663.	.5336E-01	.1853E-01
664.	.5474E-01	.1913E-01
665.	.5614E-01	.1973E-01
666.	.5758E-01	.2036E-01
667.	.5905E-01	.2100E-01
668.	.6056E-01	.2167E-01
669.	.6210E-01	.2235E-01
670.	.6368E-01	.2306E-01
671.	.6530E-01	.2377E-01
672.	.6696E-01	.2451E-01
673.	.6865E-01	.2527E-01
674.	.7039E-01	.2605E-01
675.	.7217E-01	.2686E-01
676.	.7399E-01	.2768E-01
677.	.7588E-01	.2853E-01
678.	.7777E-01	.2940E-01
679.	.7972E-01	.3030E-01
680.	.8172E-01	.3122E-01
681.	.8377E-01	.3217E-01
682.	.8586E-01	.3314E-01
683.	.8801E-01	.3414E-01

T (k)	sodium	potassium
684.	.9020E-01	.3517E-01
685.	.9245E-01	.3622E-01
686.	.9475E-01	.3730E-01
687.	.9710E-01	.3841E-01
688.	.9951E-01	.3955E-01
689.	.1020E+00	.4072E-01
690.	.1045E+00	.4193E-01
691.	.1071E+00	.4316E-01
692.	.1097E+00	.4443E-01
693.	.1124E+00	.4573E-01
694.	.1152E+00	.4706E-01
695.	.1180E+00	.4843E-01
696.	.1209E+00	.4983E-01
697.	.1238E+00	.5128E-01
698.	.1269E+00	.5275E-01
699.	.1300E+00	.5427E-01
700.	.1331E+00	.5583E-01
701.	.1364E+00	.5742E-01
702.	.1397E+00	.5906E-01
703.	.1431E+00	.6074E-01
704.	.1465E+00	.6246E-01
705.	.1501E+00	.6422E-01
706.	.1537E+00	.6603E-01
707.	.1574E+00	.6789E-01
708.	.1612E+00	.6979E-01
709.	.1650E+00	.7174E-01
710.	.1690E+00	.7374E-01
711.	.1731E+00	.7579E-01
712.	.1772E+00	.7789E-01
713.	.1814E+00	.8004E-01
714.	.1857E+00	.8224E-01
715.	.1902E+00	.8450E-01
716.	.1947E+00	.8681E-01
717.	.1993E+00	.8918E-01
718.	.2040E+00	.9161E-01
719.	.2088E+00	.9410E-01
720.	.2138E+00	.9665E-01
721.	.2188E+00	.9926E-01
722.	.2240E+00	.1019E+00
723.	.2292E+00	.1047E+00
724.	.2346E+00	.1075E+00
725.	.2401E+00	.1103E+00
726.	.2457E+00	.1133E+00
727.	.2515E+00	.1163E+00
728.	.2573E+00	.1194E+00
729.	.2633E+00	.1225E+00
730.	.2694E+00	.1257E+00
731.	.2757E+00	.1290E+00
732.	.2821E+00	.1324E+00
733.	.2886E+00	.1359E+00
734.	.2953E+00	.1394E+00
735.	.3021E+00	.1430E+00
736.	.3090E+00	.1467E+00
737.	.3161E+00	.1505E+00
738.	.3234E+00	.1544E+00
739.	.3308E+00	.1584E+00
740.	.3384E+00	.1624E+00
741.	.3461E+00	.1666E+00
742.	.3540E+00	.1708E+00
743.	.3620E+00	.1752E+00
744.	.3703E+00	.1796E+00
745.	.3787E+00	.1841E+00
746.	.3873E+00	.1888E+00
747.	.3960E+00	.1935E+00

T (k)	sodium	potassium
748.	.4050E+00	.1984E+00
749.	.4141E+00	.2033E+00
750.	.4234E+00	.2084E+00
751.	.4329E+00	.2136E+00
752.	.4426E+00	.2189E+00
753.	.4525E+00	.2243E+00
754.	.4627E+00	.2298E+00
755.	.4730E+00	.2355E+00
756.	.4835E+00	.2412E+00
757.	.4943E+00	.2471E+00
758.	.5053E+00	.2530E+00
759.	.5165E+00	.2593E+00
760.	.5279E+00	.2656E+00
761.	.5396E+00	.2720E+00
762.	.5515E+00	.2786E+00
763.	.5636E+00	.2853E+00
764.	.5760E+00	.2922E+00
765.	.5887E+00	.2992E+00
766.	.6016E+00	.3063E+00
767.	.6147E+00	.3136E+00
768.	.6281E+00	.3211E+00
769.	.6418E+00	.3287E+00
770.	.6558E+00	.3364E+00
771.	.6701E+00	.3444E+00
772.	.6846E+00	.3525E+00
773.	.6994E+00	.3607E+00
774.	.7146E+00	.3692E+00
775.	.7300E+00	.3778E+00
776.	.7457E+00	.3868E+00
777.	.7617E+00	.3955E+00
778.	.7781E+00	.4047E+00
779.	.7948E+00	.4140E+00
780.	.8118E+00	.4235E+00
781.	.8291E+00	.4333E+00
782.	.8468E+00	.4432E+00
783.	.8648E+00	.4533E+00
784.	.8832E+00	.4637E+00
785.	.9020E+00	.4742E+00
786.	.9211E+00	.4849E+00
787.	.9405E+00	.4959E+00
788.	.9604E+00	.5071E+00
789.	.9806E+00	.5185E+00
790.	.1001E+01	.5301E+00
791.	.1022E+01	.5420E+00
792.	.1044E+01	.5541E+00
793.	.1066E+01	.5664E+00
794.	.1088E+01	.5790E+00
795.	.1110E+01	.5918E+00
796.	.1134E+01	.6049E+00
797.	.1157E+01	.6182E+00
798.	.1181E+01	.6318E+00
799.	.1206E+01	.6457E+00
800.	.1230E+01	.6598E+00
801.	.1256E+01	.6742E+00
802.	.1282E+01	.6889E+00
803.	.1308E+01	.7038E+00
804.	.1335E+01	.7191E+00
805.	.1362E+01	.7346E+00
806.	.1390E+01	.7504E+00
807.	.1418E+01	.7665E+00
808.	.1447E+01	.7830E+00
809.	.1477E+01	.7997E+00

T (k)	sodium	potassium
810.	.1507E+01	.8168E+00
811.	.1537E+01	.8342E+00
812.	.1568E+01	.8519E+00
813.	.1600E+01	.8699E+00
814.	.1632E+01	.8883E+00
815.	.1665E+01	.9070E+00
816.	.1699E+01	.9260E+00
817.	.1733E+01	.9455E+00
818.	.1767E+01	.9652E+00
819.	.1803E+01	.9854E+00
820.	.1838E+01	.1006E+01
821.	.1875E+01	.1027E+01
822.	.1912E+01	.1048E+01
823.	.1950E+01	.1070E+01
824.	.1989E+01	.1092E+01
825.	.2028E+01	.1114E+01
826.	.2068E+01	.1137E+01
827.	.2109E+01	.1160E+01
828.	.2150E+01	.1184E+01
829.	.2192E+01	.1208E+01
830.	.2235E+01	.1233E+01
831.	.2279E+01	.1257E+01
832.	.2323E+01	.1283E+01
833.	.2368E+01	.1309E+01
834.	.2414E+01	.1336E+01
835.	.2461E+01	.1362E+01
836.	.2509E+01	.1389E+01
837.	.2557E+01	.1417E+01
838.	.2606E+01	.1445E+01
839.	.2656E+01	.1474E+01
840.	.2707E+01	.1503E+01
841.	.2759E+01	.1533E+01
842.	.2812E+01	.1563E+01
843.	.2866E+01	.1594E+01
844.	.2920E+01	.1625E+01
845.	.2976E+01	.1657E+01
846.	.3032E+01	.1689E+01
847.	.3090E+01	.1722E+01
848.	.3148E+01	.1755E+01
849.	.3208E+01	.1790E+01
850.	.3268E+01	.1824E+01
851.	.3329E+01	.1859E+01
852.	.3392E+01	.1895E+01
853.	.3455E+01	.1932E+01
854.	.3520E+01	.1969E+01
855.	.3585E+01	.2006E+01
856.	.3652E+01	.2045E+01
857.	.3720E+01	.2083E+01
858.	.3789E+01	.2123E+01
859.	.3859E+01	.2163E+01
860.	.3930E+01	.2204E+01
861.	.4003E+01	.2246E+01
862.	.4076E+01	.2288E+01
863.	.4151E+01	.2331E+01
864.	.4227E+01	.2374E+01
865.	.4304E+01	.2419E+01
866.	.4383E+01	.2464E+01
867.	.4463E+01	.2510E+01
868.	.4544E+01	.2556E+01
869.	.4626E+01	.2604E+01
870.	.4710E+01	.2652E+01
871.	.4795E+01	.2700E+01
872.	.4881E+01	.2750E+01
873.	.4969E+01	.2800E+01

T (k)	sodium	potassium
874.	.5058E+01	.2852E+01
875.	.5149E+01	.2904E+01
876.	.5241E+01	.2957E+01
877.	.5334E+01	.3010E+01
878.	.5429E+01	.3065E+01
879.	.5525E+01	.3120E+01
880.	.5623E+01	.3177E+01
881.	.5723E+01	.3234E+01
882.	.5824E+01	.3292E+01
883.	.5926E+01	.3351E+01
884.	.6031E+01	.3411E+01
885.	.6136E+01	.3472E+01
886.	.6244E+01	.3533E+01
887.	.6353E+01	.3596E+01
888.	.6464E+01	.3660E+01
889.	.6576E+01	.3724E+01
890.	.6690E+01	.3790E+01
891.	.6806E+01	.3857E+01
892.	.6924E+01	.3924E+01
893.	.7043E+01	.3993E+01
894.	.7164E+01	.4063E+01
895.	.7287E+01	.4134E+01
896.	.7412E+01	.4206E+01
897.	.7539E+01	.4279E+01
898.	.7668E+01	.4353E+01
899.	.7798E+01	.4428E+01
900.	.7931E+01	.4504E+01
901.	.8065E+01	.4582E+01
902.	.8202E+01	.4661E+01
903.	.8340E+01	.4740E+01
904.	.8481E+01	.4821E+01
905.	.8623E+01	.4904E+01
906.	.8768E+01	.4987E+01
907.	.8915E+01	.5072E+01
908.	.9063E+01	.5157E+01
909.	.9215E+01	.5246E+01
910.	.9368E+01	.5333E+01
911.	.9523E+01	.5423E+01
912.	.9681E+01	.5514E+01
913.	.9841E+01	.5606E+01
914.	.1000E+02	.5700E+01
915.	.1017E+02	.5795E+01
916.	.1033E+02	.5891E+01
917.	.1050E+02	.5989E+01
918.	.1067E+02	.6088E+01
919.	.1085E+02	.6189E+01
920.	.1103E+02	.6291E+01
921.	.1120E+02	.6395E+01
922.	.1139E+02	.6500E+01
923.	.1157E+02	.6606E+01
924.	.1176E+02	.6714E+01
925.	.1194E+02	.6824E+01
926.	.1214E+02	.6936E+01
927.	.1233E+02	.7047E+01
928.	.1253E+02	.7161E+01
929.	.1273E+02	.7277E+01
930.	.1293E+02	.7396E+01
931.	.1313E+02	.7514E+01
932.	.1334E+02	.7634E+01
933.	.1355E+02	.7757E+01
934.	.1377E+02	.7881E+01
935.	.1398E+02	.8007E+01

T (k)	sodium	potassium
936.	.1420E+02	.8134E+01
937.	.1442E+02	.8264E+01
938.	.1465E+02	.8395E+01
939.	.1488E+02	.8528E+01
940.	.1511E+02	.8662E+01
941.	.1534E+02	.8799E+01
942.	.1558E+02	.8937E+01
943.	.1582E+02	.9077E+01
944.	.1606E+02	.9219E+01
945.	.1631E+02	.9363E+01
946.	.1656E+02	.9509E+01
947.	.1681E+02	.9657E+01
948.	.1707E+02	.9807E+01
949.	.1733E+02	.9959E+01
950.	.1759E+02	.1011E+02
951.	.1785E+02	.1027E+02
952.	.1812E+02	.1043E+02
953.	.1840E+02	.1059E+02
954.	.1867E+02	.1075E+02
955.	.1895E+02	.1091E+02
956.	.1924E+02	.1108E+02
957.	.1952E+02	.1125E+02
958.	.1981E+02	.1142E+02
959.	.2011E+02	.1159E+02
960.	.2040E+02	.1177E+02
961.	.2071E+02	.1195E+02
962.	.2101E+02	.1213E+02
963.	.2132E+02	.1231E+02
964.	.2163E+02	.1249E+02
965.	.2195E+02	.1268E+02
966.	.2227E+02	.1287E+02
967.	.2259E+02	.1306E+02
968.	.2292E+02	.1326E+02
969.	.2325E+02	.1345E+02
970.	.2358E+02	.1365E+02
971.	.2392E+02	.1386E+02
972.	.2427E+02	.1406E+02
973.	.2462E+02	.1427E+02
974.	.2497E+02	.1448E+02
975.	.2532E+02	.1469E+02
976.	.2568E+02	.1490E+02
977.	.2606E+02	.1512E+02
978.	.2641E+02	.1534E+02
979.	.2679E+02	.1557E+02
980.	.2716E+02	.1579E+02
981.	.2754E+02	.1602E+02
982.	.2793E+02	.1625E+02
983.	.2833E+02	.1649E+02
984.	.2871E+02	.1672E+02
985.	.2911E+02	.1696E+02
986.	.2952E+02	.1721E+02
987.	.2992E+02	.1745E+02
988.	.3034E+02	.1770E+02
989.	.3075E+02	.1796E+02
990.	.3117E+02	.1821E+02
991.	.3160E+02	.1847E+02
992.	.3203E+02	.1873E+02
993.	.3246E+02	.1900E+02
994.	.3290E+02	.1928E+02
995.	.3335E+02	.1954E+02
996.	.3380E+02	.1981E+02
997.	.3425E+02	.2009E+02
998.	.3471E+02	.2037E+02
999.	.3518E+02	.2065E+02

OXYGEN PRESSURE = 1. atm

T (k)	sodium	potassium
500.	.5284E-05	.2064E-06
501.	.5452E-05	.2181E-06
502.	.5625E-05	.2304E-06
503.	.5803E-05	.2434E-06
504.	.5986E-05	.2570E-06
505.	.6175E-05	.2714E-06
506.	.6370E-05	.2866E-06
507.	.6571E-05	.3023E-06
508.	.6778E-05	.3190E-06
509.	.6991E-05	.3365E-06
510.	.7210E-05	.3549E-06
511.	.7436E-05	.3743E-06
512.	.7669E-05	.3946E-06
513.	.7909E-05	.4159E-06
514.	.8156E-05	.4383E-06
515.	.8410E-05	.4619E-06
516.	.8673E-05	.4865E-06
517.	.8943E-05	.5124E-06
518.	.9221E-05	.5396E-06
519.	.9507E-05	.5681E-06
520.	.9802E-05	.5979E-06
521.	.1011E-04	.6292E-06
522.	.1042E-04	.6621E-06
523.	.1074E-04	.6965E-06
524.	.1107E-04	.7325E-06
525.	.1141E-04	.7703E-06
526.	.1176E-04	.8098E-06
527.	.1213E-04	.8513E-06
528.	.1250E-04	.8947E-06
529.	.1288E-04	.9401E-06
530.	.1328E-04	.9876E-06
531.	.1368E-04	.1037E-05
532.	.1410E-04	.1089E-05
533.	.1453E-04	.1144E-05
534.	.1498E-04	.1201E-05
535.	.1543E-04	.1260E-05
536.	.1590E-04	.1323E-05
537.	.1639E-04	.1388E-05
538.	.1688E-04	.1456E-05
539.	.1739E-04	.1527E-05
540.	.1792E-04	.1601E-05
541.	.1846E-04	.1679E-05
542.	.1902E-04	.1760E-05
543.	.1959E-04	.1845E-05
544.	.2018E-04	.1933E-05
545.	.2079E-04	.2025E-05
546.	.2142E-04	.2122E-05
547.	.2206E-04	.2222E-05
548.	.2272E-04	.2327E-05
549.	.2340E-04	.2437E-05
550.	.2410E-04	.2551E-05
551.	.2482E-04	.2670E-05
552.	.2556E-04	.2794E-05
553.	.2632E-04	.2924E-05
554.	.2711E-04	.3059E-05
555.	.2791E-04	.3199E-05

T (k)	sodium	potassium
556.	.2874E-04	.3346E-05
557.	.2959E-04	.3498E-05
558.	.3047E-04	.3658E-05
559.	.3137E-04	.3824E-05
560.	.3230E-04	.3997E-05
561.	.3325E-04	.4177E-05
562.	.3423E-04	.4364E-05
563.	.3523E-04	.4559E-05
564.	.3627E-04	.4762E-05
565.	.3733E-04	.4973E-05
566.	.3843E-04	.5193E-05
567.	.3955E-04	.5421E-05
568.	.4071E-04	.5659E-05
569.	.4190E-04	.5907E-05
570.	.4312E-04	.6164E-05
571.	.4438E-04	.6432E-05
572.	.4567E-04	.6710E-05
573.	.4698E-04	.6999E-05
574.	.4836E-04	.7300E-05
575.	.4978E-04	.7612E-05
576.	.5120E-04	.7937E-05
577.	.5268E-04	.8274E-05
578.	.5420E-04	.8624E-05
579.	.5576E-04	.8988E-05
580.	.5737E-04	.9366E-05
581.	.5902E-04	.9758E-05
582.	.6071E-04	.1017E-04
583.	.6245E-04	.1059E-04
584.	.6424E-04	.1103E-04
585.	.6608E-04	.1148E-04
586.	.6797E-04	.1196E-04
587.	.6991E-04	.1245E-04
588.	.7190E-04	.1296E-04
589.	.7394E-04	.1348E-04
590.	.7605E-04	.1403E-04
591.	.7820E-04	.1460E-04
592.	.8042E-04	.1519E-04
593.	.8270E-04	.1580E-04
594.	.8504E-04	.1643E-04
595.	.8744E-04	.1709E-04
596.	.8990E-04	.1776E-04
597.	.9243E-04	.1847E-04
598.	.9503E-04	.1920E-04
599.	.9770E-04	.1995E-04
600.	.1004E-03	.2074E-04
601.	.1033E-03	.2155E-04
602.	.1061E-03	.2239E-04
603.	.1091E-03	.2326E-04
604.	.1122E-03	.2416E-04
605.	.1153E-03	.2509E-04
606.	.1185E-03	.2605E-04
607.	.1218E-03	.2705E-04
608.	.1252E-03	.2808E-04
609.	.1286E-03	.2915E-04
610.	.1322E-03	.3026E-04
611.	.1358E-03	.3140E-04
612.	.1396E-03	.3259E-04
613.	.1434E-03	.3381E-04
614.	.1474E-03	.3508E-04
615.	.1514E-03	.3638E-04
616.	.1556E-03	.3774E-04
617.	.1598E-03	.3914E-04
618.	.1642E-03	.4058E-04
619.	.1687E-03	.4207E-04

T (k)	sodium	potassium
620.	.1733E-03	.4362E-04
621.	.1781E-03	.4521E-04
622.	.1829E-03	.4686E-04
623.	.1879E-03	.4856E-04
624.	.1930E-03	.5032E-04
625.	.1982E-03	.5214E-04
626.	.2036E-03	.5402E-04
627.	.2091E-03	.5595E-04
628.	.2148E-03	.5795E-04
629.	.2206E-03	.6002E-04
630.	.2265E-03	.6215E-04
631.	.2326E-03	.6436E-04
632.	.2388E-03	.6662E-04
633.	.2452E-03	.6897E-04
634.	.2518E-03	.7138E-04
635.	.2586E-03	.7388E-04
636.	.2655E-03	.7645E-04
637.	.2725E-03	.7911E-04
638.	.2798E-03	.8185E-04
639.	.2873E-03	.8467E-04
640.	.2949E-03	.8758E-04
641.	.3027E-03	.9058E-04
642.	.3107E-03	.9368E-04
643.	.3189E-03	.9687E-04
644.	.3274E-03	.1002E-03
645.	.3360E-03	.1036E-03
646.	.3449E-03	.1070E-03
647.	.3539E-03	.1107E-03
648.	.3632E-03	.1144E-03
649.	.3728E-03	.1182E-03
650.	.3825E-03	.1221E-03
651.	.3925E-03	.1262E-03
652.	.4028E-03	.1304E-03
653.	.4133E-03	.1347E-03
654.	.4241E-03	.1391E-03
655.	.4351E-03	.1437E-03
656.	.4464E-03	.1484E-03
657.	.4580E-03	.1532E-03
658.	.4698E-03	.1582E-03
659.	.4820E-03	.1633E-03
660.	.4945E-03	.1686E-03
661.	.5072E-03	.1740E-03
662.	.5203E-03	.1796E-03
663.	.5336E-03	.1853E-03
664.	.5474E-03	.1913E-03
665.	.5614E-03	.1973E-03
666.	.5758E-03	.2036E-03
667.	.5905E-03	.2100E-03
668.	.6056E-03	.2167E-03
669.	.6210E-03	.2235E-03
670.	.6368E-03	.2305E-03
671.	.6530E-03	.2377E-03
672.	.6696E-03	.2451E-03
673.	.6865E-03	.2527E-03
674.	.7039E-03	.2605E-03
675.	.7217E-03	.2686E-03
676.	.7399E-03	.2768E-03
677.	.7586E-03	.2853E-03
678.	.7777E-03	.2940E-03
679.	.7972E-03	.3030E-03
680.	.8172E-03	.3122E-03
681.	.8377E-03	.3217E-03

T (k)	sodium	potassium
682.	.8586E-03	.3314E-03
683.	.8801E-03	.3414E-03
684.	.9020E-03	.3517E-03
685.	.9245E-03	.3622E-03
686.	.9475E-03	.3730E-03
687.	.9710E-03	.3841E-03
688.	.9961E-03	.3965E-03
689.	.1020E-02	.4072E-03
690.	.1045E-02	.4193E-03
691.	.1071E-02	.4316E-03
692.	.1097E-02	.4443E-03
693.	.1124E-02	.4573E-03
694.	.1152E-02	.4706E-03
695.	.1180E-02	.4843E-03
696.	.1209E-02	.4983E-03
697.	.1238E-02	.5128E-03
698.	.1269E-02	.5275E-03
699.	.1300E-02	.5427E-03
700.	.1331E-02	.5583E-03
701.	.1364E-02	.5742E-03
702.	.1397E-02	.5906E-03
703.	.1431E-02	.6074E-03
704.	.1465E-02	.6246E-03
705.	.1501E-02	.6422E-03
706.	.1537E-02	.6603E-03
707.	.1574E-02	.6789E-03
708.	.1612E-02	.6979E-03
709.	.1650E-02	.7174E-03
710.	.1690E-02	.7374E-03
711.	.1731E-02	.7579E-03
712.	.1772E-02	.7789E-03
713.	.1814E-02	.8004E-03
714.	.1857E-02	.8224E-03
715.	.1902E-02	.8450E-03
716.	.1947E-02	.8681E-03
717.	.1993E-02	.8918E-03
718.	.2040E-02	.9161E-03
719.	.2088E-02	.9410E-03
720.	.2138E-02	.9665E-03
721.	.2188E-02	.9926E-03
722.	.2240E-02	.1019E-02
723.	.2292E-02	.1047E-02
724.	.2346E-02	.1075E-02
725.	.2401E-02	.1103E-02
726.	.2457E-02	.1133E-02
727.	.2515E-02	.1163E-02
728.	.2573E-02	.1194E-02
729.	.2633E-02	.1225E-02
730.	.2694E-02	.1257E-02
731.	.2757E-02	.1290E-02
732.	.2821E-02	.1324E-02
733.	.2886E-02	.1359E-02
734.	.2953E-02	.1394E-02
736.	.3021E-02	.1430E-02
736.	.3090E-02	.1467E-02
737.	.3161E-02	.1505E-02
738.	.3234E-02	.1544E-02
739.	.3308E-02	.1584E-02
740.	.3384E-02	.1624E-02
741.	.3461E-02	.1666E-02
742.	.3540E-02	.1708E-02
743.	.3620E-02	.1752E-02
744.	.3703E-02	.1796E-02
745.	.3787E-02	.1841E-02

T (k)	sodium	potassium
746.	.3873E-02	.1888E-02
747.	.3984E-02	.1935E-02
748.	.4096E-02	.1984E-02
749.	.4141E-02	.2033E-02
750.	.4234E-02	.2084E-02
751.	.4328E-02	.2136E-02
752.	.4426E-02	.2189E-02
753.	.4525E-02	.2243E-02
754.	.4627E-02	.2298E-02
755.	.4730E-02	.2355E-02
756.	.4836E-02	.2412E-02
757.	.4943E-02	.2471E-02
758.	.5053E-02	.2532E-02
759.	.5165E-02	.2593E-02
760.	.5279E-02	.2656E-02
761.	.5396E-02	.2720E-02
762.	.5515E-02	.2786E-02
763.	.5636E-02	.2853E-02
764.	.5760E-02	.2922E-02
765.	.5887E-02	.2992E-02
766.	.6016E-02	.3063E-02
767.	.6147E-02	.3136E-02
768.	.6281E-02	.3211E-02
769.	.6418E-02	.3287E-02
770.	.6558E-02	.3364E-02
771.	.6701E-02	.3444E-02
772.	.6846E-02	.3525E-02
773.	.6994E-02	.3607E-02
774.	.7146E-02	.3692E-02
775.	.7300E-02	.3778E-02
776.	.7457E-02	.3866E-02
777.	.7617E-02	.3955E-02
778.	.7781E-02	.4047E-02
779.	.7948E-02	.4140E-02
780.	.8118E-02	.4236E-02
781.	.8291E-02	.4333E-02
782.	.8468E-02	.4432E-02
783.	.8648E-02	.4533E-02
784.	.8832E-02	.4637E-02
785.	.9020E-02	.4742E-02
786.	.9211E-02	.4849E-02
787.	.9405E-02	.4959E-02
788.	.9604E-02	.5071E-02
789.	.9806E-02	.5185E-02
790.	.1001E-01	.5301E-02
791.	.1022E-01	.5420E-02
792.	.1044E-01	.5541E-02
793.	.1066E-01	.5664E-02
794.	.1088E-01	.5790E-02
795.	.1110E-01	.5918E-02
796.	.1134E-01	.6049E-02
797.	.1157E-01	.6182E-02
798.	.1181E-01	.6318E-02
799.	.1206E-01	.6457E-02
800.	.1230E-01	.6598E-02
801.	.1256E-01	.6742E-02
802.	.1282E-01	.6889E-02
803.	.1308E-01	.7038E-02
804.	.1335E-01	.7191E-02
805.	.1362E-01	.7346E-02
806.	.1390E-01	.7504E-02
807.	.1418E-01	.7665E-02

T (k)	sodium	potassium
808.	.1447E-01	.7830E-02
809.	.1477E-01	.7997E-02
810.	.1507E-01	.8168E-02
811.	.1537E-01	.8342E-02
812.	.1568E-01	.8519E-02
813.	.1600E-01	.8699E-02
814.	.1632E-01	.8883E-02
815.	.1665E-01	.9070E-02
816.	.1699E-01	.9260E-02
817.	.1733E-01	.9455E-02
818.	.1767E-01	.9652E-02
819.	.1803E-01	.9854E-02
820.	.1838E-01	.1006E-01
821.	.1875E-01	.1027E-01
822.	.1912E-01	.1048E-01
823.	.1950E-01	.1070E-01
824.	.1989E-01	.1092E-01
825.	.2028E-01	.1114E-01
826.	.2068E-01	.1137E-01
827.	.2109E-01	.1160E-01
828.	.2150E-01	.1184E-01
829.	.2192E-01	.1208E-01
830.	.2236E-01	.1233E-01
831.	.2279E-01	.1257E-01
832.	.2323E-01	.1283E-01
833.	.2368E-01	.1309E-01
834.	.2414E-01	.1335E-01
835.	.2461E-01	.1362E-01
836.	.2509E-01	.1389E-01
837.	.2557E-01	.1417E-01
838.	.2606E-01	.1445E-01
839.	.2656E-01	.1474E-01
840.	.2707E-01	.1503E-01
841.	.2759E-01	.1533E-01
842.	.2812E-01	.1563E-01
843.	.2866E-01	.1594E-01
844.	.2920E-01	.1625E-01
845.	.2976E-01	.1657E-01
846.	.3032E-01	.1689E-01
847.	.3090E-01	.1722E-01
848.	.3148E-01	.1755E-01
849.	.3208E-01	.1790E-01
850.	.3268E-01	.1824E-01
851.	.3329E-01	.1859E-01
852.	.3390E-01	.1896E-01
853.	.3455E-01	.1932E-01
854.	.3520E-01	.1969E-01
855.	.3585E-01	.2006E-01
856.	.3652E-01	.2046E-01
857.	.3720E-01	.2083E-01
858.	.3789E-01	.2123E-01
859.	.3859E-01	.2163E-01
860.	.3930E-01	.2204E-01
861.	.4003E-01	.2246E-01
862.	.4078E-01	.2288E-01
863.	.4151E-01	.2331E-01
864.	.4227E-01	.2374E-01
865.	.4304E-01	.2419E-01
866.	.4383E-01	.2464E-01
867.	.4463E-01	.2510E-01
868.	.4544E-01	.2556E-01
869.	.4626E-01	.2604E-01
870.	.4710E-01	.2652E-01
871.	.4795E-01	.2700E-01

T (k)	sodium	potassium
872.	.4881E-01	.2760E-01
873.	.4969E-01	.2800E-01
874.	.5058E-01	.2852E-01
875.	.5149E-01	.2904E-01
876.	.5241E-01	.2957E-01
877.	.5334E-01	.3010E-01
878.	.5429E-01	.3066E-01
879.	.5525E-01	.3120E-01
880.	.5623E-01	.3177E-01
881.	.5723E-01	.3234E-01
882.	.5824E-01	.3288E-01
883.	.5926E-01	.3361E-01
884.	.6031E-01	.3411E-01
885.	.6136E-01	.3478E-01
886.	.6244E-01	.3533E-01
887.	.6353E-01	.3596E-01
888.	.6464E-01	.3660E-01
889.	.6576E-01	.3724E-01
890.	.6690E-01	.3790E-01
891.	.6806E-01	.3857E-01
892.	.6924E-01	.3924E-01
893.	.7043E-01	.3993E-01
894.	.7164E-01	.4063E-01
895.	.7287E-01	.4134E-01
896.	.7412E-01	.4206E-01
897.	.7539E-01	.4279E-01
898.	.7668E-01	.4353E-01
899.	.7798E-01	.4428E-01
900.	.7931E-01	.4504E-01
901.	.8065E-01	.4582E-01
902.	.8202E-01	.4661E-01
903.	.8340E-01	.4740E-01
904.	.8481E-01	.4821E-01
905.	.8623E-01	.4904E-01
906.	.8768E-01	.4987E-01
907.	.8915E-01	.5072E-01
908.	.9063E-01	.5157E-01
909.	.9215E-01	.5246E-01
910.	.9368E-01	.5333E-01
911.	.9523E-01	.5423E-01
912.	.9681E-01	.5514E-01
913.	.9841E-01	.5606E-01
914.	.1000E+00	.5700E-01
915.	.1017E+00	.5795E-01
916.	.1033E+00	.5891E-01
917.	.1050E+00	.5989E-01
918.	.1067E+00	.6088E-01
919.	.1085E+00	.6189E-01
920.	.1103E+00	.6291E-01
921.	.1120E+00	.6395E-01
922.	.1139E+00	.6500E-01
923.	.1157E+00	.6606E-01
924.	.1176E+00	.6714E-01
925.	.1194E+00	.6824E-01
926.	.1214E+00	.6935E-01
927.	.1233E+00	.7047E-01
928.	.1253E+00	.7161E-01
929.	.1273E+00	.7277E-01
930.	.1293E+00	.7396E-01
931.	.1313E+00	.7514E-01
932.	.1334E+00	.7634E-01
933.	.1356E+00	.7757E-01
934.	.1377E+00	.7881E-01
935.	.1398E+00	.8007E-01
936.	.1420E+00	.8134E-01
937.	.1442E+00	.8264E-01
938.	.1465E+00	.8395E-01
939.	.1488E+00	.8528E-01
940.	.1511E+00	.8662E-01
941.	.1534E+00	.8799E-01
942.	.1558E+00	.8937E-01
943.	.1582E+00	.9077E-01
944.	.1606E+00	.9219E-01
945.	.1631E+00	.9363E-01
946.	.1656E+00	.9509E-01
947.	.1681E+00	.9657E-01
948.	.1707E+00	.9807E-01
949.	.1733E+00	.9959E-01
950.	.1759E+00	.1011E+00
951.	.1785E+00	.1027E+00
952.	.1812E+00	.1043E+00
953.	.1840E+00	.1059E+00
954.	.1867E+00	.1075E+00
955.	.1896E+00	.1091E+00
956.	.1924E+00	.1108E+00
957.	.1952E+00	.1125E+00
958.	.1981E+00	.1142E+00
959.	.2011E+00	.1159E+00
960.	.2040E+00	.1177E+00
961.	.2071E+00	.1195E+00
962.	.2101E+00	.1213E+00
963.	.2132E+00	.1231E+00
964.	.2163E+00	.1249E+00
965.	.2195E+00	.1268E+00
966.	.2227E+00	.1287E+00
967.	.2259E+00	.1306E+00
968.	.2292E+00	.1326E+00
969.	.2325E+00	.1345E+00
970.	.2358E+00	.1365E+00
971.	.2392E+00	.1386E+00
972.	.2427E+00	.1406E+00
973.	.2462E+00	.1427E+00
974.	.2497E+00	.1448E+00
975.	.2532E+00	.1469E+00
976.	.2568E+00	.1490E+00
977.	.2605E+00	.1512E+00
978.	.2641E+00	.1534E+00
979.	.2679E+00	.1557E+00
980.	.2716E+00	.1579E+00
981.	.2754E+00	.1602E+00
982.	.2793E+00	.1625E+00
983.	.2832E+00	.1649E+00
984.	.2871E+00	.1672E+00
985.	.2911E+00	.1696E+00
986.	.2952E+00	.1721E+00
987.	.2992E+00	.1745E+00
988.	.3034E+00	.1770E+00
989.	.3075E+00	.1796E+00
990.	.3117E+00	.1821E+00
991.	.3160E+00	.1847E+00
992.	.3203E+00	.1873E+00
993.	.3246E+00	.1900E+00
994.	.3290E+00	.1926E+00
995.	.3335E+00	.1954E+00
996.	.3380E+00	.1981E+00
997.	.3425E+00	.2009E+00

APPENDIX B

COMPUTATION OF THE FACTOR EFFECT FOR A TWENTY-RUN PLACKETT-BURMAN EXPERIMENT ON THERMAL DECOMPOSITION OF MOLTEN NITRATE SALTS

1. Refer to Table B1. Run 20 experiments (trials) for each experiment, set each variable at its high (+) or low (-) value. Measure the responses of interest for each experiment.

2. Write the average response (measured dependent variable, such as % carbonate) for each trial in a column on Table B1.

3. For each column, sum the values of the responses on the lines with plus signs.

4. For each column, sum the values of the responses on the lines with minus signs.

5. Calculate the difference between the totals in (3) and (4) for each column. Call these numbers the Differences.

6. Divide the Difference computed for each of the 19 columns by 10 (because there are ten "plus" experiments and ten "minus" experiments). These numbers are the factor effects of the variables in columns 1-10 and the unassigned factor effects for columns 11-19.

7. Find the experimental noise level by taking the sum of the squares of the unassigned factor effects dividing by 9, and taking the square root. This is called S_{FE}.

8. The minimum significant factor effect (min) is calculated by $S_{FE} \cdot t$ (t is 1.833 for this experimental design with a 95% confidence level for 9 degrees of freedom). All factor effects greater than the min influence the response being evaluated.

TABLE B1

PLACKETT BURMAN TEST MATRIX

Expt. Order	Trial #1	Temp. 1	O_2 2	N_2 3	CO_2 4	RH 5	Flow Rate 6	Surf. Area 7	KNO_3/ $NaNO_3$ 8	Size 9	Purity 10	11	12	13	14	15	16	17	18	19
14	1	+	+	-	-	+	+	+	+	-	+	-	+	-	-	-	-	+	+	-
19	2	+	-	-	+	+	+	+	-	+	-	+	-	-	-	-	+	+	-	+
11	3	-	-	+	+	+	+	-	+	-	+	-	-	-	-	+	+	-	+	+
10	4	-	+	+	+	+	-	+	-	+	-	-	-	-	+	+	-	+	+	-
17	5	+	+	+	+	-	+	-	+	-	-	-	-	+	+	-	+	+	-	-
8	6	+	+	+	-	+	-	+	-	-	-	-	+	+	-	+	+	-	-	+
13	7	+	+	-	+	-	+	-	-	-	-	+	+	-	+	+	-	-	+	+
7	8	+	-	+	-	+	-	-	-	-	+	+	-	+	+	-	-	+	+	+
15	9	-	+	-	+	-	-	-	-	+	+	-	+	+	-	-	+	+	+	+
18	10	+	-	+	-	-	-	-	+	+	-	+	+	-	-	+	+	+	+	-
6	11	-	+	-	-	-	-	+	+	-	+	+	-	-	+	+	+	+	-	+
5	12	+	-	-	-	-	+	+	-	+	+	-	-	+	+	+	+	-	+	-
3	13	-	-	-	-	+	+	-	+	+	-	-	+	+	+	+	-	+	-	+
9	14	-	-	-	+	+	-	+	+	-	-	+	+	+	+	-	+	-	+	-
12	15	-	-	+	+	-	+	+	-	-	+	+	+	+	-	+	-	+	-	-
20	16	-	+	+	-	+	+	-	-	+	+	+	+	-	+	-	+	-	-	-
2	17	+	+	-	+	+	-	-	+	+	+	+	-	+	-	+	-	-	-	-
1	18	+	-	+	+	-	-	+	+	+	+	-	+	-	+	-	-	-	-	+
16	19	-	+	+	-	-	+	+	+	+	-	+	-	+	-	-	-	-	+	+
4	20	-	-	-	-	-	-	-	-	-	-	-	-	-	-	-	-	-	-	-

INDEPENDENT VARIABLES OR FACTORS

UNASSIGNED FACTORS

APPENDIX C

THERMOGRAVIMETRY EXPERIMENTS

On the following pages are graphs of the thermogravimetric data collected from TG experiments in 1 atm and in vacuum. Each of the following pages has the data from one experiment. Each page has 4 graphs which show 1) the weight and the weight per unit surface area versus time on 1 graph (in the upper lefthand corner), 2) the natural logarithm of the fraction of the sample remaining versus time (in the upper righthand corner), 3) the temperature profile during the experiment (in the lower lefthand corner), and 4) the percent weight loss versus time (in the lower righthand corner). Graphs 1, 2, and 4 also have the best linear least squares fit to the data plotted with the experimental data in accordance with Equations (51), (53), and (54) respectively. The experimental data points are simply connected by straight lines. A marker is shown on the graph periodically (not for each data point) to identify the experimental data. There is no marker on the lines representing the best least squares fit to the data.

The following is a list of the experiments shown in this index.

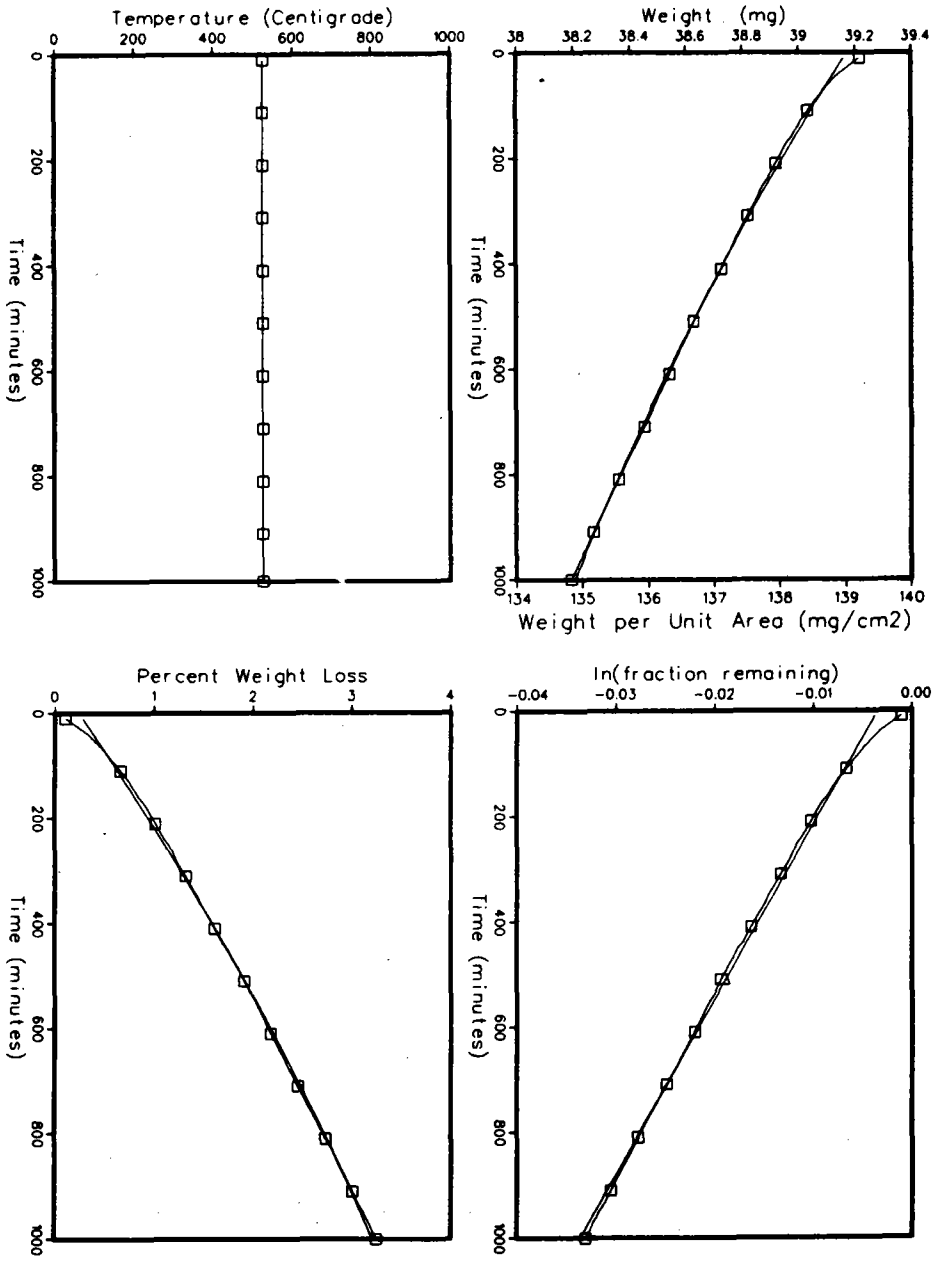

T-25G NaNO3 -air

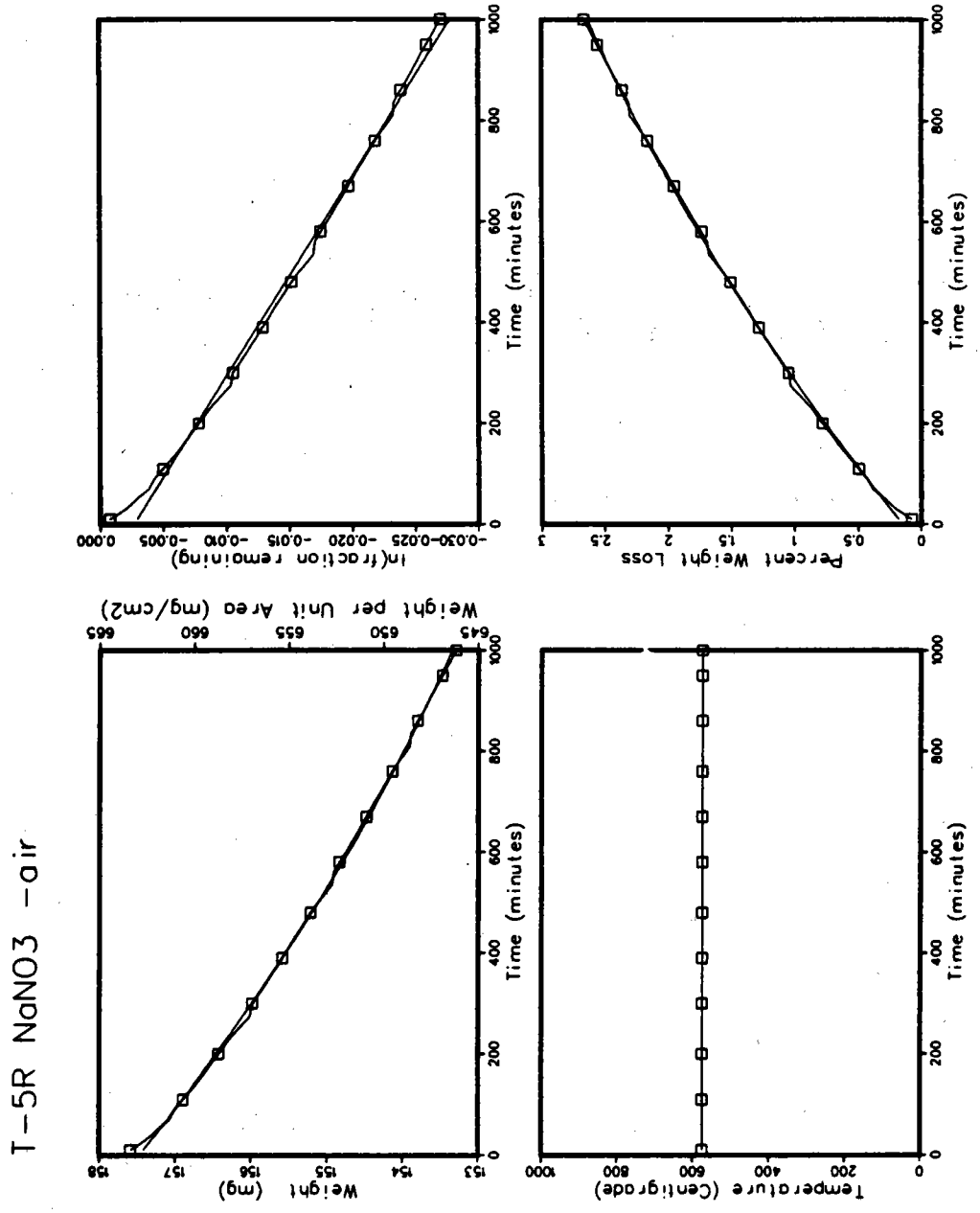
T-5R NaNO3 -air
Temperature (Centigrade)
Time (minutes)
Weight (mg)
Time (minutes)
Weight per Unit Area (mg/cm2)
Percent Weight Loss
Time (minutes)
ln(fraction remaining)
Time (minutes)

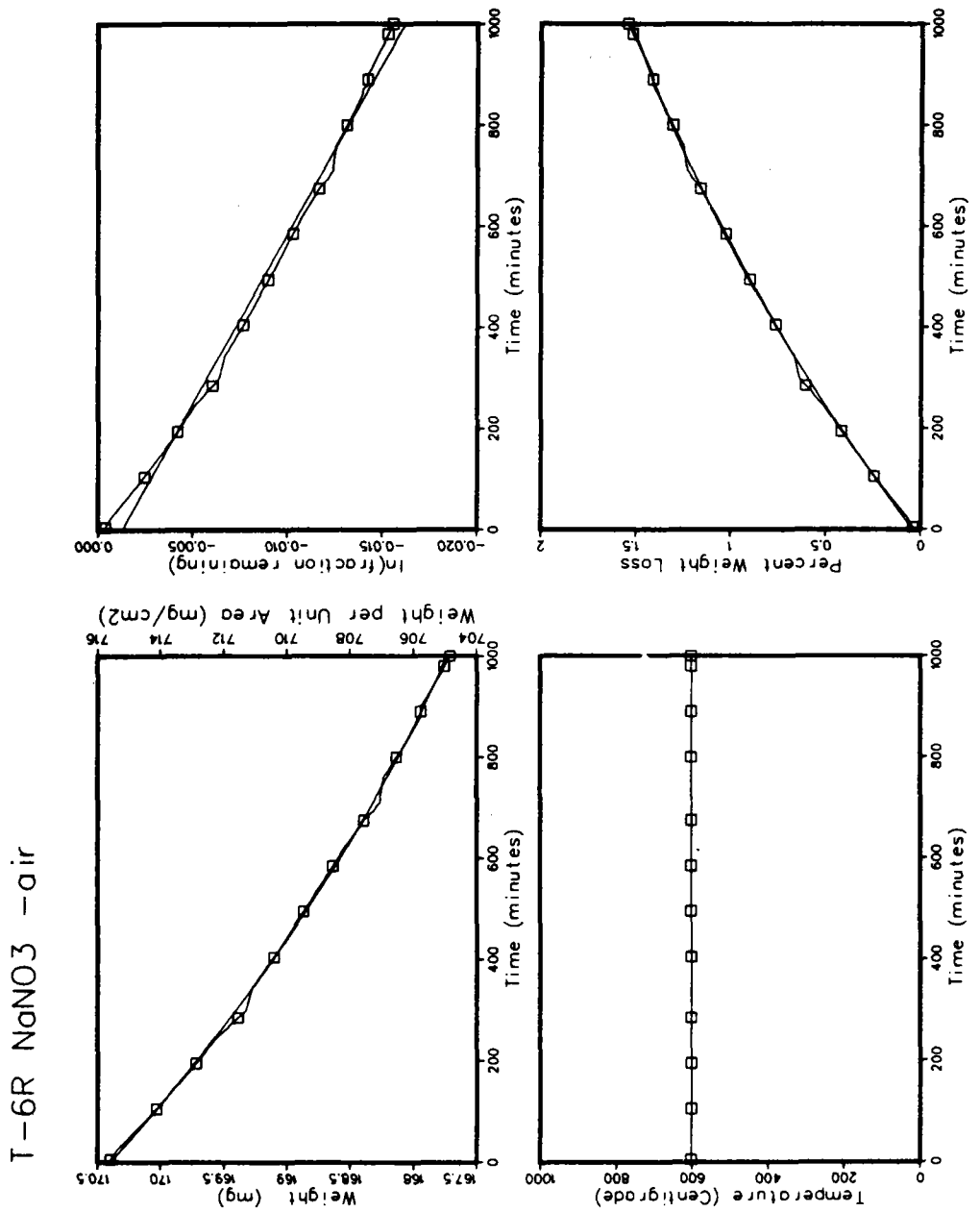
T-6R NaNO3 -air
Weight (mg)
Time (minutes)
Weight per Unit Area (mg/cm2)
ln(fraction remaining)
Percent Weight Loss
Temperature (Centigrade)

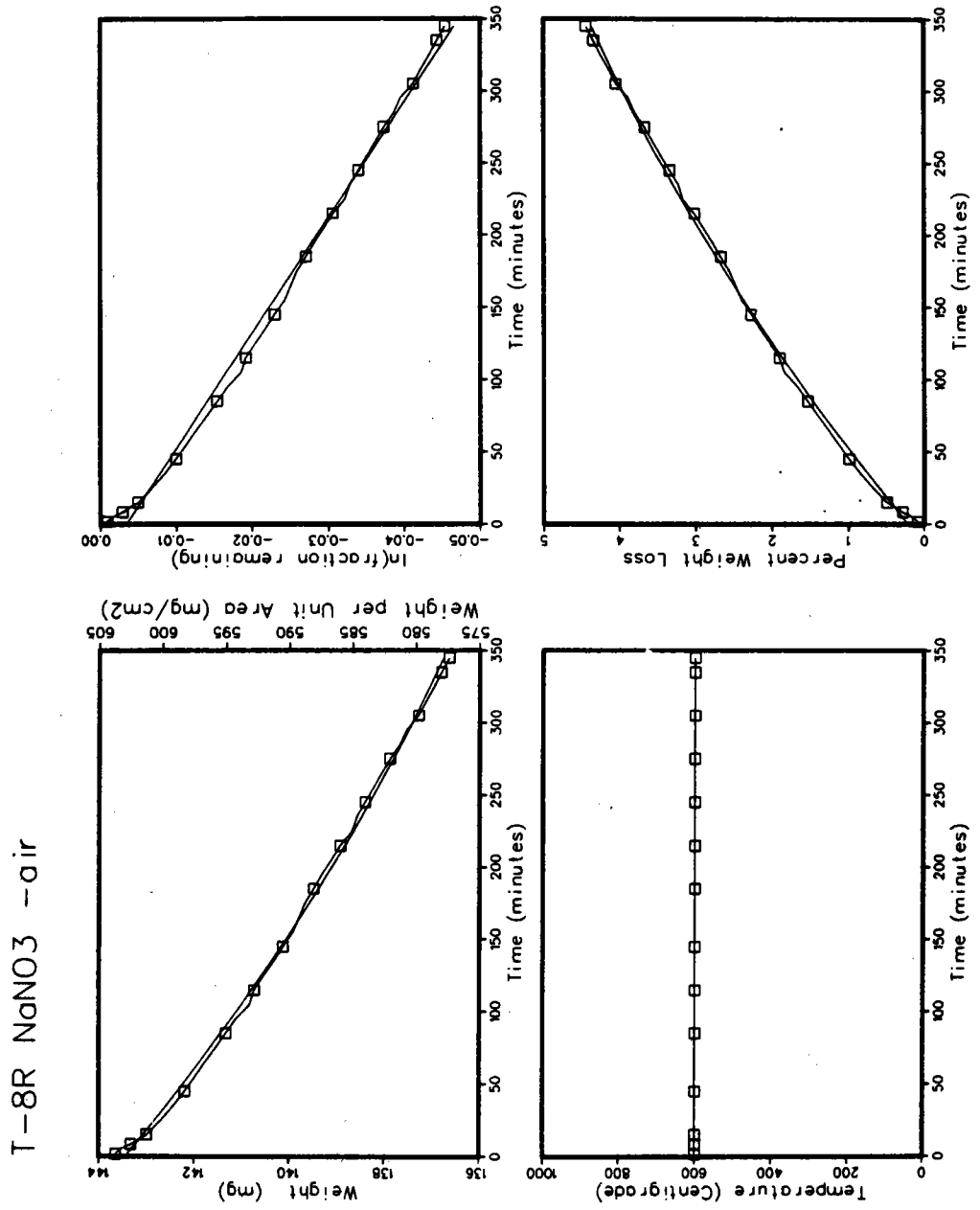
T-8R NaNO3 -air
Weight (mg)
Time (minutes)
Weight per Unit Area (mg/cm2)
ln(fraction remaining)
Percent Weight Loss
Temperature (Centigrade)

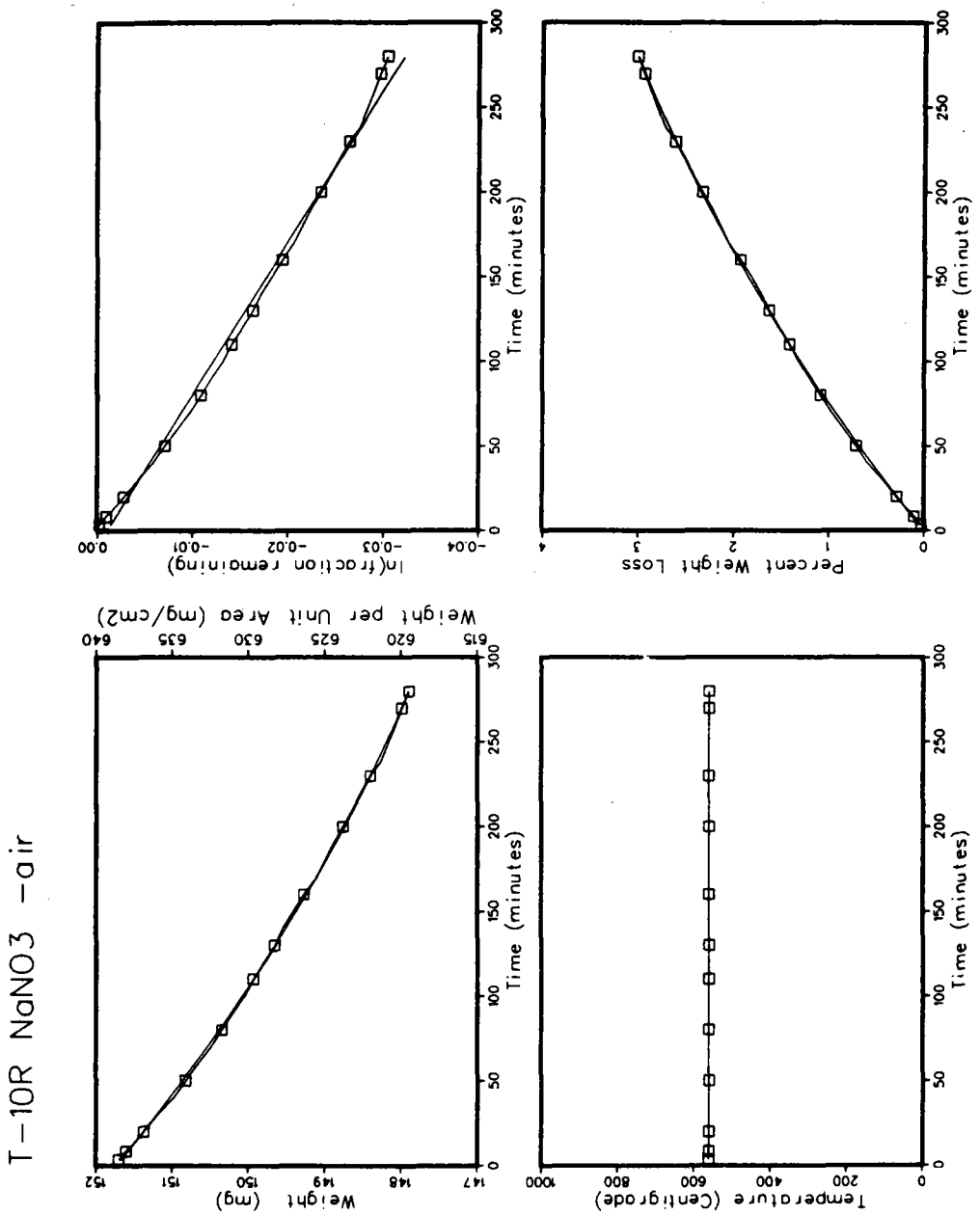
T-10R NaNO3 -air
Weight (mg)
Time (minutes)
Weight per Unit Area (mg/cm2)
ln(fraction remaining)
Percent Weight Loss
Temperature (Centigrade)

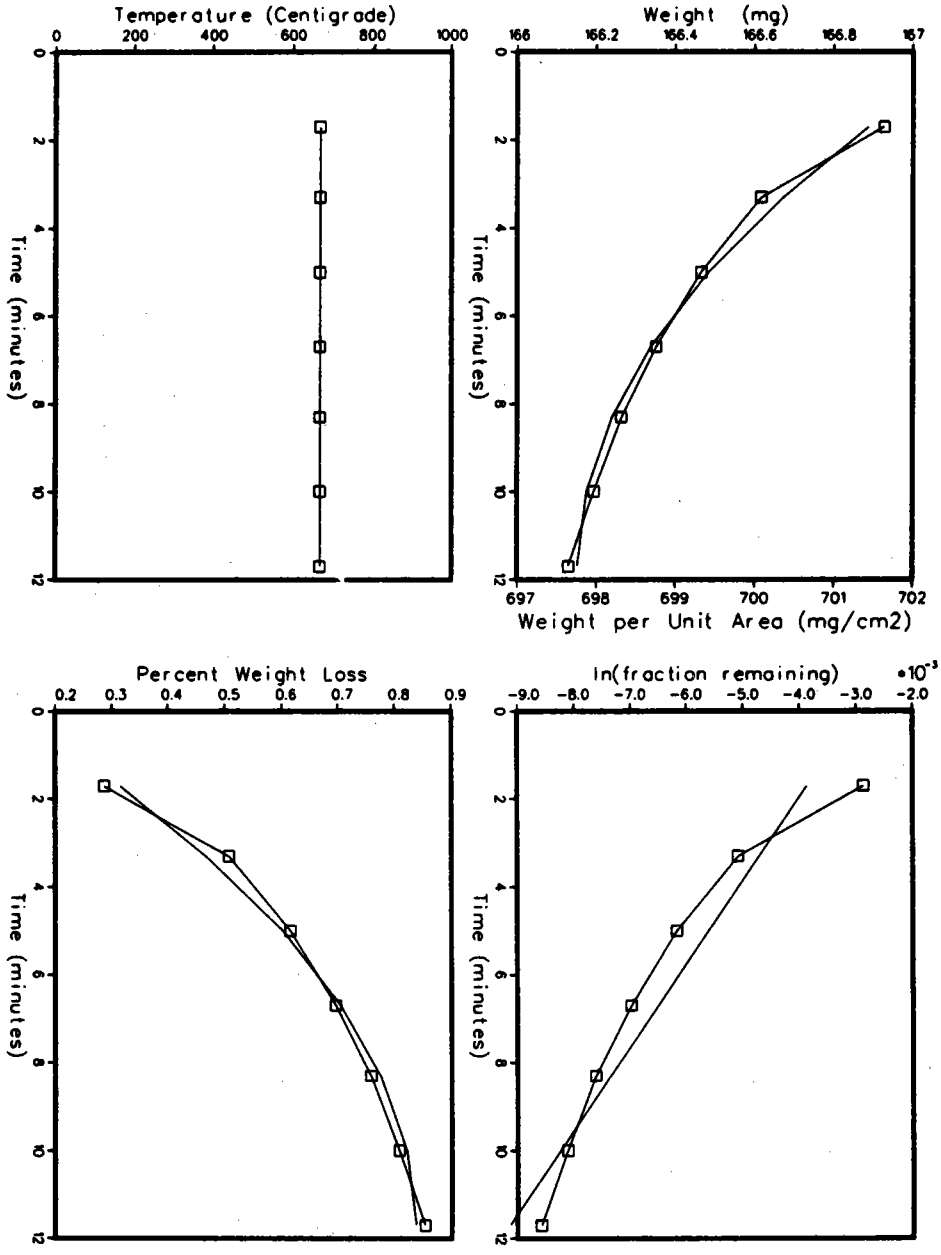

T-11R NaNO3-air

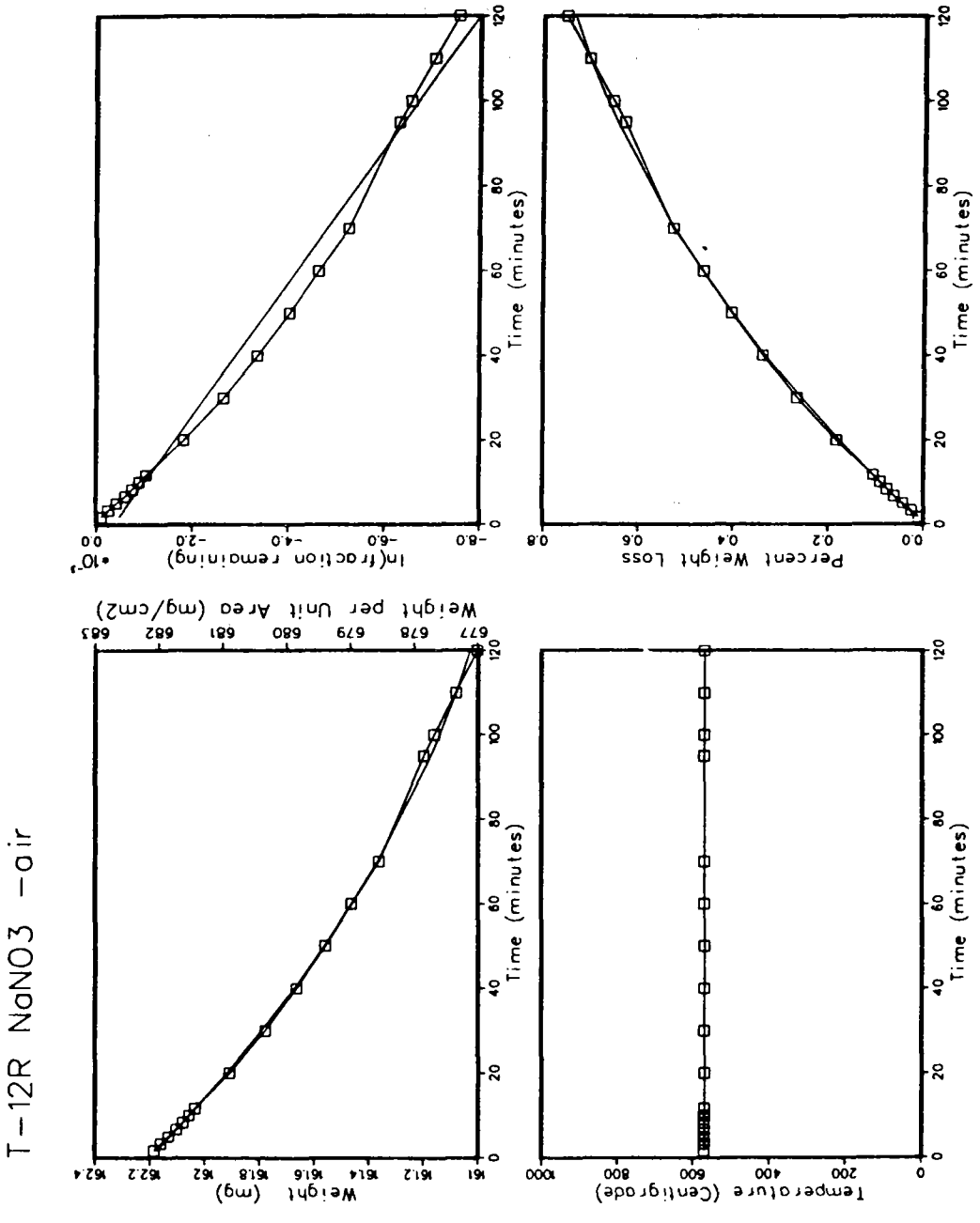
T-12R NaNO3 -air
Weight (mg)
Time (minutes)
Weight per Unit Area (mg/cm2)
Temperature (Centigrade)
Percent Weight Loss
ln(fraction remaining)
*10^-3

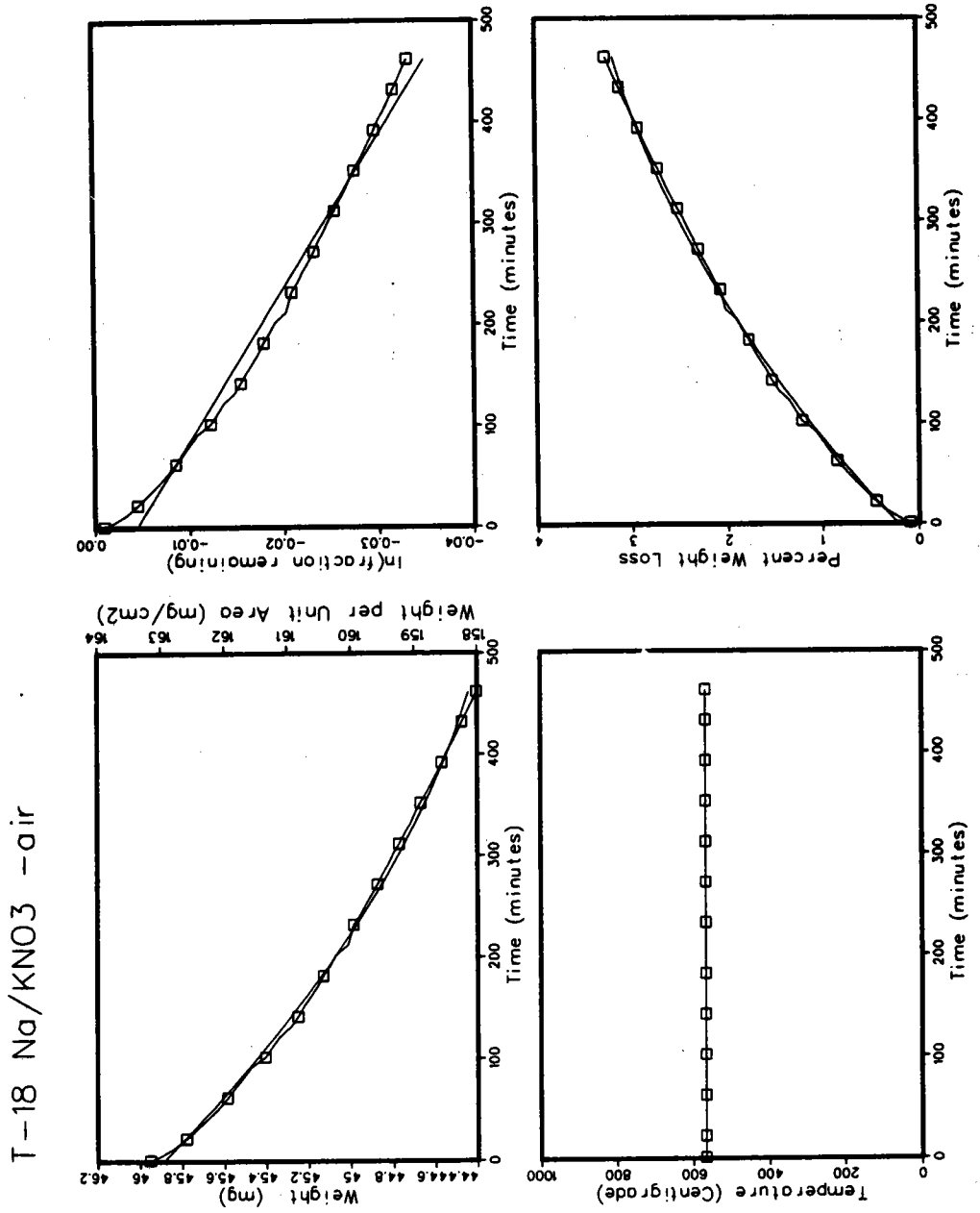
T-18 Na/KNO3 -air
Weight (mg)
Time (minutes)
Weight per Unit Area (mg/cm2)
ln(fraction remaining)
Percent Weight Loss
Temperature (Centigrade)

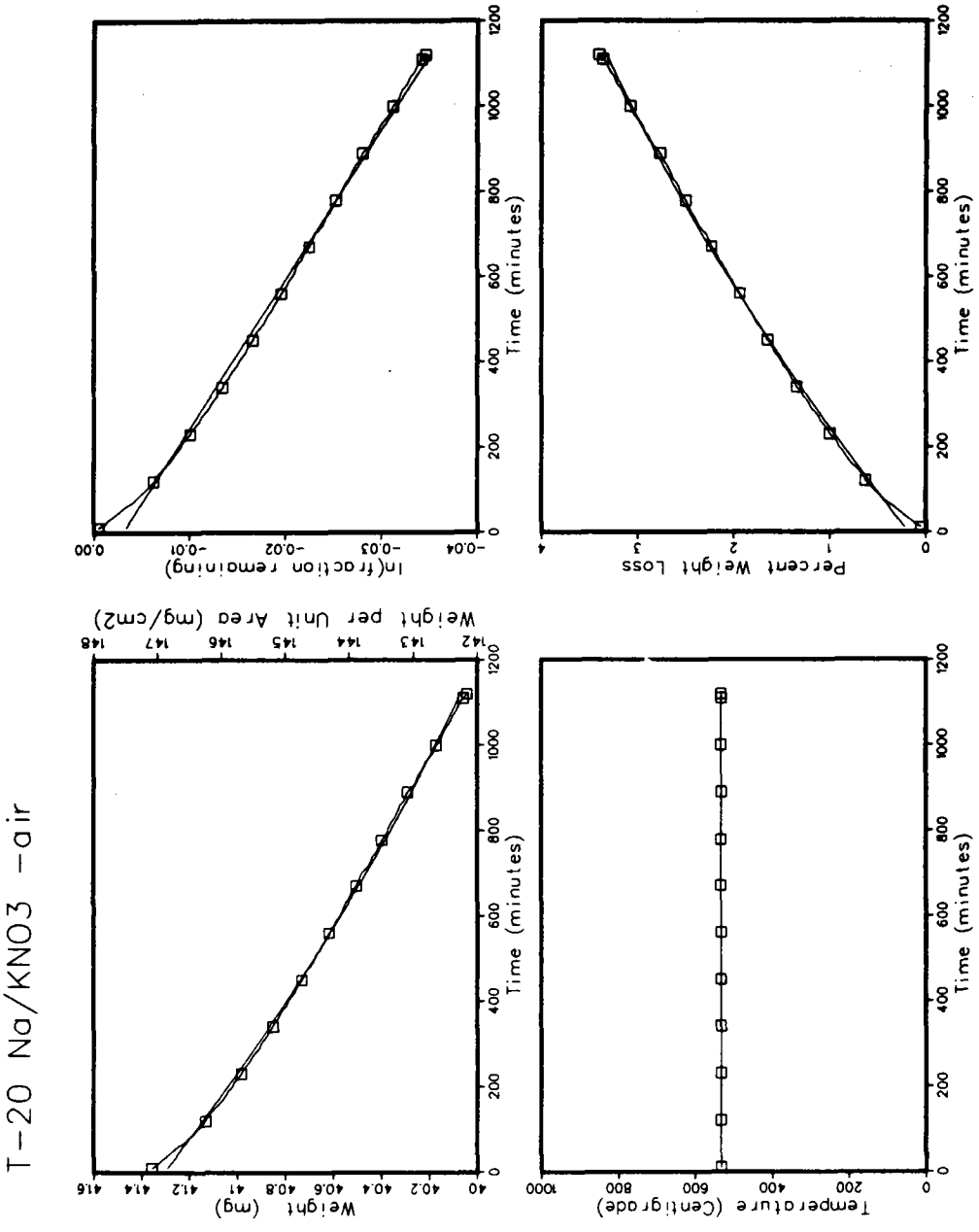
T-20 Na/KNO3 -air
Temperature (Centigrade)
Time (minutes)
Percent Weight Loss
Time (minutes)
Weight (mg)
Time (minutes)
ln(fraction remaining)
Time (minutes)
Weight per Unit Area (mg/cm2)

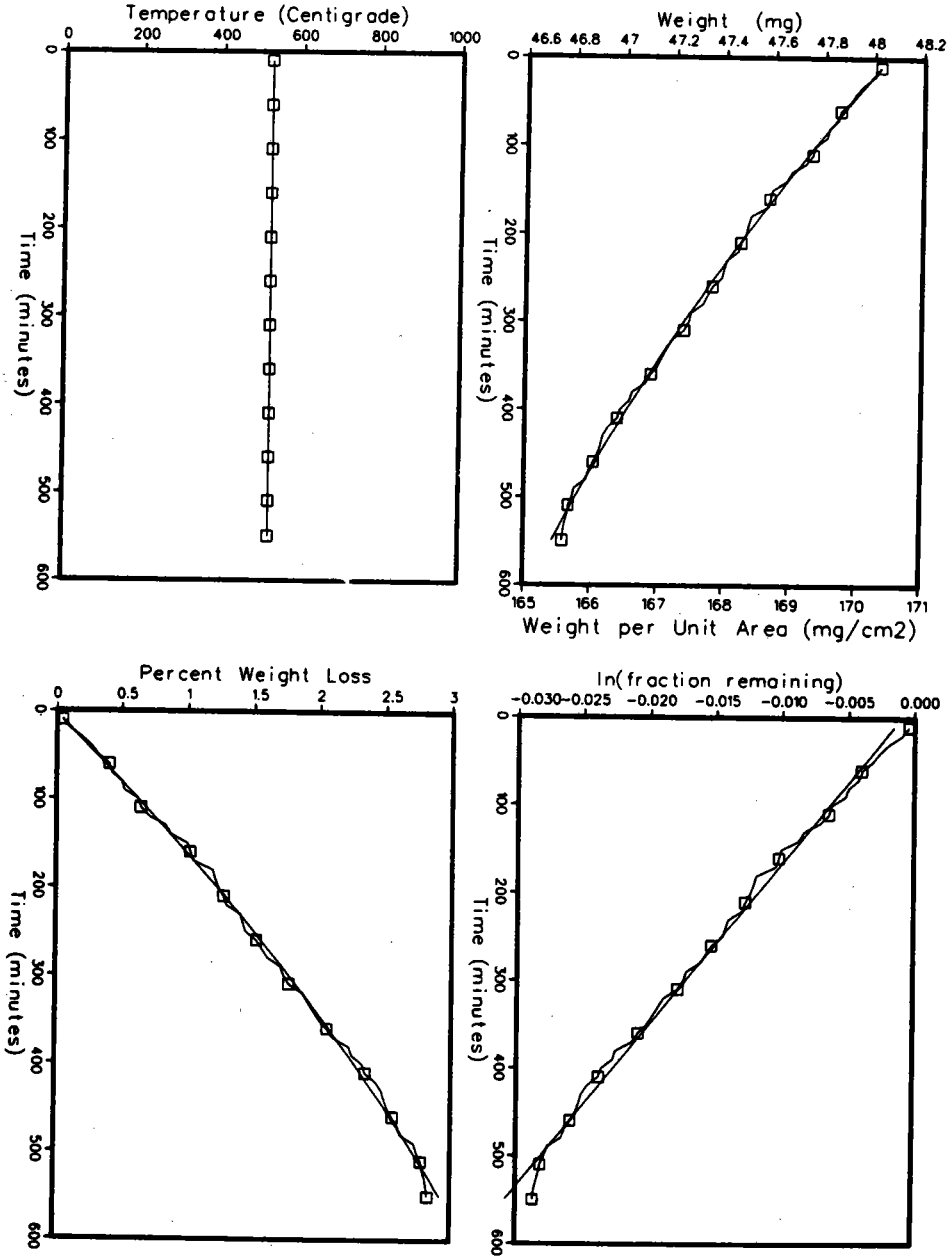
Temperature (Centigrade)
0
200
400
600
800
1000
Time (minutes)
0
100
200
300
400
500
600
Weight (mg)
46.6
46.8
47
47.2
47.4
47.6
47.8
48
48.2
Time (minutes)
165
166
167
168
169
170
171
Weight per Unit Area (mg/cm2)
Percent Weight Loss
0
0.5
1
1.5
2
2.5
3
Time (minutes)
ln(fraction remaining)
-0.030
-0.025
-0.020
-0.015
-0.010
-0.005
0.000
Time (minutes)

T-15 P430 -air

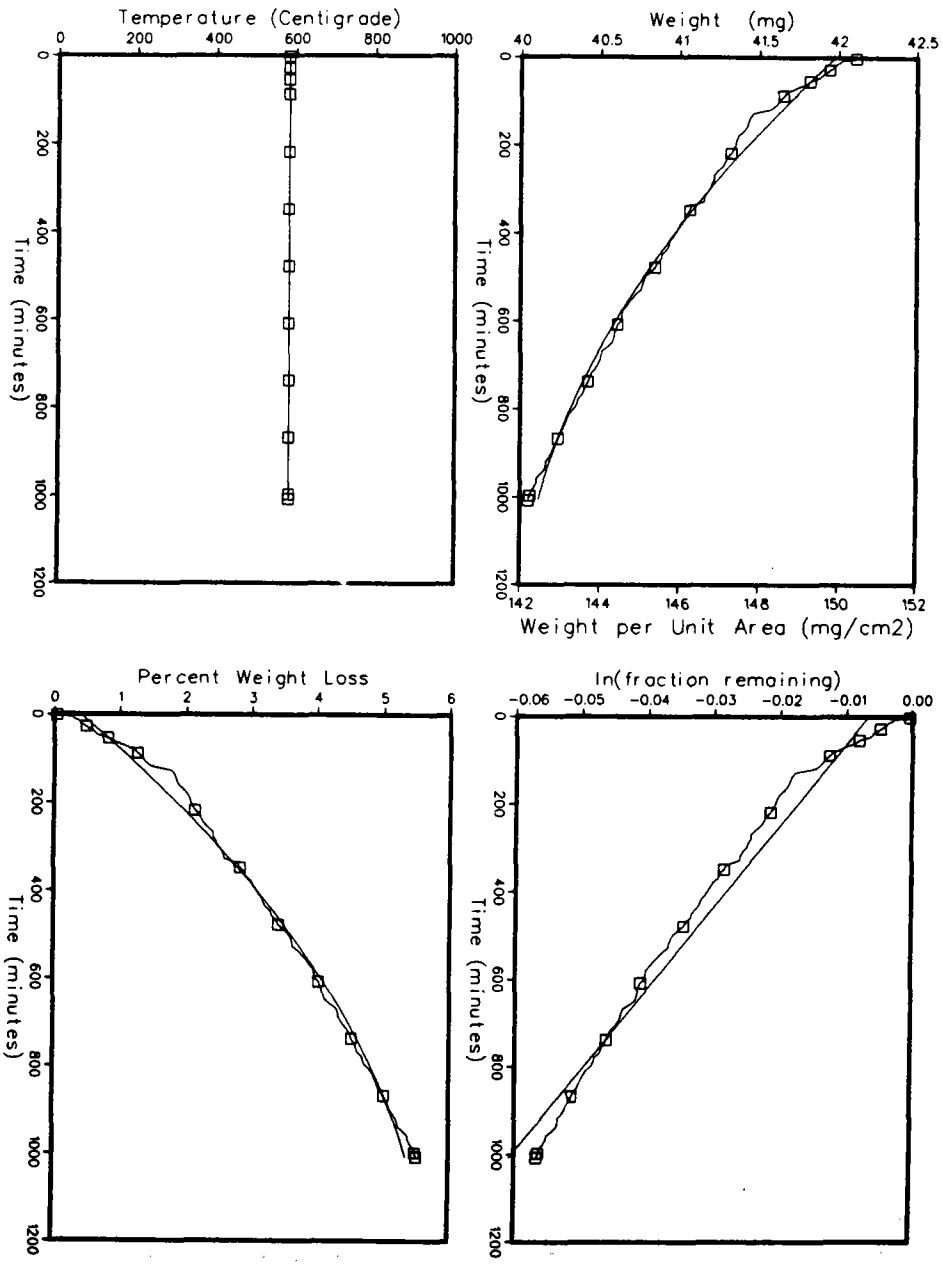
Temperature (Centigrade)
0
200
400
600
800
1000
Time (minutes)
0
200
400
600
800
1000
1200
Weight (mg)
40
40.5
41
41.5
42
42.5
Time (minutes)
142
144
146
148
150
152
Weight per Unit Area (mg/cm2)
Percent Weight Loss
0
1
2
3
4
5
6
Time (minutes)
ln(fraction remaining)
-0.06
-0.05
-0.04
-0.03
-0.02
-0.01
0.00
Time (minutes)

T-16 P430 -air

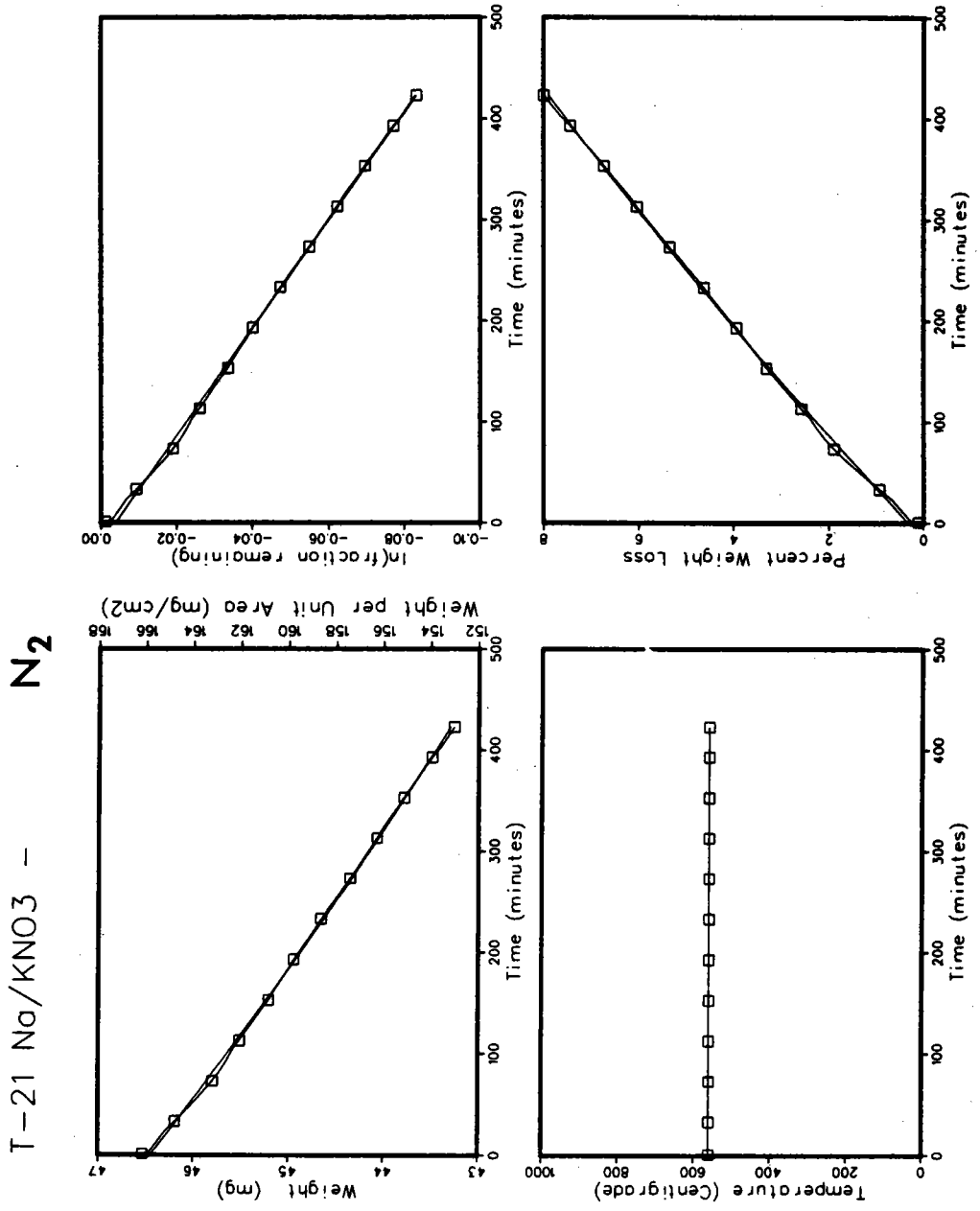
T-21 Na/KNO3 - N2
Weight (mg)
Time (minutes)
Temperature (Centigrade)
Time (minutes)
Percent Weight Loss
Time (minutes)
ln(fraction remaining)
Time (minutes)
Weight per Unit Area (mg/cm2)

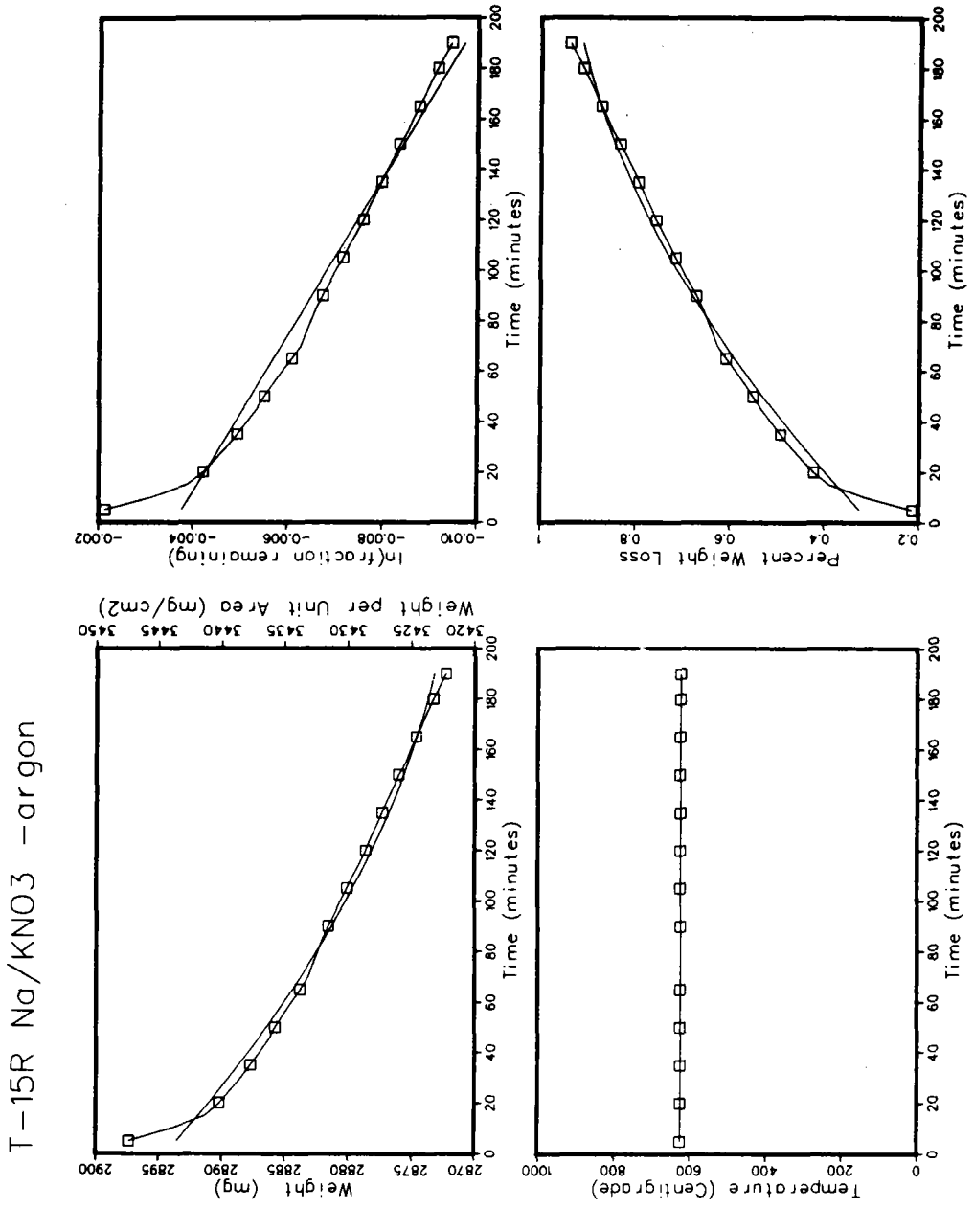
T-15R Na/KNO3 -argon
Weight (mg)
Time (minutes)
Weight per Unit Area (mg/cm2)
ln(fraction remaining)
Percent Weight Loss
Temperature (Centigrade)

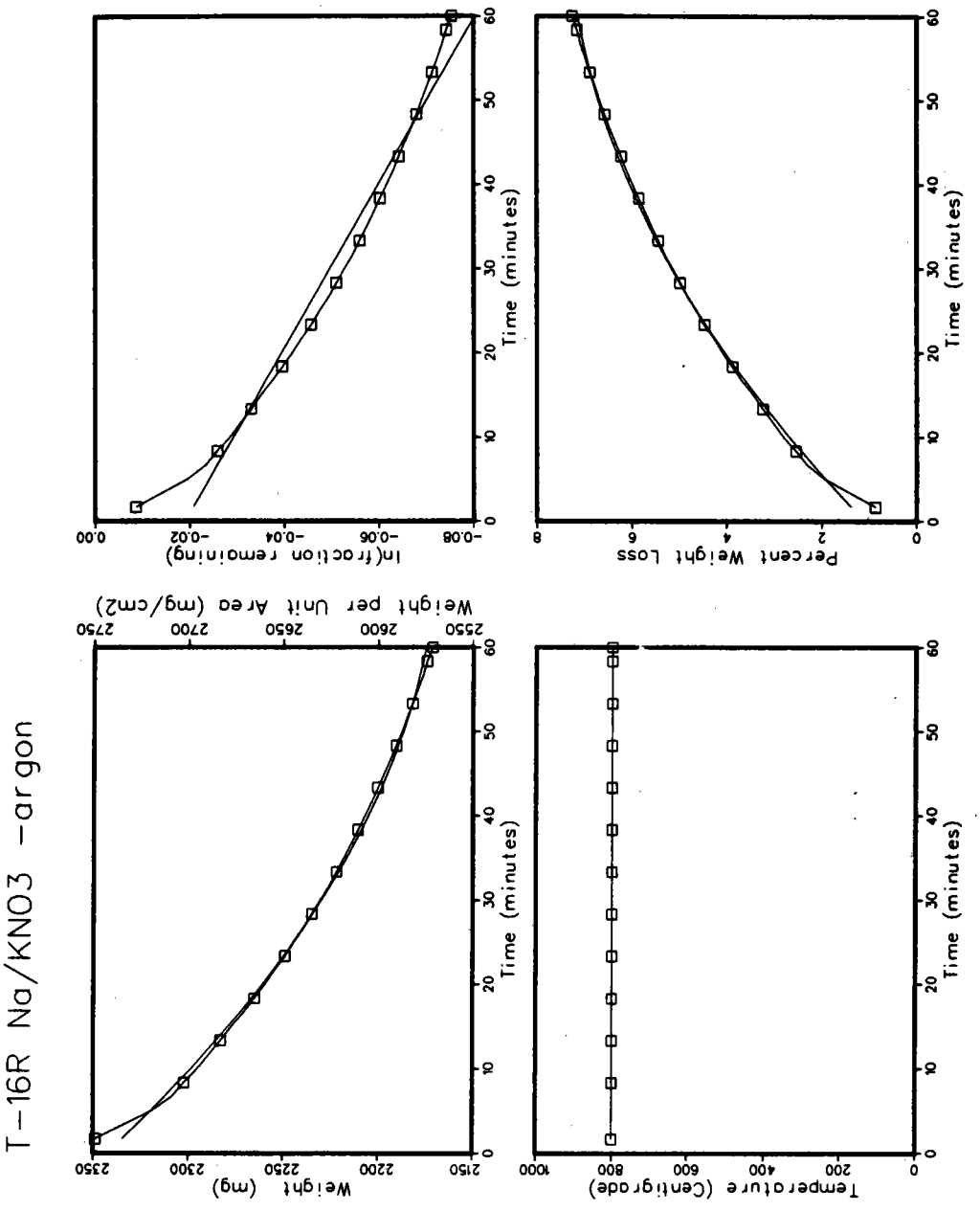
T-16R Na/KNO3 -argon
Weight (mg)
Time (minutes)
Weight per Unit Area (mg/cm2)
ln(fraction remaining)
Percent Weight Loss
Temperature (Centigrade)

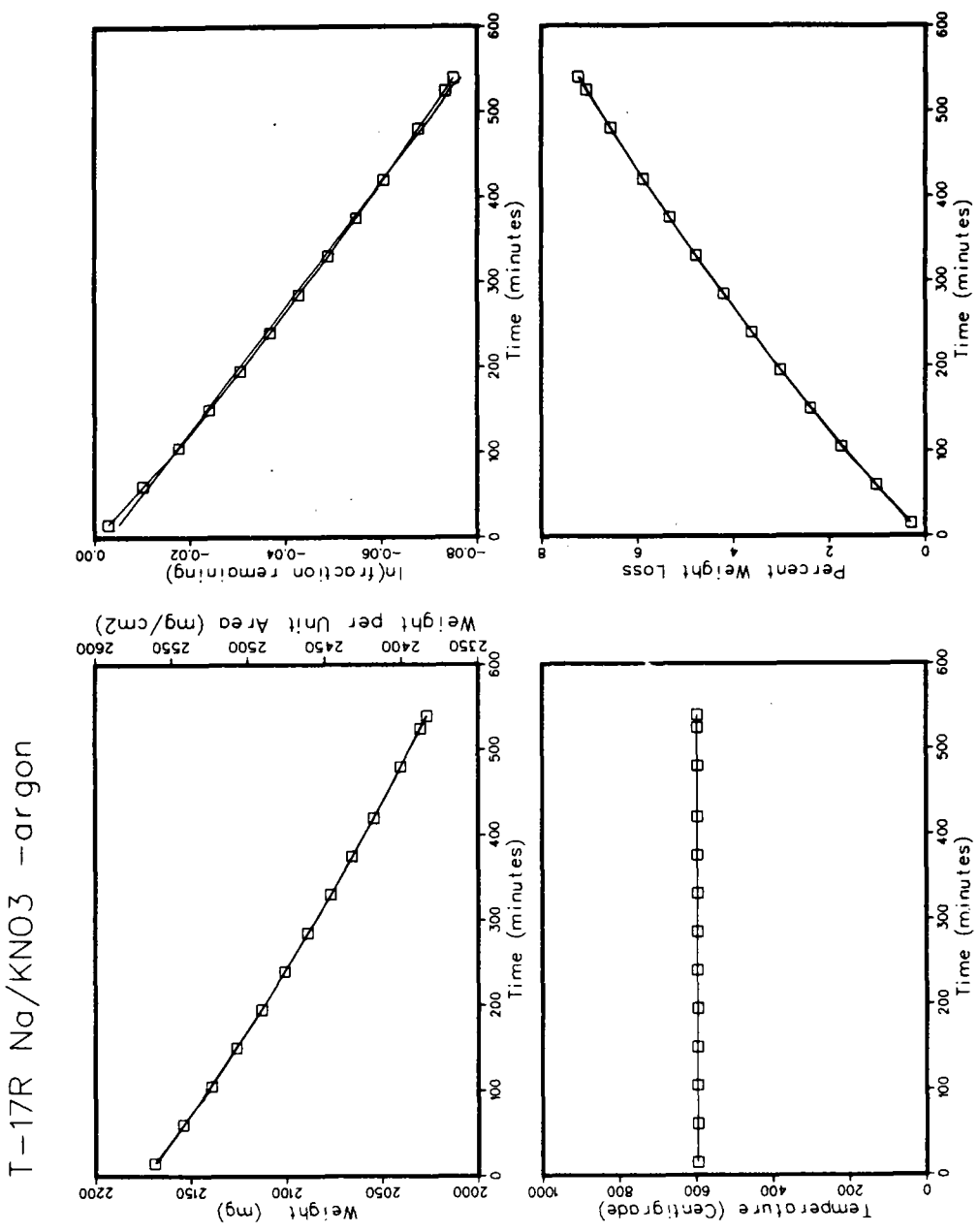
T-17R Na/KNO3 -argon
Weight (mg)
Time (minutes)
Weight per Unit Area (mg/cm2)
ln(fraction remaining)
Percent Weight Loss
Temperature (Centigrade)

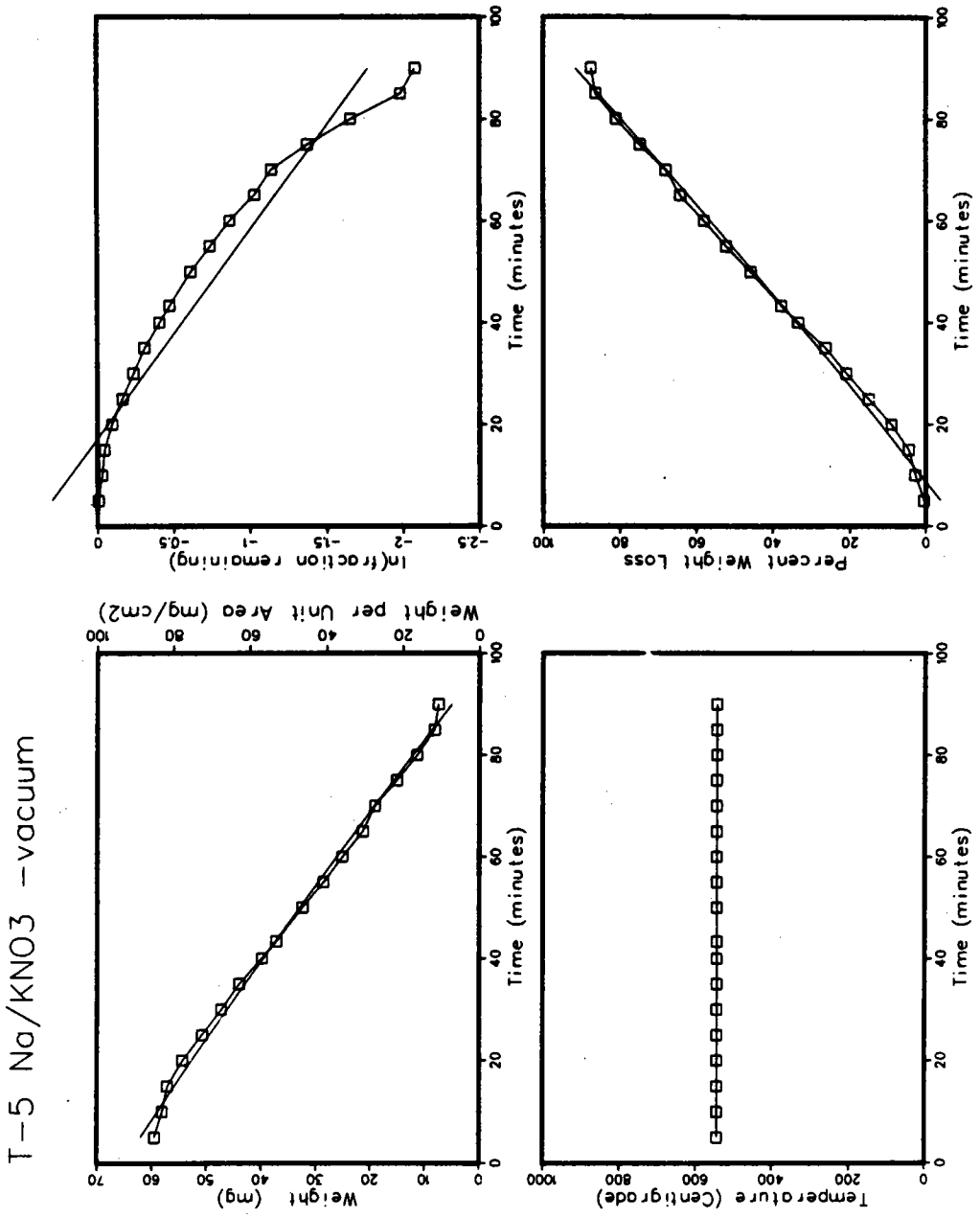
T-5 Na/KNO3 -vacuum
Weight (mg)
Weight per Unit Area (mg/cm2)
Time (minutes)
Temperature (Centigrade)
Time (minutes)
Percent Weight Loss
Time (minutes)
ln(fraction remaining)
Time (minutes)

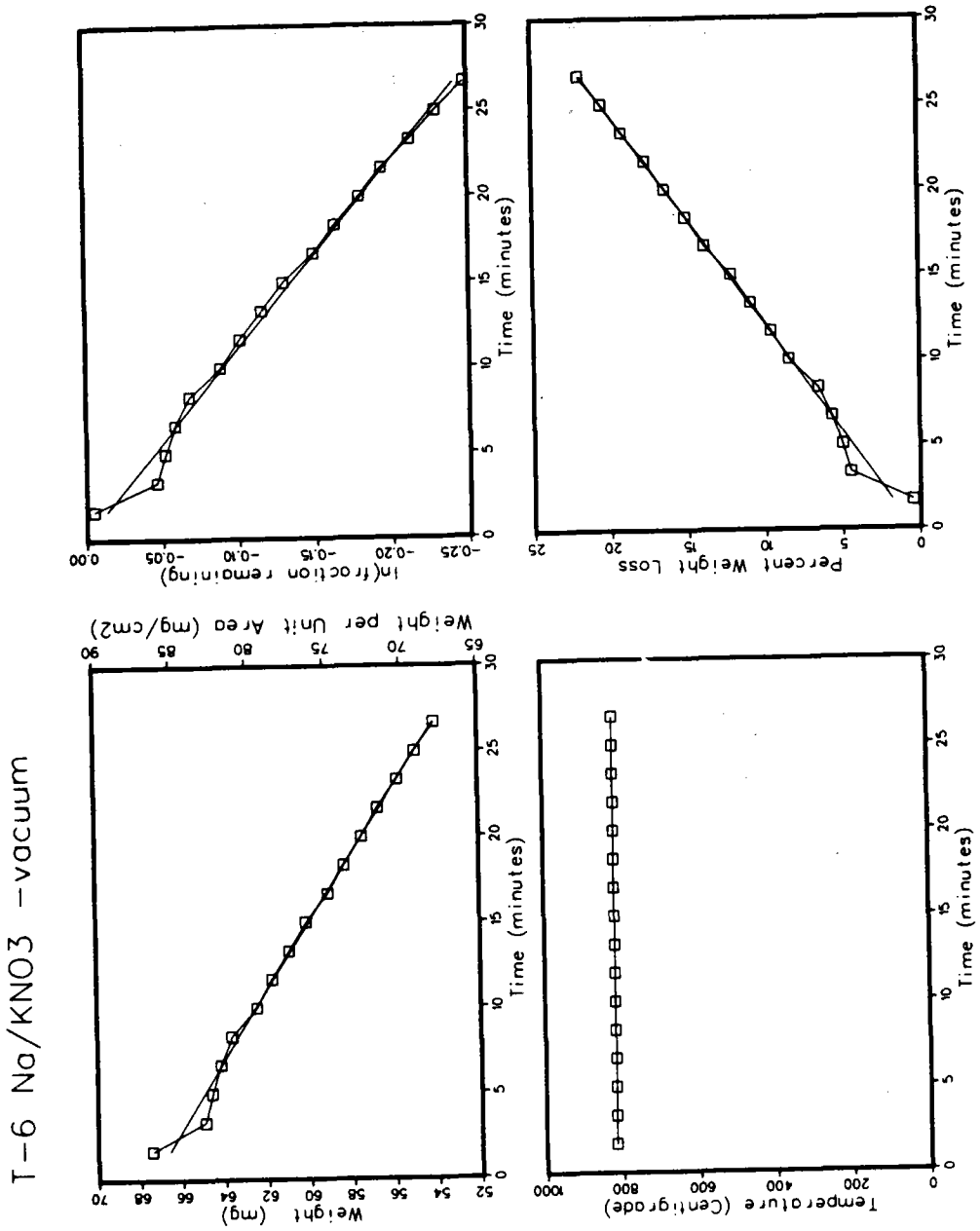
T-6 Na/KNO3 -vacuum
Weight (mg)
Time (minutes)
Weight per Unit Area (mg/cm2)
ln(fraction remaining)
Percent Weight Loss
Temperature (Centigrade)

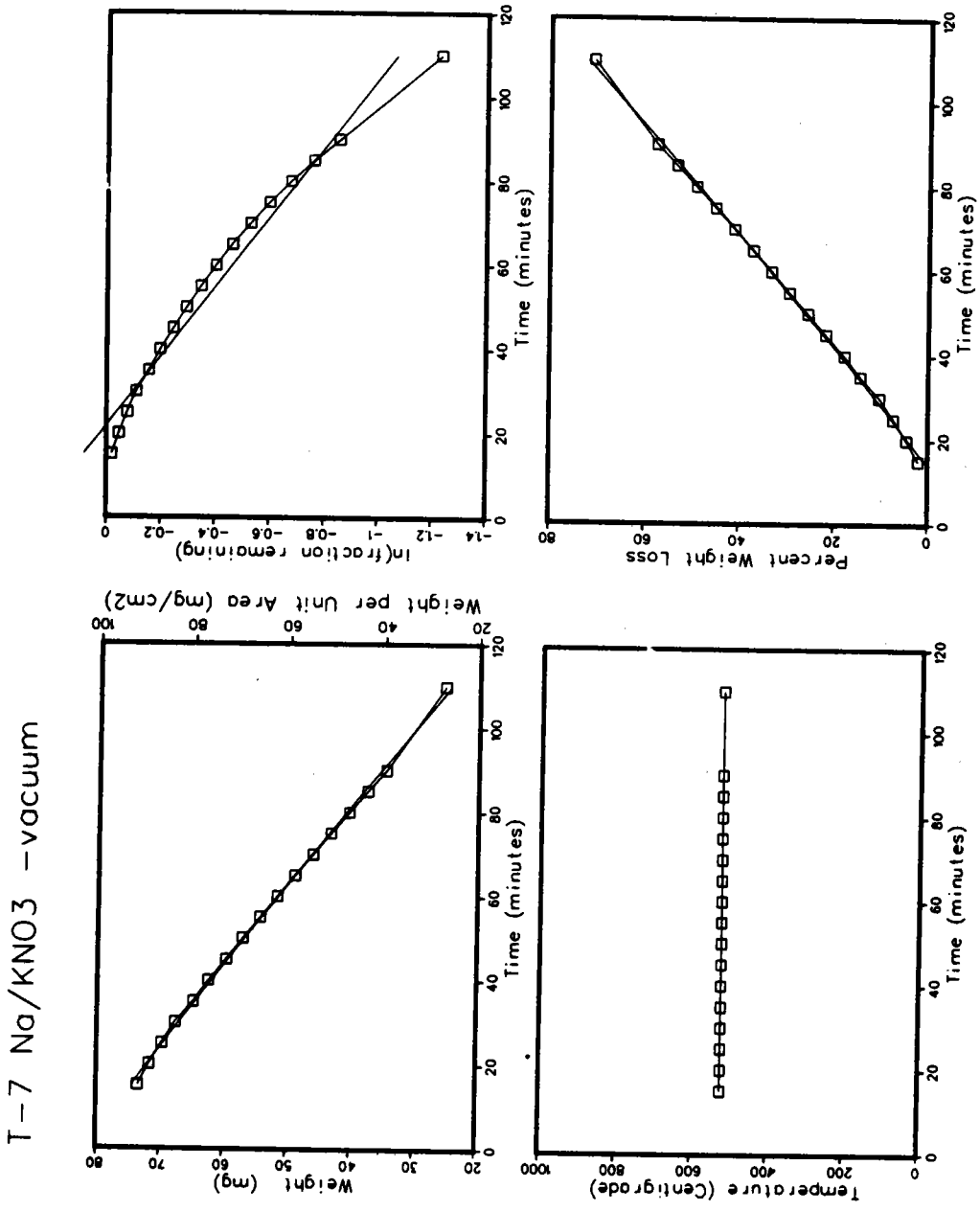
T-7 Na/KNO3 -vacuum
Weight (mg)
Time (minutes)
Temperature (Centigrade)
Time (minutes)
Percent Weight Loss
Time (minutes)
ln(fraction remaining)
Time (minutes)
Weight per Unit Area (mg/cm2)

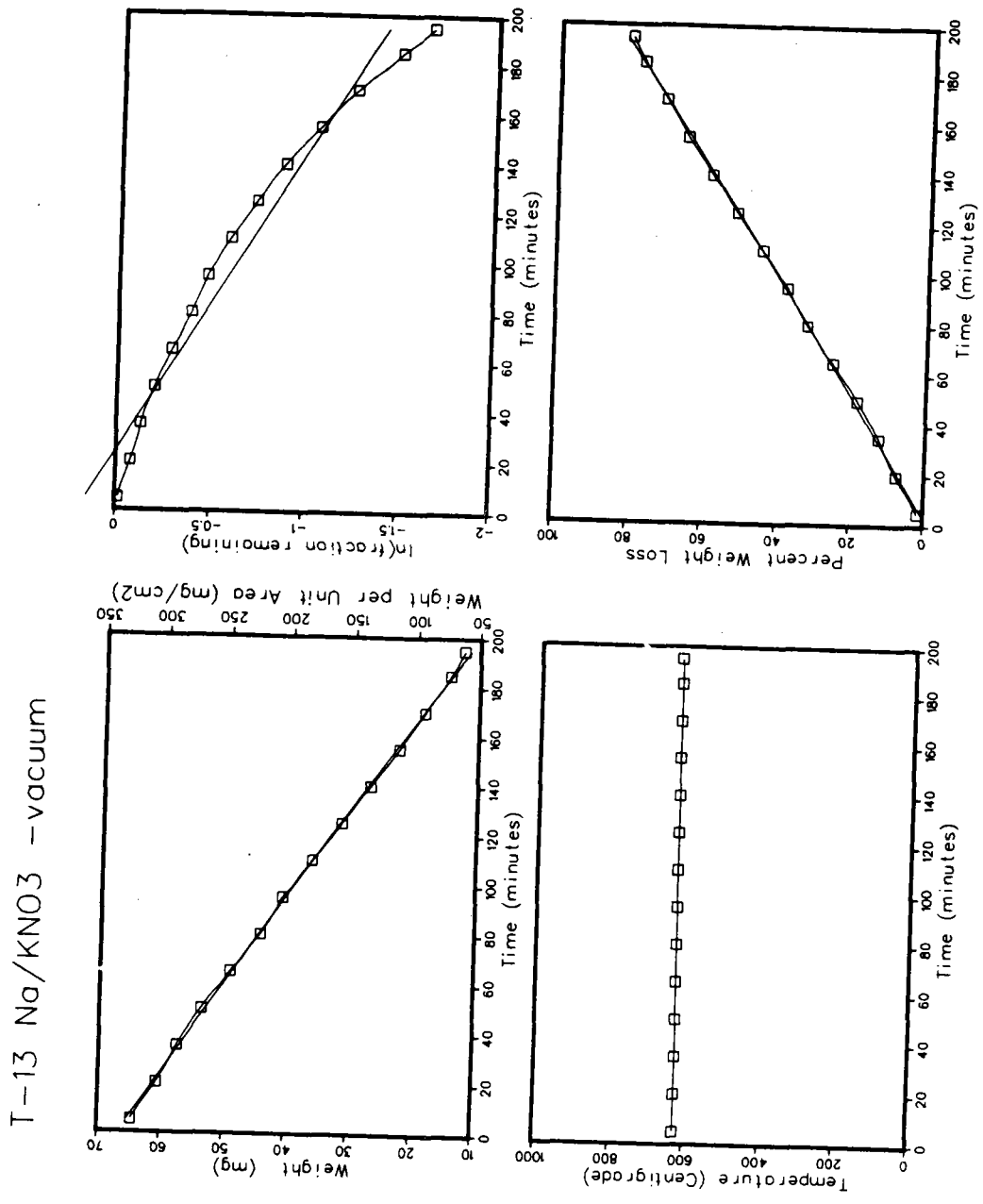
T-13 Na/KNO3 -vacuum
Weight (mg)
Time (minutes)
Weight per Unit Area (mg/cm2)
ln(fraction remaining)
Percent Weight Loss
Temperature (Centigrade)

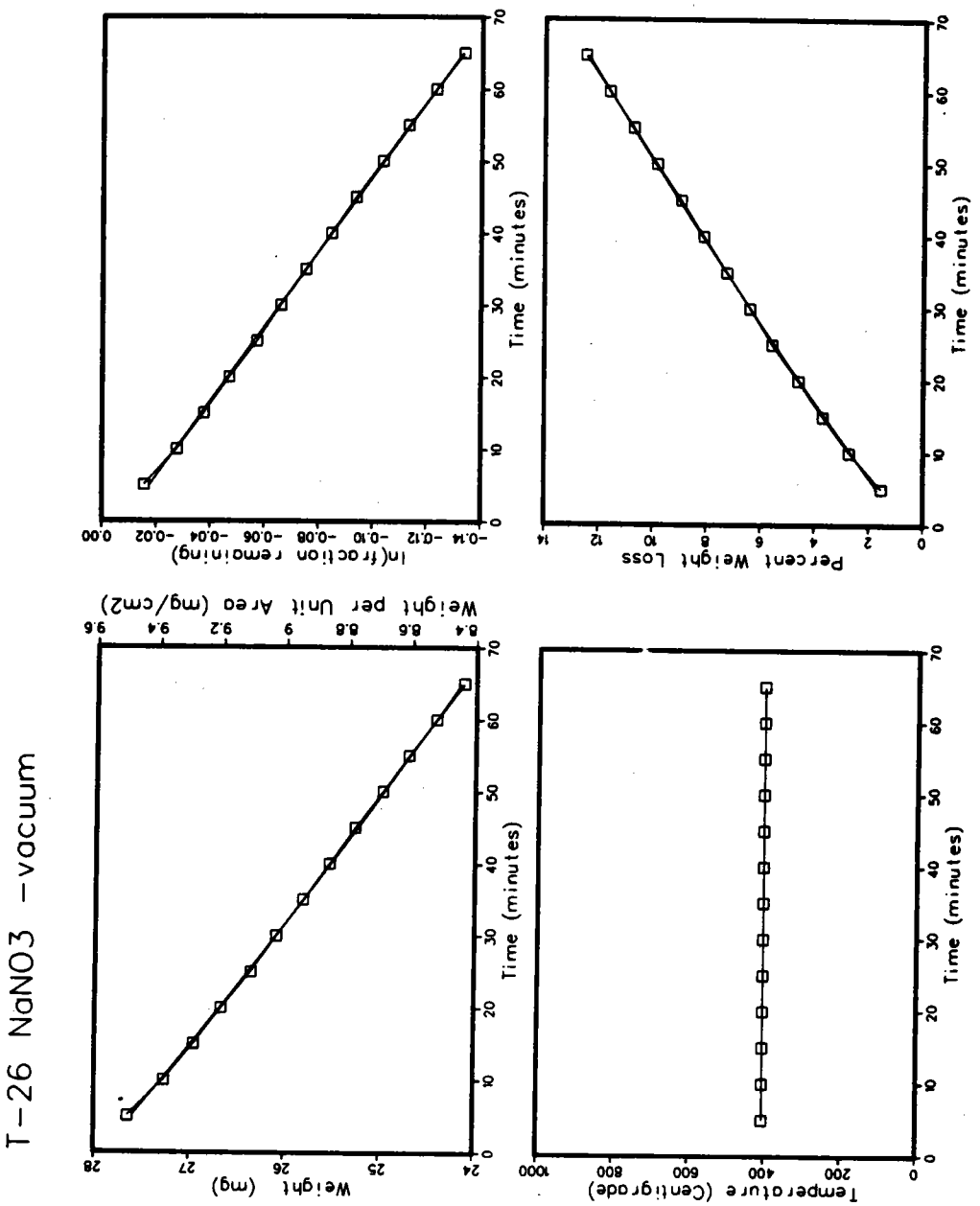
T-26 NaNO3 -vacuum
Temperature (Centigrade)
Time (minutes)
Weight (mg)
Weight per Unit Area (mg/cm2)
Time (minutes)
Percent Weight Loss
Time (minutes)
ln(fraction remaining)
Time (minutes)

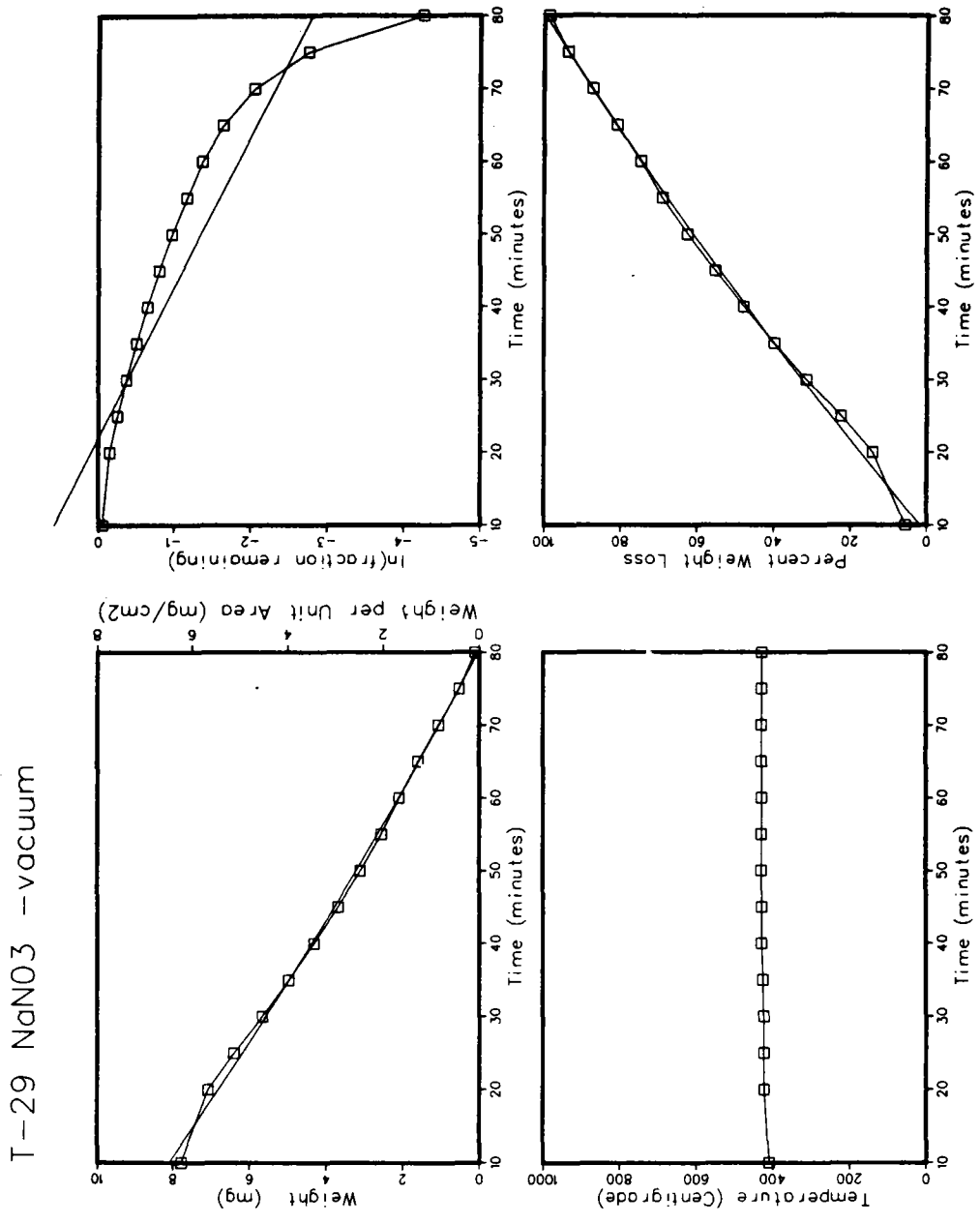
T-29 NaNO3 -vacuum
Temperature (Centigrade)
Time (minutes)
Weight (mg)
Weight per Unit Area (mg/cm2)
Percent Weight Loss
ln(fraction remaining)

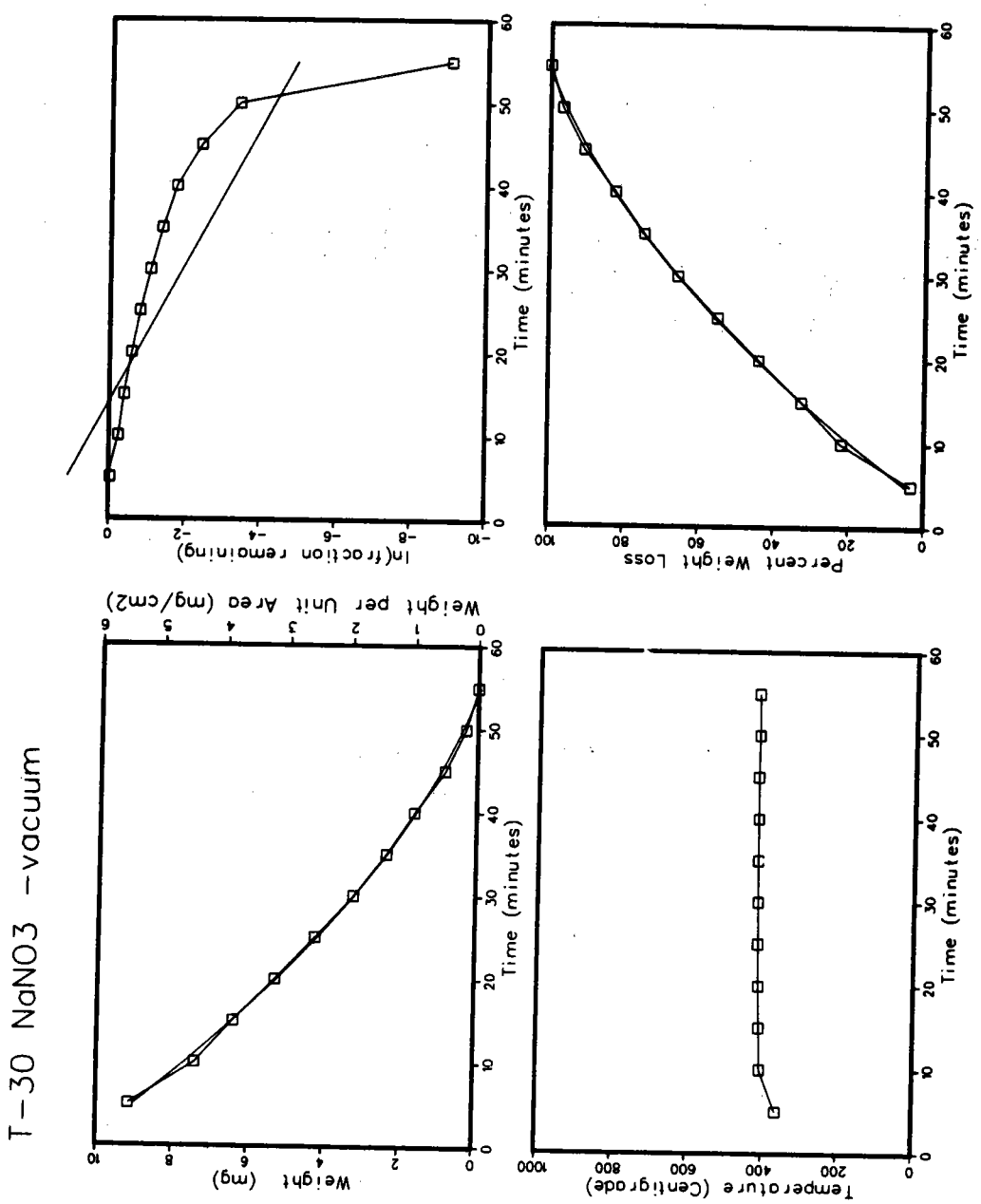
T-30 NaNO3 -vacuum
Weight (mg)
Time (minutes)
Weight per Unit Area (mg/cm2)
ln(fraction remaining)
Percent Weight Loss
Temperature (Centigrade)

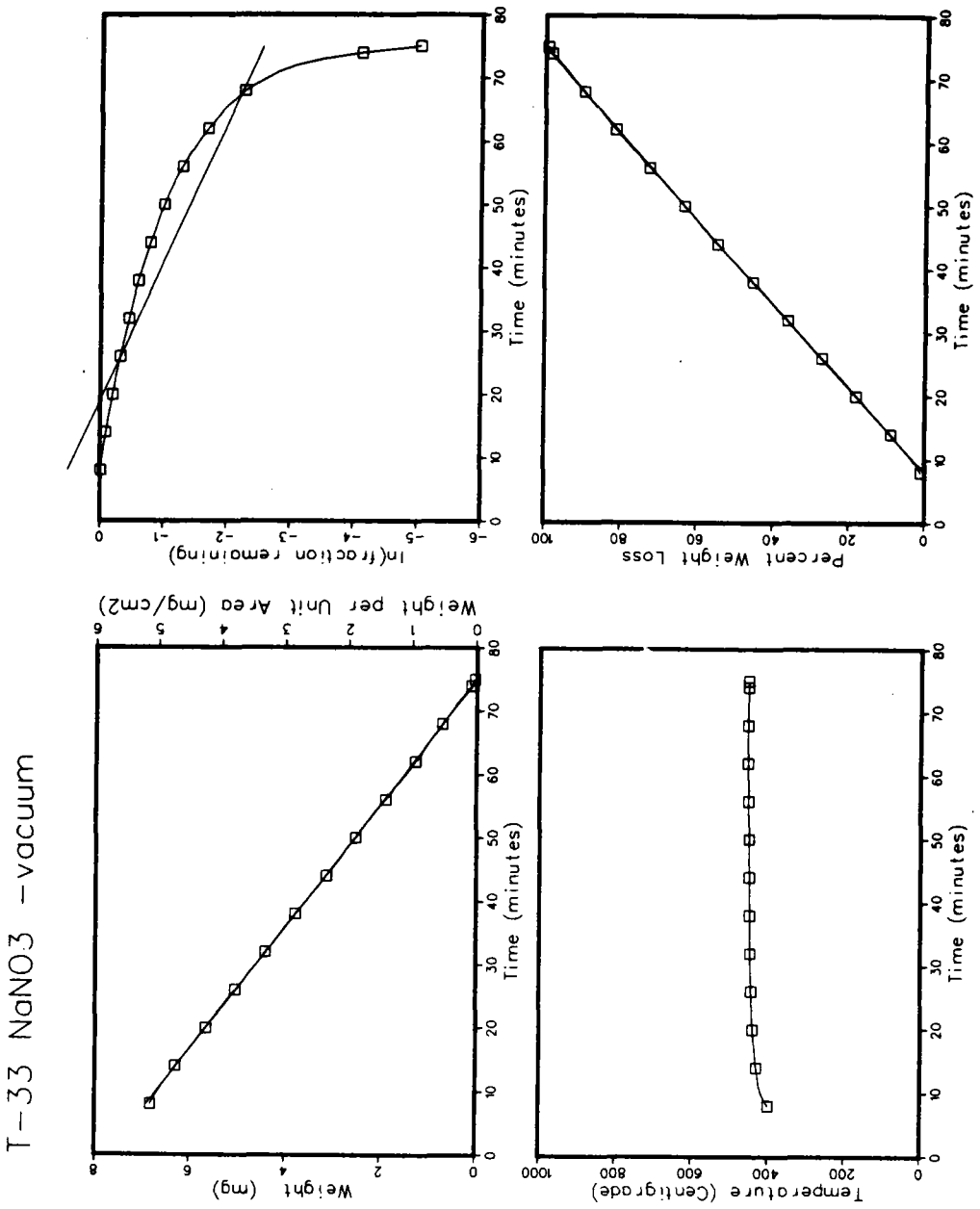
T-33 NaNO3 -vacuum
Weight (mg)
Time (minutes)
Weight per Unit Area (mg/cm2)
ln(fraction remaining)
Percent Weight Loss
Temperature (Centigrade)

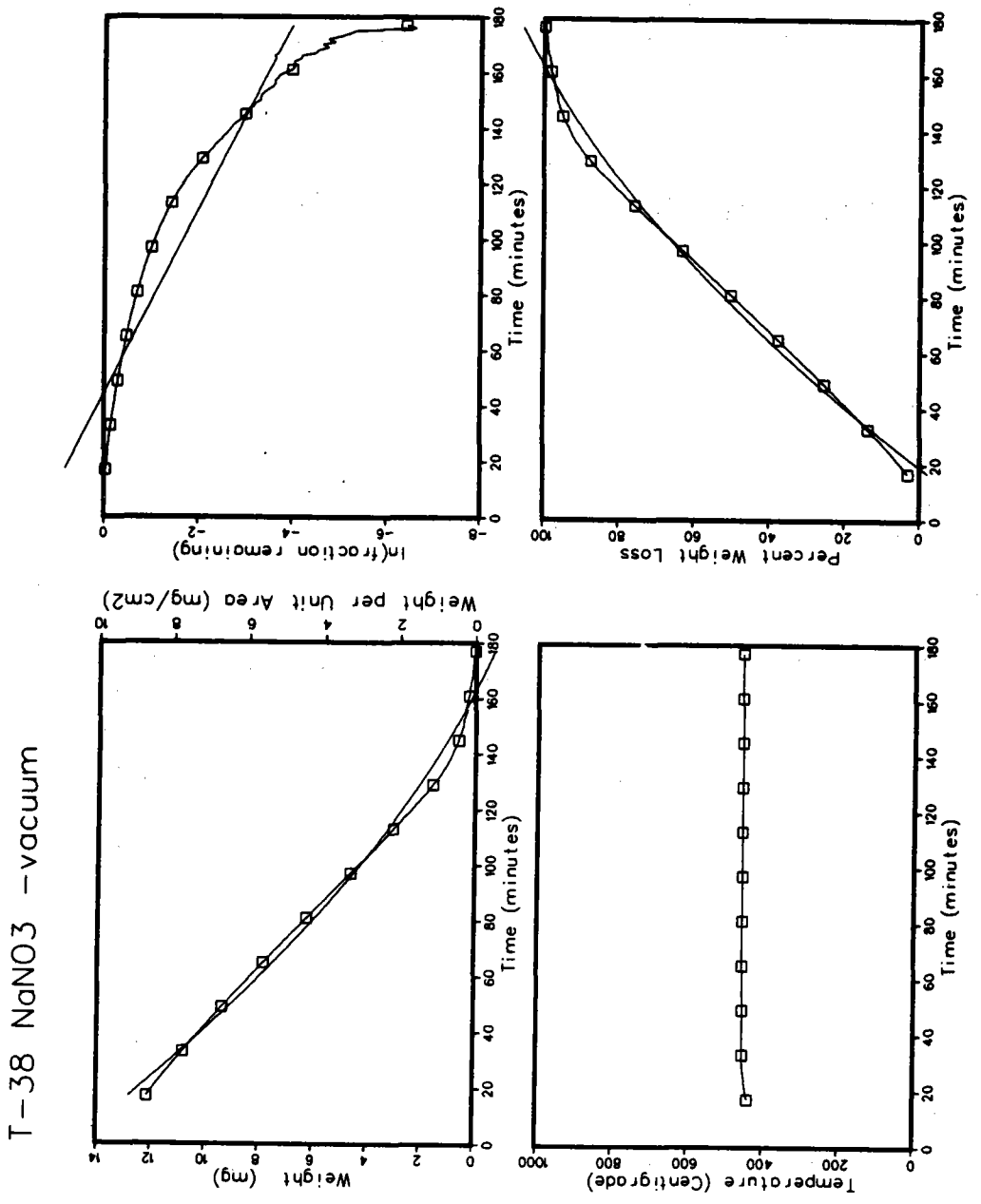
T-38 NaNO3 -vacuum
Temperature (Centigrade)
Time (minutes)
Weight (mg)
Time (minutes)
Weight per Unit Area (mg/cm2)
Time (minutes)
Percent Weight Loss
Time (minutes)
ln(fraction remaining)
Time (minutes)

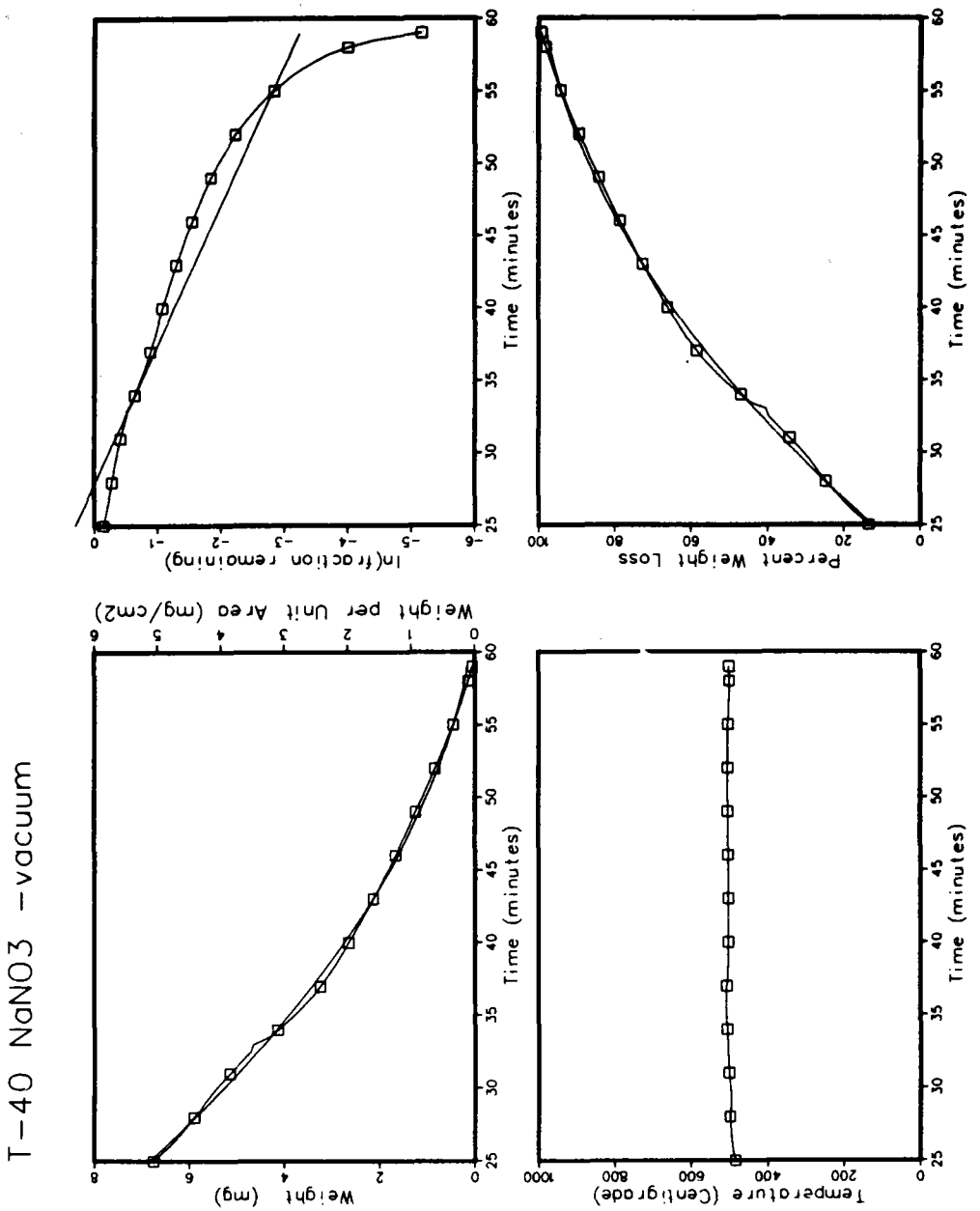
T-40 NaNO3 -vacuum
Weight (mg)
Time (minutes)
Weight per Unit Area (mg/cm2)
ln(fraction remaining)
Percent Weight Loss
Temperature (Centigrade)

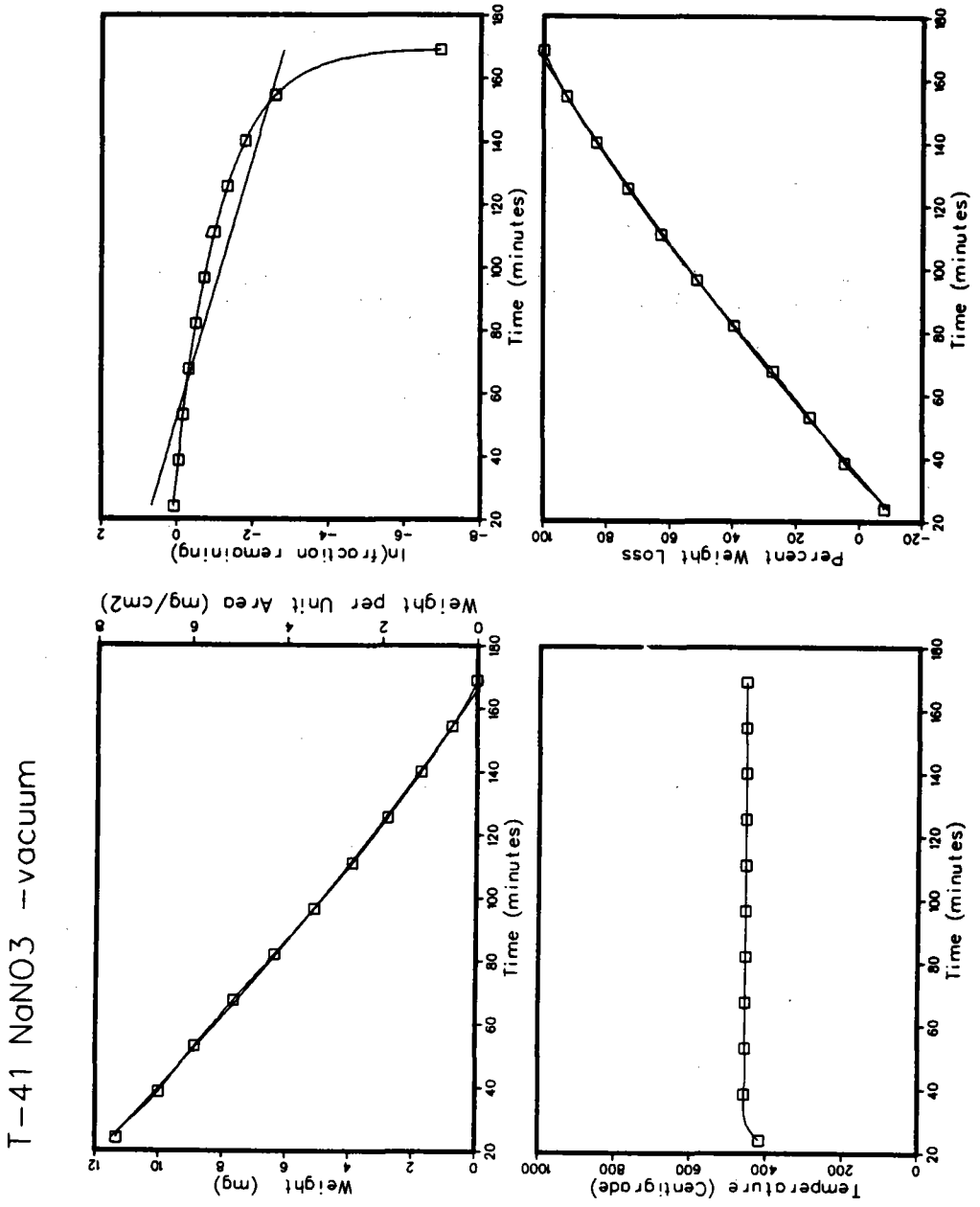
T-41 NaNO3 -vacuum
Weight (mg)
Time (minutes)
Weight per Unit Area (mg/cm2)
ln(fraction remaining)
Percent Weight Loss
Temperature (Centigrade)

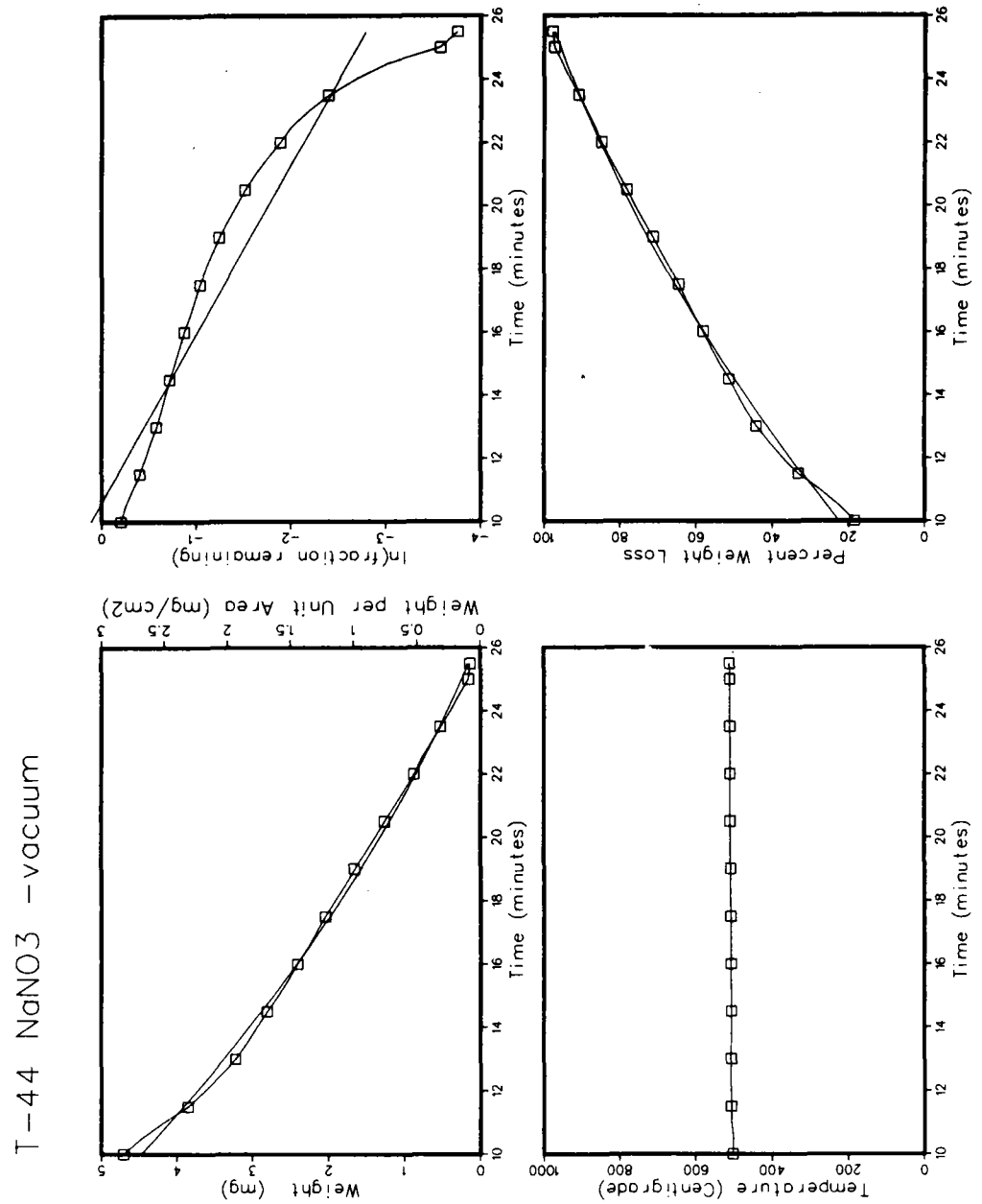
T-44 NaNO3 -vacuum
Weight (mg)
Time (minutes)
Weight per Unit Area (mg/cm2)
ln(fraction remaining)
Percent Weight Loss
Temperature (Centigrade)

T-47 NaNO3 -vacuum

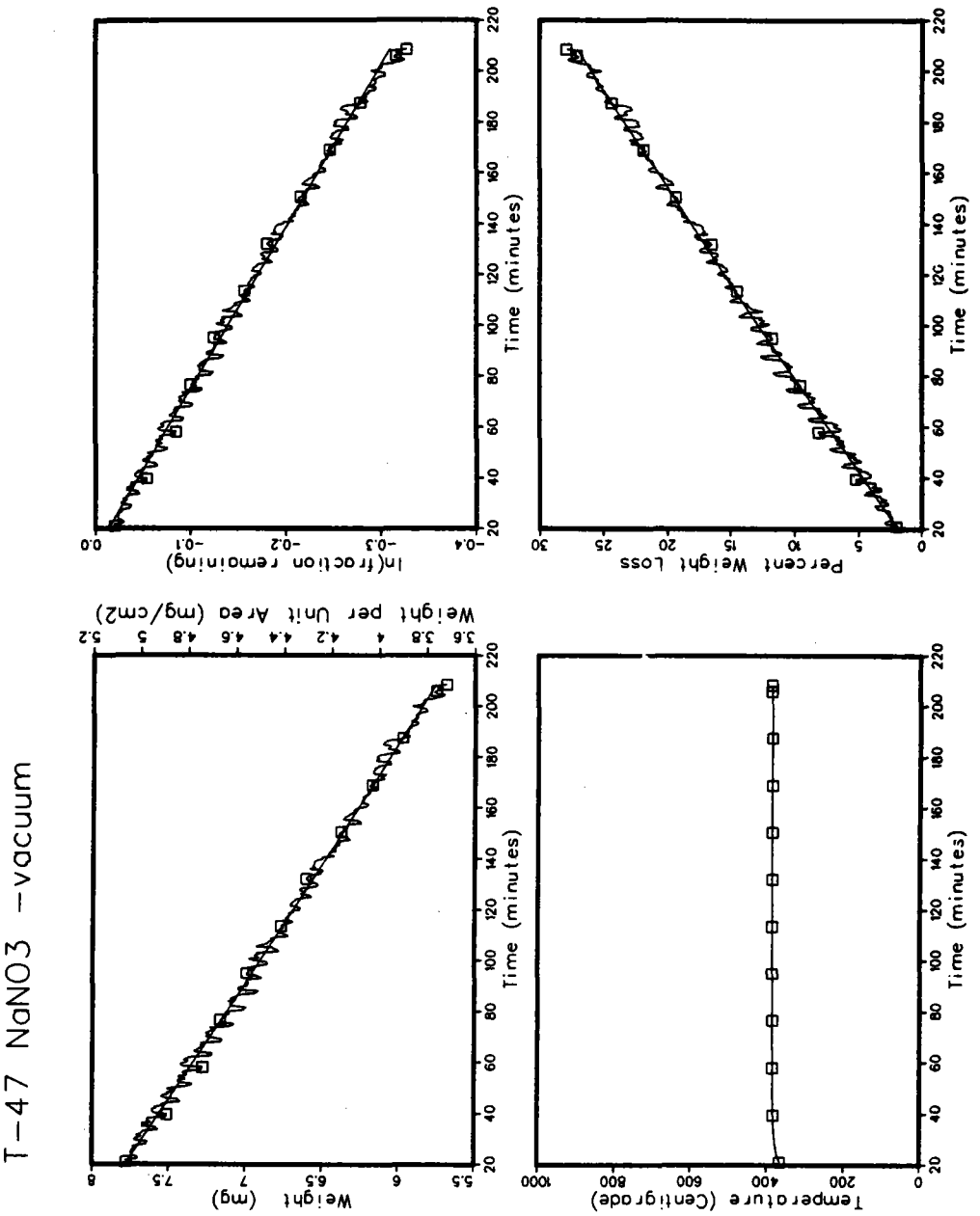

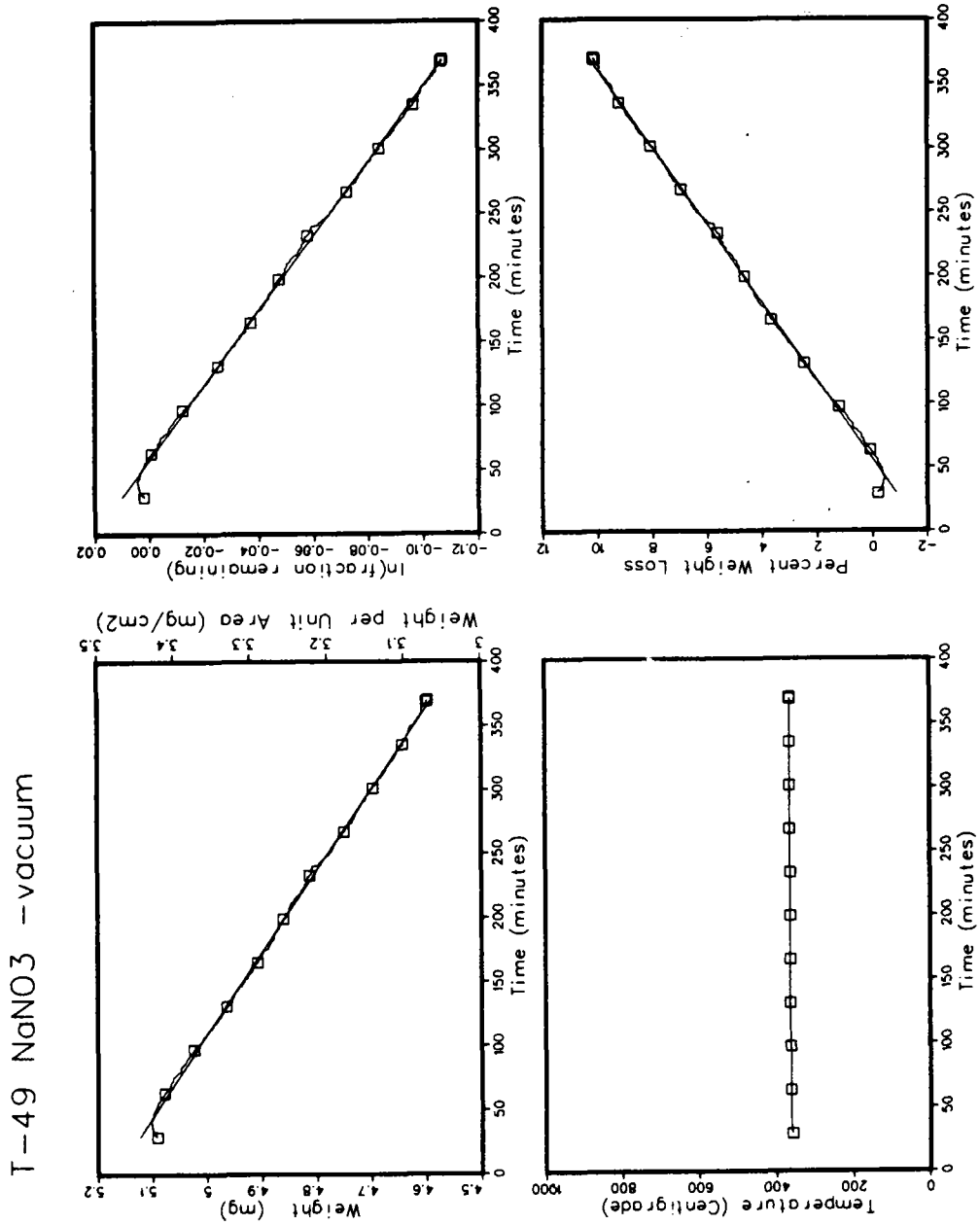
T-49 NaNO3 -vacuum
Weight (mg)
Time (minutes)
Weight per Unit Area (mg/cm2)
ln(fraction remaining)
Percent Weight Loss
Temperature (Centigrade)

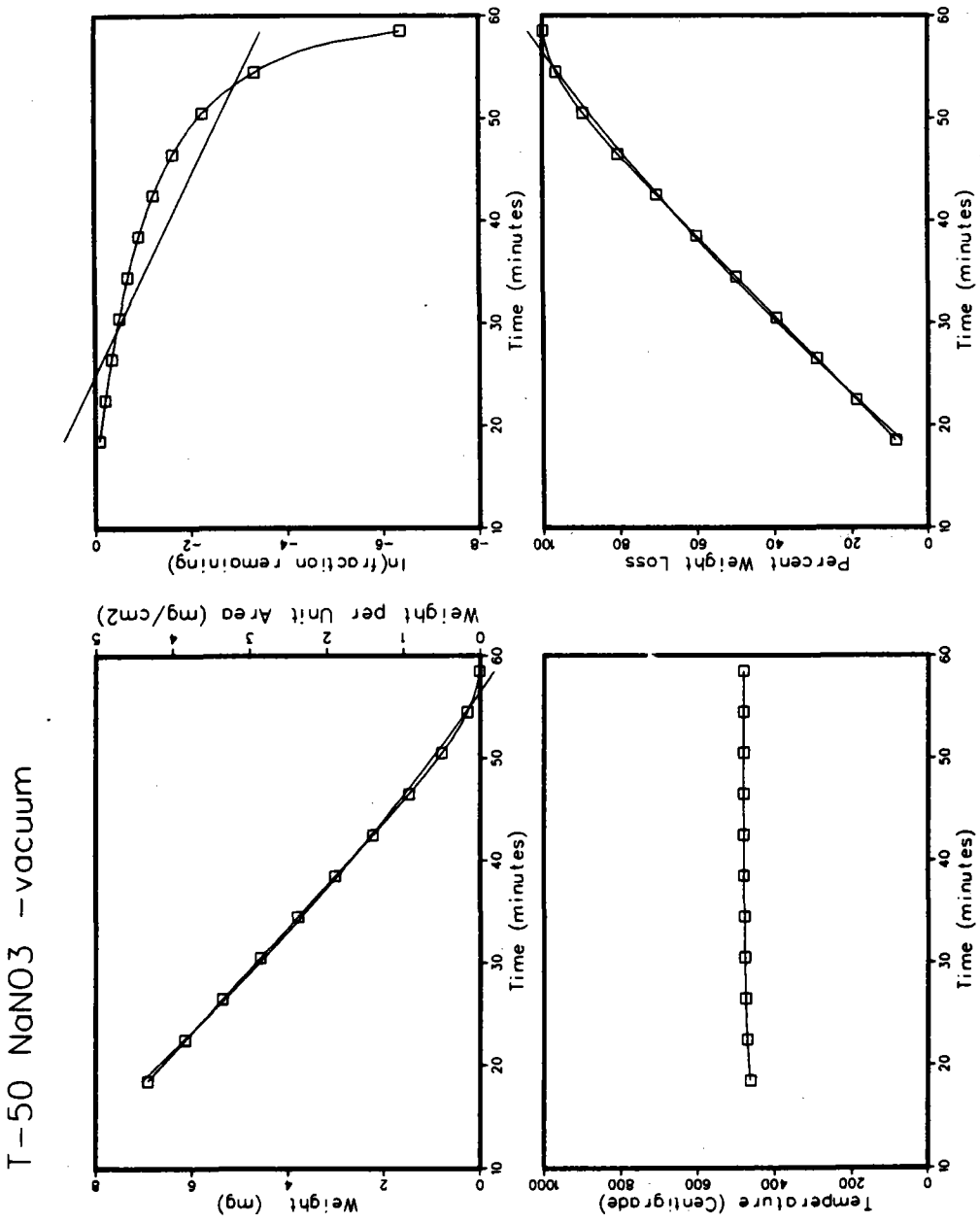
T-50 NaNO3 -vacuum
Weight (mg)
Time (minutes)
Weight per Unit Area (mg/cm2)
Temperature (Centigrade)
Time (minutes)
Percent Weight Loss
Time (minutes)
ln(fraction remaining)
Time (minutes)

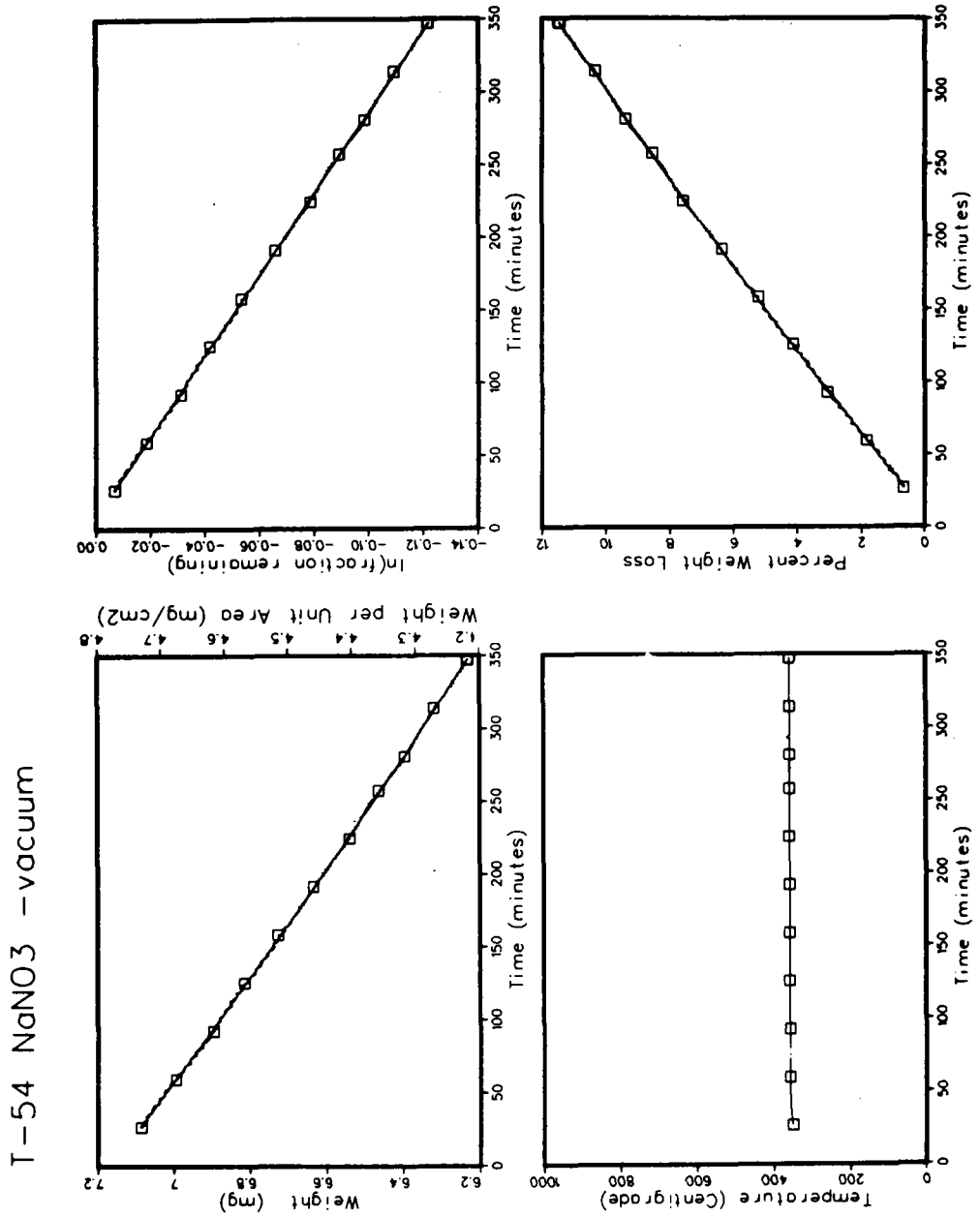
T-54 NaNO3 -vacuum
Weight (mg)
Time (minutes)
Weight per Unit Area (mg/cm2)
ln(fraction remaining)
Percent Weight Loss
Temperature (Centigrade)

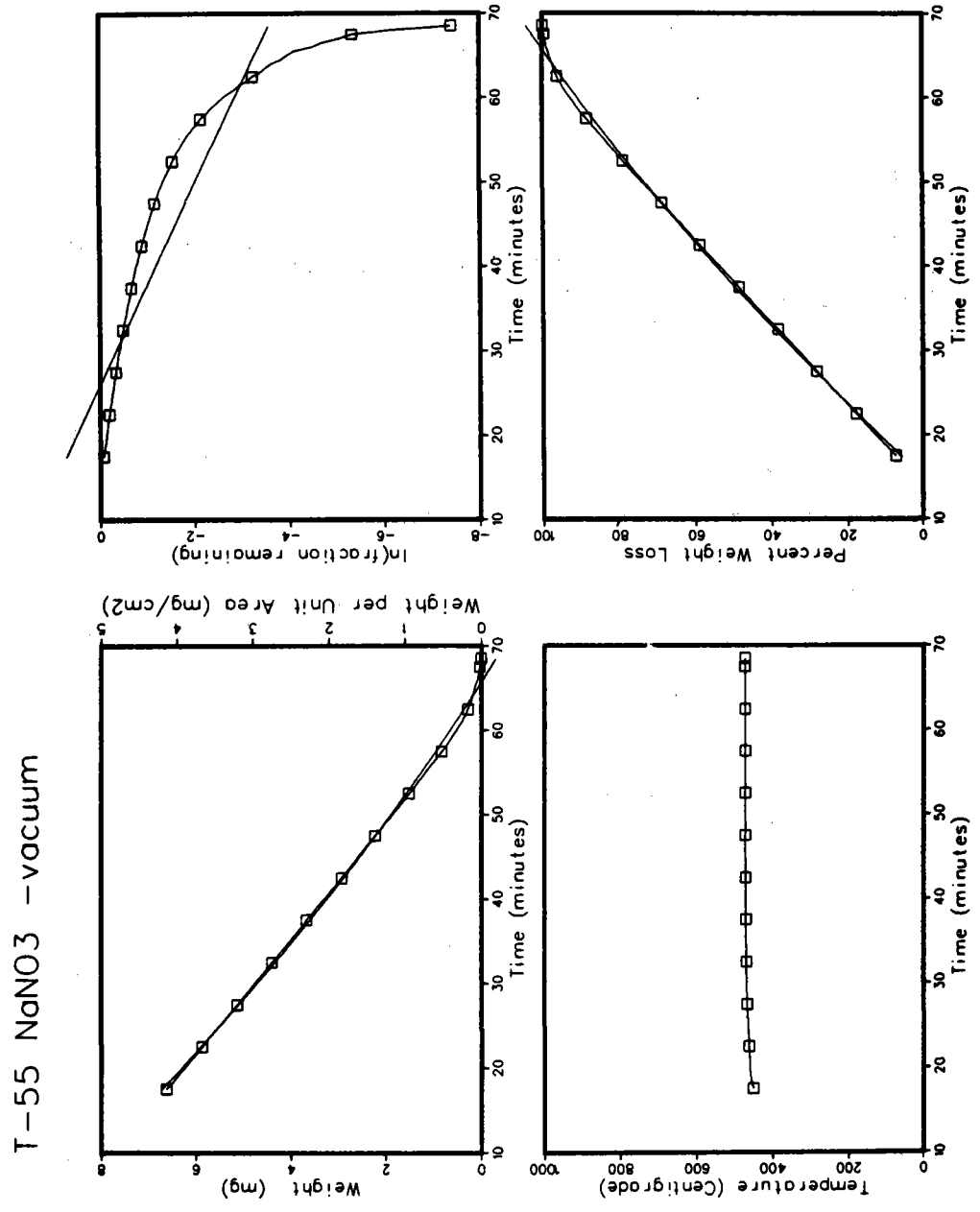
T-55 NaNO3 -vacuum
Weight (mg)
Time (minutes)
Weight per Unit Area (mg/cm2)
ln(fraction remaining)
Percent Weight Loss
Temperature (Centigrade)

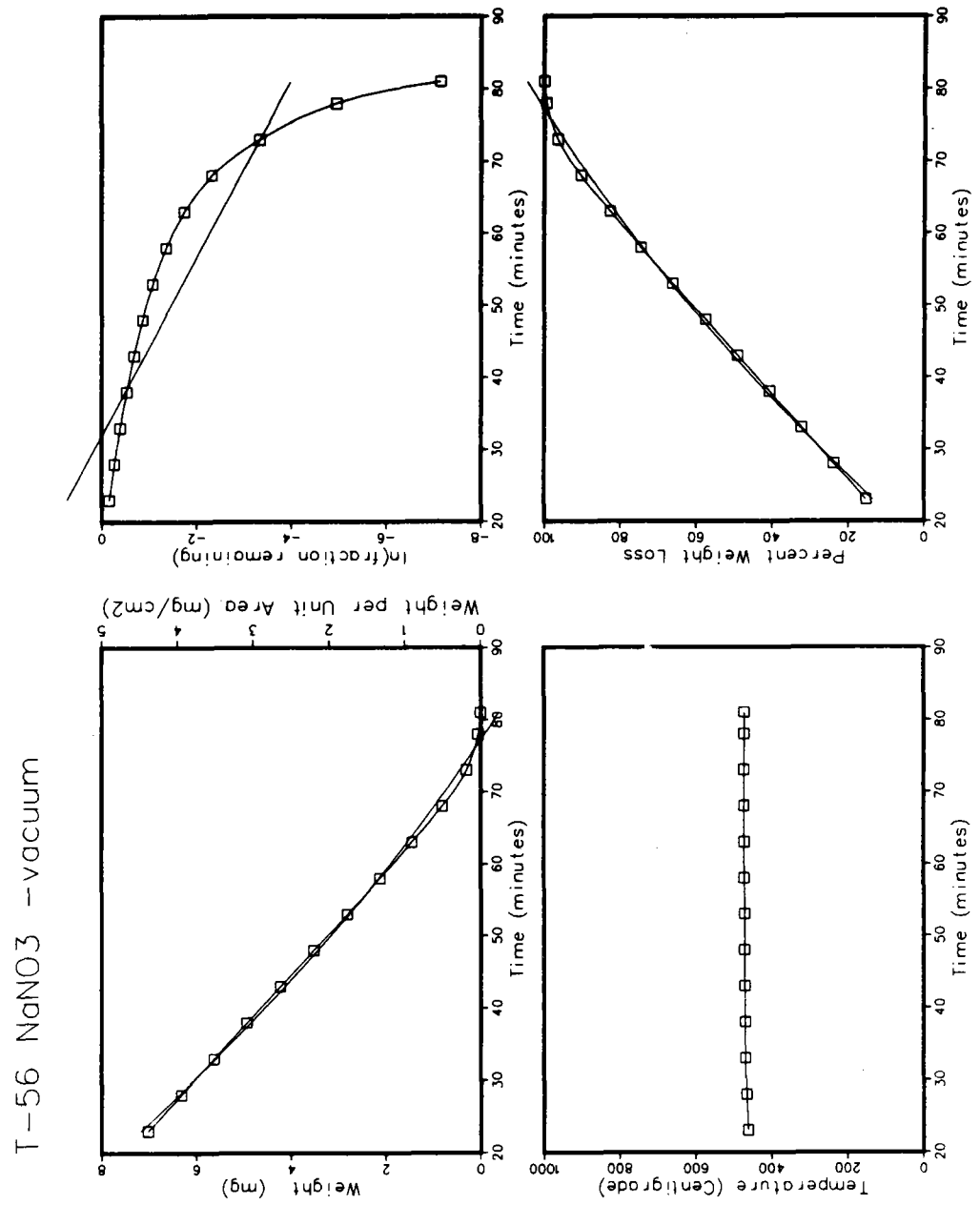
T-56 NaNO3 -vacuum
Weight (mg)
Time (minutes)
Weight per Unit Area (mg/cm2)
ln(fraction remaining)
Time (minutes)
Percent Weight Loss
Time (minutes)
Temperature (Centigrade)
Time (minutes)

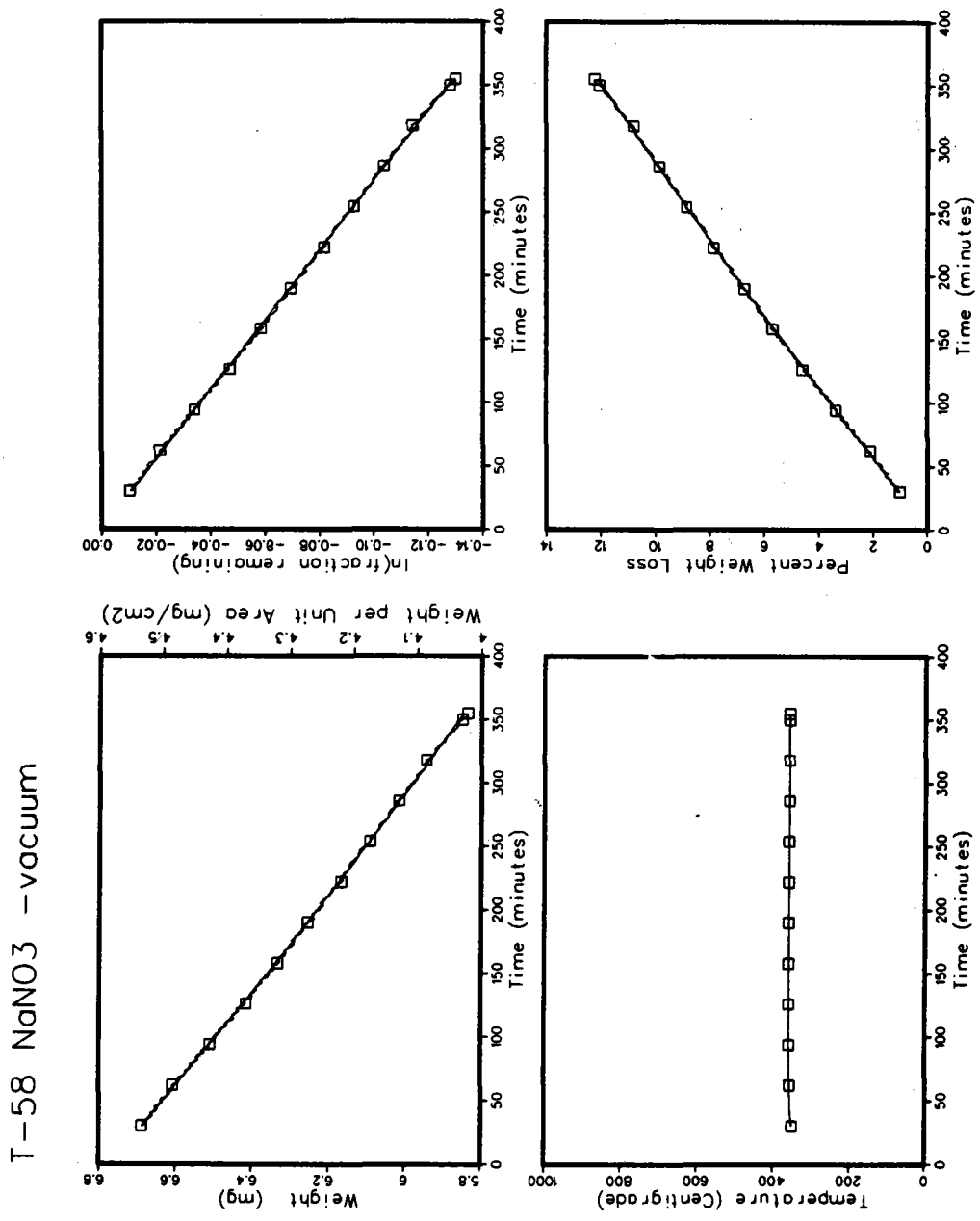
T-58 NaNO3 -vacuum
Weight (mg)
Time (minutes)
Weight per Unit Area (mg/cm2)
ln(fraction remaining)
Percent Weight Loss
Temperature (Centigrade)

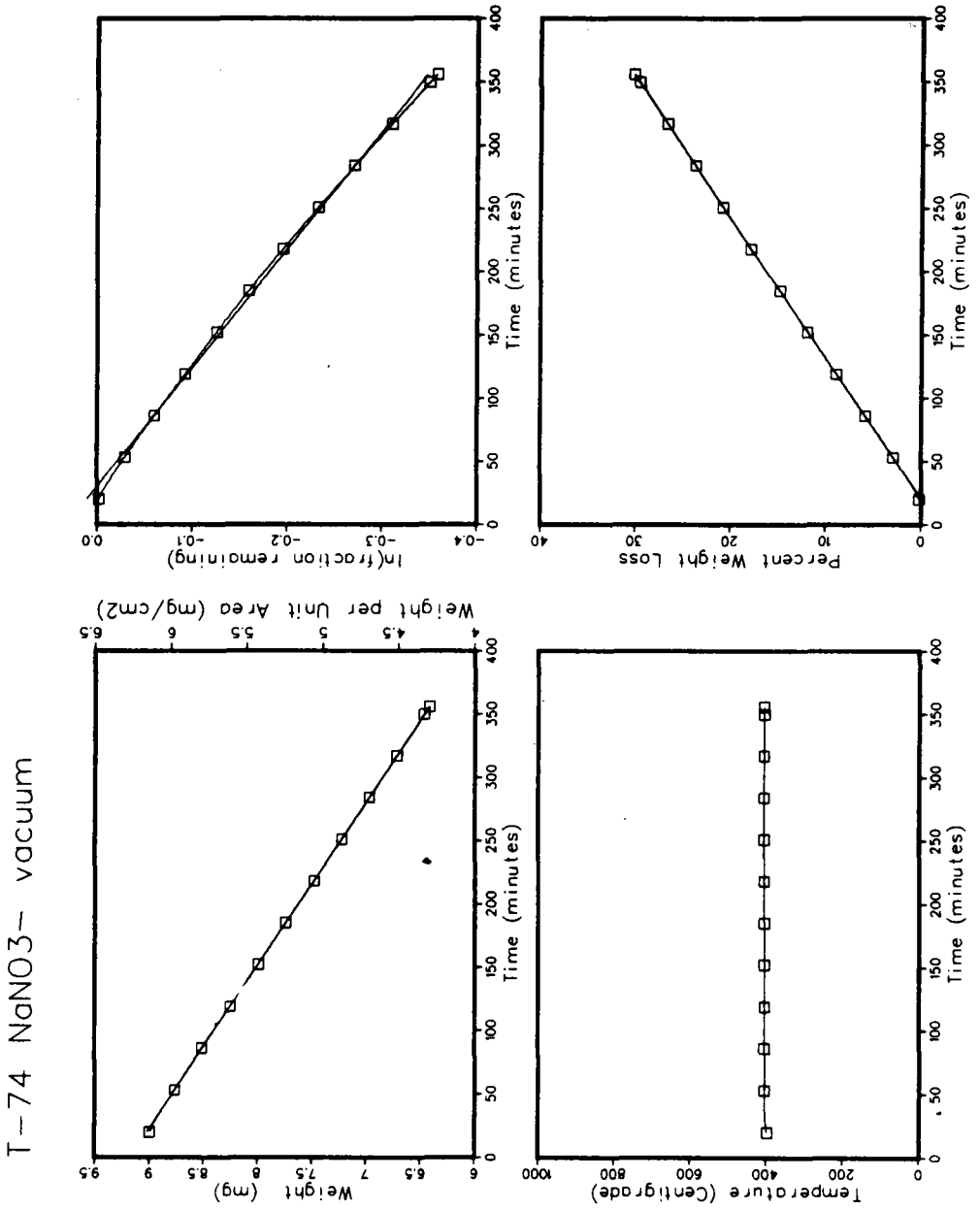
T-74 NaNO3- vacuum
Weight (mg)
Time (minutes)
Weight per Unit Area (mg/cm2)
ln(fraction remaining)
Percent Weight Loss
Temperature (Centigrade)

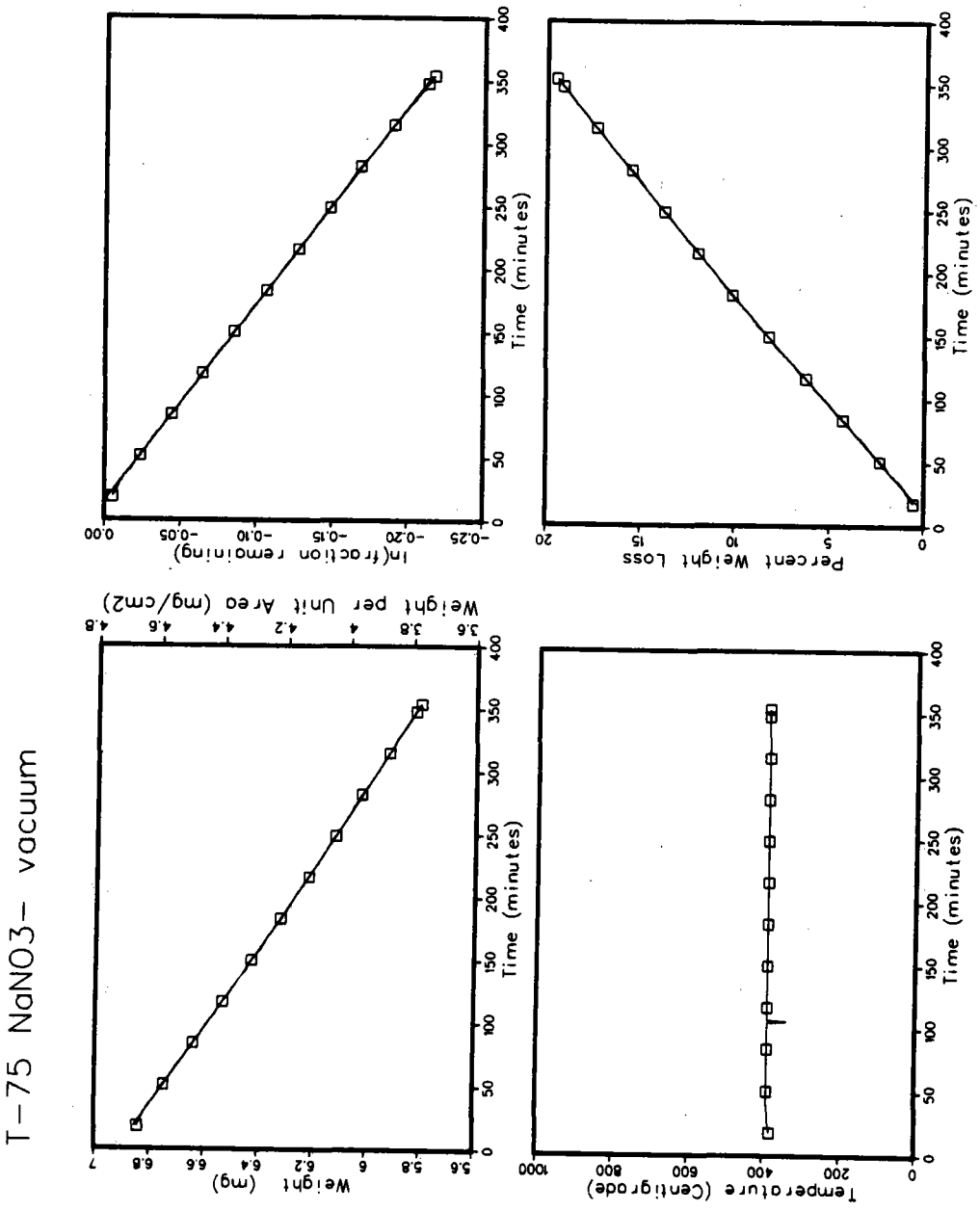
T-75 NaNO3- vacuum
Weight (mg)
Time (minutes)
Weight per Unit Area (mg/cm2)
ln(fraction remaining)
Percent Weight Loss
Temperature (Centigrade)

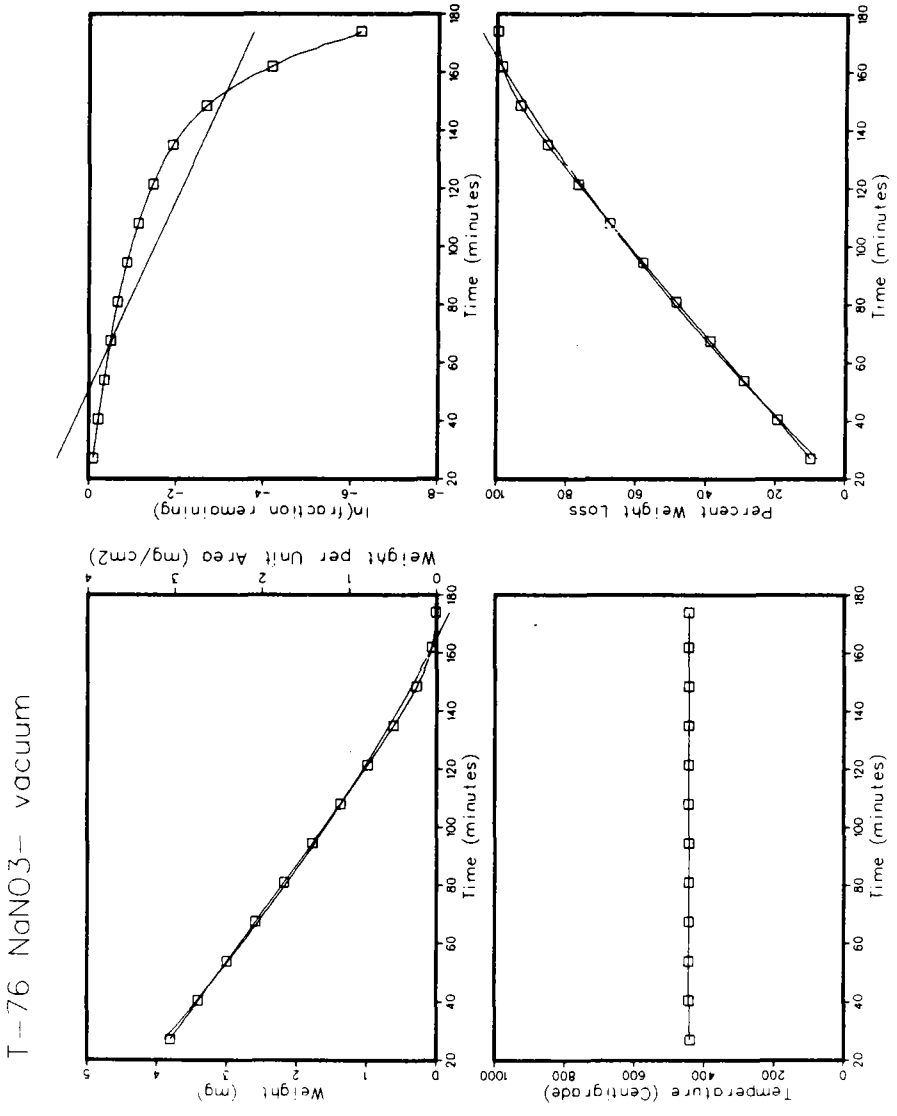
T-76 NaNO3- vacuum
Weight (mg)
Weight per Unit Area (mg/cm2)
Time (minutes)
Temperature (Centigrade)
Time (minutes)
Percent Weight Loss
Time (minutes)
ln(fraction remaining)
Time (minutes)

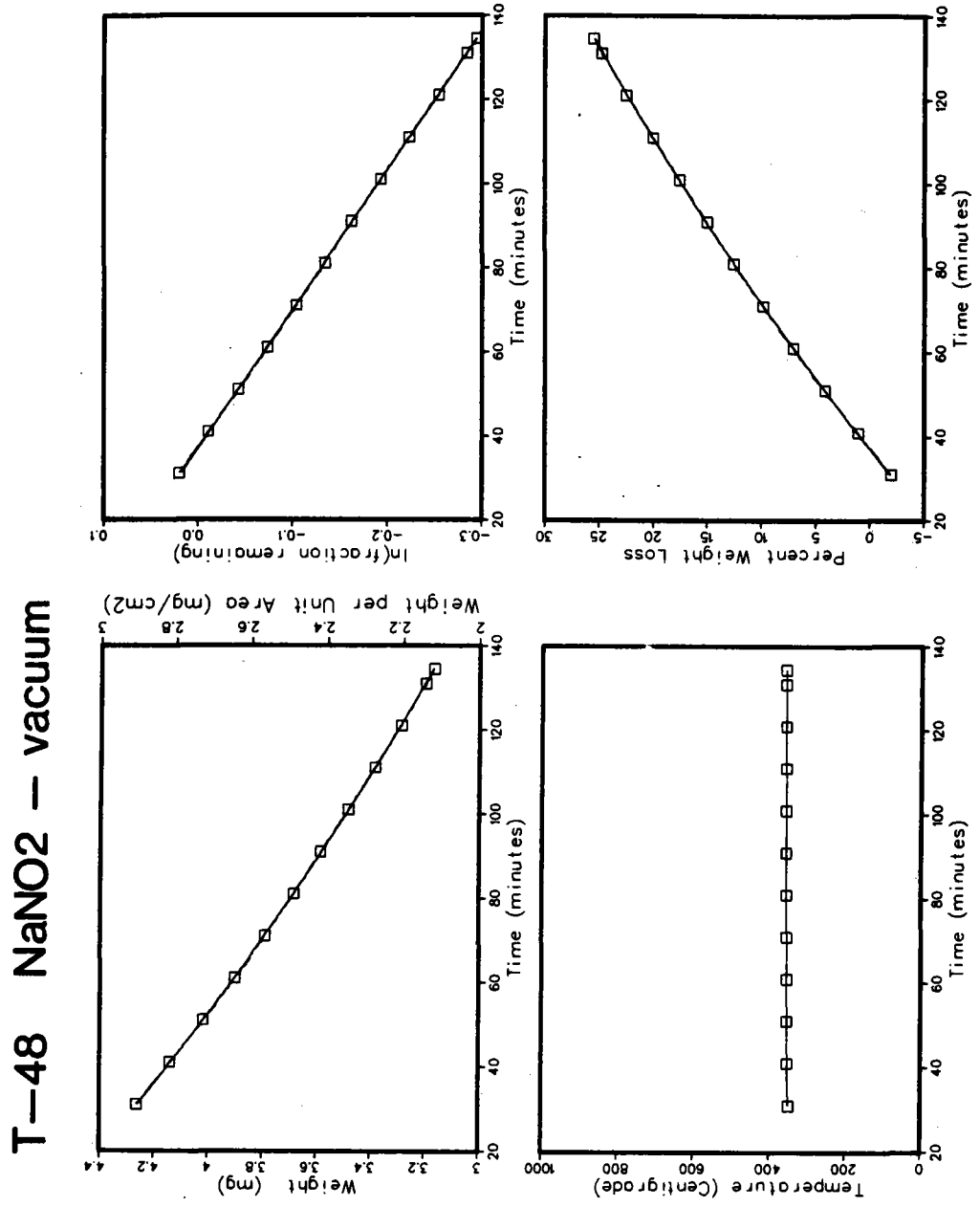
T−48 NaNO2 − vacuum
Weight (mg)
Weight per Unit Area (mg/cm2)
Time (minutes)
ln(fraction remaining)
Percent Weight Loss
Temperature (Centigrade)

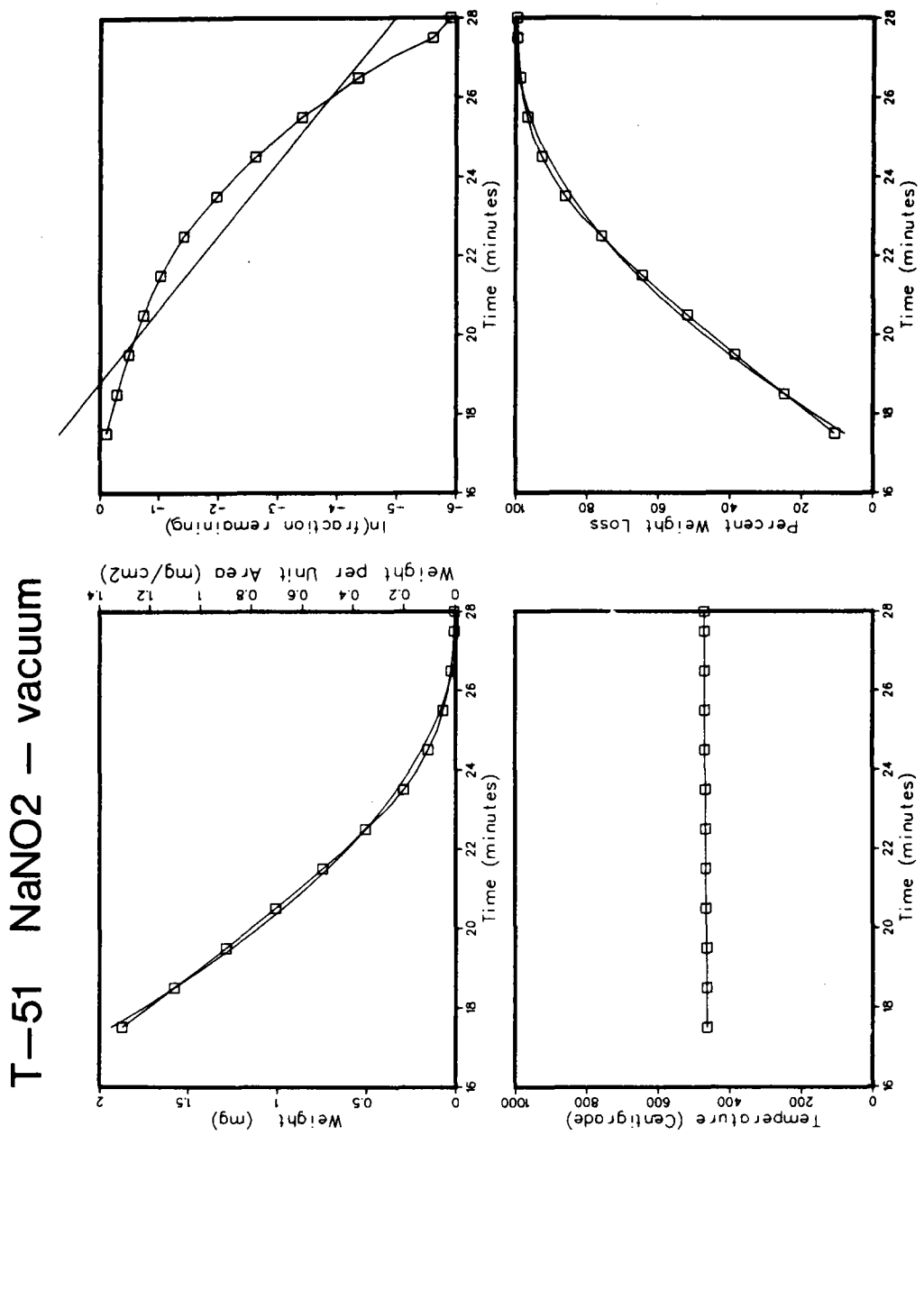
T−51 NaNO2 − vacuum
Weight (mg)
Time (minutes)
Weight per Unit Area (mg/cm2)
ln(fraction remaining)
Percent Weight Loss
Temperature (Centigrade)

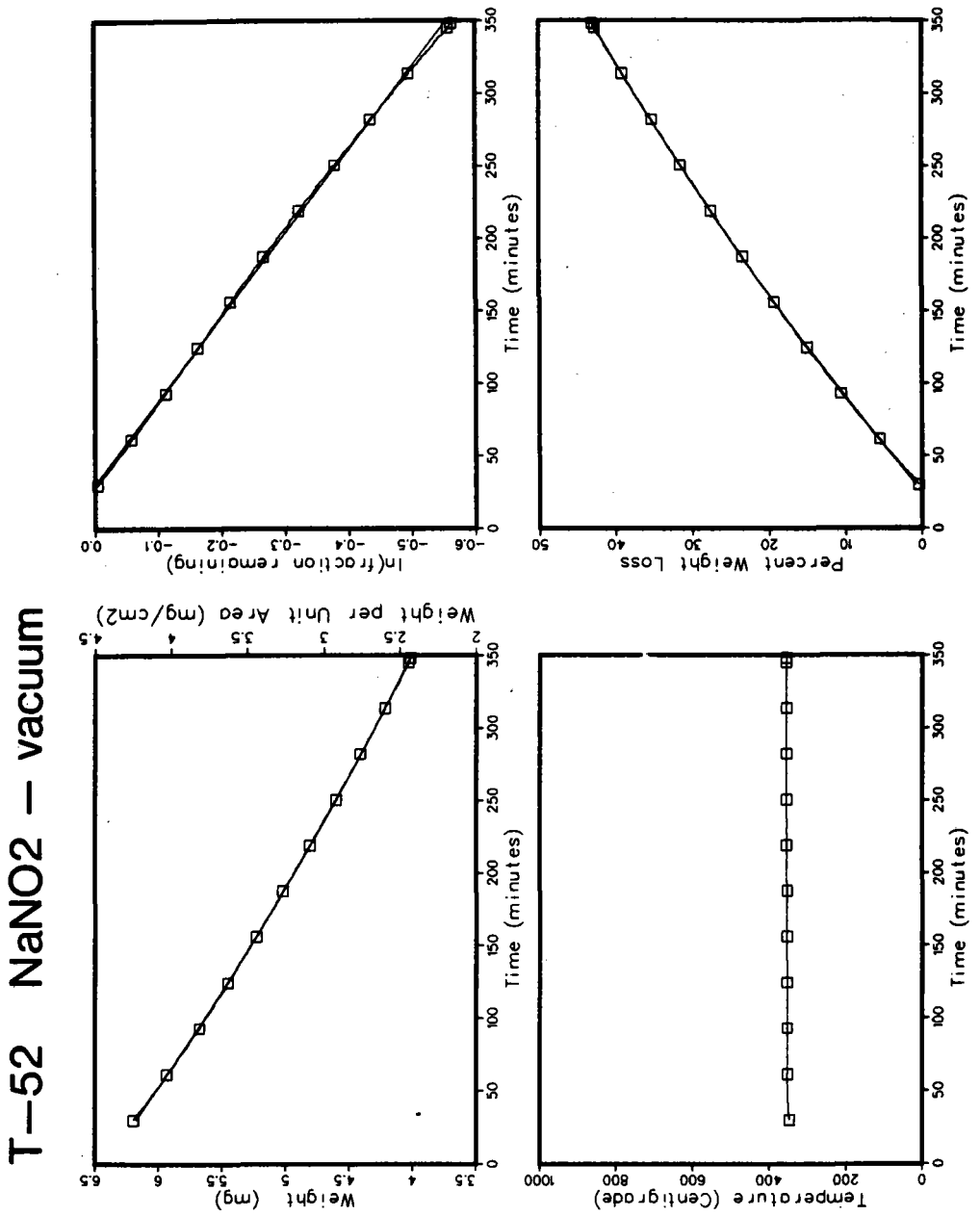
T–52 NaNO2 – vacuum
Weight (mg)
Time (minutes)
Weight per Unit Area (mg/cm2)
ln(fraction remaining)
Percent Weight Loss
Temperature (Centigrade)

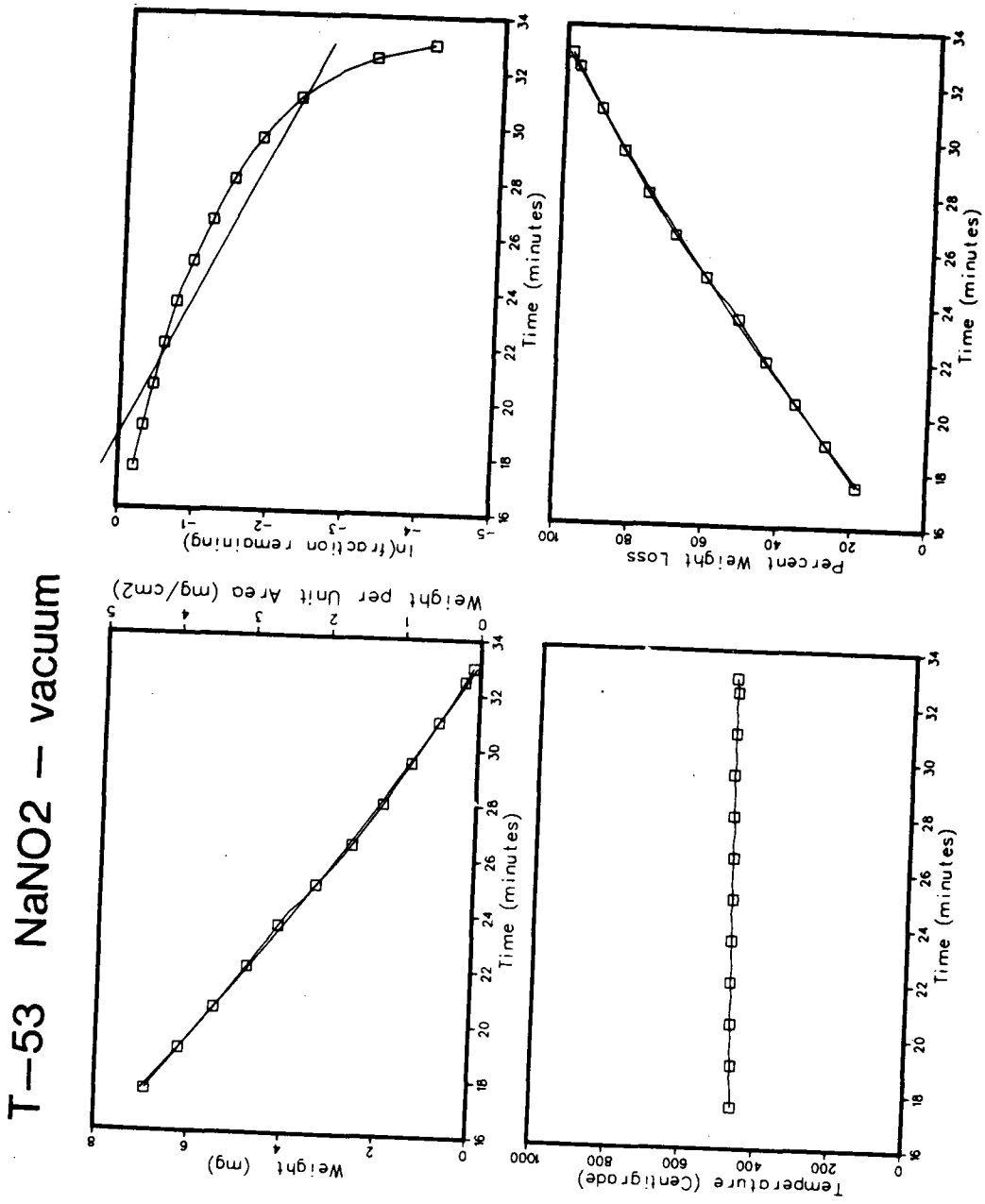
T-53 NaNO2 - vacuum
Weight (mg)
Time (minutes)
Weight per Unit Area (mg/cm2)
ln(fraction remaining)
Percent Weight Loss
Temperature (Centigrade)

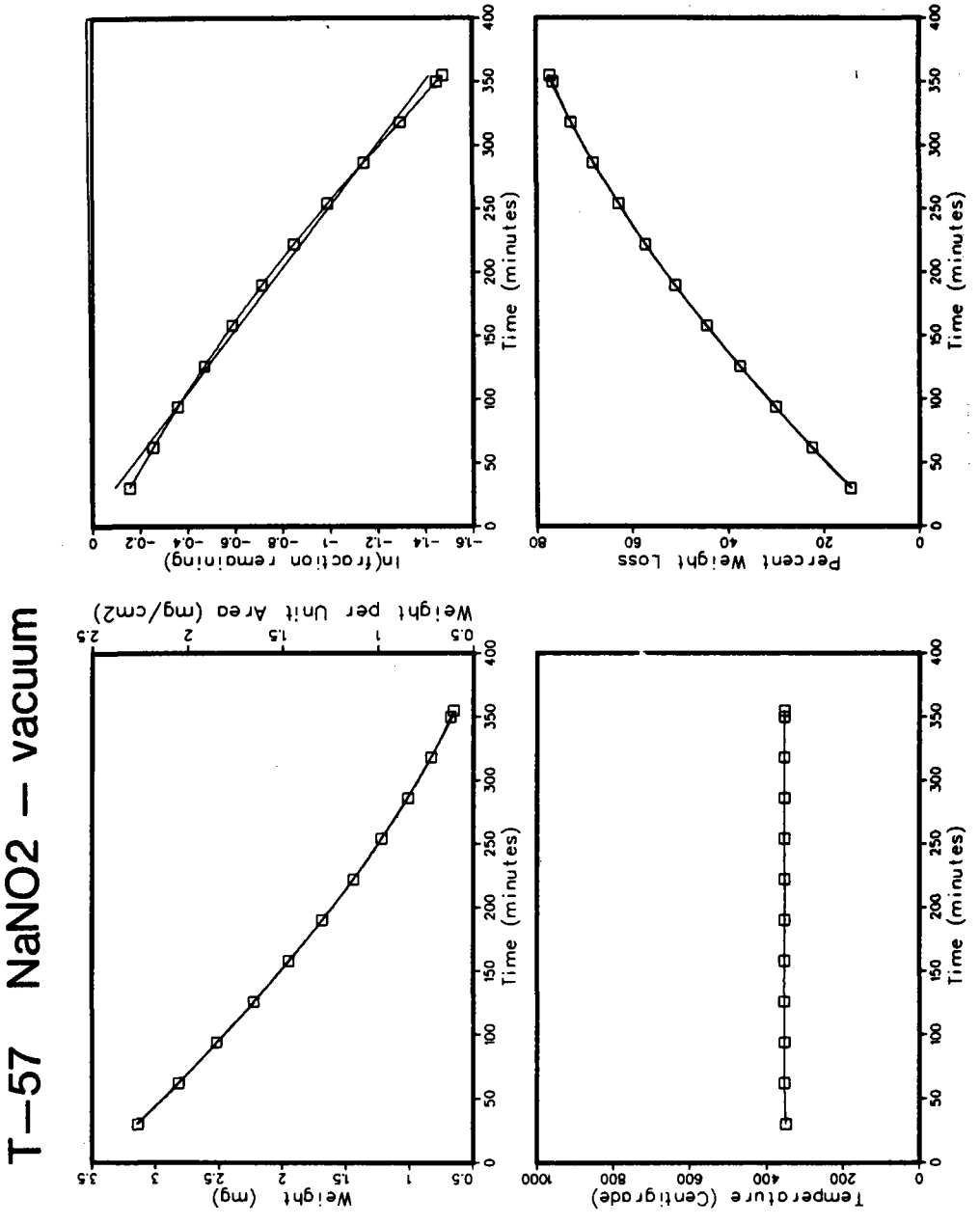
T—57 NaNO2 — vacuum
Weight (mg)
Time (minutes)
Weight per Unit Area (mg/cm2)
ln(fraction remaining)
Percent Weight Loss
Temperature (Centigrade)

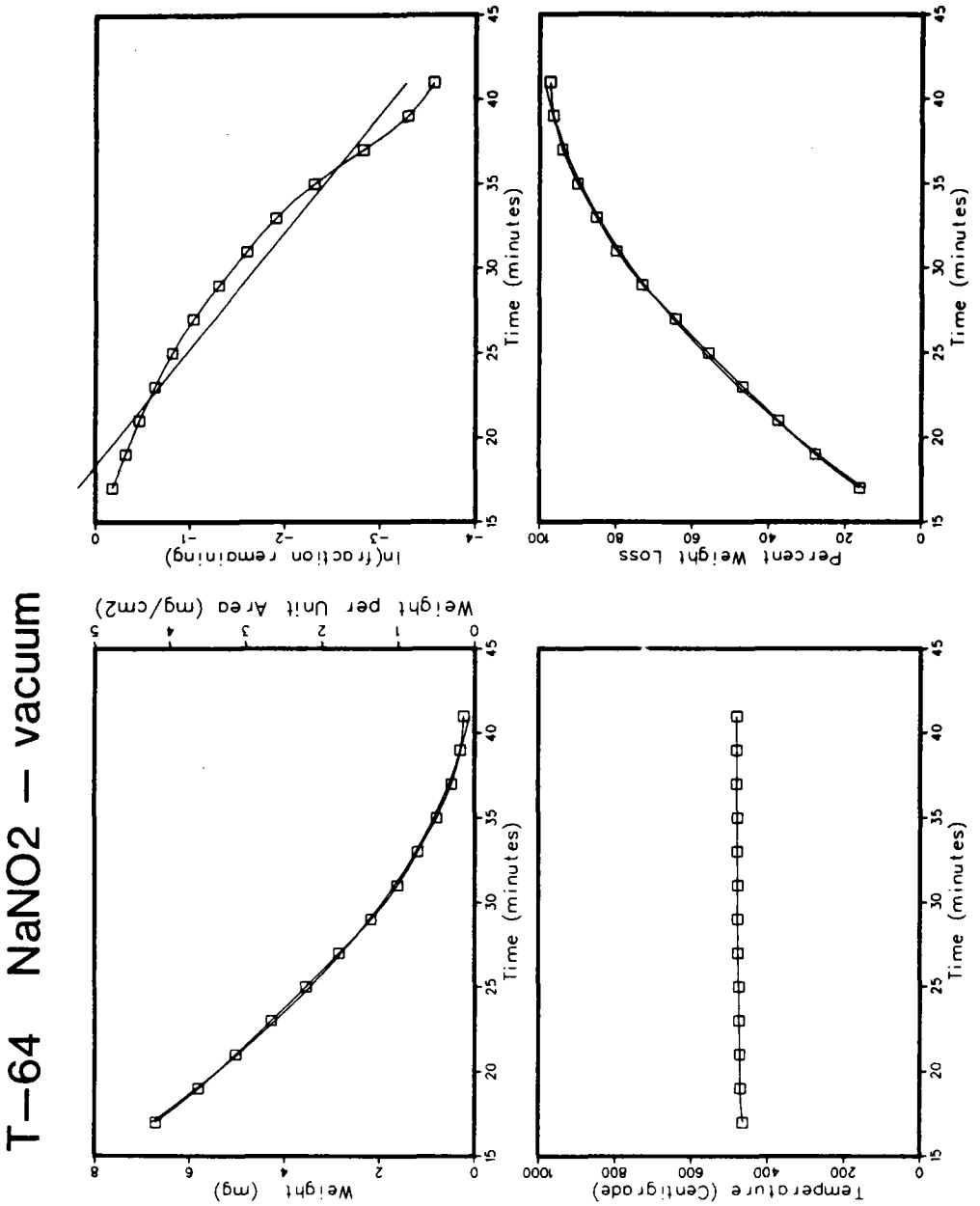
T−64 NaNO2 − vacuum
Weight (mg)
Weight per Unit Area (mg/cm2)
Time (minutes)
Temperature (Centigrade)
Percent Weight Loss
ln(fraction remaining)

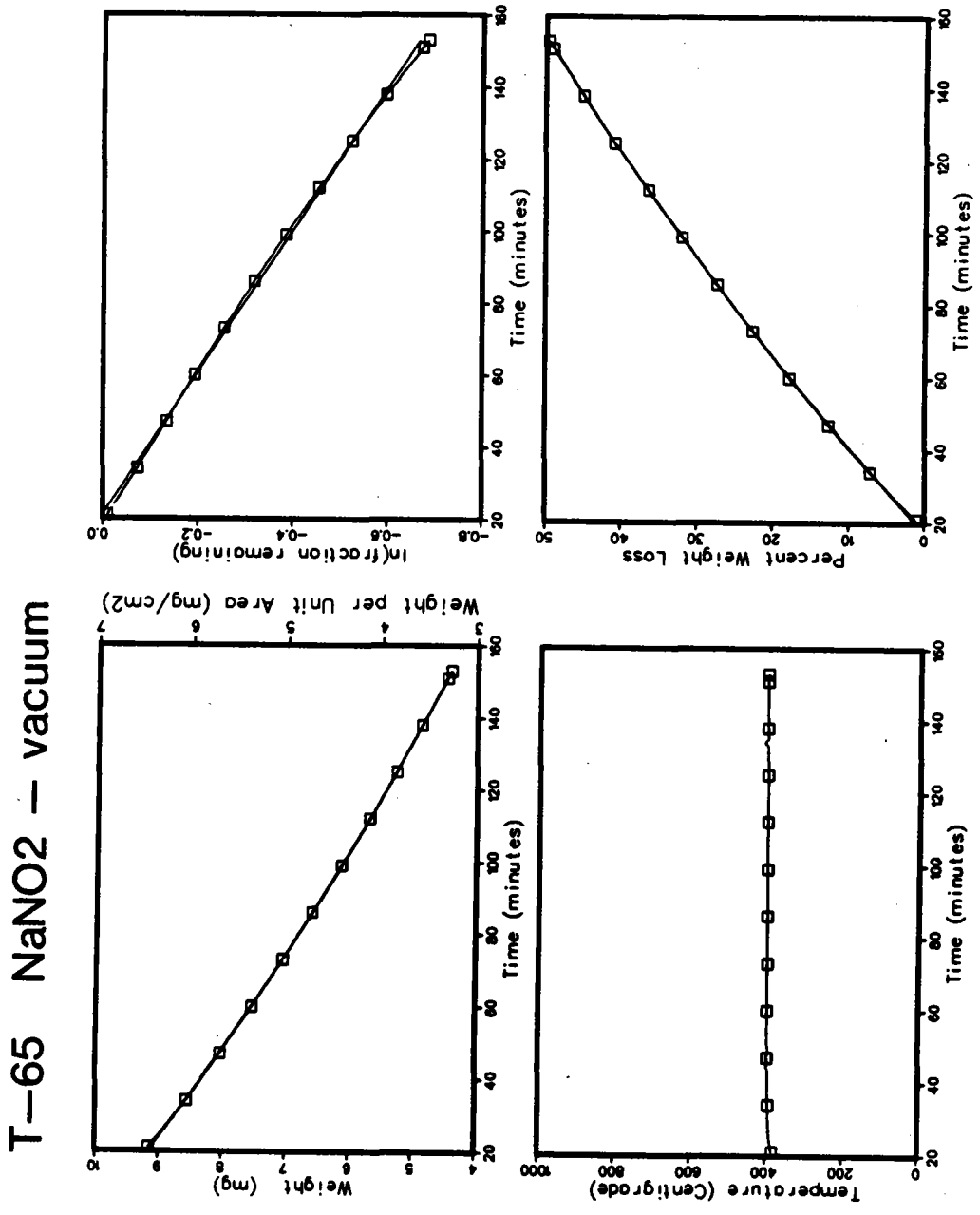
T—65 NaNO2 — vacuum
Temperature (Centigrade)
Time (minutes)
Weight (mg)
Time (minutes)
Weight per Unit Area (mg/cm2)
Percent Weight Loss
Time (minutes)
ln(fraction remaining)
Time (minutes)

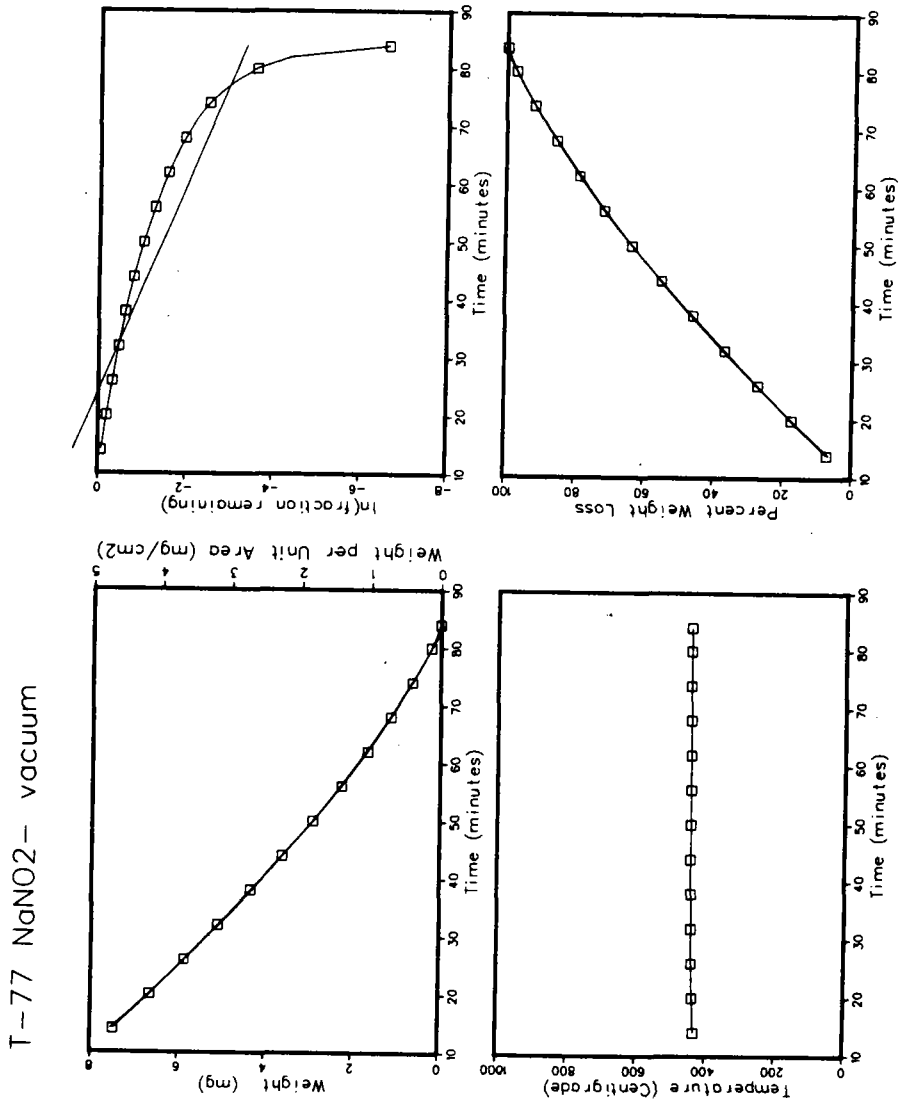
T-77 NaNO2- vacuum
Weight (mg)
Time (minutes)
Weight per Unit Area (mg/cm2)
ln(fraction remaining)
Percent Weight Loss
Temperature (Centigrade)

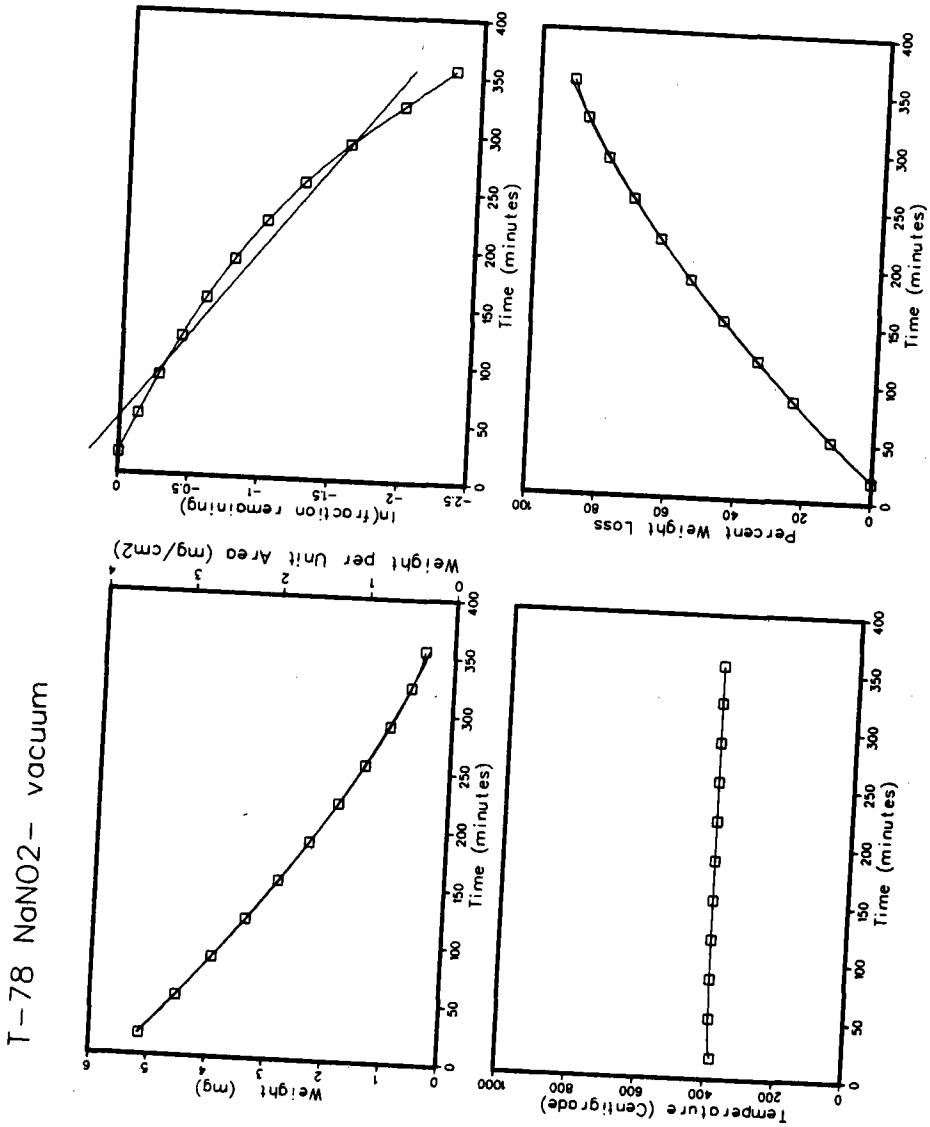
T-78 NaNO2- vacuum
Weight (mg)
Time (minutes)
Temperature (Centigrade)
Time (minutes)
Percent Weight Loss
Time (minutes)
ln(fraction remaining)
Time (minutes)
Weight per Unit Area (mg/cm2)

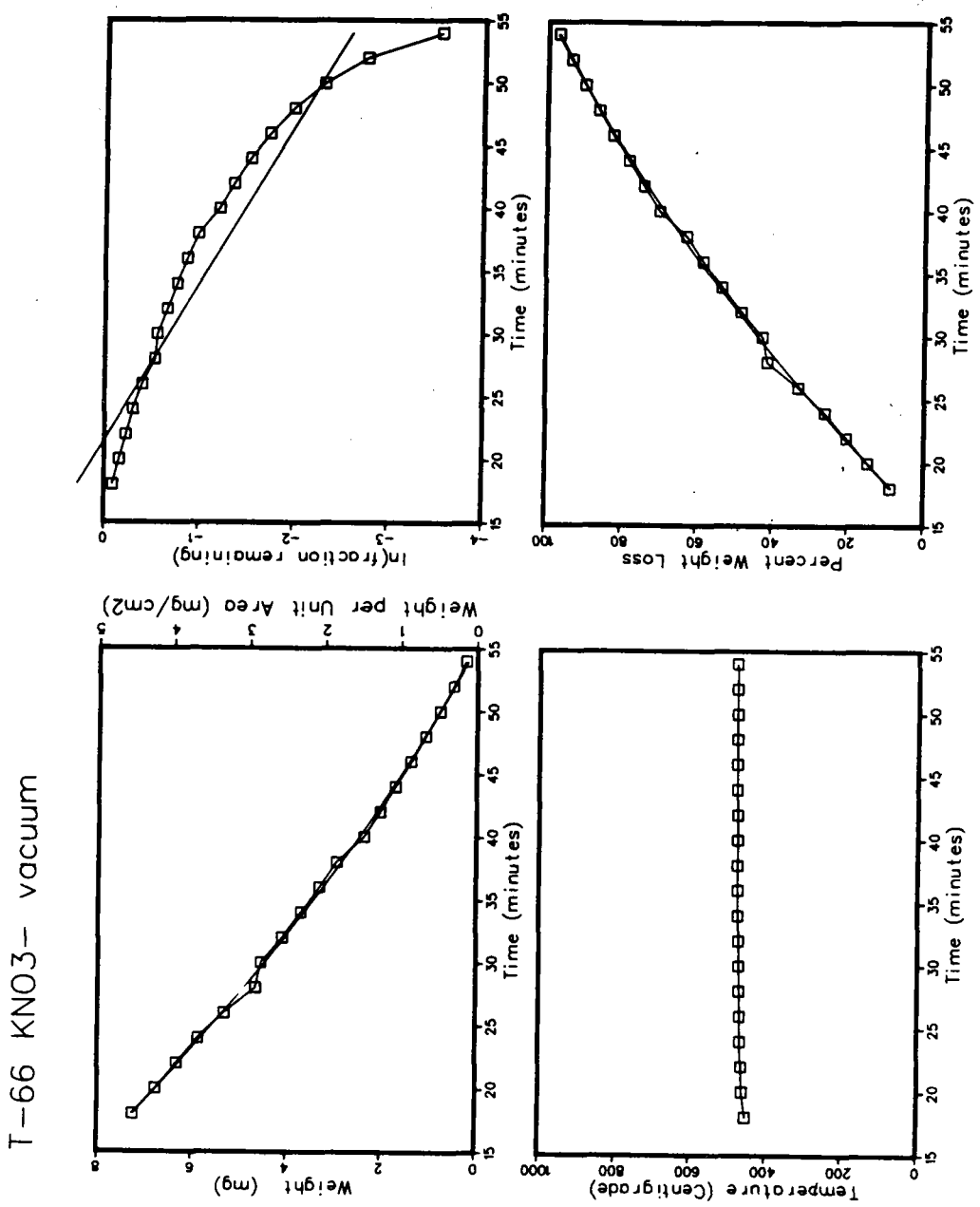
T-66 KNO3- vacuum
Weight (mg)
Time (minutes)
Weight per Unit Area (mg/cm2)
ln(fraction remaining)
Percent Weight Loss
Temperature (Centigrade)

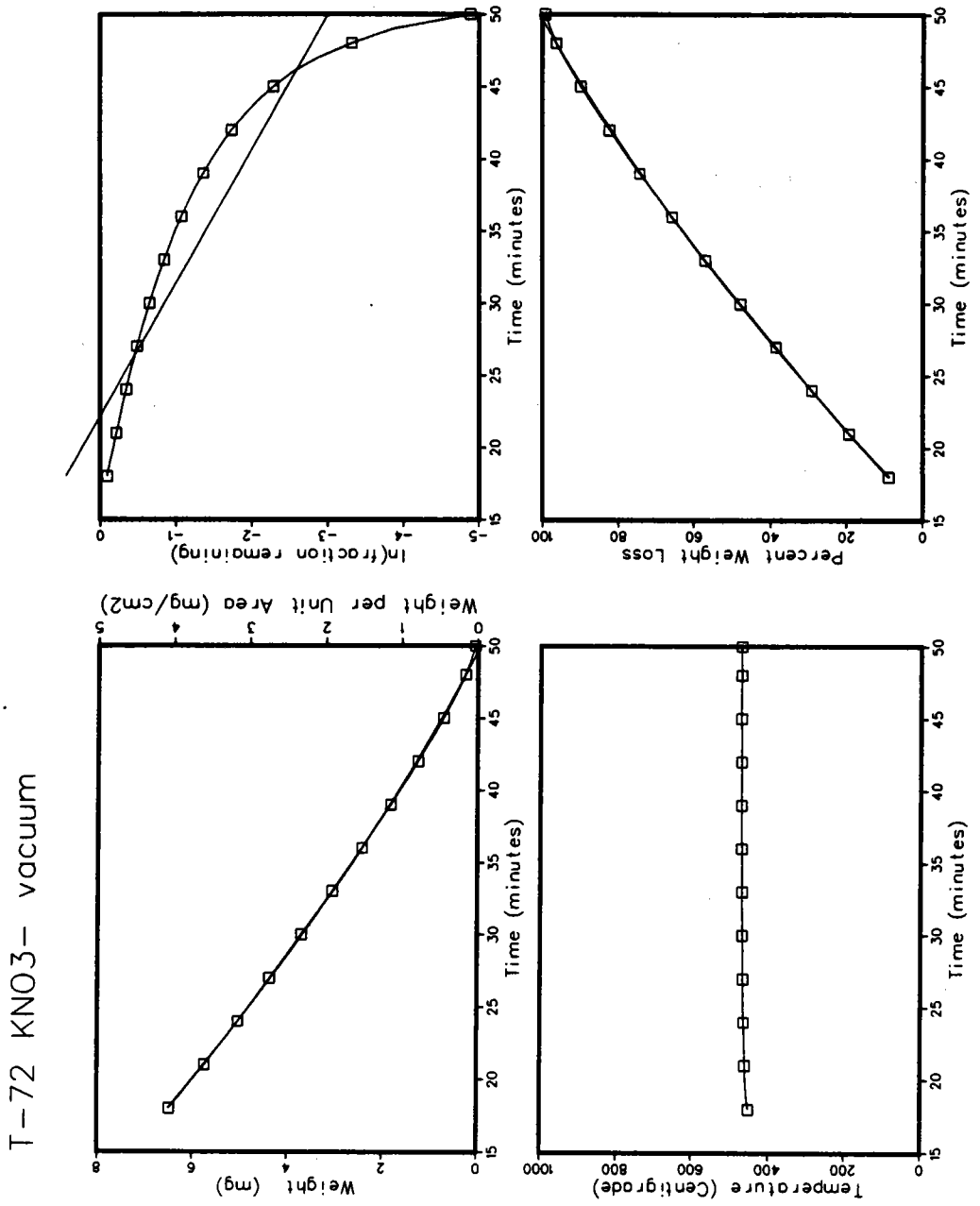
T-72 KNO3- vacuum
Weight (mg)
Time (minutes)
Weight per Unit Area (mg/cm2)
Temperature (Centigrade)
Time (minutes)
Percent Weight Loss
Time (minutes)
ln(fraction remaining)
Time (minutes)

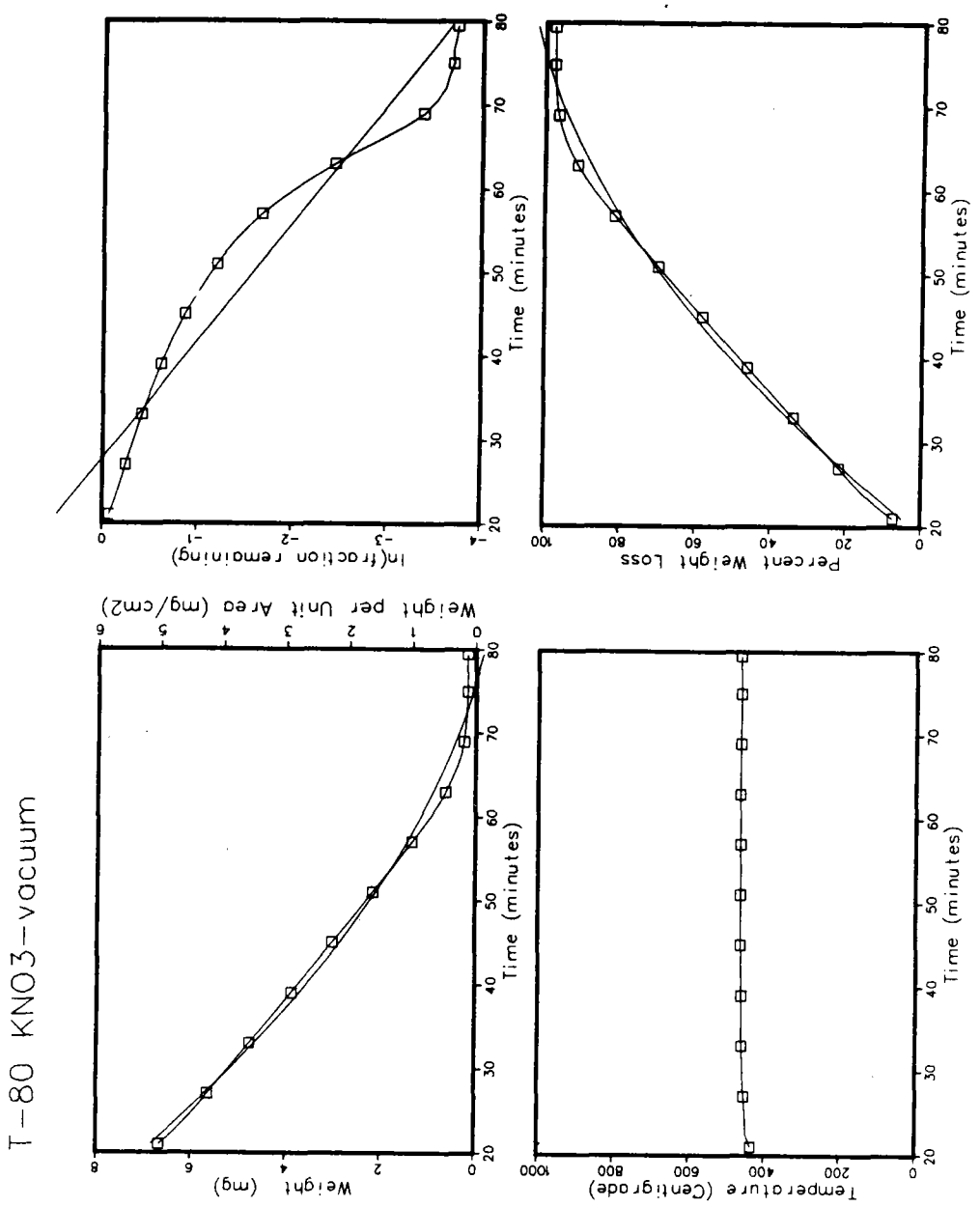
T-80 KNO3-vacuum
Weight (mg)
Time (minutes)
Weight per Unit Area (mg/cm2)
Temperature (Centigrade)
Percent Weight Loss
ln(fraction remaining)

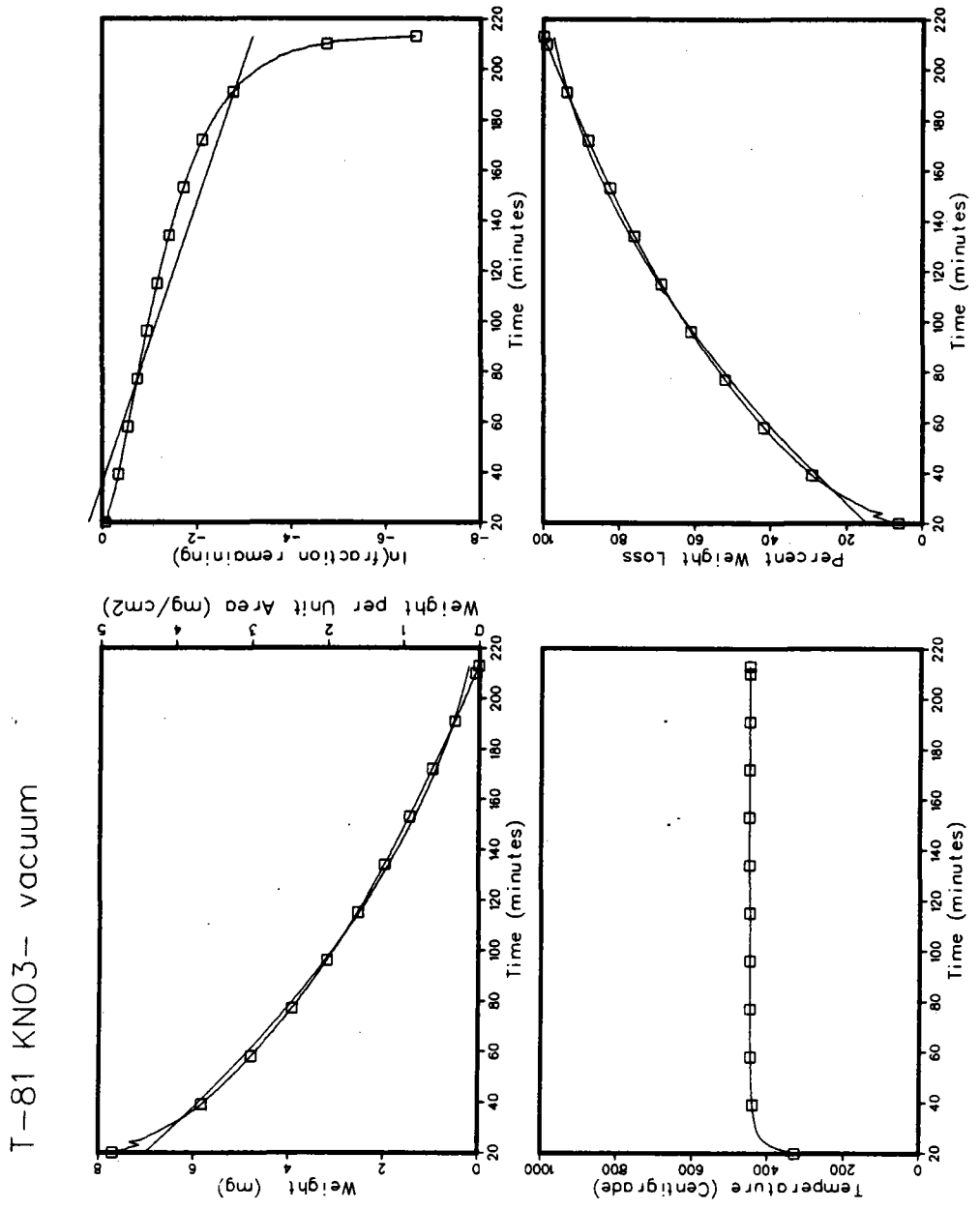
T-81 KNO3- vacuum
Weight (mg)
Time (minutes)
Weight per Unit Area (mg/cm2)
ln(fraction remaining)
Percent Weight Loss
Temperature (Centigrade)

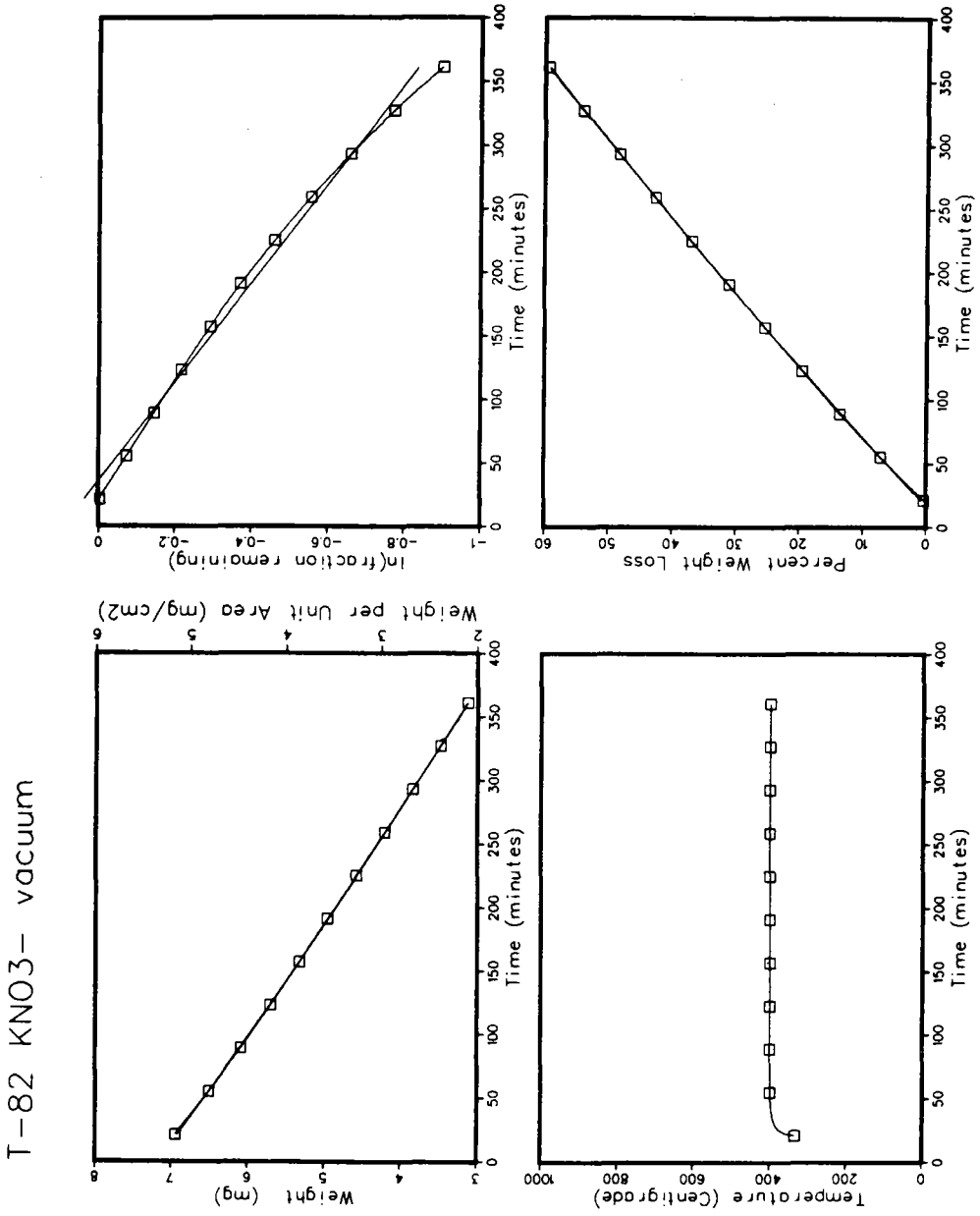
T-82 KNO3- vacuum
Weight (mg)
Time (minutes)
Weight per Unit Area (mg/cm2)
ln(fraction remaining)
Percent Weight Loss
Temperature (Centigrade)

T-83 KNO3 -vacuum

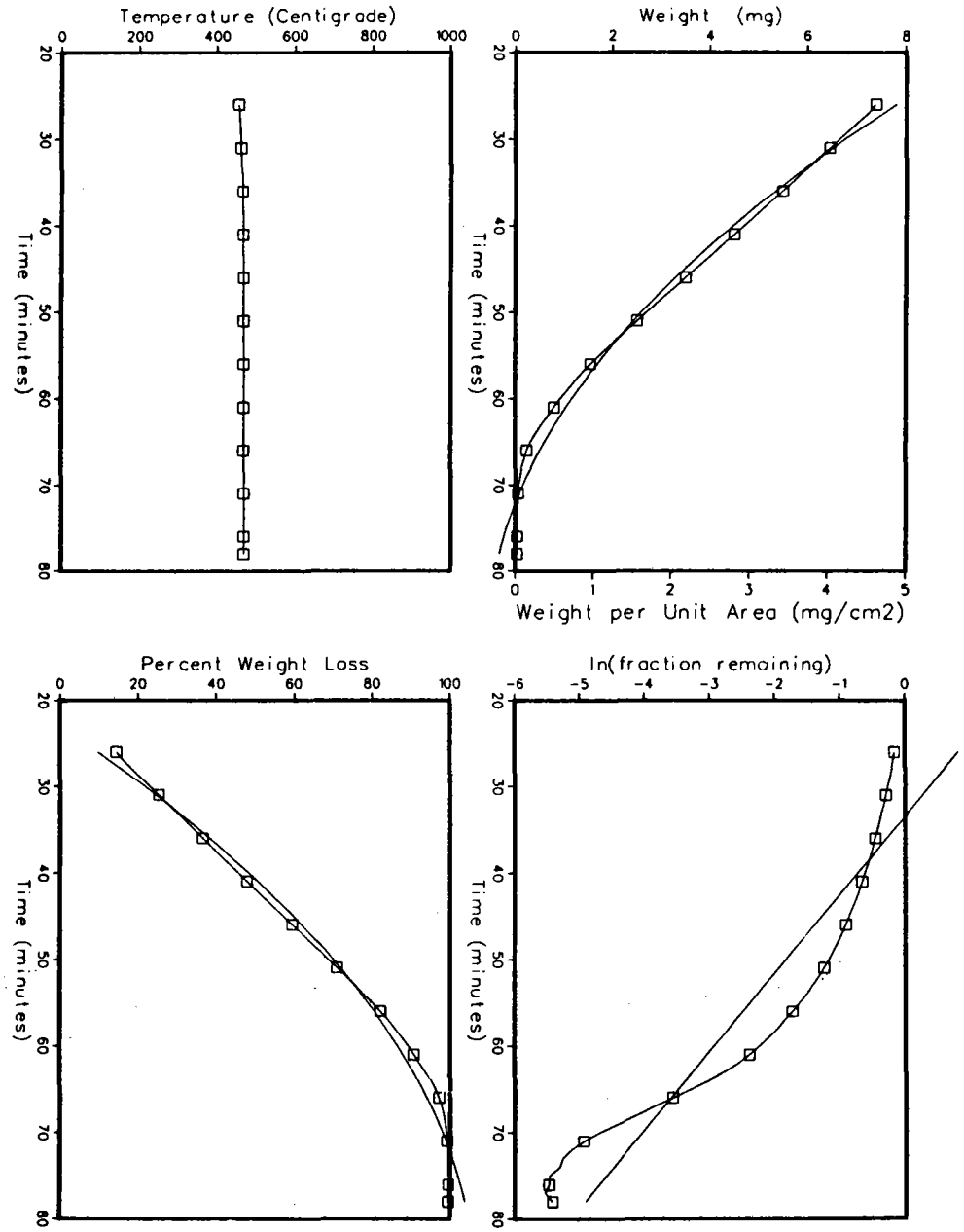

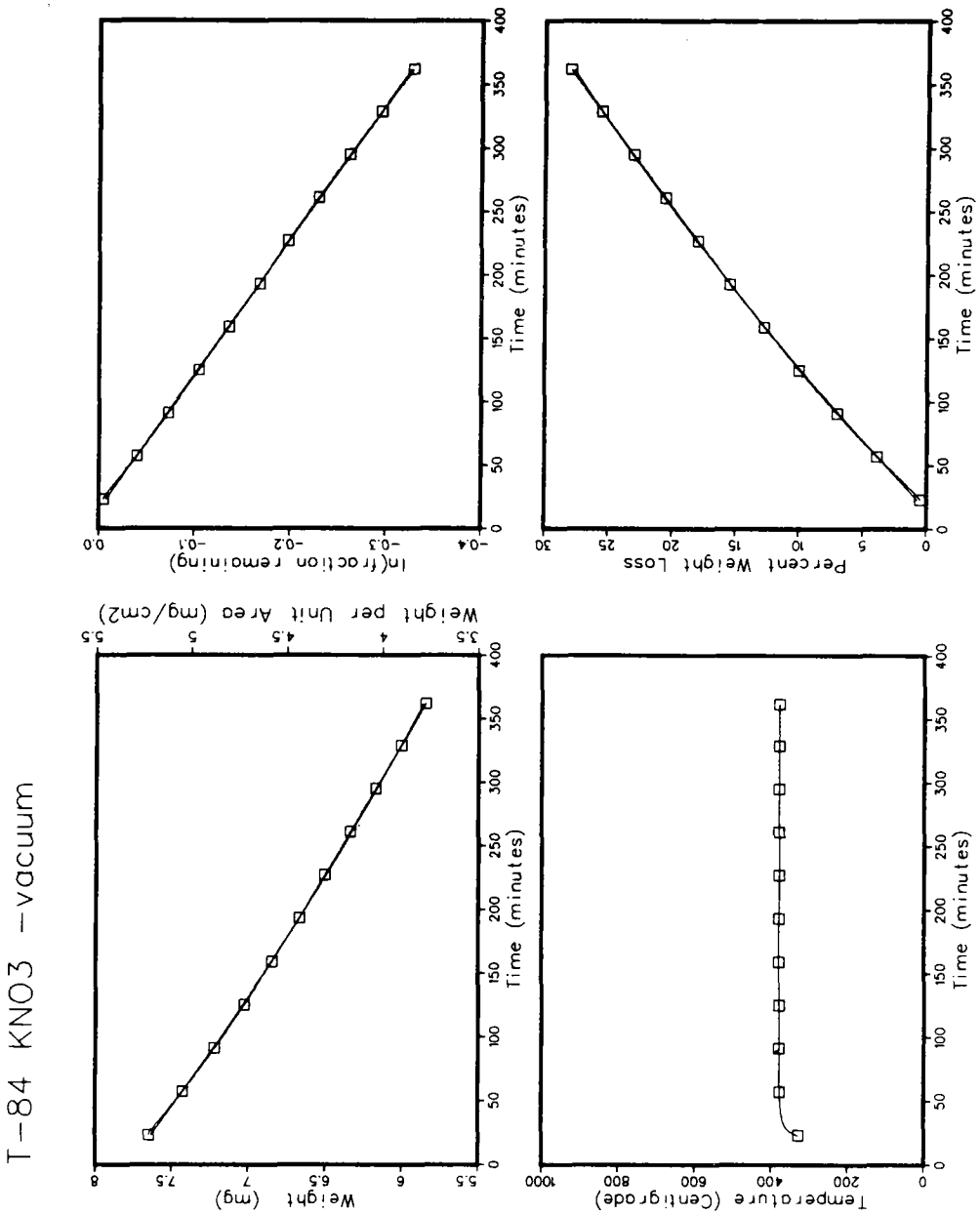
T-84 KNO3 -vacuum
Weight (mg)
Time (minutes)
Weight per Unit Area (mg/cm2)
ln(fraction remaining)
Percent Weight Loss
Temperature (Centigrade)

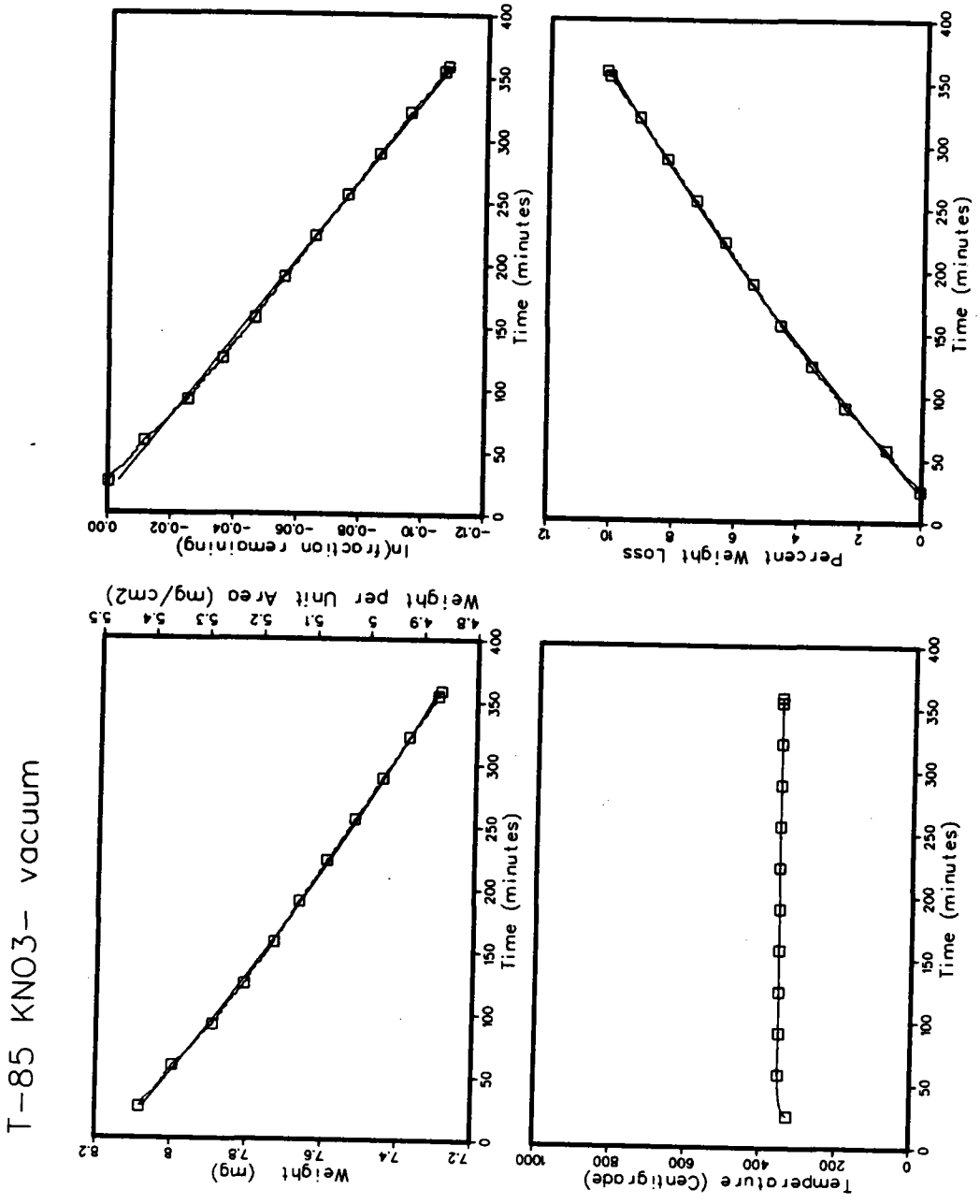
T-85 KNO3- vacuum
Temperature (Centigrade)
Time (minutes)
Weight (mg)
Time (minutes)
Weight per Unit Area (mg/cm2)
Percent Weight Loss
Time (minutes)
ln(fraction remaining)
Time (minutes)

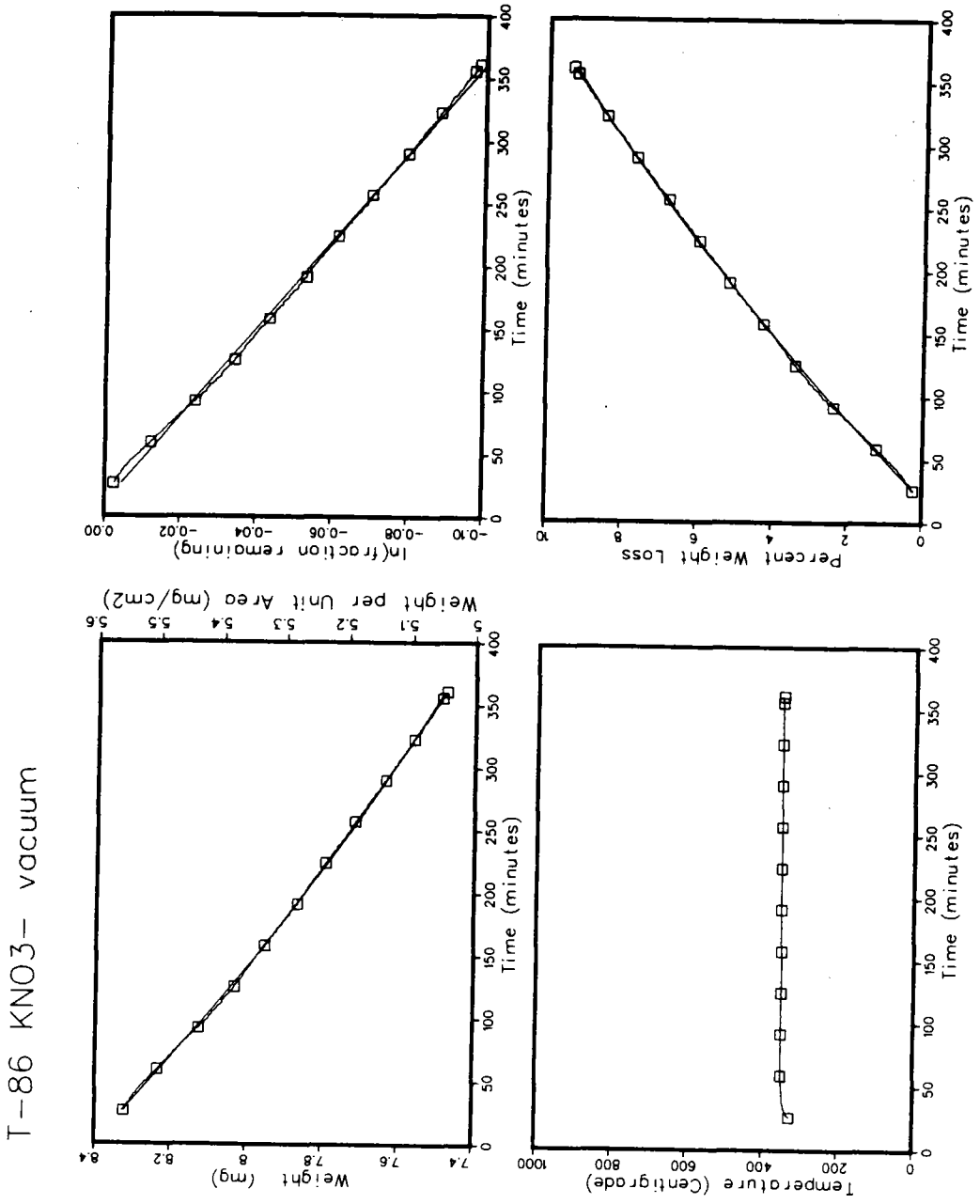
T-86 KNO3- vacuum
Weight (mg)
Time (minutes)
Weight per Unit Area (mg/cm2)
ln(fraction remaining)
Percent Weight Loss
Temperature (Centigrade)

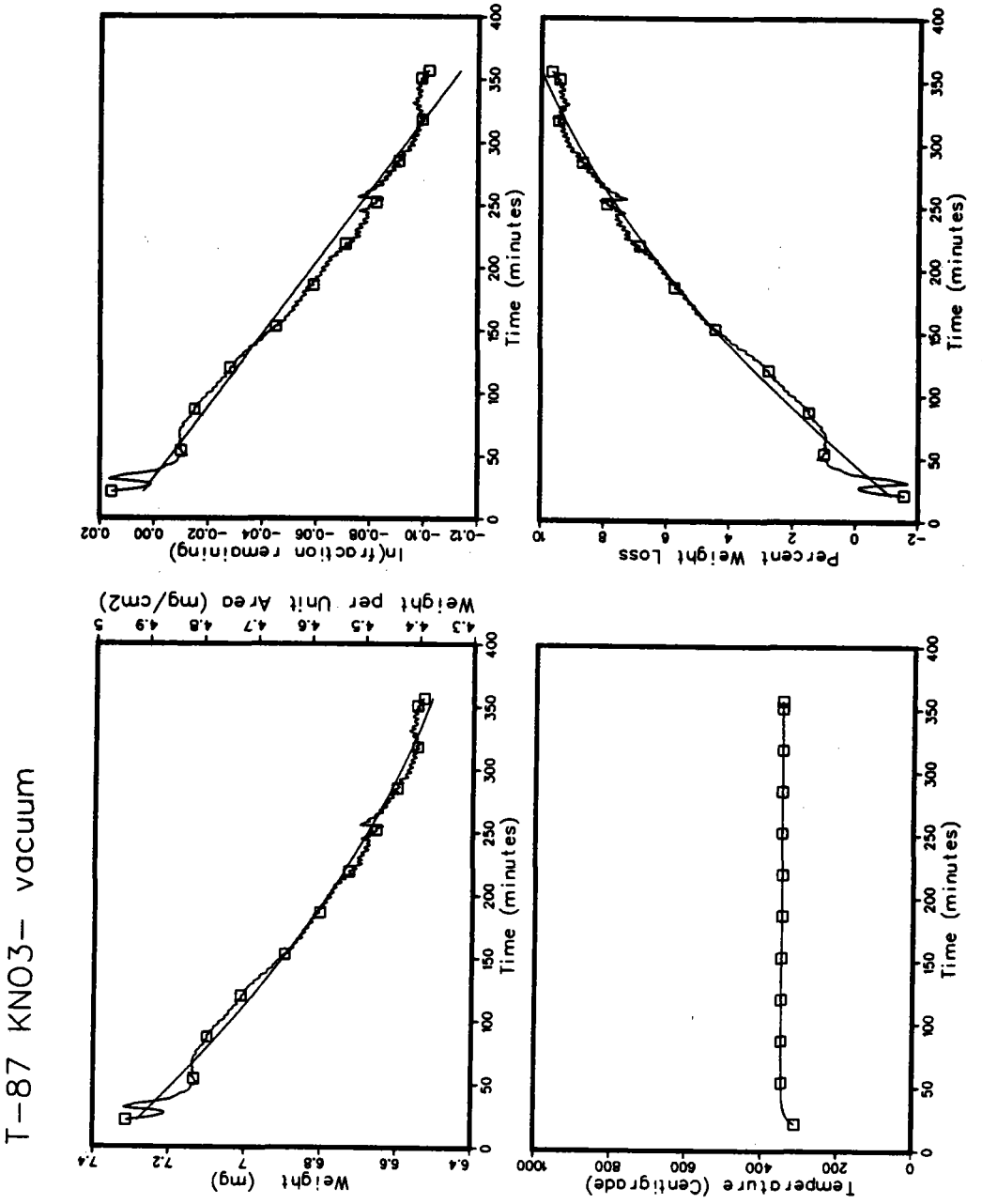
T-87 KNO3- vacuum
Weight (mg)
Weight per Unit Area (mg/cm2)
Time (minutes)
ln(fraction remaining)
Percent Weight Loss
Temperature (Centigrade)

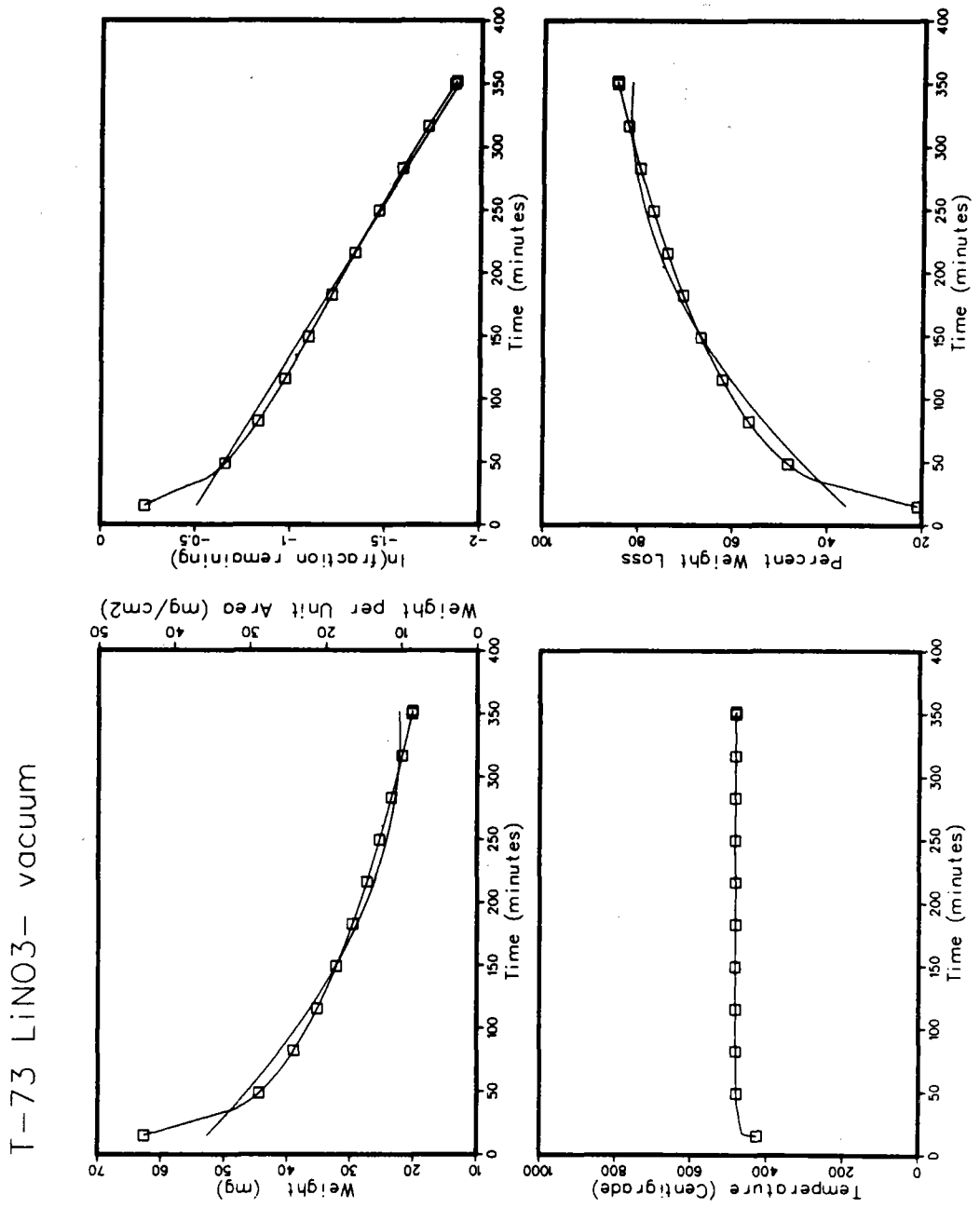
T-73 LiNO3- vacuum
Weight (mg)
Time (minutes)
Weight per Unit Area (mg/cm2)
Temperature (Centigrade)
Percent Weight Loss
ln(fraction remaining)

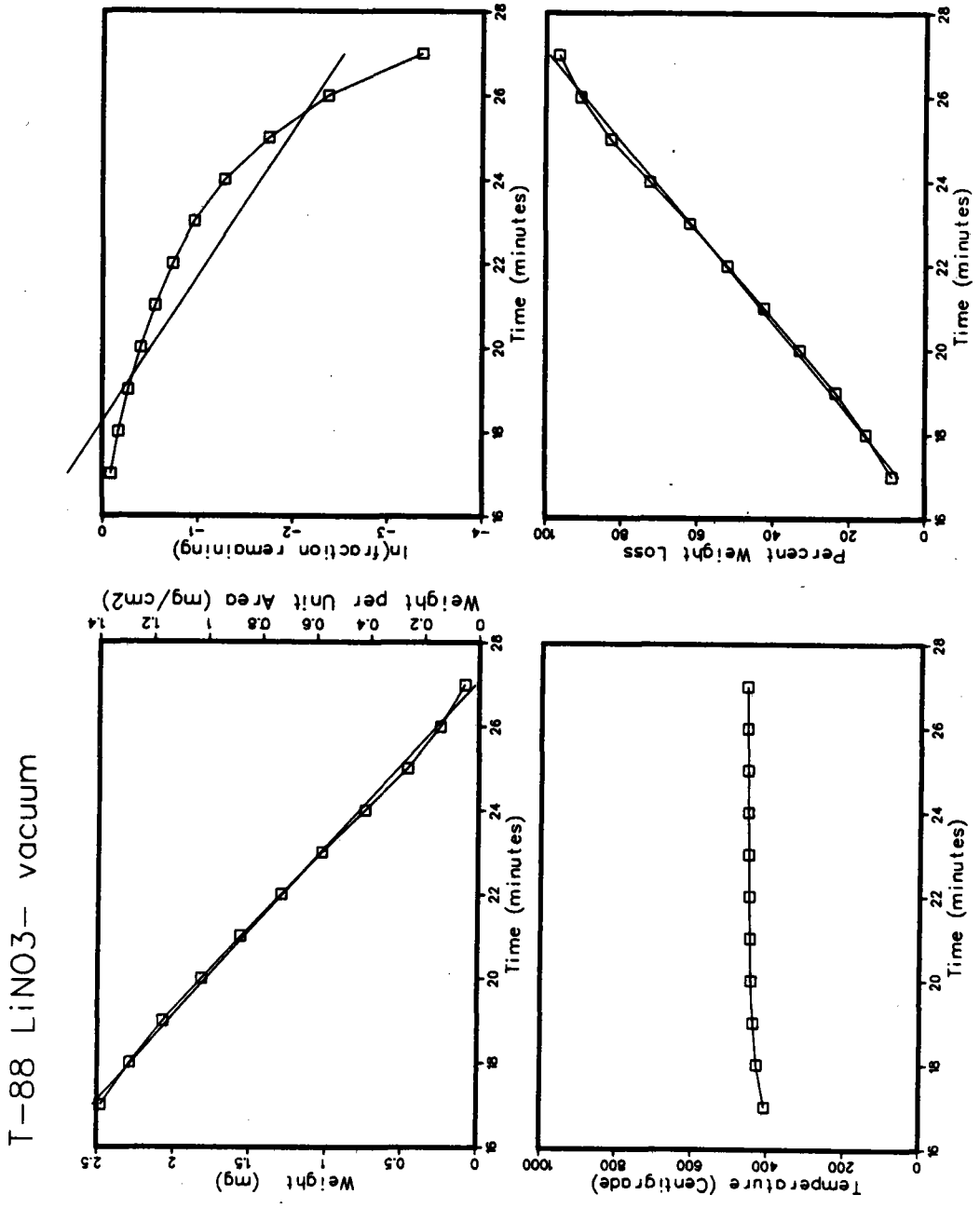
T-88 LiNO3- vacuum
Temperature (Centigrade)
Time (minutes)
Weight (mg)
Weight per Unit Area (mg/cm2)
Time (minutes)
Percent Weight Loss
Time (minutes)
ln(fraction remaining)
Time (minutes)

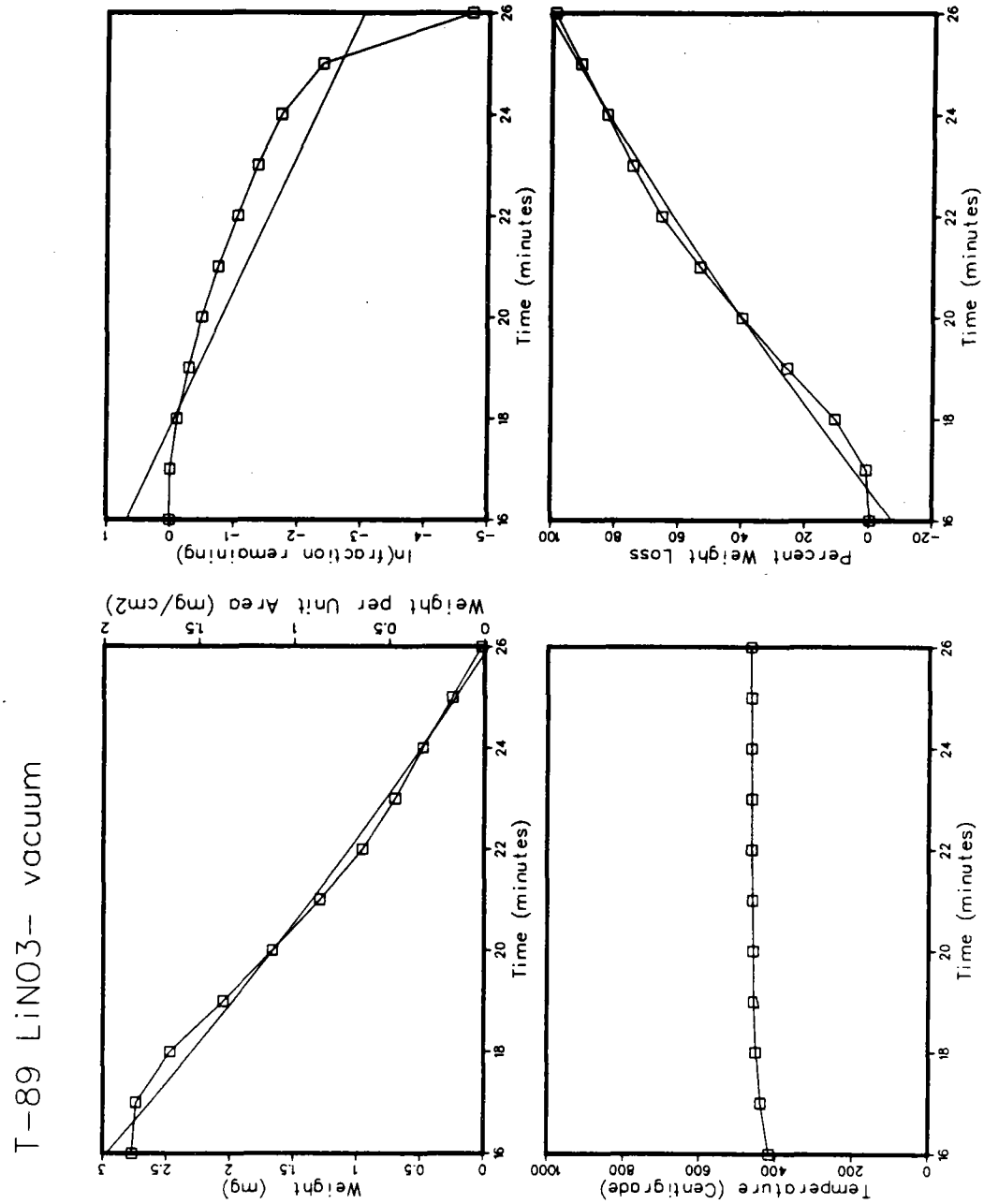
T-89 LiNO3- vacuum
Weight (mg)
Weight per Unit Area (mg/cm2)
Time (minutes)
Temperature (Centigrade)
Percent Weight Loss
ln(fraction remaining)

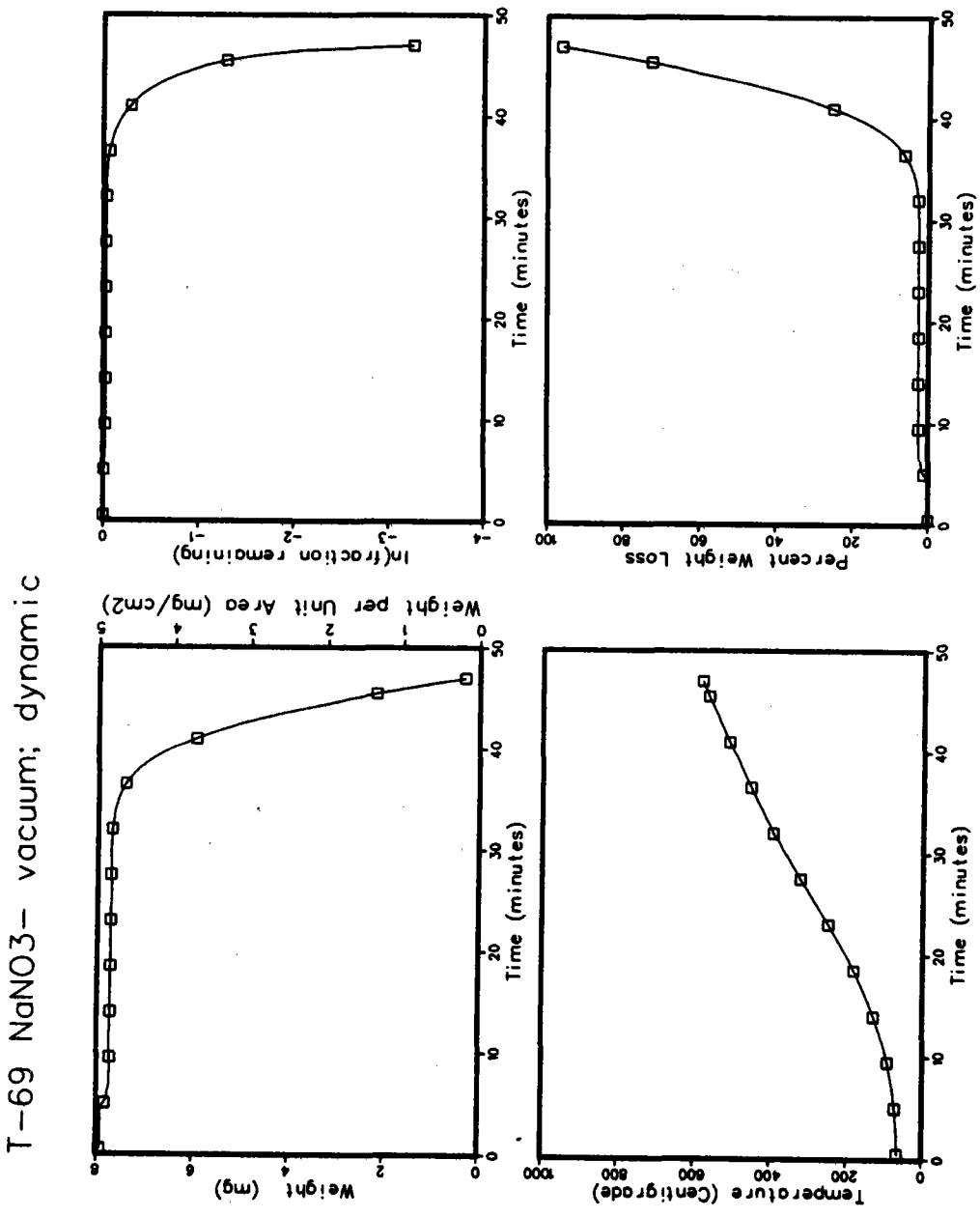
T-69 NaNO3- vacuum; dynamic
Temperature (Centigrade)
Time (minutes)
Weight (mg)
Weight per Unit Area (mg/cm2)
Time (minutes)
Percent Weight Loss
Time (minutes)
ln(fraction remaining)
Time (minutes)

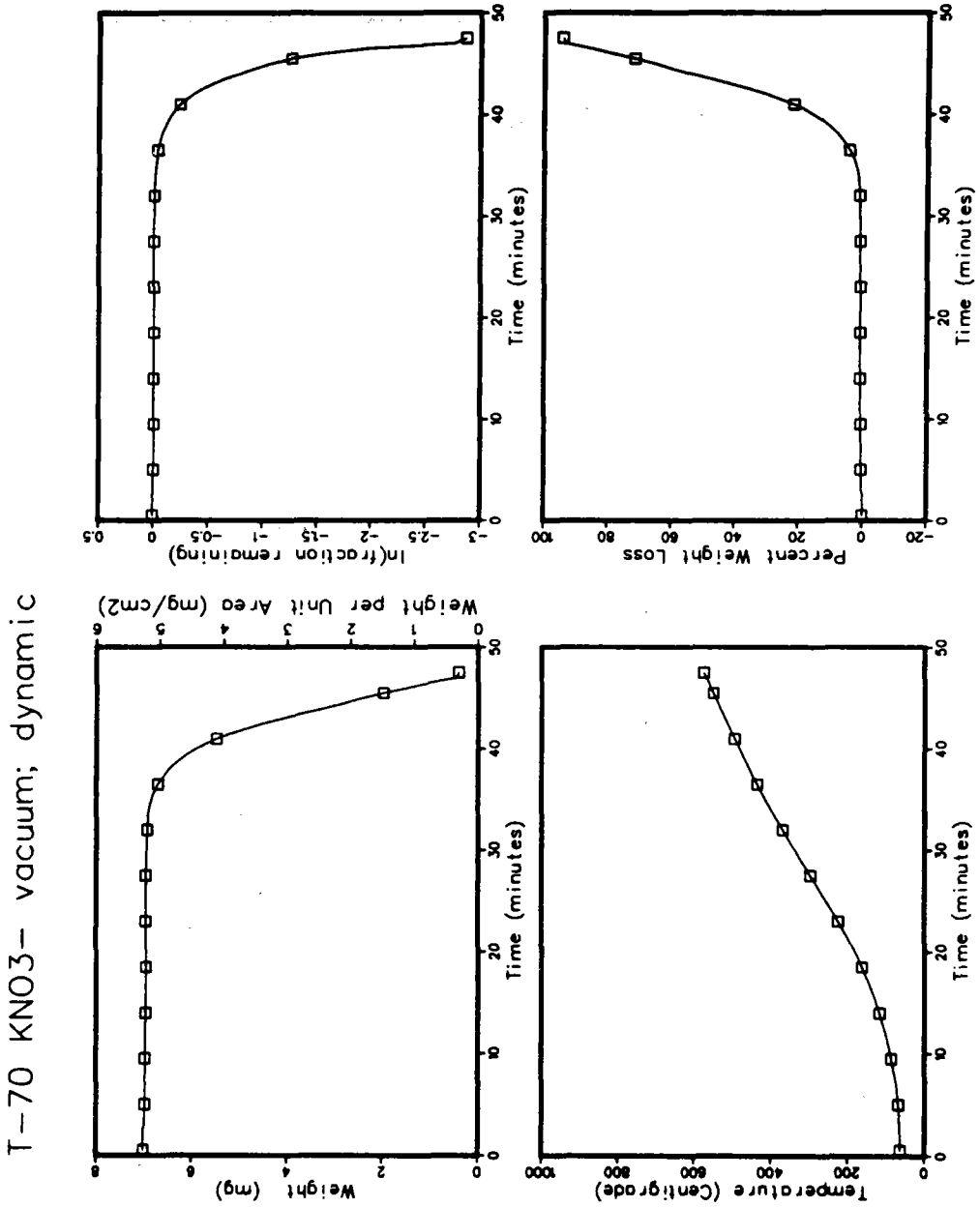
T-70 KNO3- vacuum; dynamic
Temperature (Centigrade)
Time (minutes)
Weight (mg)
Weight per Unit Area (mg/cm2)
Percent Weight Loss
ln(fraction remaining)

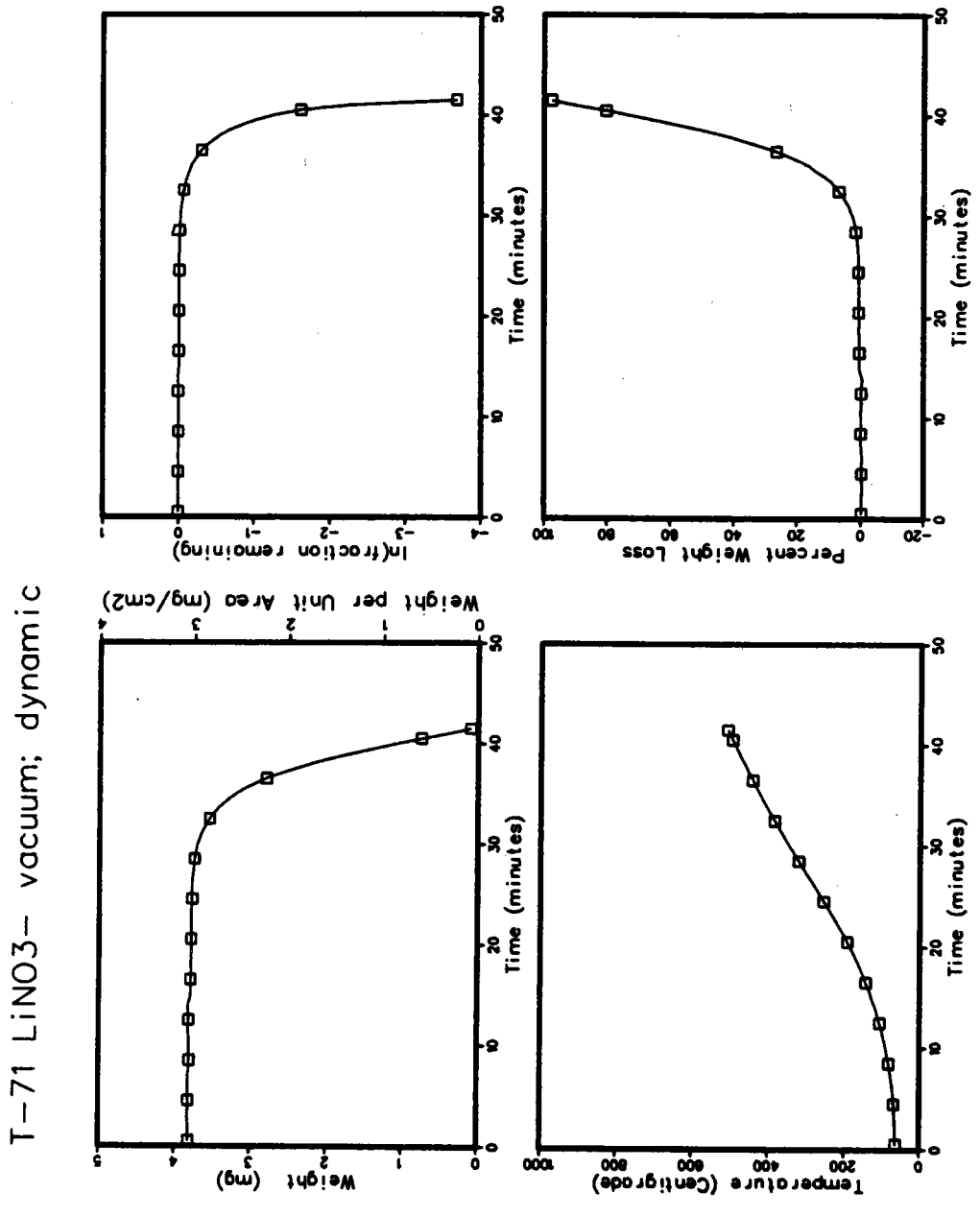
T-71 LiNO3- vacuum; dynamic
Temperature (Centigrade)
Time (minutes)
Weight (mg)
Time (minutes)
Weight per Unit Area (mg/cm2)
Time (minutes)
Percent Weight Loss
Time (minutes)
ln(fraction remaining)
Time (minutes)